INTRA-ARTICULAR DEPOT FORMING DRUG DELIVERY SYSTEM FOR OSTEOARTHRITIS

Matthew Freddi, BSc (Hons)

Thesis submitted to the University of Nottingham

for the degree of Doctor of Philosophy

May 2012

Abstract

Osteoarthritis (OA) is a chronic degenerative disease of the joint. Current treatments for this disease (such as glucocorticoid steroids) aim to reduce pain and increase mobility. Intra-articular injection is used in OA as treatment can be targeted to affected joints only. There is currently a lack of sustained release formulations for intra-articular injection.

The aim of this thesis was to produce and characterise an injectable intra-articular drug delivery system capable of providing delivery of the steroid dexamethasone phosphate (DXMP) over 3 months. This would be an injectable hydrogel that contains drug loaded nanoparticles.

Initially two systems Pluronic F127 gels and polyelectrolyte complexes between hyaluronic acid (HA) and chitosan were investigated. The complexes between HA and chitosan were selected for the hydrogel portion of this system as they showed the greatest stability and promise in initial studies. To improve the polyelectrolyte complex properties a modified HA was synthesised. This modified polymer caused faster complex formation and produced stronger, more resilient complexes.

DXMP was incorporated into poly(glycerol-adipate) (PGA) nanoparticles. A low but sufficient drug loading was achieved and particles were found to give a sustained drug release over 28 days.

Nanoparticles were found to be efficiently incorporated and well retained within complexes. Nanoparticles slightly improved complex formation and properties. Composites were able to be formulated into an injectable form.

Drug release from directly loaded complexes was rapid. A full release profile was not determined from composites of nanoparticle loaded complexes; however, over 60% of the loaded drug was recovered after 56 days of release study. Dexamethasone crystals were also incorporated directly into complexes to investigate the necessity of the use of nanoparticles. This gave a sustained drug release over 90 days making this system worthy of further investigation. These results highlight the different responses of these systems using drugs with different hydrophobicities.

Acknowledgments

Firstly and most importantly I would like to thank my supervisors Dr. Martin Garnett and Dr. Snow Stolnik whose guidance and support were invaluable. I would also like to thank my AstraZeneca supervisors Simon Cruyws, Terry Woolley and Paul Gellert for their useful input. My thanks are also due to the EPSRC and AstraZeneca for funding and presenting me with this opportunity.

I would like to thank the people who helped with my work during this project: Sanya Puri, Ahmed Abushrida and Mieke Heyde for help with the polymers; Bettina Wolf and Lloyd Hamilton for support with rheology. I would also like to thank the technical staff for their amazing work and dedication: Christy Grainger-Boultby, Paul Cooling, Teresa Marshall and Lee Hibbett.

I would also like to acknowledge other students who have contributed to the results in this thesis: Fabrice Bayard who carried out the work on the PAA hydrogels in Chapter 3; Salome Gamble and Shy Lih Teo who both made contributions to some initial studies.

My thanks are also due to Chris Grindon and Claudia Matz for emotional and administrative support as DTC project officer. Finally I would like to thank the other members of the Targeted Therapeutics DTC for their friendship and support, particularly Vicky Hutter, Klara Lovrics, Adnan Khan, Helen Angell and Gavin Hackett. Lastly I would like to thank all my friends and family for their constant support and love; especially my grandmother Sylvia Hope Butters who passed away in 2010 aged 94 and is greatly missed.

Table of Contents

List of Figures

List of Tables

Abbreviations

ACI- autologous chondrocyte implantation

ADAM - a disintegrin and metalloproteinase

ADAMTS- a disintegrin and metalloproteinase with thrombospondin motifs

ANOVA- analysis of variance

ASF- artificial synovial fluid

ASFP- artificial synovial fluid with protein

bFGF- basic fibroblast growth factor

BMP- bone morphogenetic protein

Ch- chitosan

CMC- carboxymethyl cellulose

COMP- cartilage oligomeric matrix protein

COX- cyclooxygenase

Da- Daltons

DCM- dichloromethane

Dex- dexamethasone

DMOAD- disease-modifying osteoarthritis drug

DTC- Doctoral Training Centre

DVS- divinylsulfone

DXMP- dexamethasone phosphate

E/S- emulsification and solvent evaporation method

ECM- extracellular matrix

EDAC- 1-ethyl-3-(3-dimethylaminopropyl) carbodiimide

eNOS- endothelial nitric oxide synthase

FDA- Food and Drug Administration

FGF- fibroblast growth factor

G'- storage modulus

G"- loss modulus

GAG- glycosaminoglycan

GP- General Practitioner

GPI- glycosylphosphatidylinositol

HA- hyaluronic acid

HAase- hyaluronidase

HAM- cysteamine modified hyaluronic acid

HAS- hyaluronic acid synthase

HBSS- Hank's balanced salt solution

HYAL- hyaluronidase

HEPES- 4-(2-hydroxyethyl)-1-piperazineethanesulfonic acid

HIF-1α- hypoxia inducible factor-1α

HRP- horseradish peroxidise

IA- intra-articular

IGF- insulin-like growth factor

IL- interleukin

IL-1Ra- interleukin-1 receptor antagonist

iNOS- inducible nitric oxide synthase

IPN- interpenetrating network

JSN- joint space narrowing

LIF- leukaemia inhibitory factor

LVR- linear viscoelastic region

MDR-1- multidrug resistance-associated protein 1

MMP- matrix metalloproteinase

MMPi- matrix metalloproteinase inhibitors

MRI- magnetic resonance imaging

MRP-5- multidrug resistance-associated protein 5

MRT- mean retention time

Mw- molecular weight

NASHA- non-animal stabilised hyaluronic acid

NMR- nuclear magnetic resonance

NO- nitric oxide

NOS- nitric oxide synthase

NP- nanoparticle

NSAID- non-steroidal anti-inflammatory drug

OA- osteoarthritis

PBCA- poly(butylcyanoacrylate)

PBS- phosphate buffered saline

PC- phosphatidylcholine

PDLLA- poly(DL-lactic acid)

PEG- (poly(ethylene glycol)

PEI- poly(ethyleneimine)

PGA- poly(glycerol-adipate)

PGE_2- prostaglandin E_2

PLA- poly(lactic acid)

PLGA- poly(lactic-co-glycolic acid)

PLLA- poly(L-lactic acid)

PNIPAM- poly(N-isopropylacrylamide)

PPG- poly(propylene glycol)

PPS- poly(propylene sulphide)

PVA- poly(vinyl alcohol)

RA- rheumatoid arthritis

RBITC- rhodamine B isothiocyanate

ROS- reactive oxygen species

SEM- scanning electron microscopy

siRNA- small interfering ribonucleic acid

SLC- synovial lining cell

SOD- superoxide dismutase

TGF-β- transforming growth factor-beta

THF- tetrahydrofuran

TIMP- tissue inhibitor of metalloproteinases

TNF- tumour necrosis factor

VEGF- vascular endothelial growth factor

CHAPTER 1 - INTRODUCTION

1.1 General Introduction to Osteoarthritis

1.1.1 Introduction

Osteoarthritis (OA) is a degenerative disorder of the synovial joint that is characterised by a progressive loss of articular cartilage (Brandt et al., 2003, Buckwalter and Martin, 2006). As the disease progresses the entire joint becomes affected (Pollard et al., 2008, Brandt et al., 2003). Osteoarthritis is a monoarthritis as it develops within individual joints; this contrasts with rheumatoid arthritis (RA), the most prevalent polyarthritis, which affects many joints in sufferers (Woolf and Pfleger, 2003).

Any synovial joint can be affected by osteoarthritis, but the joints most commonly affected are the knee, hip, hand, foot, and spine (Woolf and Pfleger, 2003). The main symptom of this disease is joint pain. Other symptoms include tenderness, stiffness and loss of movement in affected joints (Pelletier et al., 2001, Woolf and Pfleger, 2003, Buckwalter and Martin, 2006).

1.1.2 Risk Factors

A number of risk factors for osteoarthritis have been identified and include obesity (Woolf and Pfleger, 2003, Aspden, 2011), joint deformity or malalignment (Brandt et al., 2003, Buckwalter and Martin, 2006), gender (OA shows a higher prevalence in females) (Woolf and Pfleger, 2003, Brandt et al., 2003), age (Woolf and Pfleger, 2003, Buckwalter and Martin, 2006), genetics

(Woolf and Pfleger, 2003, MacGregor et al., 2000) and joint trauma (Buckwalter and Martin, 2006, Gelber et al., 2000, Woolf and Pfleger, 2003).

Age is one of the primary risk factors for OA as physiological changes that occur in the aging joint make it more susceptible to OA. These include a softening of the cartilage surface and decreases in the strength of the cartilage matrix components (Goldring and Goldring, 2007, Aigner et al., 2007). Despite the strong link with age it is not unknown for osteoarthritis to develop in individuals under 45 years old. This is relatively uncommon and the prevalence increases rapidly after this age (Woolf and Pfleger, 2003).

The link between obesity and osteoarthritis has been found to be more complex than it might initially seem. The increased loads on the joints due to obesity might be expected to explain this link. However there is growing evidence that other metabolic factors may be more important. The hormones leptin and adiponectin are produced by adipose tissue and have been found to increase the levels of degradative factors that are important in OA (Aspden, 2011, Dumond et al., 2003, Aspden et al., 2001, Clouet et al., 2009, Kang et al., 2010).

1.1.3 Prevalence

Osteoarthritis is the world's most common arthritis and the most common joint disease. The World Health Organisation estimates that 18% of women and 10% of men over 60 years of age worldwide have symptomatic osteoarthritis (Woolf and Pfleger, 2003). In the UK it has been estimated by Arthritis Care that there are 8.5 million people living with symptomatic osteoarthritis (Arthritis Care, 2004). Due to the slow development of OA changes in joints

can occur long before symptoms are experienced. Radiographic evidence of OA is found in about 25% of adults over 50 years old (National Collaborating Centre for Chronic Conditions, 2008, Woolf and Pfleger, 2003, Peat et al., 2006), but only about half of these people are symptomatic.

1.1.4 Impact

Osteoarthritis has a huge impact and it has been estimated that OA was the eighth leading non-fatal burden of disease in the world in 1990 (Woolf and Pfleger, 2003). We are living in an aging population and as OA has a strong association with aging it is predicted to become the fourth leading cause of disability by 2020 (Woolf and Pfleger, 2003).

The demands that this disease places on the health services are therefore huge. In the UK 2 million adults visit their GP every year due to osteoarthritis. Over 60,000 hip replacements, costing around £450 million, were carried out in 2006/7 in the UK of which 94% were due to OA (National Collaborating Centre for Chronic Conditions, 2008). The total cost of this disease in the UK has been estimated to be equivalent to 1% of Gross National Product per year (National Collaborating Centre for Chronic Conditions, 2008), which includes the effect of 36 million lost working days due to osteoarthritis in 1999/2000.

1.2 Synovial Joint Physiology

To understand osteoarthritis it is necessary to be familiar with the physiology of synovial joints and so a brief overview is included in the following sections.

1.2.1 General Structure

Synovial joints are the most common and most mobile type of joint present in the human body. The other two types of structural joint in the body are simpler and less mobile. They are fibrous and cartilaginous joints, in which the bones are directly connected by collagen fibres and cartilage respectively.

The healthy synovial joint is an organ composed of a number of different cell and tissue types (Brandt et al., 2003). These include the subchondral bone, articular cartilage, synovial membrane and the joint capsule. The basic structure of a synovial joint shown in Figure 1-1, and consists of two bones held in position by the joint capsule. The articulating surfaces of the bones are covered in cartilage and separated by the synovial cavity which is filled with synovial fluid. More detailed descriptions of these components follow below.

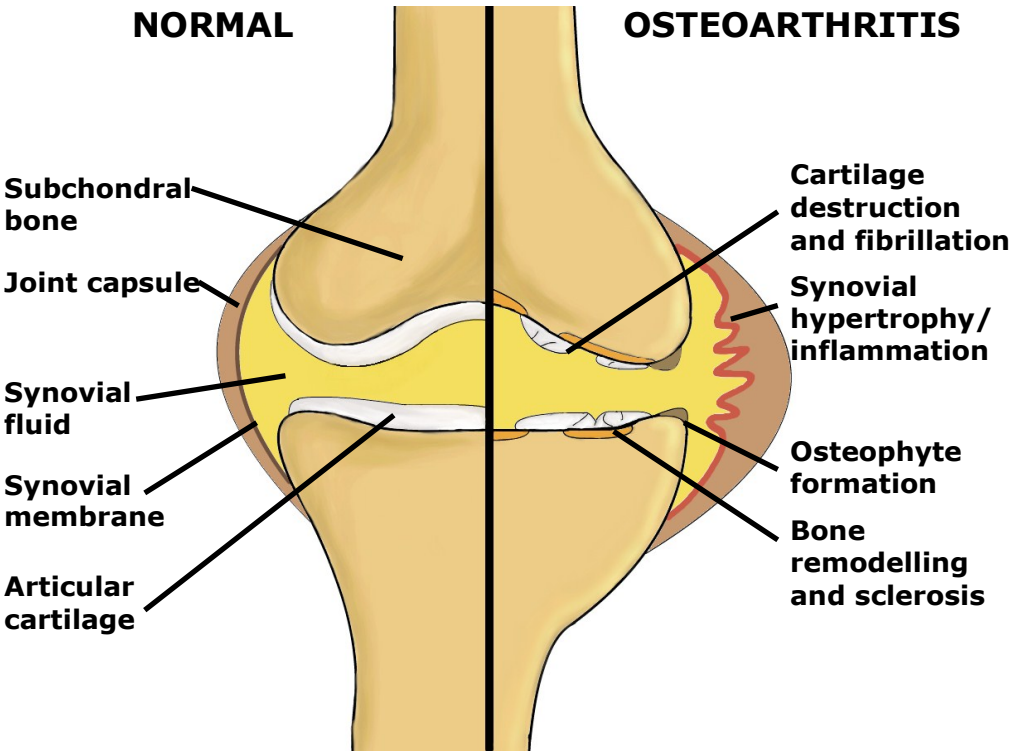

Figure 1-1 Diagram showing the features of a normal synovial joint and the major changes observed in osteoarthritis.

1.2.2 Cartilage

The bone surface within the joint is covered by a protective layer of hyaline cartilage known as articular cartilage. This layer helps to resist the mechanical forces within the joint, protects the bone and provides a low friction surface for joint movement (Aigner et al., 2006). Cartilage is a relatively acellular tissue with chondrocytes being the only cells present. The primary component of cartilage is its specialised extracellular matrix.

Cartilage can be divided into zones depending on its depth. The layer exposed to the synovial fluid is called the superficial zone. In that order below that are the middle zone, deep zone and calcified zone (Buckwalter et al., 2005). The calcified zone links the cartilage to the bone and acts to relieve the shear stresses that would occur with a straight division (Pollard et al., 2008).

1.2.2.1 Extracellular matrix

The extracellular matrix (ECM) is the major component of articular cartilage. It is composed of structural and connective proteins, as well as proteoglycans and tissue fluid- 80% of the wet weight of cartilage is water (Pollard et al., 2008). The major structure of hyaline cartilage is shown in Figure 1-2. It is a network of fibrillar type II collagen fibres which retains the proteoglycan aggrecan (Buckwalter et al., 2005). Collagen is a protein rich in glycine (found roughly every third residue) and proline. Three individual collagen chains of around 1000 amino acids come together to form triple-helical fibrils which further associate to form long collagen fibres.

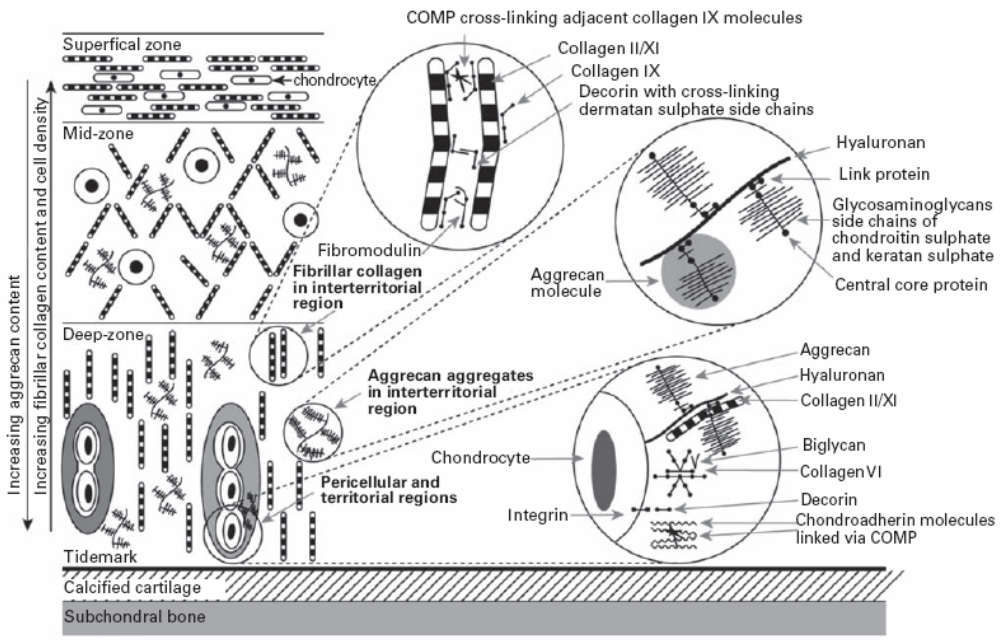

Figure 1-2 Diagram showing the zonal differences in biochemical composition and organisation of articular cartilage.
Reproduced with permission and copyright © of the British Editorial Society of Bone and Joint Surgery (Pollard et al., 2008).

Aggrecan is a proteoglycan consisting of a core protein linked to a large number (c. 100-300) of glycosaminoglycan (GAGs) molecules, mostly chondroitin sulphate and keratan sulphate. GAGs are polysaccharides composed of disaccharides of a hexuronic acid and a hexosamine with various sulphations. Aggrecan molecules are bound to large hyaluronan molecules by a link protein to make a huge complex (Brandt et al., 2003).

The sulphate groups present in GAGs make aggrecan highly negatively charged. These charges cause a high osmotic pressure and leads to the large volume of water in cartilage (Alford and Cole, 2005). The high water content combined with the repulsive forces between negative charges causes expansion, which the tensile strength of the collagen fibres acts to contain. The expanded structure provides cartilage with its compressive strength and it can resist loads of up to 15 to 20 MPa, which occur for short periods (less than a

second) during vigorous activity (Seireg and Arvikar, 1975, Sharma et al., 2007).

A number of minor components are present in articular cartilage, as shown in Figure 1-2. These include various other collagens, such as types VI, X, XI and XVI (Buckwalter et al., 2005), which have various functions, for example Type IX acts as a link to other components of the ECM (Buckwalter et al., 2005, Aigner et al., 2006) and type XI is involved in fibril synthesis (Aigner et al., 2006). Cartilage also contains a variety of other proteins and proteoglycans such as decorin, biglycan, chondroadherin, fibronectin, and cartilage oligomeric matrix protein (COMP) (Pollard et al., 2008, Aigner et al., 2006, Sofat, 2009). These components fulfil a variety of roles such as stabilising the collagen framework and regulating matrix turnover (Pollard et al., 2008).

The composition and organisation of cartilage varies by zone (Buckwalter et al., 2005). The superficial zone is relatively rich in collagen, with relatively thin fibres arranged parallel to the surface. This arrangement provides resistance to shear forces and produces a protective surface. In the middle zone the collagen fibres are thicker and arranged at angles to the surface. The deep zone is the richest in aggrecan and has the thickest collagen fibres, which are arranged perpendicular to the surface and help provide compressive strength (Buckwalter et al., 2005).

1.2.2.2 Chondrocytes

Chondrocytes make up about 1% of the volume of articular cartilage (Buckwalter et al., 2005). Chondrocytes are found within cavities known as lacunae and are adapted to anoxic, high pressure conditions (Holland and Mikos, 2003). The main function of chondrocytes is to synthesise the ECM components of cartilage (Buckwalter et al., 2005). Chondrocytes within mature articular cartilage are quiescent and do not undergo mitosis (Goldring and Goldring, 2007). Chondrocyte numbers and morphology vary between cartilage zones (Buckwalter et al., 2005).

The turnover rate for healthy cartilage is very slow, with the estimated half-life for collagen in cartilage being 100 years and for aggrecan is around 5 years (Brandt et al., 2003). The natural turnover requires the breakdown of old molecules which is carried out by enzymes in the matrix metalloproteinase (MMP) and the ADAMTS (a disintegrin and metalloproteinase with thrombospondin motif) families (Aigner et al., 2006). MMP-1 and MMP-13 are the most important enzymes in the degradation of type II collagen (Pollard et al., 2008). ADAMTS-4 and ADAMTS-5 are responsible for the initial cleavage of aggrecan, which is further degraded by MMPs (Pollard et al., 2008), particularly MMP-3 (Aigner et al., 2006). The ability of chondrocytes to maintain and repair cartilage diminishes with age, which has been attributed to a reduction in their anabolic capacity (Buckwalter et al., 2005, Goldring and Goldring, 2007, Aigner et al., 2007).

Cartilage can be categorised according to its proximity to chondrocytes. These zones are identified and characterised in Figure 1-2. The zone surrounding the chondrocytes is the pericellular zone which is rich in proteoglycans and lacking in fibrillar collagen. It is also rich in type VI collagen which links chondrocytes to type II collagen fibrils (Aigner et al., 2006). Surrounding this zone is the territorial zone which contains a 'basket' of thin collagen fibres that gives the cells some mechanical protection (Buckwalter et al., 2005). Well away from chondrocytes is the interterritorial zone which makes up about 90% of cartilage volume (Pollard et al., 2008, Buckwalter et al., 2005).

1.2.3 Synovial Membrane and Joint Capsule

1.2.3.1 Synovial membrane

The synovial membrane contains the only other population of cells in the synovial joint. The intima layer of the synovial membrane faces the synovial cavity and is composed of a thin layer of cells known as synovial lining cells (SLCs) (Momberger et al., 2005). SLCs can be divided into two distinct types. Type A SLCs are macrophage like cells that make up around a third of the SLC population (Gerwin et al., 2006), and act to remove large molecular weight debris from the joint. Type B SLCs are fibroblasts that secrete the components of synovial fluid (Athanasou, 1995, Momberger et al., 2005).

Below the intima is the subsynovium or subintima which is composed of loose connective tissue with an extracellular matrix rich in collagen, hyaluronan, decorin and biglycan (Gerwin et al., 2006, Burt et al., 2009). It also contains adipose cells, blood and lymph vessels (Burt et al., 2009).

The synovial membrane is highly vascularised and allows an ultrafiltrate of plasma to enter the synovial cavity (Gerwin et al., 2006). This fluid makes up the liquid portion of synovial fluid and supplies nutrients and oxygen to the cartilage. The synovium also contains the only nerves within the joint which provide pain feedback and control synovial blood flow (Gerwin et al., 2006).

1.2.3.2 Joint capsule

The joint capsule surrounds the synovium and along with associated ligaments and muscles acts to hold the joint together by resisting the expansive forces from cartilage and joint loading (Aigner et al., 2006).

1.2.4 Synovial Fluid

Synovial fluid is a viscous fluid that fills the synovial cavity. A human joint contains between 0.5 and 2ml of this fluid (Brandt et al., 2003). The fluid is an ultrafiltrate of blood plasma containing similar plasma proteins but in reduced amounts (Ropes et al., 1940). Synovial fluid also contains other glycoprotein components that are permanently present within the joint.

The defining characteristic of synovial fluid is that it contains a high concentration of hyaluronic acid (around 3.5mg/ml) (Gerwin et al., 2006, Curtiss, 1964). Hyaluronic acid (HA) has an average molecular weight in healthy joints of between 4 and 10 mDa (Dahl et al., 1985) and is the primary reason for the high viscosity and characteristic viscoelastic properties of synovial fluid (Mensitieri et al., 1995).

1.2.4.1 Hyaluronic acid

Hyaluronic acid is composed of a repeating disaccharide of D-glucuronic acid and D-N-acetyl glucosamine (Liao et al., 2005), as shown in Figure 1-3. Unlike all other GAGs HA is not sulphated (Volpi et al., 2009, Ponedel'kina et al., 2008). HA is often referred to as hyaluronan as it is ionised at a physiological pH (Liao et al., 2005).

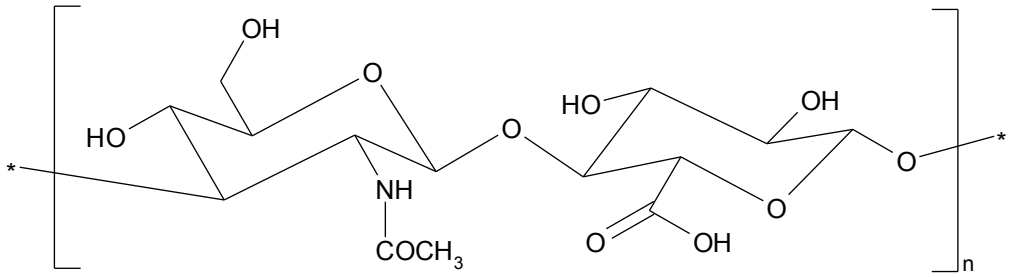

Figure 1-3 Structure of hyaluronic acid showing disaccharide repeating unit.

In solution HA has a level of ordered structure (Scott and Heatley, 1999) which is stabilised by hydrogen bonding between neighbouring disaccharide repeats, interactions between hydrophobic patches and interchain hydrogen bonding (Scott and Heatley, 1999, Scott and Heatley, 2002). HA adopts a twisted chain secondary structure, which can further associate to form an antiparallel β-sheet like tertiary structure (Scott and Heatley, 1999, Liao et al., 2005). Antiparallel means that the HA chains in this structure run parallel but in opposite directions. Chain interactions can also lead to the formation of weak and transient molecular networks in high molecular weight HA (Scott, 1998). These structures are more stable than a random coil but can be disrupted and reversibly denatured (Scott and Heatley, 2002).

HA is synthesised by hyaluronan synthase (HAS) enzymes and in humans there are three isoforms of this enzyme. HAS2 is the isoform predominantly

expressed in the joint and produces high molecular weight hyaluronan (c. 2MDa) (Liao et al., 2005, Bastow et al., 2008). Synthesis occurs at the plasma membrane of the type B synoviocytes, with the polymer being simultaneously exported by a transmembrane pore. The multi-drug resistance transporters MDR-1 (multidrug resistance-associated protein 1) and MRP-5 (multidrug resistance-associated protein 5) have been implicated as these transporters (Momberger et al., 2005, Prehm and Schumacher, 2004).

HA is degraded by two mechanisms *in vivo* which are enzymatic hydrolysis and scission reactions involving reactive oxygen species (ROS) (Volpi et al., 2009). Little is known about the relative contributions of these two mechanisms to overall HA degradation. Enzymatic hydrolysis occurs through the action of hyaluronidases (HYAL), which can also degrade other GAGs. Mammalian hyaluronidases are β-endo-N-acetylglucosaminidase and hydrolase enzymes (Volpi et al., 2009). There are 3 functionally active HYAL enzymes in humans. HYAL-1 (lysosomal) and HYAL-2 (glycosylphosphatidylinositol (GPI) linked to the external surface of the cell membrane) are the major hyaluronidases (Volpi et al., 2009, Stern et al., 2007). PH-20 is an enzyme involved in sperm penetration of the ovum (Volpi et al., 2009, Stern et al., 2007).

It has been suggested that these enzymes work in tandem to mediate HA degradation. HYAL-2, CD44, HARE and RHAMM, act as extracellular receptors for HA (Liao et al., 2005, Bastow et al., 2008) which traffic HA to acidic endosomes. In these endosomes HYAL-2 digests HA to medium sized

fragments. These fragments are moved to the lysosomes for further degradation by HYAL-1 and other lysosomal enzymes (Volpi et al., 2009, Yoshida et al., 2004, Liao et al., 2005, Bastow et al., 2008). Enzymatic degradation of HA produces fragments with an identical chemical structure to the full chain polymer.

Degradation by ROS produces fragments that contain products of O_2 metabolism such as aldehydes and hydroperoxides (Volpi et al., 2009). The ROS species mainly responsible for HA degradation are the hydroxyl radical ($OH^{\cdot}$), hypochlorous acid (HOCl) and peroxynitrite ($ONOO^{-}$) (Volpi et al., 2009, Stern et al., 2007). There are various mechanisms for these degradations which have been reviewed by Volpi et al. and Stern et al. (Stern et al., 2007, Volpi et al., 2009). It is possible that HA degradation by ROS is sacrificial to scavenge and remove free radicals (Liao et al., 2005, Volpi et al., 2009).

1.2.4.2 Other constituents

Synovial fluid also contains lubricin (0.05 mg/ml), which is a glycoprotein that helps provide lubrication (Bao et al., 2011). The synovial ECM prevents plasma proteins greater than 160 kDa entering the joint and causes overall protein levels to be a third of those found in plasma (c. 20 mg/ml) (Curtiss, 1964, Mavraki and Cann, 2009). The filtering also acts to relatively enrich albumin, which makes up around 60% of protein in synovial fluid but only around 40% of that in plasma (Curtiss, 1964, Mavraki and Cann, 2009). The majority of the rest of the protein in synovial fluid is globulins.

1.2.4.3 Functions

The main functions of synovial fluid are to facilitate joint movement and protect the articular surfaces. Synovial fluid acts as a lubricating layer between the bones but its viscoelastic properties allow it to also act as an elastic shock absorber upon impacts (Mensitieri et al., 1995). Synovial fluid also has an essential role in supplying nutrients to chondrocytes (Momberger et al., 2005).

Synovial fluid undergoes a rapid turnover with the blood acting as a sink for small molecules, which is seen by ions in synovial fluid being in equilibrium with plasma (Brandt et al., 2003). Synovial fluid is also drained by the well-developed lymphatic vessels in the subsynovium (Burt et al., 2009, Xu et al., 2003). HA is retained for longer due to its high molecular weight partially excluding it from lymph vessels. HA is still completely turned over in around 36h (Gerwin et al., 2006, Butoescu et al., 2009a).

1.3 Disease Progression in Osteoarthritis

Osteoarthritis causes changes throughout the synovial joint. The most important is the progressive loss of articular cartilage. Other changes include sclerosis of subchondral bone, osteophyte formation, synovial thickening and changes in synovial fluid (Aigner et al., 2006, Brandt et al., 2003). Figure 1-1 summarises the main changes seen in osteoarthritis.

The early stages of the disease are outlined below, followed by a summary of how the disease progresses beyond this point. Finally the most important changes in the later stage disease are summarised.

1.3.1 Early Osteoarthritis

Investigation into early osteoarthritis has been challenging due to the long development before symptoms appear. Changes naturally occur in the joint, for example with aging, that increase the risk of osteoarthritis but that are not necessarily a precursor to OA. Despite the challenges a picture of the early stages of OA is beginning to emerge.

The first observed change in the development of osteoarthritis is a loss of aggrecan from the outer layers of articular cartilage (Arden and Cooper, 2006). Changes in proteoglycan levels cause changes in the swelling behaviour of cartilage and can lead to oedema. Oedema causes stretching and thinning of the collagen which makes fibres more susceptible to breakage (Brandt et al., 2003). Breakage of fibres leads to the formation of surface cracks, and surface fibrillation is one of the first macroscopic changes observed in osteoarthritis (Brandt et al., 2003, Buckwalter et al., 2005).

Chondrocytes counteract decreased proteoglycan levels by increasing synthesis and removing damaged cartilage components (Dijkgraaf et al., 1995). This increases anabolic and catabolic processes in an attempt to repair the cartilage.

1.3.2 Progression to Clinical Osteoarthritis

A key transition occurs in the development of osteoarthritis, which is a shift from hypertrophic cartilage, where there is an increase in both anabolism and catabolism, to catabolic processes dominating. The causes of this progression are not fully known but there are contributions from numerous factors.

In early osteoarthritis increased levels of anabolic factors which mediate cartilage repair have been observed. These include TGF-β (transforming growth factor-beta) and IGF-1 (insulin-like growth factor 1) (Goldring and Goldring, 2007, Blom et al., 2004). As OA progresses these become overwhelmed by larger increases in catabolic cytokines (Aigner et al., 2006, Freemont, 2006, Bondeson et al., 2006).

Changes in the cartilage repair process are thought to be important. Over time repair can become ineffectual, for example due to aging chondrocytes or further damage to the cartilage (Buckwalter et al., 2005). This causes a decline in cartilage quality leading to an increased susceptibility to further damage. Repeated damage may eventually cause dysregulation of the repair process and lead to increased degradation. At a molecular level it has been suggested that the activation of MMP-13 is important. Activation is thought to occur due to aggrecan depletion around chondrocytes allowing collagen fibrils to interact with a receptor that activates MMP-13 (Xu et al., 2007).

1.3.3 Cytokines

Aberrant cytokine signalling is a major factor in osteoarthritis. The two key cytokines in osteoarthritis are IL-1β (interleukin-1 beta) and TNF-α (tumour necrosis factor-alpha). Levels of both are increased in osteoarthritis (Furuzawa-Carballeda and Alcocer-Varela, 1999, Benito et al., 2005, Bondeson et al., 2006). IL-1β and TNF-α cause cartilage destruction both individually and synergistically, as in combination their effects exceed those from one alone (Page Thomas et al., 1991).

IL-1β and TNF-α are expressed by synovial macrophages and chondrocytes. These cytokines cause increased expression of ECM degrading enzymes (Pelletier et al., 2001, Sofat, 2009, Goldring and Goldring, 2007). They cause an overexpression and activation of iNOS (inducible nitric oxide synthase) in chondrocytes (Grabowski et al., 1997, McInnes et al., 1996). They also induce the release of inflammatory mediators including reactive oxygen species (Mathy-Hartert et al., 2008), prostaglandin E_2 (PGE_2), IL-6, IL-17, IL-18 and leukaemia inhibitory factor (LIF) (Van den Berg, 2002, Alaaeddine et al., 1999, Atik, 1990, Benito et al., 2005, Furuzawa-Carballeda and Alcocer-Varela, 1999, Farahat et al., 1993).

Other pro-inflammatory cytokines have also been implicated in osteoarthritis. These include oncostatin M (Barksby et al., 2006), IL-8 (also known as CCL2) (Alaaeddine et al., 1999, Furuzawa-Carballeda and Alcocer-Varela, 1999, Sellam and Berenbaum, 2010), other prostaglandins (Wittenberg et al., 1993, Benito et al., 2005) and leukotriene B_4 (Atik, 1990, Wittenberg et al., 1993). Normally there is a balance between pro- and anti- inflammatory cytokines. This balance is further disrupted in OA by reductions in anti-inflammatory cytokines such as IL-4, IL-10, IL-13 and IL-1Ra (IL-1 receptor antagonist) (Furuzawa-Carballeda and Alcocer-Varela, 1999, Smith et al., 1997, Sutton et al., 2009).

1.3.4 Enzymes

Enzymes are responsible for the majority of degradation seen in osteoarthritis. These are mostly enzymes naturally involved in cartilage turnover, with the

enzymes most responsible being the MMP and ADAMTS families (Cawston and Wilson, 2006, Aigner et al., 2006). There is evidence that enzymes of the cathepsin family are also increased in OA (Konttinen et al., 2002, Hou et al., 2002). A minor role in aggrecan degradation may be played by glycosidase enzymes (Pasztoi et al., 2009, Ortutay et al., 2003, Sugimoto et al., 2004).

MMPs and ADAMTS are extracellular proteinase enzymes involved in ECM turnover throughout the body. The most important in OA are considered to be MMP-1 (Catterall and Cawston, 2003), MMP-3 (Sandell and Aigner, 2001), MMP-13 (Catterall and Cawston, 2003, Sandell and Aigner, 2001), ADAMTS-4 (Sandell and Aigner, 2001, Davidson et al., 2006) and ADAMTS-5 (Sandell and Aigner, 2001, Davidson et al., 2006). The synovium and chondrocytes are both sources of these enzymes (Davidson et al., 2006, Goldring and Berenbaum, 2004). MMP-13 is considered to be highly important in OA as raised levels are found in patients and its preferential inhibition significantly reduces collagen cleavage (Sofat, 2009, Davidson et al., 2006, Billinghurst et al., 1997, Mitchell et al., 1996, Johnson et al., 2007). ADAMTS-5 is the most important aggrecanase (Glasson et al., 2005, Plaas et al., 2007) and is the enzyme primarily responsible for aggrecan release in OA (Little et al., 1999).

Other MMPs and members of the ADAM (a disintegrin and metalloproteinase-enzymes closely related to ADAMTS) family have been implicated in osteoarthritis. These include MMP-2 (Aigner et al., 2006, Davidson et al., 2006, Arican et al., 2000), MMP-7 (Aigner et al., 2006), MMP-8 (Aigner et al., 2006, Sofat, 2009), MMP-9 (Davidson et al., 2006, Sofat, 2009, Arican et al.,

2000), MMP-14 (Aigner et al., 2006, Davidson et al., 2006, Sofat, 2009), ADAM-10 (Aigner et al., 2006) and ADAM-15 (Aigner et al., 2006).

TIMPs (tissue inhibitor of metalloproteinases) are natural regulators of MMP activity (Cawston and Wilson, 2006). Four TIMPs are known which have variable activities toward different MMPs (Le Graverand-Gastineau, 2010), and TIMP-3 is also active against ADAMTS-4 and ADAMTS-5 (Le Graverand-Gastineau, 2010). TIMP-1 is the most expressed TIMP in the joint (Davidson et al., 2006), and shows reduced expression in OA (Sandell and Aigner, 2001, Davidson et al., 2006). Increases in MMP levels overwhelm the capacity of TIMPs and this contributes to the degradation seen in OA.

Due to their potency and to provide a greater control of their action most MMPs are secreted as proenzymes (Nagase et al., 2006). Activation of these pro-MMPs often occurs through the action of proteinases, including other MMPs and active versions of the same enzyme (Nagase et al., 2006, Dreier et al., 2004). Once the degradative state emerges in OA and if enzyme expression continues then a self-perpetuating, uncontrolled activation occurs.

1.3.5 Synovial Inflammation

Osteoarthritis is not considered to be an inflammatory arthritis. Inflammation is not a primary factor in the disease and no neutrophils are found in the synovium. Rheumatoid arthritis (RA) is an inflammatory arthritis and shows extensive neutrophil infiltrates.

In most osteoarthritis patients there are some signs of inflammation in the synovium (Hill et al., 2007, Pelletier et al., 2008, Haraoui et al., 1991). A magnetic resonance imaging study showed a thickening of the synovial lining cell layer in 73% of OA patients (Bonnet and Walsh, 2005). The inflammation varies with time and between individuals. For much of the time it may be localised and at sub-clinical levels (Myers et al., 1990, Bonnet and Walsh, 2005), with acute flares occurring that can reach the inflammation levels seen in RA (Haraoui et al., 1991, Myers et al., 1990).

Synovial inflammation may be initiated and driven by molecular fragments from cartilage destruction (Sellam and Berenbaum, 2010, Ghosh and Cheras, 2001). These fragments can lead to the activation and proliferation of synovial lining cells (Hamerman and Klagsbrun, 1985, Aigner et al., 2006). Often a moderate synovial hyperplasia is seen in early OA which becomes a general synovitis as the disease progresses (Oehler et al., 2002, Aigner et al., 2006).

Cytokines and other soluble factors are known to be important mediators of synovial inflammation. The inflamed synovial membrane is also an important source of cytokines and enzymes in osteoarthritis. Synovial macrophage depletion has caused a significant reduction in TNF-α, IL-1 and MMP levels in OA (Bondeson et al., 2006, Blom et al., 2007).

Extensive immune cell infiltration doesn't occur in OA. However there can be a scattered infiltration of the subsynovium (Nakamura et al., 1999, Sakkas and Platsoucas, 2007). This infiltration includes activated T cells, B cells and

macrophages (Nakamura et al., 1999, Benito et al., 2005, Sakkas and Platsoucas, 2007). Mast cells are naturally present in the joint to provide an immune response (Dean et al., 1993) and have been found to be increased in number and activated in OA (Dean et al., 1993). Mast cells may have a role in maintaining chronic synovitis in OA, as mast cell accumulation is associated with many chronic inflammatory conditions (Nigrovic and Lee, 2007).

Synovial synovitis causes remodelling within the synovium. Angiogenesis is closely related to inflammation throughout the body and has been observed in inflamed osteoarthritic synovium (Walsh et al., 2007). This angiogenesis is driven by the proangiogenic factors VEGF (vascular endothelial growth factor) (Haywood et al., 2003), with a smaller contribution from HIF-1α (hypoxia inducible factor-1α) (Giatromanolaki et al., 2003). As VEGF causes tissue remodelling it causes increased expression of MMPs (Murata et al., 2008). Remodelling of the lymph system has also been observed in OA with lymph vessels extending further into the subintima (Xu et al., 2003).

1.3.6 Chondrocytes

Chondrocytes in OA can change from their quiescent form, and undergo apoptosis or aberrantly divide or gain an altered phenotype (Aigner et al., 2001, Aigner et al., 2006). The most common phenotypic change is dedifferentiation as this can be induced by IL-1β and TNF-α (Seifarth et al., 2009, Aigner et al., 2006). Dedifferentiation causes chondrocytes to change into a more fibroblast like cell leading to changes in gene expression. Cartilage specific genes are no longer expressed and other genes are aberrantly

expressed (Aigner et al., 1997, Vondermark et al., 1977). For example collagen types I and III as well as tenascin have been detected in OA cartilage (Aigner et al., 1993, Salter, 1993).

Abnormal proliferation of chondrocytes occurs in an attempt to repair cartilage and leads to cells in OA often being found in clusters (Aigner et al., 2001, Rothwell and Bentley, 1973). The accumulation of matrix components in chondrocytes can lead to their apoptosis (Horton et al., 2005, Yang et al., 2005). There is an increased turnover of type VI collagen in OA (McDevitt et al., 1988, Buckwalter et al., 2005). This molecule helps to provide a protective layer around the chondrocytes, and its increased turnover be responsible for some of the changes seen in chondrocytes (Aigner et al., 2006).

1.3.7 Reactive Oxygen Species

Reactive oxygen species (ROS) are highly toxic oxygen species produced by metabolic processes in the mitochondria. In general they are free radicals and contain an unpaired electron, however some ROS such as hydrogen peroxide are not radicals (Volpi et al., 2009). Superoxide ($O_2^{\cdot -}$) is a ROS that is produced in the mitochondria. The amount of superoxide radical in the cell is controlled by superoxide dismutase (SOD) which reduces it to hydrogen peroxide, which itself is eliminated by catalase or glutathione peroxidase (Afonso et al., 2007). If not controlled, superoxide and hydrogen peroxide can react together in the presence of transition metals to form the highly damaging hydroxyl ($OH^{\cdot}$) and peroxyl radicals ($ROO^{\cdot}$) (Afonso et al., 2007).

There is a plenty of evidence of ROS involvement in osteoarthritis. Measures of oxidative damage in cartilage increase with age and OA stage (Afonso et al., 2007). This suggests that ROS and oxidative stress play a role in both OA and chondrocyte senescence (Henrotin et al., 2005). Further evidence comes from a greater SOD activity in OA synovial fluid, which as an inducible enzyme would suggest there are higher radical levels (Ostalowska et al., 2006). IL-1β is known to deregulate cellular ROS defences (Mathy-Hartert et al., 2008). ROS are also associated with sites of inflammation as they are produced in the oxidative burst associated with phagocytosis (Afonso et al., 2007), and it is therefore likely that ROS have a role in maintaining the synovitis in OA.

Another radical produced in cells is nitric oxide ($NO^{\cdot}$), which is a reactive nitrogen species that has an important role in cellular signalling. Nitric oxide is produced by the enzyme nitric oxide synthase (NOS), which has three isoforms: endothelial (eNOS), neuronal and inducible (iNOS).

Chondrocytes express both eNOS and iNOS (Henrotin et al., 2005). TNF-α and IL-β have been found to cause overexpression of iNOS in chondrocytes (Henrotin et al., 2005), with IL-1β being more potent (Mazzetti et al., 2001). Mechanical stress also induces NO production (Henrotin et al., 2005). These factors lead to increased levels of NO in osteoarthritis. NO has been found to inhibit collagen and proteoglycan synthesis (Henrotin et al., 2005, Mazzetti et al., 2001); activate MMPs (Mazzetti et al., 2001); induce chondrocyte apoptosis (Nesic et al., 2006, Mazzetti et al., 2001, Goldring and Berenbaum, 2004); cause matrix stiffness and brittleness (Nesic et al., 2006); and cause

insensitivity to the anabolic effects of IGF-1 (Henrotin et al., 2005). There is some evidence that ROS may be more important in RA and that NO is more important in OA (Mazzetti et al., 2001).

1.3.8 Synovial Fluid

The major change seen in osteoarthritic synovial fluid is a reduction in concentration and mass of hyaluronic acid (Volpi et al., 2009). HA in OA is generally found at a concentration of 0.5-1.2 mg/ml (Praest et al., 1997, Yoshida et al., 2004), compared to around 3.6mg/ml in a healthy joint. The molecular weight of HA in healthy individuals is around 7 MDa weight average (M_w), and around 2 MDa number average (M_n) (Dahl et al., 1985). In OA these values are reduced to a molecular weight of around 5 MDa M_w, and around 0.5 MDa M_n (Dahl et al., 1985). The difference in these changes is caused by changes in the weight distributions of HA. There is a reduction in the number of the largest HA molecules and a large increase in smaller fragments (Dahl et al., 1985). There is also a high variation in HA distributions between patients.

There are a number of potential explanations for these changes in OA. Firstly it has been found that the expression of hyaluronic acid synthase-2 (HAS-2) is reduced in OA (Momberger et al., 2005, Volpi et al., 2009, Bastow et al., 2008). HAS-3 has been found to be upregulated by IL-1β and TNF-α (Volpi et al., 2009), but it produces lower weight HA (around 200kDa) and so would contribute to the reduced molar mass (Volpi et al., 2009). Also the level of hyaluronidase enzyme HYAL-2 is increased in OA (Yoshida et al., 2004).

ROS are also capable of breaking down HA, but the contribution of ROS to HA degradation is not well known (Volpi et al., 2009). In OA ROS levels are increased and cellular ROS defences are depleted, so it is therefore likely that ROS do make a significant contribution to HA degradation (Stern et al., 2007, Afonso et al., 2007, Nagaya et al., 1999).

Increases in the volume of synovial fluid also occur in OA, but the magnitude of this change varies widely between patients. Volumes of synovial fluid have been found to range from just above normal to over 20 ml in some cases (Dahl et al., 1985, Balazs, 2009). Synovial inflammation increases the vascular permeability which causes a dilution of synovial fluid and allows proteins to enter more easily. Protein levels in inflamed joints are between 30 to 70% of those in plasma, compared to around 30% normally (Burt et al., 2009). This also leads to an increase in the relative abundance of globulins in OA synovial fluid (Larsen et al., 2008).

These changes in synovial fluid act to drastically alter its properties. Healthy synovial fluid acts as a lubricating fluid at low shear rates but forms an elastic shock absorbing solid at higher shear rates (Gerwin et al., 2006, Mensitieri et al., 1995). In osteoarthritic synovial fluid these shock absorbing properties are lost, and these changes can be seen clearly in the rheology of the fluid, as shown in Figure 1-4. In healthy fluid at low frequencies of shear stress the G″ (representing liquid properties) exceeds the G′ (representing solid properties) and synovial fluid is liquid. At higher frequencies, which occur during physical

exercise, the G′ exceeds the G″ meaning that the elastic properties dominate and it acts as a solid shock absorber. The cross-over point between G′ and G″ shift to higher frequencies with age and OA. These frequencies come to exceed those naturally found (Balazs, 2009, Mensitieri et al., 1995). In OA the shock absorbing properties are lost, reducing the protective mechanisms in the joint and leading to an increase in damage.

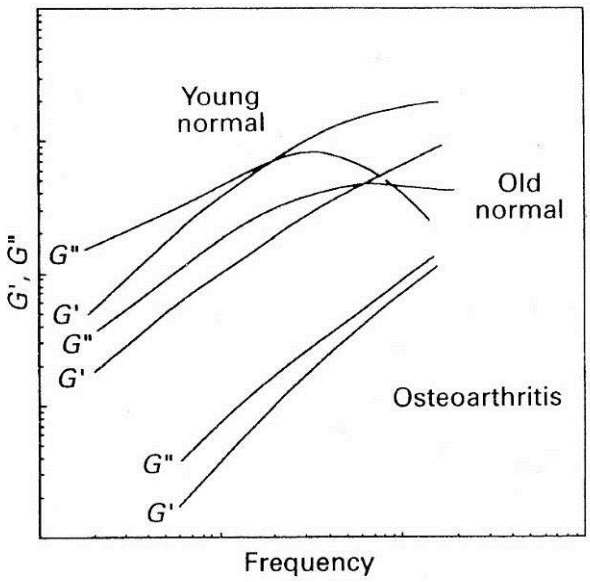

Figure 1-4 Rheology frequency sweeps of healthy, aged and osteoarthritic synovial fluid. Reproduced with kind permission from Springer Science and Business Media: (Mensitieri et al., 1995) © 1995 Chapman and Hall

1.3.9 Osteophytes, Subchondral Bone Sclerosis and Capsular Fibrosis

1.3.9.1 Osteophytes

Osteophytes are aberrant growths of new bone thought to occur in an attempt to stabilise the degenerating joint. Their formation is driven by overexpressed anabolic cytokines. Exogenous application of TGF-β and BMP-2 (bone morphogenetic protein-2) caused osteophyte formation (Aigner et al., 2006, van Lent et al., 2004) showing that these cytokines are key mediators.

Osteophyte development starts with mesenchymal precursor cells following normal processes that occur during development to produce a structure that resembles adult articular cartilage (Aigner et al., 2006). However there are differences as osteophytes show no distinct transition between calcified and non-calcified cartilage and have a more random cell organisation. These factors suggest that the new tissue lacks the mechanical properties of the original.

The fact that OA is a disease of the whole joint is highlighted by the fact that the depletion of synovial macrophages prevents osteophyte formation (van Lent et al., 2004). This shows that synovial cells play an essential role in this process, which could be due to synthesis and secretion of BMP-2 and BMP-4 (Sellam and Berenbaum, 2010, van Lent et al., 2004, Blom et al., 2004).

1.3.9.2 Subchondral bone sclerosis

Subchondral bone sclerosis is a thickening and remodelling of the underlying bone (Aigner et al., 2006). There is some debate as to whether this remodelling acts as an effect (as is generally accepted) or is a cause of changes in cartilage (Aigner et al., 2006, Goldring and Goldring, 2007, Ge et al., 2006). Changes in the subchondral bone are evident in the early stages of osteoarthritis. Greater and more significant changes are seen in more developed OA focused below areas of cartilage destruction and include sclerosis, necrosis, formation of subchondral cysts and fibrosis in bone marrow (Aigner et al., 2006, Dijkgraaf et al., 1995). Where a total destruction of the cartilage has occurred, the bone plate becomes exposed and this can allow synovial fluid to enter the bone and

access the bone marrow. The synovial fluid induces changes in mesenchymal precursor cells and leads to the development of cartilage 'tufts' (Aigner et al., 2006, Buckwalter and Martin, 2006).

1.3.9.3 Capsular fibrosis

Capsular fibrosis can occur in late stage osteoarthritis and is a thickening of collagen within the joint capsule, which is the structure that surrounds the joint to stabilise it. Capsular fibrosis is often responsible for the reduction in joint motion that occurs in osteoarthritis (Aigner et al., 2006).

1.3.10 Vicious Cycle

Advanced OA develops into a situation where a vicious cycle propagates and maintains the disease (Sofat, 2009). Matrix fragments in synovial fluid lead to the activation of chondrocytes and synoviocytes, causing the production of various factors such as TNF-α, IL-1β and hydrolytic enzymes (Benito et al., 2005, Page Thomas et al., 1991, Sellam and Berenbaum, 2010). This is supported by evidence that collagen fragments upregulate chondrocyte expression of MMP-2, MMP-9 and MMP-13 (Fichter et al., 2006); Cathepsins B, L and K (Ruettger et al., 2008); IL-1β, IL-6 and IL-8 (Klatt et al., 2009). These soluble factors cause further cartilage damage, releasing more fragments and thus propagating the cycle. The cycle can be further enhanced by the autocrine action of TNF-α and IL-1β (Sadouk et al., 1995).

1.4 Drug Treatments for Osteoarthritis

1.4.1 Current Treatments

A number of drug treatments are currently used against osteoarthritis, but none are able to cure this disease and reverse the joint damage. Current treatments focus on providing symptomatic relief by reducing pain as well as maintaining and increasing joint mobility. This reduces disability and improves the quality of life of sufferers. Disease modifying drugs, known as DMOADs (disease-modifying OA drugs) have been, and continue to be, the subject of extensive research and more details on these are given in a following section.

A number of non-pharmacological treatments are used for the treatment of osteoarthritis, including weight loss, exercise, transcutaneous electrical nerve stimulation, acupuncture and nutraceuticals (National Collaborating Centre for Chronic Conditions, 2008). Nutraceuticals are food supplements with potential health effects, but there is no evidence of any efficacy of these in OA.

The most common first line treatments for osteoarthritis are paracetamol and a topical non-steroidal anti-inflammatory drug (NSAID). Paracetamol is preferred to an oral NSAID due to its better long term safety profile, particularly in relation to the gastric tract. If these treatments are not sufficient to relieve pain then an oral NSAID or cyclooxygenase (COX-2) inhibitor is usually considered. Further treatments include intra-articular steroids or hyaluronic acid. Opioids are used only when other treatments have failed or are contraindicated. Capsaicin (the chemical that gives chilli peppers their ‘heat’) is an alternative topical treatment that provides pain relief.

When all other treatments have been considered surgical options are available. A variety of surgical treatments have been used to treat osteoarthritis. These range from joint lavage to attempted joint repair to total joint replacement. Joint replacement has been shown to be a very effective last resort treatment and over 55,000 hip replacements were carried out in 2006/7 to treat osteoarthritis (National Collaborating Centre for Chronic Conditions, 2008).

1.4.2 Intra-articular Delivery for Osteoarthritis

1.4.2.1 Current treatments

Intra-articular (IA) delivery is an attractive delivery route for OA and is currently utilised in main line therapy. OA is not a systemic disease and affects individual joints; therefore this form of local delivery targeted to joints where drug is needed reduces systemic exposure and side effects. The reduction of side effects is particularly important for OA as it is a chronic disease so there is a need for well tolerated long term treatments (Gerwin et al., 2006). Intra-articular delivery avoids problems associated with other administration routes.

Various steroid and hyaluronic acid formulations are approved for administration by IA injection (Gerwin et al., 2006). Corticosteroids are anti-inflammatory drugs used to treat a wide variety of diseases and for OA provide relief from pain and inflammation. The chronic systemic administration of steroids can lead to severe side effects, such as diabetes, hypertension, glaucoma and cataracts. Therefore systemic delivery of these drugs is not used in OA and they are administered by IA injection (National Collaborating Centre for Chronic Conditions, 2008). Corticosteroids formulated as solutions

(e.g. dexamethasone phosphate) are rapidly removed from the synovial cavity. They have half-lives of only a couple of hours (Larsen et al., 2008) and are completely cleared within 5 days (Bias et al., 2001). Despite this rapid clearance, trials have found they can reduce pain for up to 4 weeks (Bellamy et al., 2005a).

Suspension formulations (e.g. dexamethasone acetate, triamcinolone acetonide) have been used to increase the retention time of corticosteroid drugs within the joint (Derendorf et al., 1986). These suspensions are composed of drug crystals and only give a slight increase in retention time as they simply rely on their limited solubility (Bias et al., 2001, Derendorf et al., 1986). Crystals cause irritation or inflammation in the joint and they can even cause cartilage damage. Gout and pseudogout are known as crystal induced arthritis. Corticosteroid suspension formulations therefore have a closely controlled crystal size (around 20μm) to reduce the risk of damage (Derby et al., 2008).

A Cochrane review on steroid injections for knee osteoarthritis concluded that there was proof of a reduction in pain for up to 3 weeks (Bellamy et al., 2005a). The effectiveness of this treatment has also been shown in other joints such as the ankle (Ward et al., 2008). The risks associated with intra-articular administration have led the American College of Rheumatology to recommend a minimum of 3 months between intra-articular corticosteroid injections (Butoescu et al., 2009a, Clouet et al., 2009). In the UK corticosteroid injections are recommended only as an adjuvant therapy in moderate to severe pain (National Collaborating Centre for Chronic Conditions, 2008).

The other major intra-articular treatment for osteoarthritis is hyaluronic acid. This treatment was first proposed in the 1970s (Rydell and Balazs, 1971). The rationale was to restore the natural protective viscoelastic properties of synovial fluid which are lost in osteoarthritis, which has led to this treatment also being known as viscosupplementation. A number of HA preparations for IA injection are marketed and these have various molecular weights. There are also a number of cross linked preparations available. A summary of different hyaluronic products for osteoarthritis is given in Table 1-1.

Trade Name	Molecular weight (kDa)	Cross-Linking	Manufacturer
Hyalgan®	500-730	No	Fidia (Italy)
Artz®/ Supartz®	600- 1,200	No	Seikagaku (Japan)
Othrovisc®	1,000 -2,900	No	Anika Therapeutics (USA)
Euflexxa®	2,400-3,600	No	Ferring Pharameuticals (USA)
Fermathron®	1,000 average	No	Biomet (Belgium)
Synvisc-One® (Hylan GF-20)	6,000 average	Yes	Genzyme (USA)
Monovisc®	High	Yes	Anika Therapeutics (USA)
Durolane®	N/A	Yes	Q-Med (Sweden)
Gel-One®	N/A	Yes	Seikagaku (Japan)

Table 1-1 Marketed intra-articular hyaluronic acid treatments.
Information on cross-linking taken from (Prestwich and Kuo, 2008).

A Cochrane review on viscosupplementation in the knee found similar benefits to NSAIDs and a prolonged effectiveness compared to corticosteroids for up to 13 weeks (Bellamy et al., 2005b). This period of effectiveness is despite the rapid clearance of HA, which is not quite as fast as the clearance of small molecules. For example Hyalgan has a half-life of 17 hours and the high molecular weight component of Synvisc has a half-life of around 9 days in the

joint (Brandt et al., 2000). HA injections are not available on the National Health Service in the UK due to the costs of this treatment (National Collaborating Centre for Chronic Conditions, 2008).

There is *in vitro* evidence that HA has anti-inflammatory and chondroprotective effects (Moreland, 2003). With these effects there could be a disease modifying effect of HA; however clinical trials have found no such effect (Pelletier and Martel-Pelletier, 2007).

1.4.2.2 Challenges for intra-articular delivery

Intra-articular administration has a number of challenges. One of the greatest is the rapid clearance that occurs from the synovial cavity. Molecules that are smaller than around 500 Daltons have a half-life of around an hour in the joint (Larsen et al., 2008). This rapid clearance can be seen in the fact that after intra-articular injection drug can be detected in blood plasma within an hour (Bias et al., 2001). Larger molecules are resident for longer but are still cleared within a few hours (Larsen et al., 2008).

Intra-articular delivery is a physically tricky route for administration. Even with experienced practitioners there is the risk of infection or that the injection will be incorrectly sited. The correct localisation of injections can be ensured by using imaging techniques (Schumacher, 2003), however this increases the cost and complexity. Aspiration of synovial fluid before IA injection is an easier way to ensure correct localisation and is beneficial as it reduces oedema in the joint, reducing the pressure and discomfort (Schumacher, 2003, Jones et

al., 1993). Good sterile practice and avoidance of injecting through inflamed skin can reduce the risk of infection to acceptable levels (Jones et al., 1993, Gerwin et al., 2006). These challenges mean that it is recommended to limit the frequency of administration by intra-articular injection, which creates a currently unmet need for sustained release formulations (Burt et al., 2009).

1.4.2.3 Drug delivery systems for intra-articular delivery

Various advanced drug delivery systems for intra-articular delivery have been investigated. A summary of systems is given in Table 1-2 and includes nanoparticles, microspheres and liposomes. These systems have followed four main methods to improve drug delivery. The first was to target the system for uptake by synovial macrophages to avoid release to the systemic circulation. The other three methods attempt to provide a sustained drug release. Firstly this was achieved by increasing the residence time in synovial fluid, which in the majority of cases was done by using particles too large to be taken up by phagocytosis. The other two methods were to produce systems that adhere to or penetrate the cartilage matrix or the synovium. The most interesting systems and results are described in more detail below.

Intra-articularly administered liposomes are taken up by phagocytosis (Blom et al., 2007, Bias et al., 2001). One intra-articular liposome formulation under the trade name of Lipotalon® has been approved for use in human therapy in Germany. It consists of dexamethasone 21-palmitate in lecithin coated vesicles of around 200nm in diameter (Bias et al., 2001). This liposome therapy can

cause a reduction in pain for 28 days, but the drug is not detected in serum beyond 5 days (Bias et al., 2001).

Particulate based drug delivery systems for intra-articular delivery have focused mainly on microparticles designed to avoid phagocytosis through their size. Studies have shown that the size limit for phagocytosis in the joint is around 10 to 15μm (Butoescu et al., 2009b, Liggins et al., 2004, Greis et al., 1994). Latex particles of 15μm were sparingly taken up by a minority of cells and 45μm particles were not taken up at all (Greis et al., 1994).

Various materials used in the production of particles have been found to be compatible in the joint; PLGA (poly(lactic-co-glycolic acid)) (Burt et al., 2009, Mountziaris et al., 2010), PLLA (poly(L-lactic acid)) (Burt et al., 2009, Ratcliffe et al., 1984), and albumin (Burt et al., 2009, Ratcliffe et al., 1984) were all well tolerated within the joint. Some materials are not well tolerated, for example certain synthetic materials caused collagenase synthesis which would lead to further joint damage (Greis et al., 1994). Injected particles have been found in general to penetrate or associate to the synovium (Ratcliffe et al., 1987, Burgess and Davis, 1988, Mountziaris et al., 2010).

Other approaches have been used to increase residence time in the joint. One example is a system containing magnetic iron nanoparticles that were retained in the joint using magnets (Schulze et al., 2005). Another system used cartilage adhesive nanoparticles (Rothenfluh et al., 2008). These particles used a cartilage binding peptide and 38nm particles were found to penetrate and bind

the cartilage matrix (Rothenfluh et al., 2008), however the particles were only followed for 96 hours *in vivo* and there was no investigation with any drug.

Some more complex systems have also been investigated and are included at the end of Table 1-2. These include a system described as lipogelosomes, which contained liposomes within a carboxymethyl cellulose (CMC) hydrogel (Turker et al., 2005), but this system gave only a moderate increase in retention time. Another system used elastin-like polymers that thermally aggregate to form a depot after injection (Betre et al., 2006), however this system has not yet been loaded with drug.

System	Materials	Drug	Size	Results	References
Nanoparticles	PLGA	Betamethasone phosphate	300-500nm	*In vitro* release over 20 days, 21 day reduction in inflammation in rabbits	(Horisawa et al., 2002a)
Nanoparticles	PVA Iron NPs	Fluorescent label	Undefined	External magnets used to retain particles in joint	(Schulze et al., 2005)
Nanoparticles	PPS and Pluronic F127 with collagen binding peptide	Fluorescent label	38nm or 96nm	36nm penetrate cartilage and are retained, 96nm are held in cartilage surface layers	(Rothenfluh et al., 2008)
*Nanoparticles	PEG-PLGA	Betamethasone phosphate	51 - 178nm	Inflammation reduced for 9 days in rats	(Ishihara et al., 2009)
Nano/microparticles	PLGA	Fluorescent label	265nm/25µm	Nanospheres phagocytosed, Microparticles adhere to synovial membrane surface	(Horisawa et al., 2002b)
Microparticles	PLA, PBCA, gelatin or albumin	None	1 - 10µm	Albumin well tolerated in rabbits, Others caused some inflammation	(Ratcliffe et al., 1984)
Microparticles	PLGA Iron oxide NPs	Dexamethasone	1 or 10µm	Taken up by phagocytosis, No inflammation in joint	(Butoescu et al., 2009)

System	Materials	Drug	Size	Results	References
Microparticles	PDLLA	Dexamethasone	40-60µm 90-110µm	*In vitro* release over 10 days, Drug recovered from particles after 7 days in joint	(Ramesh et al., 1999)
Microparticles	Albumin	Prednisolone Triamcinolone	23µm	Release in rabbit joint over 10 days, Particles located to synovium surface not phagocytosed	(Burgess and Davis, 1988)
Microparticles	Albumin	Radiolabel	3.5µm	Release in joint over 7 days, Particles localise to synovium	(Ratcliffe et al., 1987)
Microparticles	PDLLA	Fluorescent label	Under 20µm 20 - 100µm	All microspheres localised to fat, Particles degrade in 5 to 14 days depending on polymer mw in rabbit, No inflammation in joint	(Nishide et al., 1999)
Microparticles	PLGA Albumin	Naproxen	PLGA 9µm Albumin 10µm	*In vitro* release over 5 days for PLGA and 8 hours for albumin	(Bozdag et al., 2001)
Microparticles	Gelatin and Chondroitin sulfate	Proteins	10µm	*In vitro* release over 48 h, Non inflammatory	(Brown et al., 1998)
Microparticles	Albumin	Diclofenac	15µm	*In vitro* release over 7 days	(Tuncay et al., 2000b)

System	Materials	Drug	Size	Results	References
Microparticles	PLGA	Diclofenac	5 - 10µm	*In vitro* release over 5 days	(Tuncay et al., 2000a)
Microparticles	Chitosan	Celocoxib	8 - 12µm	*In vitro* release over 5 days, Anti-inflammatory in rats over 18 days	(Thakkar et al., 2004a)
Microparticles	Chitosan	Celecoxib	8 - 16µm	*In vitro* release over 4 days, Celocoxib detected in blood for over 24h	(Thakkar et al., 2004b)
*Microparticles	Gelatin	Diclofenac	37 - 46µm	*In vitro* release over 30 days	(Saravanan et al., 2011)
*Microparticles	Gelatin	Flubioprofen	3 - 12µm	*In vitro* release over 24 hours, MRT in rabbit joint increase 10 fold	(Lu et al., 2007)
*Microparticles	PLGA	Paclitaxel	50µm	Increased transynovial fluid flow in horse, Minimal inflammation seen	(Bragdon et al., 2001)
*Microparticles	PLGA PLLA	Paclitaxel	10-35µm 35-105µm	*In vitro* release over 28 days, Reduced inflammation in rabbit	(Liggins et al., 2004)
*Microparticles	PLLA	Methotrexate	77µm	*In vitro* release over 24h, No difference in plasma compared to free drug	(Liang et al., 2005, Liang et al., 2004)
*Microparticles	PLLA	Radionuclide	2 - 13µm	High retention in rabbit joints over 5 days, No uptake to lymph nodes	(Mumper et al., 1992)

System	Materials	Drug	Size	Results	References
**Microparticles	PLGA	Fluorescent label	20μm	Particles retained in synovial lining and well tolerated in rats	(Mountziaris et al., 2010)
**Microparticles	PLGA	siRNA PEI	29 - 34μm	*In vitro* release over about 14 days	(Mountziaris et al., 2011)
Liposomes	Lipid with HA or collagen	Dexamethasone Diclofenac	Undefined	Bioadhesive liposomes, Reduced inflammation in rats over 17 days	(Elron-Gross et al., 2009)
*Liposomes	Mixed lipids	Triamcinolone acetonide 21-palmitate	Undefined	Prolonged retention in joint compared to free drug over 24 hours	(Lopez-Garcia et al., 1993)
*Liposomes	Mixed lipids	Cortisol 21-palmitate	Undefined	Anti-inflammatory effect for 14 days in RA patients	(Silva et al., 1979)
*Liposomes	Mixed lipids	Clodronate	160 - 180nm	Anti-inflammatory and protected cartilage in rabbit arthritis model with weekly injections	(Monkkonen et al., 1995) (Ceponis et al., 2001)
*Liposomes	PC and cholesterol	Clodronate	120 - 160nm	Macrophage depletion in RA patients.	(Barrera et al., 2000)
*Liposomes	Various lipids	Lipid conjugated methotrexate	1.2μm	Anti-inflammatory effect for 21 days	(Williams et al., 1996)

System	Materials	Drug	Size	Results	References
Hydrogel microparticles	Gelatin	bFGF	70μm	Retention in rabbit joint over 7 days	(Inoue et al., 2006)
*Lipogelosomes	Liposomes in CMC gel	Radiolabel	250nm	*In vitro* release over 2 days, Half-life in joint of over 24h	(Turker et al., 2005)
Hydrogel	Calcium alginate	TGF-β	Undefined	*In vitro* release over 5 days	(Mierisch et al., 2002)
*Hydrogel	HA-tyramine H_2O_2 and HRP	Dexamethasone	Undefined	*In vitro* and *in vivo* release over 28 days, Reduction in cytokine levels.	(Kim et al., 2011)
Thermal aggregates	Elastin-like polypeptides	None	Undefined	Aggregating polymer was retained in joint 25 times longer than non-aggregating	(Betre et al., 2006)
In situ precipitates	Modified peptides	None	Undefined	Peptides precipitate in water to form depot	(Pedersen et al., 2011)

Table 1-2 Intra-articular drug delivery systems.
* designates system that was designed for RA ** designates system that was designed for temporomandibular joint disorders. Abbreviations used in table: bFGF- basic fibroblast growth factor; CMC- carboxymethyl cellulose; HA- hyaluronic acid; HRP- horseradish peroxidise; MRT- mean retention time; mw- molecular weight; NP- nanoparticle; PBCA- poly(butylcyanoacrylate); PC- phosphatidylcholine; PDLLA- poly(DL-lactic acid); PEG- (poly(ethylene glycol); PEI- poly(ethyleneimine); PLA- poly(lactic acid); PLGA- poly(lactic-co-glycolic acid); PLLA- poly(L-lactic acid); PPS- poly(propylene sulphide); PVA- poly(vinyl alcohol); RA- rheumatoid arthritis; siRNA- small interfering ribonucleic acid; TGF β- transforming growth factor-beta.

1.4.3 Disease Modifying Drugs for Osteoarthritis

Currently there are a lack of treatments for osteoarthritis that have a disease modifying effect (DMOAD) either by slowing disease progression or reversing changes that have already occurred. The effectiveness of any DMOAD could also be increased by earlier diagnosis and treatment (Qvist et al., 2008). OA is generally diagnosed once significant changes have occurred within the joint. Improvements in imaging techniques such as MRI (magnetic resonance imaging) (Burstein, 2006), or the identification of suitable biomarkers would allow for improved early diagnosis of OA (Pollard et al., 2008).

1.4.3.1 DMOAD potential of current treatments

There has been evidence that some current treatments can have a disease modifying effect. For example *in vitro* corticosteroids have been shown to inhibit production of IL-1, TNFα and iNOS (Pelletier et al., 2001, Tung et al., 2002). Reductions in these key cytokines have the potential to exert a disease modifying effect, however clinical trials have found no evidence of this. A similar situation has been found with NSAIDs (Jiang et al., 2010).

Effectiveness in OA animal models has often not translated to success in clinical trials. The animal models used may be partly to blame for this, as OA models mostly focus on recreating the cartilage damage seen (Bonnet and Walsh, 2005) and ignore the contributions of other structures within the joint.

It is also challenging to prove a disease modifying effect in OA clinical trials. The regulatory guidelines to establish DMOAD efficacy are primarily focused

on joint space narrowing (JSN) (Hogenmiller and Lozada, 2006). JSN has a high deviation between patients (Le Graverand-Gastineau, 2010) but changes very slowly; the average change is 0.1mm/year (Hogenmiller and Lozada, 2006). This slow change can lead to control groups undergoing such a small progression that it is not possible for a statistically significant improvement to be seen (Le Graverand-Gastineau, 2010). To overcome these problems clinical trials using JSN need large numbers of subjects and a long time frame, both of which increase costs (Le Graverand-Gastineau, 2010). Advances in MRI imaging techniques allow detailed imaging of the joint and give hope that more accurate measurements can be used in the future (Burstein, 2006).

1.4.3.2 Novel DMOADs

Novel DMOADs have targeted a number of systems, and include inhibitors of MMPs, iNOS, Cathepsin K and cytokine signalling. The recent history of DMOADs has been dominated by failed drugs.

A good example of this is the field of MMP inhibitors (MMPi). These drugs have the potential to treat a number of diseases and have been the focus of much research. Safety problems have caused the termination of some clinical trials, with the main problem having been unexplained muscle pain (Cawston and Wilson, 2006). In other trials the *in vitro* promise has again failed to translate to benefits in clinical trials (Catterall and Cawston, 2003, Rengel et al., 2007). The search for MMP inhibitors continues due their huge therapeutic potential, and novel strategies are being pursued to produce more specific inhibitors. In OA, MMP-13 is an obvious target due its high expression and

novel specific MMP-13 inhibitors have been produced (Johnson et al., 2007, Li et al., 2011).

Interfering in cytokine signalling is another approach that has been investigated and can be achieved in a number of ways including using neutralising soluble factors, receptor blockade or blocking intercellular signalling pathways. TNF-α neutralising antibodies have been successful in the treatment of RA, but have caused little or no improvement in OA trials (Qvist et al., 2008). Blockade of the IL-1 receptor with the drug anakinra is utilised for the treatment of RA, but clinical trials in knee OA found no significant benefit (Clouet et al., 2009, Qvist et al., 2008, Chevalier et al., 2009).

Potential drugs with DMOAD activity are currently undergoing clinical trials. Pfizer currently has an inhibitor of iNOS (SD 6010) in phase II trials with results due in 2012. Medivir has two candidate cathepsin K inhibitors (MIV-710 and MIV-711) in preclinical development. Compounds with aggrecanase inhibitory activity are also in preclinical development (Le Graverand-Gastineau, 2010, De Rienzo et al., 2009, Shiozaki et al., 2011). OA is a complex disease and it is likely that MMPs, aggrecanases and cathepsins are all involved in the degradation seen (Nagase and Kashiwagi, 2003). It may prove that combinations of inhibitors are required for successful therapy.

A number of biological molecules with potential DMOAD action have been identified. These include the anti-inflammatory cytokines IL-10 (Pelletier et al., 2001) and IL-6 (Sellam and Berenbaum, 2010); as wells as osteogenic

protein 1 (Le Graverand-Gastineau, 2010); human growth hormone (Dunn, 2010); BMP-7 (Hayashi et al., 2010); and lubricin (Le Graverand-Gastineau, 2010, Bao et al., 2011).

1.4.3.3 DMOAD potential of other drugs

Drugs for other conditions have been investigated for potential DMOAD activity, for example some drugs have been found to have MMP inhibitory activity. Tetracyclines were developed as antibiotics but have been found to possess MMP inhibitory activity (Pelletier et al., 2001, Catterall and Cawston, 2003). This inhibition is thought to be due to the ability of the tetracyclines to chelate the zinc in the MMP active site (Pelletier et al., 2001). Doxycycline hyclate is the only current FDA (Food and Drug Administration) approved MMPi treatment and is used for peridontitis (Catterall and Cawston, 2003, Li et al., 2011).

For osteoarthritis minocycline and doxycycline have been shown to inhibit expression of MMP-1, MMP-3, aggrecanases and iNOS in chondrocytes and synoviocytes (Pelletier et al., 2001). However the only clinical trial undertaken has led to doxycycline not being recommended for OA treatment as it showed a minimal effect that was outweighed by safety concerns (Nuesch et al., 2009).

Bisphosphonates were first used as a bone protective therapy (Catterall and Cawston, 2003). Tiludronate has been shown to inhibit MMP-1 and MMP-3 (Catterall and Cawston, 2003). Intra-articularly delivered clodronate loaded liposomes deplete the synovial macrophages and cause reductions in

expression of IL-1β, TNF-α, NO, MMP and cartilage damage (Barrera et al., 2000, Blom et al., 2007, van Lent et al., 2004, Monkkonen et al., 1995, Ceponis et al., 2001). A clinical trial for clodronate in knee OA found it give a similar level of symptomatic relief as intra-articular HA (Rossini et al., 2009), however no assessment of DMOAD activity was made.

Calcitonin is a thyroid hormone involved in calcium and phosphorous homeostasis which inhibits osteoclast bone resorption leading to its use as a treatment for osteoporosis (Le Graverand-Gastineau, 2010, Sondergaard et al., 2010). It has also been shown to have chondroprotective properties in animal models (Qvist et al., 2008, Sondergaard et al., 2010, Karsdal et al., 2006). Two phase III trials for knee OA using oral formulations of salmon calcitonin are currently under way with results due shortly (Le Graverand-Gastineau, 2010, Qvist et al., 2008, Holm-Bentzen et al., 2010).

1.5 Plan for Delivery System

At the outset of this project the aim for this thesis was to investigate advanced delivery systems for osteoarthritis, with a focus on a targeted or environmentally activated delivery. Intra-articular injection is an established delivery route for osteoarthritis (Gerwin et al., 2006). It is a form of local delivery and therefore has a level of targeting by drug only being administered to diseased joints. However this delivery route has a number of challenges that are yet to be overcome (Burt et al., 2009). An advanced delivery system could therefore improve the efficacy of this delivery route for osteoarthritis.

The main challenge is the rapid clearance experienced from the synovial cavity. Also the American College of Rheumatology guidelines recommend a period of at least three months between IA steroid administrations. Together these factors have led to an unmet need for sustained release formulations. A delivery system that provided drug release over a three month period would improve the therapy available for osteoarthritis. This period is far greater than has currently been achieved (Kim et al., 2011).

The period of delivery desired in this project exceeds what is possible from a particle based delivery systems and is also unlikely to be achieved with a hydrogel directly retaining drug. This project will therefore investigate an injectable hydrogel that contains a nanoparticle drug delivery system. The hydrogel will retain the nanoparticle system within the joint and allow a sustained release to occur over three months.

1.6 Introduction to Hydrogels and Injectable Hydrogels

1.6.1 Hydrogels

Hydrogels are defined as colloidal gels where water is the dispersion medium, or as swollen macromolecular networks in water (Berger et al., 2004). Hydrogels can be formed by many substances but for this project only polymer hydrogels will be considered. Hydrogels have an extremely high water content of up to 99% and can vary from rigid to quite liquid-like (Hoffman, 2002). Hydrogels can be stabilised by physical and chemical means, including covalent cross linking, ionic bonding, hydrogen bonding, amphipathic stabilisation or by forming an interpenetrating network (IPN) (Hoffman, 2002).

IPNs are a strongly entangled combination of two polymers both in individual networks (Sperling and Mishra, 1996).

Of particular interest in this project are injectable hydrogel systems and polyelectrolyte complexes, which can produce resilient hydrogels. These systems will both be introduced in more detail below.

1.6.2 Injectable Hydrogels

To allow administration of the proposed delivery system an injectable hydrogel is required. The most common approaches that have been investigated for producing injectable hydrogels are *in situ* polymerisation (Jagur-Grodzinski, 2010, Yu and Ding, 2008), *in situ* cross-linking (Jagur-Grodzinski, 2010, Yu and Ding, 2008) and stimuli responsive polymers (Yu and Ding, 2008, Alexander and Shakesheff, 2006, Bajpai et al., 2008). Other approaches include the co-injection of polymers to form an IPN (Barbucci et al., 2010), stereocomplexation between different enantiomers (Jeong et al., 2002) or the action of enzymes to produce hydrogels (Chen et al., 2003).

Chemical methods for the *in situ* polymerisation and *in situ* cross-linking have issues with biocompatibility. Polymerisation methods have focused on free radical polymerisations initiated by photosensitive or thermally sensitive initiators (Yu and Ding, 2008, Jeong et al., 2002). Cross-linking methods require additional cross linking agents or the use of polymers with highly reactive groups (Hoffman, 2002). All of these have the potential to cause damage in the body and so their biocompatibility is questionable.

Polymers that are responsive to many stimuli have been synthesised, including pH, temperature and ionic conditions. To produce an injectable system an obvious stimulus to utilise is temperature. A number of thermogelling polymers have been investigated, which include natural polymers such as cellulose derivatives (Ruel-Gariepy and Leroux, 2004), and synthetic polymers such as Pluronics (Ruel-Gariepy and Leroux, 2004, Yu and Ding, 2008), PLGA (Ruel-Gariepy and Leroux, 2004), PEG-PLGA (Yu and Ding, 2008), PNIPAM (poly(N-isopropylacrylamide)) (Jagur-Grodzinski, 2010, Ruel-Gariepy and Leroux, 2004).

1.6.3 Polyelectrolyte Complexes

1.6.3.1 Introduction to polyelectrolyte polymers

The term polyelectrolyte is applied to any polymer that has an ionisable group within its repeating unit. In aqueous solution polyelectrolytes undergo dissociation, which can be full or partial, to give repeating charges. It is possible for a polyelectrolyte to have mixed positive and negative charges on a single polymer chain.

Polyelectrolyte solutions have unique properties due to their charges. Neutral polymers tend to have a random coil conformation in solution. The repulsive charges mean that polyelectrolytes often have a more extended and rigid structure. This structure can affect many other properties of the solution such as viscosity. Polyelectrolyte polymers are common in nature; for example nucleic acids contain a repeating phosphate group so are an anionic polyelectrolyte and polypeptides are mixed charge polyelectrolytes.

1.6.3.2 Polyelectrolyte complexation

Mixing polymer solutions often results in immiscibility and phase separation (Harding et al., 1995). Phase separation can result from a segregation of the polymers into the different phases or the collection of the polymers into a polymer rich phase (Harding et al., 1995). The mixing of different polyelectrolyte solutions is no different and phase separation is common. This study will focus on complexation between oppositely charged polyelectrolytes.

The mixing of oppositely charge polyelectrolyte solutions results in the formation of a polymer rich phase. This is caused by attractions between the polymers and can be described as associative phase separation or complex coacervation (Harding et al., 1995). Strong electrostatic interactions between oppositely charged polymers promote their association. However the close association of polymer chains restricts movement and causes an entropic barrier. The association of polymers also causes the release of associated counterions which become free to move. There are many of these ions and so the increase in their entropy balances the losses from polymer association (Harding et al., 1995).

Phase separation can form different structures under different conditions. When there is a low overall charge in solution an insoluble polyelectrolyte complex network can form (Berger et al., 2004, Hamman, 2010). At high overall charge, such as when there is a large imbalance in the polymer concentrations, soluble small polyelectrolyte particles can form (Garnett, 1999, Hamman, 2010, Kabanov and Kabanov, 1998, Lee et al., 1997).

Polyelectrolyte particles have been utilised in drug and gene delivery (Garnett et al., 2009, Brown et al., 1998, Wu et al., 2007, Kabanov and Kabanov, 1998).

For the intended application as a slow release delivery system it is desired to form a precipitated polyelectrolyte complex network. These will be referred to as polyelectrolyte complexes through the rest of this thesis. These polyelectrolyte complexes have many similarities to hydrogels, however as they are precipitates they cannot be strictly considered to be hydrogels.

The production and stability of polyelectrolyte complexes is influenced by many different factors, with the most important factor being pH as both polymers must ionised for complexation to occur (Berger et al., 2004). Temperature, the ratio of polymers/charges (Hamman, 2010), molecular weight of the polymers (Hamman, 2010, Harding et al., 1995), polymer charge density (Hamman, 2010) and other ions present (Berger et al., 2004, Harding et al., 1995) can all affect the formation and stability of polyelectrolyte complexes. Salt ions can be highly disruptive to polyelectrolyte complex formation as the ions shield the polymer charges and prevent long range interactions. There is also a reduction in the counterion effect as there are more ions present in solution (Harding et al., 1995). A thorough mixing is required for a good complex formation (Hamman, 2010), and to achieve optimal complex formation mixing needs to be conducted under conditions where interaction does not occur (Berger et al., 2004).

Polyelectrolyte complexes have been found to be generally biocompatible (Lee et al., 1999). Polyelectrolyte complexes have been investigated for a number of applications including as membrane materials for drug release (Berger et al., 2004, Lee et al., 1997); as medical materials for implants (Berger et al., 2004); for the isolation of proteins and nucleic acids (Dumitriu and Chornet, 1998); for wound healing and tissue engineering scaffold materials (Sechriest et al., 1999, Suh and Matthew, 2000).

1.7 Introduction to Nanoparticle Drug Delivery Systems

1.7.1 General Introduction

Colloidal drug delivery systems have been widely investigated for their potential to improve delivery of a variety of drugs. Drugs encapsulated within a colloidal carrier can provide a sustained or targeted drug delivery. There are many systems that fit within the category of colloidal carriers and the most commonly investigated systems are liposomes, polymer micelles and polymer nanoparticles (Johnston et al., 2011). Liposomes are a very successful drug delivery system and a number of liposomal formulations are on the market for cancer treatment (Johnston et al., 2011). Liposomes can however have problems with leakage and long term stability (Johnston et al., 2011). For these reasons a polymeric nanoparticle system was chosen for use in this project and an introduction to these systems is given below.

1.7.2 Nanoparticle Drug Delivery Systems

Particulate drug delivery systems are composed of polymer with drug entrapped within the polymer matrix or adsorbed onto the particle surface.

These particles can be formulated in a variety of sizes, but are generally in the micrometre to nanometre size range. Two key parameters in a particle delivery system are the polymer used and the formation method. These two factors can affect the drug loading and drug release of the particles.

1.7.2.1 Polymers

The polymer used for a drug delivery system must be biocompatible and have no toxic degradation products. A wide range of natural and synthetic polymers have been investigated for particulate systems, with the most common polymers being PLA (poly(lactic acid)), PLG (poly(glycolic acid)) and their copolymer PLGA (poly(lactide-co-glycolide) (Brewer et al., 2011). Many other polymers have also been investigated including poly(caprolactone) (Brewer et al., 2011, Rao and Geckeler, 2011), poly(alkylcyanoacrylate) (Rao and Geckeler, 2011, Cai and Xu, 2011) and poly(orthoesters) (Puri, 2007).

1.7.2.2 Particle preparation

Many methods have been investigated and used for the production of polymeric particles. The two methods most widely used are the emulsification solvent evaporation method and the interfacial deposition method. Other methods that have been used include spray drying, salting out and methods using supercritical carbon dioxide (Rao and Geckeler, 2011).

The emulsification solvent evaporation method uses a water immiscible solvent to dissolve the polymer, which is emulsified into an aqueous phase containing surfactant. The organic solvent is evaporated causing the formation

of small polymer particles. This method was originally described by Beck et al (Beck et al., 1979) and has been widely used since (Rao and Geckeler, 2011). The main drawbacks are that particles cannot be produced without the presence of surfactant and residual organic solvent always remains.

The interfacial deposition method uses a water miscible solvent to dissolve the polymer. This is added drop wise to an aqueous phase in which the polymer is insoluble. The rapid diffusion of solvent into the aqueous phase causes a decrease in interfacial tension, and there is also an increased interfacial surface area due to turbulence from magnetic stirring. Together this causes the formation of small solvent droplets without high speed mechanical mixing. This method has also been widely used and can be used to produce particles with or without surfactant present (Fessi et al., 1989). A disadvantage of this method is that it can give poor entrapment of water soluble drugs due to the accessible aqueous phase (Mishra et al., 2010).

1.7.2.3 Drug loading

The incorporation of drug into polymeric nanoparticles is a key factor for their use as a drug delivery system. A high drug loading level is desirable as a lower amount of nanoparticles will be required to deliver the desired drug dose. There are two methods used to load drug into nanoparticles. The most common is that drug is entrapped whilst the particles are being formed, alternatively drug can be adsorbed to the particle surface after formation.

When investigating drug loading two parameters can be calculated. Encapsulation efficiency refers to the proportion of drug available that is encapsulated within the particles and can be calculated using the formula:

$$\text{Encapsulation efficiency (\%)} = \frac{\text{Mass of drug in nanoparticles}}{\text{Mass of drug used}} \times 100$$

Drug loading refers to the proportion of drug in a particle by mass and can be calculated using the formula:

$$\text{Drug loading (\%)} = \frac{\text{Mass of drug in nanoparticles}}{\text{Mass of nanoparticles}} \times 100$$

Encapsulation efficiency is of most interest in terms of particle manufacture but the drug loading level is a more useful measure therapeutically as it relates to the dose of drug available within nanoparticles. Drug loading is also comparable between different nanoparticle samples.

1.7.2.4 Drug release

Drug release from nanoparticles can occur through a number of mechanisms. Firstly drug can diffuse out of the solid matrix leaving the particles intact (Washington, 1990). A subtly different mechanism involves penetration of release medium into the particles, which dissolves the drug and allows its diffusion into the bulk solution (Washington, 1990). Both these mechanisms are diffusion driven and affected by the surrounding concentration of drug.

The final release mechanism occurs through the degradation of polymer and the breakdown of the particles (Washington, 1990). Polymer degradation can occur either through bulk hydrolysis or surface erosion. Bulk eroding polymers undergo chain cleavage throughout the system and overall tend to have less

reactive functional groups so generally degrade more slowly than surface eroding particles. For a sustained release it is desirable to have a bulk eroding polymer such as PLGA (Anderson and Shive, 1997). In most cases drug release occurs through a combination of mechanisms, and often leads to an initial rapid release known as a burst. A burst is not desirable as can give a high concentration of drug which can cause side effects and also reduces the ability of the system to give a sustained release.

Drug release from nanoparticles is affected by a number of factors, with particle size considered to be the most important. With all other factors equal a slower, more sustained release with a smaller initial burst will occur with larger particles (Washington, 1990, Hans and Lowman, 2002, Dawes et al., 2009). The properties of the polymer and drug also have important contributions to the rate of drug release.

1.8 Thesis Aims

The aim of this thesis was to produce and characterise a delivery system for OA and the initial plan for this system was outlined in section 1.5. This slow release drug delivery system for intra-articular injection was to be composed of a nanoparticle drug delivery system held within an injectable hydrogel. The aim was that the system will be able to provide a sustained release for three months as no current systems are able to give a delivery over such a timeframe.

In order to identify the most suitable hydrogel an initial investigation of different hydrogels was undertaken. In chapter 3, two hydrogel systems using

different formation methods were investigated. Pluronic F127 was one selected system as this thermosetting polymer has been widely studied and has the required thermosetting properties. The other system used a different approach and selected a system capable of producing resilient gels, which were polyelectrolyte complexes between hyaluronic acid and chitosan. These two hydrogel systems are illustrated in Figure 1-5 with the nanoparticles that will also be included. This figure shows the proposed structure for this delivery system once it has formed after injection.

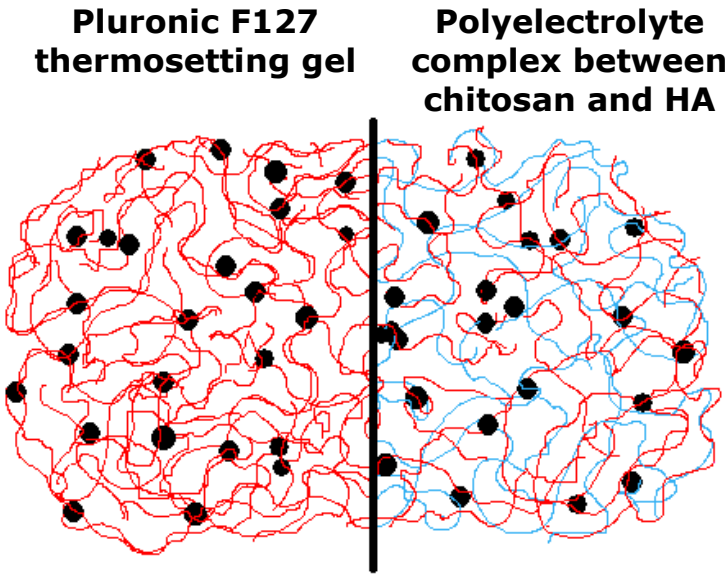

Figure 1-5 Diagram of the two selected hydrogel systems for the proposed delivery system with nanoparticles.

A number of the key properties of these hydrogels were investigated, which were the hydrogel formation, the complex strength and the stability of the hydrogels under physiological conditions. A formation within 30 minutes was required to avoid clearance from the synovial cavity and resilient hydrogels were required to withstand the challenging conditions within the joint. The production of an injectable formulation of the polyelectrolyte complexes was also investigated.

There are also further considerations for the polyelectrolyte system particularly for their long term stability. Therefore a further investigation, within chapter 4, was carried out into a modified hyaluronic acid that would provide cross-links in the complexes to produce more resilient complexes that were more resistant to degradation. To improve the biocompatibility of the complexes reduced chitosan concentrations in the complexes were also investigated throughout this project.

Glucocorticoid steroids are a current intra-articular therapy that is effective at relieving pain and other symptoms for up to three weeks. This short period of action means that this treatment could benefit from incorporation into a delivery system. This project therefore used the glucocorticoid steroid dexamethasone phosphate. This drug was incorporated into a nanoparticle delivery system which was then characterised, and this investigation was carried out in chapter 5.

The combined nanoparticle and hydrogel system was also characterised, in chapter 6, for its ability to hold and retain high concentrations of nanoparticles to allow for the desired drug release. Finally the drug release from this system was characterised to ensure that it meets the aims.

CHAPTER 2 - GENERAL METHODS

2.1 Materials

2.1.1 Polymer Materials

Pluronic F127 was purchased from Sigma-Aldrich (Poole, UK). Hyaluronic acid (sodium salt) with a molar mass of 2.2 MDa was purchased from Optima chemicals (Middlessex, UK) and was used as supplied. Chitosan chloride with a molecular weight of 330 kDa (which corresponds to a mass of 275 kDa in free base form) and a degree of deacetylation of 95% was purchased from Novamatrix Biopolymers (Oslo, Norway) and was used as supplied. Poly(glycerol-adipate) backbone polymer was provided by Dr. G. Hutcheon (Liverpool John Moores University, UK), preparation is detailed in (Kallinteri et al., 2005) and polymer was used as received.

2.1.2 Drug Materials

Dexamethasone 21-phosphate disodium salt (98% minimum), dexamethasone (98% minimum), and RBITC (mixed isomers) were obtained from Sigma-Aldrich (Poole, UK).

2.1.3 Other Reagents

All solvents were obtained from Fisher Scientific (Loughborough, UK) and were of laboratory reagent grade or better. All solvents used for HPLC were obtained from Fisher Scientific and were of HPLC grade. Purified water used was from an ELGA purification system (minimum resistivity 18.2 MΩcm, ELGA, Marlow, UK). Hyaluronidase enzyme (E.C. 3.2.1.35) of bovine

testicular source (1600 U/mg) was obtained from MP Biomedicals (Cambridge, UK). All dialysis membranes used were SpectraPor membranes (Spectrum Europe, Netherlands). Bovine serum and HBSS buffer (10X) were obtained from Invitrogen (Life Technologies, Paisley, UK). All other reagents, unless otherwise stated, were obtained from Sigma-Aldrich (Poole, UK) and were of laboratory reagent grade or better.

2.2 Buffers

2.2.1 Artificial Synovial Fluid

As this study was investigating intra-articular injection it was desirable to utilise a buffer that is biologically relevant and mimetic of synovial fluid. The main components of synovial fluid are an electrolyte solution, protein and HA. A buffer that was named artificial synovial fluid (ASF) was produced that was mimetic of the salts present in synovial fluid. The salts present in synovial fluid are very similar to those present in plasma (Gerwin et al., 2006, Shanfield et al., 1988), and therefore Hank's Balanced Salt Solution (HBSS) was used as a base for ASF.

2.2.2 Artificial Synovial Fluid with Protein

Protein is another essential component of synovial fluid and so was also included into the buffer. This buffer was named ASFP (ASF with protein) and used the ASF buffer described above with added protein. The composition of synovial fluid is known to vary with disease state. As this delivery system is designed for use in osteoarthritis the composition aimed to reflect that. ASFP contained 33% (v/v) bovine serum as this is the approximate concentration of

protein in osteoarthritic synovial fluid (Gerwin et al., 2006, Curtiss, 1964, Mavraki and Cann, 2009). In healthy synovial fluid there is a greater proportion of albumin compared to globulins (Mavraki and Cann, 2009, Curtiss, 1964). In OA this balance is shifted as the vascular permeability increases allowing larger proteins to enter more easily (Burt et al., 2009, Larsen et al., 2008). Bovine serum was selected as it is readily available and is a relatively realistic mimic of the proteins in arthritic synovial fluid.

2.3 Hydrogel Preparation and Characterisation

2.3.1 Pluronics

2.3.1.1 Pluronic solution preparation

A stock Pluronic F127 solution (30% w/v) was produced by the "cold method" (Schmolka, 1972). Briefly, Pluronic polymer (15g) was slowly added to ice cold purified water (50ml) or PBS buffer (50ml, pH 7.4) under magnetic stirring. When all Pluronic polymer had been added the beaker was transferred to the fridge and left overnight to fully dissolve. Further periods of magnetic stirring were used as necessary until a fully dissolved solution was obtained.

2.3.1.2 Pluronic hydrogel preparation

Stock solution was diluted with purified water or PBS buffer (pH 7.4) to the required concentration between 5 and 20% (w/v). Hyaluronic acid (3.5mg/ml final concentration) was added during this dilution where desired. Solutions were incubated at 5°C to allow full mixing. In order to allow gel formation to occur solutions were transferred to either 22°C (room temperature in

laboratory) or a water bath at 37°C. Photographs were taken after vials containing hydrogel had been inverted for 1 minute.

Hydrogel formation was assessed by rheology time sweeps, which were carried out as described in section 2.8.1.2. 16% (w/v) Pluronic samples were used. These samples were kept at room temperature before being loaded onto the rheometer plate (37°C) and measurements were started as soon as possible after this.

2.3.1.3 Pluronic hydrogel rheology

Rheology amplitude sweeps were carried out as described in section 2.8.1.2. These were carried out on 16% (w/v) Pluronic hydrogels which were formed onto the rheometer plate at 37°C. Once the hydrogels had formed measurements were started. T-tests were used to compare the results of different samples.

2.3.1.4 Pluronic hydrogel degradation

Pluronic degradation was assessed by monitoring the release of Pluronic from the hydrogel using a colourimetric assay. To produce the hydrogel a Pluronic solution (2ml, 16% w/v) was added to a dialysis membrane (molecular weight cut-off of 250 kDa) and heated to 37°C. The hydrogel was placed in a beaker of PBS buffer (30ml, pH 7.4) and then incubated in a water bath at 37°C. Buffer was replaced at regular intervals and the released Pluronic was quantified using a colourimetric assay (Al-Hanbali et al., 2007). For this assay dichloromethane (0.5ml) was added to a microcentrifuge tube. This was

followed by the test Pluronic solution (0.5ml) and a solution containing 0.4M ammonium thiocyanate and 0.1M anhydrous iron (III) chloride (0.5ml). The tubes were shaken for 20 minutes (Rotamix RM1, ELMI Ltd) and then subjected to centrifugation (MSE microcentaur, MSE, London, UK) at 13,000rpm for 3mins. Absorbance of the organic layer was measured in a quartz cell at 510nm using a Beckman Coulter DU800 spectrophotometer (Beckman Coulter, High Wycombe, UK).

2.3.2 Polyelectrolyte Complexes between Hyaluronic Acid and Chitosan

2.3.2.1 Hyaluronic acid and chitosan solution preparation

Stock solutions of hyaluronic acid (6mg/ml) and chitosan chloride (8mg/ml) were obtained by dissolution of the polymers in purified water, 1.2M NaCl solution or ASF, under magnetic stirring. Chitosan chloride was used in this study rather than the free base due to the increased solubility of this salt form. The free base form of chitosan is only soluble in acid solution below about pH 6, however the chitosan chloride used here is soluble in water at neutral pH making it much more suitable for the intended application.

2.3.2.2 Hyaluronic acid and chitosan polyelectrolyte complex formation

Polyelectrolyte complexes between chitosan and hyaluronic acid were produced by adding hyaluronic acid (2.5ml of 6mg/ml) to a glass vial and making up the volume to 5ml with purified water or ASF. To give complexes with different polymer ratios, diluted chitosan solution (1ml of 2.5-6.2mg/ml depending on ratio) was added. To ensure a thorough mixing of the polymers a rigorous mixing protocol was followed: the vial was vigorously inverted 10

times and then agitated by vortex (Rotamixer, Hook & Tucker) for 30 seconds. The mixtures were then incubated in a 37°C water bath for 60 minutes to allow formation to occur. Photographs were taken at regular intervals during this incubation to show the formation of these complexes.

To further assess the formation of these complexes, rheology time sweeps were carried out. These were conducted using the protocol described in section 2.8.1.2. HA solution (in purified water, ASF, or ASFP) was added to the rheometer plate and allowed to equilibrate at 37°C. Chitosan was then added, the solution was thoroughly mixed and measurements were started as soon as possible.

2.3.2.3 Rheology amplitude sweeps

To assess the strength and integrity of complexes, rheology amplitude sweeps were carried out. Complexes were produced using triple volumes of all components. Complexes were extracted and placed on the plate of the rheometer. Amplitude sweeps were undertaken using the protocol described in section 2.8.1.2. T-tests and repeated measures ANOVA were used to analyse the results.

2.3.2.4 Complex degradation

A mass degradation method was used to assess the stability of complexes. Complexes were extracted and placed into purified water, ASF or ASFP (5ml). Samples were incubated in a water bath at 37°C with the buffer replaced 3

times per week. Complexes were extracted at each time point, dried in an oven and weighed. Repeated measures ANOVA was used to analyse the results.

A further study was undertaken to investigate the strength of the complexes as they degrade using rheology amplitude sweeps. Complexes were prepared as for rheology amplitude sweeps, see section 2.3.3.3. Complexes were extracted and placed into ASF (15ml). Samples were incubated in a water bath at 37°C with the buffer replaced 3 times per week. Complexes were then extracted at each time point and placed on the plate of the rheometer. Amplitude sweeps were undertaken using the protocol described in section 2.8.1.2.

2.3.2.5 Effect of salt on complex formation

Complexes were produced by adding hyaluronic acid (2.5ml of 6mg/ml) to a glass vial. This was followed by 1.2M NaCl (0.5ml, 1ml, 1.5ml, 2ml, 2.5ml- to give final concentrations of 0.1M, 0.2M, 0.3M, 0.4M, 0.5M) and the solution was made up to 5ml with purified water. Diluted chitosan solution (1ml of 2.5-6.2mg/ml) was added to give the desired polymer ratio. The solutions were then thoroughly mixed by vigorously inverting the vial 10 times and then agitating by vortex (Rotamixer, Hook & Tucker) for 30 seconds. The complexes were incubated in a 37°C water bath for 60 minutes to allow formation to occur and photographs were then taken.

2.3.2.6 Complex formation by dialysis

Hyaluronic acid in 1.2M NaCl (2.5ml of 6mg/ml) was added to a glass vial, made up to 5ml with purified water. Diluted chitosan solution (1ml of 2.5-

6.2mg/ml) was added to give the desired polymer ratio. The solution was then thoroughly mixed by vortex (Rotamixer, Hook & Tucker) for 30 seconds, and placed in a dialysis membrane (10 kDa molecular weight cut-off). This was dialysed against purified water or ASF buffer (250ml) at 37°C, under magnetic stirring. Buffer was changed every 15 minutes for the first hour and then every 30 minutes for the second hour. Photographs were taken at each buffer change.

To further assess the formation of these complexes using this formation method, rheology amplitude sweeps were carried out. These were conducted using the protocol described in section 2.8.1.2. The dialysis samples were prepared as above, except using half volumes of all reagents. At each buffer change the appropriate sample was removed and transferred to the plate of the rheometer.

2.4 Modified Hyaluronic Acid Preparation and Characterisation

2.4.1 Synthesis of Modified Hyaluronic Acid

A modified hyaluronic acid (HAM) with a cysteamine substitution of the carboxylate groups was produced. A 10% substitution of available carboxylate groups was aimed for. Three times the amount of cysteamine required by the stoichiometric ratio was used based on the expected reaction efficiency.

Hyaluronic acid (2g, 5.06 mmol COOH) was dissolved in 200ml of 0.1M potassium phosphate buffer (pH 6.4). Cysteamine hydrochloride (0.172g, 1.52 mmol) was dissolved in a small volume of buffer and added to the HA solution under magnetic stirring. To initiate the reaction 1-ethyl-3-(3-

dimethylaminopropyl) carbodiimide (EDAC, 0.353g, 2.28mmol) was added. The pH was monitored throughout the reaction and maintained at 6.4 using 0.1M HCl. After 1 hour and when there was no further change in pH the reaction solution was transferred to a dialysis membrane (10 kDa molecular weight cut-off) and dialysed against purified water for 48 hours to remove any by-products or unreacted cysteamine. The substituted hyaluronic acid was then lyophilised. HAM was then used in the same way as unmodified hyaluronic acid.

2.4.2 Characterisation of Modified Hyaluronic Acid

The sulfhydryl group concentration was determined by Ellman's test (Ellman 1959). To a microcentrifuge tube HAM solution (200µl, 3mg/ml) was added, followed by 1M Tris buffer (100µl, pH 8) and 2mM 5,5'-dithio-bis(2-nitrobenzoic acid) in 50mM sodium acetate trihydrate (50µl). The volume was made up to 1ml with purified water. These solutions were incubated on ice for 30 minutes. After this time the absorbance was measured at 412nm using a Beckman Coulter DU800 spectrophotometer (Beckman Coulter, High Wycombe, UK). A standard curve of sulfhydryl concentration was constructed using cysteine to allow quantification of sulfhydryl groups in HAM.

2.5 Nanoparticle Preparation and Characterisation

2.5.1 PGA Polymer Modification and Characterisation

12kDa backbone PGA polymer was 40% substituted with C18 acyl (stearoyl) groups, using the published method (Kallinteri et al., 2005). PGA polymer (5g, 0.42mmol) was dissolved in dried THF (50ml, dried using activated molecular

sieves) through heating under a gentle reflux in a N_2 atmosphere. To this solution stearoyl chloride (3.28g, 3.65ml, 2.15mmol) dissolved in dried THF (12.5ml) was added. This was followed by the addition of pyridine (2.5ml), which was slowly added. The reaction was allowed to continue under gentle reflux overnight.

The reaction mixture was cooled and chloroform (75ml) was added. This mixture was poured over a solution of purified water (50ml) and concentrated HCl (1.25ml) in a separating funnel. The organic layer was collected and a further 25ml of chloroform was poured over the remains in the separating funnel and the organic layer was again collected. The two organic layers were combined and poured over another solution of purified water (50ml) and concentrated HCl (1.25ml). The organic layer was collected and poured over purified water (100ml) and this was repeated once. The organic layer collected after this rinsing was dried using solid Mg_2SO_4, which was removed by filtration. The solvent was removed by rotary evaporation. The final solid was dried overnight under vacuum and the reaction was analysed using ^{1}H-NMR (Bruker 400MHz spectrometer, Bruker Corporation, Coventry, UK) using acetone-d_6 as a solvent.

2.5.2 Nanoparticle Preparation

Nanoparticles were prepared using 40% C18 substituted 12kDa PGA polymer by the interfacial deposition method as previously described (Kallinteri et al., 2005, Meng et al., 2006). PGA polymer was dissolved in acetone and this solution (2ml, 10mg/ml) was added drop wise to an aqueous phase in a glass

vial under magnetic stirring. The aqueous phase used was as follows: for unloaded (blank) nanoparticles it was purified water (5ml); for DXMP loaded particles it was of purified water (5ml) containing DXMP (8mg); for RBITC loaded particles it was 0.01M HEPES buffer (6ml, pH 7.4) containing RBITC (100μg). The acetone was allowed to evaporate off overnight. Particles were filtered through a 1.0μm cellulose nitrate membrane filters (Whatman) to remove flocculated particles where necessary.

2.5.3 Separation of Unencapsulated Drug

To separate unencapsulated drug from the DXMP particles gel permeation chromatography was used. This was carried out using a column (2.5x30cm) packed with Sepharose CL-4B gel, with purified water as an eluent. Fractions were collected by a fraction collector. Fractions containing eluted particles were combined and concentrated using Vivaspin 20 concentrators (10 kDa molecular weight cut-off, Sartorius Stedium Biotech, Germany) in a Centaur 2 centrifuge (MSE, London, UK) for 30 minutes at 3000rpm.

The separation of unencapsulated RBITC was achieved by dialysis. The nanoparticle suspensions were loaded into dialysis membrane (10kDa cut-off) and dialysed against purified water for 24h with regular changes of water.

2.5.4 Nanoparticle Characterisation

Nanoparticle size and zeta potential were determined using a Malvern Zetasizer Nano ZS (Malvern Instruments Ltd, UK) at 25°C. Size was determined by dynamic light scattering and zeta potential by laser doppler

micro-electrophoresis. Samples were diluted with purified water which had been filtered through 0.2µm membrane filters (Millipore, Watford, UK). The results were analysed using Student's T test.

2.5.5 Analysis of Nanoparticle Drug Loading Levels

2.5.5.1 Determination of RBITC loading levels

RBITC loading levels were assessed using a direct method. Freeze dried nanoparticle samples were dissolved in a solvent mixture of acetone and methanol (2:1 ratio). The fluorescence of this solution was assessed using a fluorimeter as described in section 2.8.2. A standard curve of known concentrations of RBITC in acetone and methanol (2:1 ratio) was used to quantify the RBITC present.

2.5.5.2 Method development for DXMP loading levels

This development process aimed to produce a direct method for evaluation of drug loading. For a direct method it is necessary to disrupt nanoparticles to release the encapsulated drug. As PGA is a polyester it can be broken down through the use of sodium hydroxide. Freeze dried blank nanoparticles were taken (c.4mg), DXMP (3mg) was added followed by 2M NaOH (20ml). This mixture was sonicated and incubated overnight. The pH was then neutralised using 2M HCl. DXMP was quantified using high-performance liquid chromatography (HPLC), as described in section 2.8.3.

This method was extended in an attempt to optimise the extraction of DXMP from the neutralised solution. Hexane washing was used to remove fatty acids,

where 7ml hexane was added to the neutralised solution. This mixture was vortexed, sonicated and centrifuged before the hexane was removed. A second wash using 5ml hexane was carried out. The aqueous phase was then analysed by HPLC, as described in section 2.8.3.

A biphasic extraction protocol was also investigated. Freeze dried blank nanoparticles (c.4mg) were taken and DXMP (3mg) or dexamethasone (3mg) was added. To this dry mixture 1ml of purified water and 4ml of chloroform or dichloromethane (DCM) was added. These mixtures were sonicated and incubated overnight at 22°C. The aqueous layer was extracted and DXMP and dexamethasone were quantified using HPLC, as described in section 2.8.3.

The DCM extraction method was extended to analyse the organic layer. The DCM from samples was diluted in methanol to improve its aqueous miscibility. This mixture was then analysed using HPLC, as described in section 2.8.3.

2.5.5.3 Determination of DXMP drug loading levels

An indirect method has previously been used to estimate the drug loading for DXMP loaded PGA nanoparticles (Kallinteri et al., 2005). This analysed free DXMP recovered from the column chromatography used to separate the unencapsulated drug. DXMP was quantified using HPLC, as described in section 2.8.3.

The optimised direct method for determination of DXMP drug loading was a biphasic DCM extraction. Freeze dried DXMP loaded nanoparticles had DCM added (4ml) followed by purified water (16ml). This mixture was sonicated and incubated overnight. After centrifugation the water and DCM layers were extracted. The DCM was diluted with methanol and the drug was quantified using HPLC, as described in section 2.8.3.

2.5.6 Analysis of Drug Release from Nanoparticles

2.5.6.1 RBITC release

RBITC loaded nanoparticles (1ml) were added to a dialysis membrane (10 kDa molecular weight cut-off), with purified water or bovine serum (1ml). The sealed dialysis membrane was immersed in ASF (5ml) and incubated at 37°C in a water bath. At regular intervals the buffer was replaced with fresh buffer. Released RBITC was quantified using fluorimeter as described in section 2.8.2.

2.5.6.2 DXMP release

DXMP loaded nanoparticles (1ml) were added to a dialysis membrane (10 kDa molecular weight cut-off). The sealed dialysis membrane was immersed in ASF (5ml) and incubated at 37°C in a water bath. At regular intervals the buffer was replaced with fresh buffer. Released drug was quantified using HPLC, as described in section 2.8.3.

2.6 Composite Preparation and Characterisation

2.6.1 Composite Preparation

Nanoparticle loaded polyelectrolyte complexes were produced using the same method as polyelectrolyte complexes, section 2.3.3.2. The only difference is that nanoparticle suspension (c. 4mg), as prepared in sections 2.5.2 and 2.5.3, was included in place of the purified water. The formation of the nanoparticle loaded complexes was characterised using the same methods as previously described, section 2.3.3.2.

2.6.2 Composite Characterisation

The nanoparticle loaded complexes were characterised using the same methods as previously described, except using nanoparticle loaded complexes. This was rheology amplitude sweeps as described in section 2.3.3.3 and mass degradation studies as detailed in section 2.3.3.4.

2.6.3 Determination of Nanoparticle Incorporation into Composites

Composites were removed from solution using 30μm nylon mesh filters (Millipore, Watford, UK). The fluorescence of the solution excluded from the complexes was analysed by fluorimetry, as described in section 2.8.2. Complexes were produced in the absence of nanoparticles and the complexes were removed as before; these solutions were then spiked with known concentrations of nanoparticles to allow the production of a standard curve. This allowed the concentration of particles present in solution to be calculated. Repeated measures ANOVA was used to analyse the results.

2.6.4 Nanoparticle Release

Composites loaded with RBITC nanoparticles were extracted using 30μm nylon mesh filters (Millipore, Watford, UK). These were placed into 5ml of ASF or ASFP and incubated at in a water bath 37°C. At each time point this buffer was replaced and the nanoparticle concentration in the removed buffer was determined using a fluorimeter, as detailed in section 2.8.2. Repeated measures ANOVA was used to analyse the results.

2.6.5 Enzyme Degradation

Complexes loaded with RBITC nanoparticles were prepared. These composites were removed using 30μm nylon mesh filters (Millipore, Watford, UK) and were incubated in 0.1M formate buffer (5ml, pH 4.5) containing bovine testicular hyaluronidase (0.6U/ml) in a water bath at 37°C. At each time point the buffer was replaced and fluorescence in the removed buffer was measured by fluorimetry, as detailed in section 2.8.2. At the end of the study period HAase (5ml, 30U/ml) was added, this was done to break down any remaining complex and recover any retained particles. After incubation in a water bath at 37°C for 7 days the nanoparticle concentration was estimated using fluorimetry. Repeated measures ANOVA was used to analyse the results.

2.6.6 Effect of Salt on Composite Formation

The effect of salt on composite formation was investigated using the same method as described in section 2.3.3.5. The only difference was that nanoparticle suspension (0.25ml, c. 2mg) was included in place of water.

2.6.7 Dialysis Formation Method

2.6.7.1 Composite formation by dialysis

The dialysis formation method was the same as that used for the polyelectrolyte complexes, section 2.3.3.6, except that 2.5ml of nanoparticle suspension was included in the place of purified water. Formation of composites by this method was analysed using the same methods as previously described, section 2.3.3.6.

2.6.7.2 Characterisation of composites formed by dialysis

Formed composites prepared by the dialysis formation method were characterised using the same methods as used for bulk formed composites. These was nanoparticle incorporation (section 2.6.3), rheology amplitude sweeps (section 2.6.2), degradation (section 2.6.2), particle release (section 2.6.5) and enzyme degradation (section 2.6.6).

2.7 Drug Release from Composites

2.7.1 DXMP Release from Drug Loaded Composites

Complexes containing DXMP loaded nanoparticles were prepared. Composites were removed using 30µm nylon mesh filters (Millipore, Watford, UK) and were added to ASF buffer (5ml) and incubated at 37°C. Buffer was replaced at regular time points and was filtered through 30µm nylon mesh filters (Millipore, Watford, UK) to ensure no complex was removed.

The collected release medium may contain intact nanoparticles. Therefore to allow the drug content to be analysed the direct method for the determination

of DXMP loading was used, as described in section 2.5.5.3. DXMP content was assayed by HPLC, as described in section 2.8.3. Repeated measures ANOVA was used to analyse the results.

2.7.2 Complexes Loaded with Dexamethasone Crystals

2.7.2.1 Crystal preparation and characterisation

A suspension of dexamethasone crystals (6mg/ml) in purified water was prepared by sonication. The size of particles in this suspension was determined using a Coulter Counter (Beckman Coulter LS230, Beckman Coulter, High Wycombe, UK).

2.7.2.2 Drug release from dexamethasone loaded complexes

Dexamethasone suspension was loaded into complexes. Complexes were prepared as in section 2.3.3.2 but dexamethasone suspension (1ml, 6mg/ml) was included in place of the purified water. Complexes were removed using 30µm nylon mesh filters (Millipore, Watford, UK), were added to ASF buffer (5ml) and were incubated in a water bath at 37°C. Buffer was replaced at regular time points. The release medium was diluted with methanol to solubilise dexamethasone and drug content was assayed by HPLC, as detailed in section 2.8.3. Repeated measures ANOVA was used to analyse the results.

2.8 Machine Techniques

2.8.1 Rheology

2.8.1.1 Introduction to rheology

Rheology is a technique that investigates the viscoelastic properties of materials. Viscoelasticity is the combination of the viscous (liquid) and elastic (solid) properties that are found in materials such as hydrogels. Rheology investigates the flow and deformation of these viscoelastic materials to give information about the inherent structural properties of materials under dynamic conditions.

Controlled stress deformation oscillatory rheology tests measurements were used in this study. These involve the application of a sinusoidal shear stress (τ) to a sample and measuring the induced strain (γ) and the shift in phase angle (δ) of the stress and strain. In an ideal elastic solid the applied stress and the measured strain are in phase, hence a phase angle of 0° is obtained. In an ideal viscous liquid the shear stress is in phase with the shear rate and is out of phase with the strain, and hence a phase angle of 90° is seen. Viscoelastic materials have a phase angle of between 0° and 90° and this value represents the relative elastic and viscous properties of the material.

From the measured parameters the rheological parameters G' and G'' can be calculated through mathematical associations (Mezger, 2006). G' is the elastic modulus and is a measure of the amount of deformation energy that is stored in the sample. This energy restores the original form of the sample once the strain is removed and represents the elastic (or solid) properties of a material. G'' is

the loss modulus and this is a measure of the energy applied that is dissipated as heat. Energy loss occurs when the applied stress is causing physical changes to the structure of a material. The G″ can be seen to represent the viscous (or liquid) properties of a material.

There are three main different measuring system geometries available for rheological tests (Mezger, 2006). Firstly there are concentric cylinders or cup and bob systems which are most suited to the measurement of low viscosity materials. There are also cone and plate systems but these are not recommended where a sample contains particles. Finally there are parallel plates and for the samples studied here these are the most appropriate system to use.

A number of different rheology experiments can be carried out. One common type is stress amplitude sweeps. These experiments involve performing measurements at a set angular frequency and increasing the amplitude of the stress throughout the experiment. For hydrogels at low stress values the G′ and G″ are at a plateau. This is known as the linear viscoelastic range (LVR). As the stress is increased G′ and G″ remain constant whilst the sample remains in the LVR. At the point where the values of G′ and G″ begin to decrease rapidly the sample has become irreversibly damaged. The yield point is the shear stress value where this decrease occurs and shows the maximum shear stress that a sample can withstand without irreversible damage occurring. If the stress is increased further the G′ will fall below the G″ and this cross-over is known as the flow point.

Another experiment type is time sweeps. These tests use a constant stress amplitude and frequency (such that the response is within the LVR) and the values G′ and G″ are monitored as they change with time. This is particularly useful for monitoring the formation of hydrogels. The important parameters here are the gelation and the time over which the G′ and G″ continue to evolve. From a rheological point of view gelation can be defined as the point when G′ exceeds G″, as this is when the solid properties exceed the liquid properties. The phase angle (δ) can also be useful to monitor the relative changes in G′ and G″ as these parameters are related by the equation $\tan \delta = G''/G'$.

2.8.1.2 Rheology protocols

Rheology was performed using a Physica MCR 301 rheometer (Anton Paar Ltd, Hertford, UK). Oscillatory shear stress amplitude sweeps were carried out on hydrogels or complexes at 37ºC. These used a 25mm parallel plate geometry with a gap size of 1mm, frequency of 1.59 Hz (10 rad/s) and strain ranging from 0.01 to 100% (30 measurements). From these results the value of the G′ in the LVR was extracted. The yield stress was calculated by the elastic stress method (Walls et al., 2003). This method calculates the maximum elastic stress (G′γ) which is equivalent to the yield stress, and has been shown to give better yield stress estimates than other methods (Walls et al., 2003).

Oscillatory shear stress amplitude sweeps to investigate the dialysis formation method were carried out on dialysis samples at 37ºC. These used a 50mm parallel plate geometry with a gap size of 1mm, a frequency of 1.59 Hz (10 rad/s) and a strain ranging from 0.01 to 100% (15 measurements).

For time sweep measurements solutions (2.5ml total volume) were placed on the fixed lower plate of the rheometer at 37 ºC. Measurements were started immediately using a 50mm parallel plate with a gap size of 1mm, a frequency of 1.59 Hz (10 rad/s) and a strain of 0.05 %.

2.8.2 Fluorescence Spectrophotometer

Fluorescence of RBITC containing solutions was measured using a Hitachi F-4500 fluorescence spectrophotometer (λ_{Ex}=554 nm, λ_{Em}=575 nm, slit sizes-5nm, Voltage- 700V). Standard curves of RBITC or nanoparticle suspensions were used to quantify results as appropriate.

2.8.3 HPLC

HPLC was performed using an HP 1050 machine consisting of a pump, degasser, variable wavelength UV/visible detector, autosampler and Chemstation software. A method for simultaneous dexamethasone and dexamethasone phosphate determination was used (Puri, 2007). A reversed phase Lichrosphere 100 RP-18 endcapped column (25cm × 4.6mm; 5µm particle size) with a guard column was used. Mobile phase used was 0.1M phosphate buffer (pH 3.50- produced with HPLC analytical grade potassium phosphate monobasic from Sigma-Aldrich (Poole, UK)), methanol and acetonitrile in the ratio 50:36:14 with a flow rate of 1ml/min. 20µl of sample were injected and column eluent was monitored continuously at 240 nm. Standard curves for dexamethasone and DXMP were produced using known concentration standards that were run under the same HPLC conditions.

CHAPTER 3 - HYDROGEL SELECTION

3.1 Introduction

3.1.1 Requirements and Candidates for Hydrogels

The aim of this project was to produce a long term release formulation for intra-articular injection. The properties required to achieve this include the time taken for gel formation, the stability of gels under physiological conditions and the ability to hold and retain nanoparticles. The formation of these hydrogels needs to be rapid to ensure that formation occurs before significant clearance occurs from the joint.

In order to select a suitable hydrogel system an initial study was carried out on different hydrogel systems. Two hydrogels that used different methods of formation were selected for study. This allowed the most promising system to be identified. A commonly used approach for the production of injectable hydrogels is thermosetting polymers. Pluronic F127 was selected as the polymer to be used for this approach. The formation after injection due to the change in temperature is illustrated in the schematic in Figure 3-3.

The other system selected was a polyelectrolyte system comprising of hyaluronic acid and chitosan which produces resilient gels. A more detailed introduction into each system is given in the following sections.

3.1.2 Pluronics

Pluronics, also known as poloxamers, are a family of polymers with the general structure shown in Figure 3-1. They are tri-block co-polymers of poly(ethylene glycol) (PEG) and poly(propylene glycol) (PPG) in the form PEG-PPG-PEG, with different polymers produced with varying block lengths. Pluronic polymers are amphipathic as the PPG blocks are hydrophobic and the PEG blocks are hydrophilic. These synthetic polymers are biocompatible and are an FDA approved material.

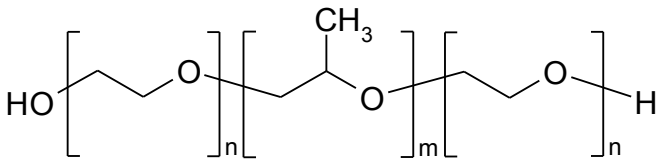

Figure 3-1 General structure of Pluronic polymers showing the tri-block composition.

Some of the polymers in the Pluronic family are thermogelling. When solutions of these polymers are heated above a critical temperature they undergo a phase change to form a hydrogel. The gelation is also concentration dependent and requires a minimum critical concentration. The gelation depends on the amphipathic nature of Pluronics and is an entropic effect. It involves two separate processes which are micelle formation and the gelation of these micelles. Analysis has found that micelle formation is the major energetic event in gelation (Yu et al., 1992). After micelles have formed, gelation occurs through micelles becoming tightly packed forming a gel (Yu et al., 1992, Nanjawade et al., 2007, He et al., 2008).

The thermogelling properties of Pluronic polymers allow them to be used as injectable hydrogels. For this project it is required to have a system that is liquid at room temperature and gels at body temperature. It is desirable to use a

room temperature solution for injection as this reduces the discomfort compared to a refrigerated solution. Pluronic F127 (also known as poloxamer 407) was chosen for study as it has been widely used in hydrogel production and forms a gel within the required temperature range (Chung et al., 2008, Malmsten and Lindman, 1992). The composition of Pluronic F127 is on average PEG_{106}-PPG_{69}-PEG_{106} with a molecular weight of around 12,500 Da (Yu et al., 1992).

Pluronic F127 hydrogels have been investigated for use in injectable drug delivery systems for controlled protein delivery (Kim and Park, 2002, Stratton et al., 1997, Chung et al., 2008) and for opthalmic delivery (Nanjawade et al., 2007). Pluronic F127 hydrogels have also been utilised for sustained drug release (Cafaggi et al., 2008, Jeong et al., 2002, Ruel-Gariepy and Leroux, 2004, Guzman et al., 1992), with a release over a maximum of 10 days achieved (Ruel-Gariepy and Leroux, 2004).

3.1.3 Polyelectrolyte Complexes between Chitosan and Hyaluronic Acid

3.1.3.1 Chitosan

Chitosan (Ch) is the partially deacetylated form of the biopolymer chitin. Chitin is found in the cell walls of fungi and the exoskeletons of insects and crustaceans. Chitosan is produced by chemical deacetylation of chitin and generally has a degree of deacetylation between 70 and 95% (Hamman, 2010, Wang et al., 2011). Chitosan is a random copolymer of D-glucosamine and N-acetylglucosamine with a molecular weight of up to 1000 kDa, structure shown in Figure 3-2 (Hamman, 2010).

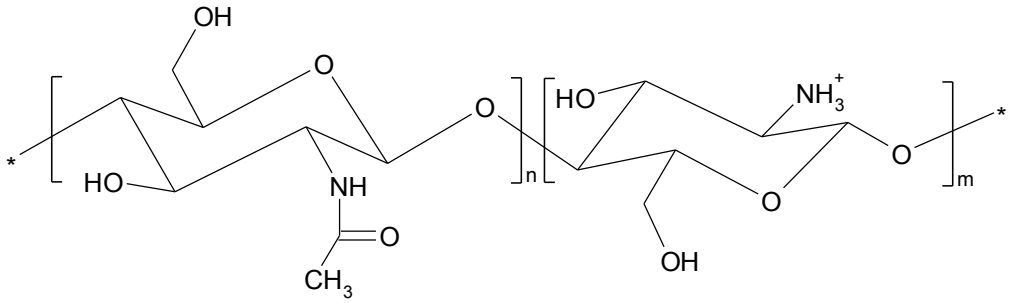

Figure 3-2 Structure of chitosan showing acetylated (left) and deacetylated (right) glucosamine monomers.

The D-glucosamine residues have a free amine group which can become protonated (pKa~6.5) (Berger et al., 2004), meaning that chitosan is a polyelectrolyte. Chitosan in its free base form is not soluble in water and needs to be dissolved in acid (El-hefian and Yahaya, 2010). Therefore for this study the more soluble chitosan chloride was used.

Chitosan is considered to be biocompatible and has been approved by the FDA for use in wound healing products. A study looking at chitosan in the joint found that chitosan caused fibrous tissue formation in the first week (Lu et al., 1999). As the experiment continued this decreased and overall chitosan was generally well tolerated despite the use of acidic chitosan solutions (Lu et al., 1999). Chitosan is also known to be biodegradable. Degradation occurs through enzymes such as lysozyme and low molecular weight chitosan is then excreted via the kidneys (Wang et al., 2011, Rani et al., 2010).

As chitosan is a polyelectrolyte it has been used for the preparation of polyelectrolyte complexes. It has been used in combination with various naturally derived polyanions including carboxymethyl cellulose (Berger et al., 2004, Dumitriu and Chornet, 1998), carrageenan (Berger et al., 2004, Hamman, 2010), liganosulphates (Fredheim and Christensen, 2003), heparin

(Berger et al., 2004, Dumitriu and Chornet, 1998), and hyaluronic acid (Denuziere et al., 1996, Berger et al., 2004, Hamman, 2010); as well with synthetic polymers such as poly(acrylic acid) (Hamman, 2010, Berger et al., 2004).

3.1.3.2 Chitosan and hyaluronic acid polyelectrolyte complexes

The structure and synthesis of hyaluronic acid has been introduced in section 1.2.4.1. The carboxylate groups (pKa~3) present in HA mean that it is a polyelectrolyte. HA has most commonly been used been investigated in polyelectrolyte complexes with chitosan, which form precipitated and phase separated complexes (Berger et al., 2004). The strong electrostatic interactions between the amine groups of chitosan and the carboxylate groups of HA mean that these complexes are stable through a wide pH range (Denuziere et al., 1996).

These precipitated polyelectrolyte complexes have been used to promote wound healing, although the efficacy has shown mixed results (Denuziere et al., 1998, Lee et al., 2003, Denuziere et al., 1996). These complexes have also been utilised for nasal protein drug delivery, and gave a release of 40% of incorporated insulin over 5 hours *in vitro* (Luppi et al., 2009). These studies have shown that these complexes are biocompatible and are tolerated by chondrocytes *in vitro* (Lee et al., 2003, Boughellam, 2007, Denuziere et al., 1998). These studies all used pre-formed complexes but this project aims to form complexes after injection.

Complexes between HA and chitosan have also been used in other forms. These include as polyelectrolyte films for tissue engineering (Cloyd et al., 2007, Feng et al., 2005); and as polyelectrolyte multilayers to confer antibacterial properties on titanium (Chua et al., 2008), or to promote lymphocyte binding (Vasconcellos et al., 2010) or in development of a 3D liver model (Kim et al., 2010). Complexes have also been produced that avoid precipitation, including polyelectrolyte nanoparticles for protein delivery (Hamman, 2010, Parajo et al., 2010, de la Fuente et al., 2008) and soluble complexes produced with PEG conjugated chitosan (Wu et al., 2007).

3.1.4 Chapter Aims

This chapter selected the hydrogel portion of the delivery system. Two potential systems were investigated and characterised, these were Pluronic F127 hydrogels and polyelectrolyte complexes between chitosan and hyaluronic acid. The formation, degradation and rheological properties of the hydrogels were assessed to allow the selection of the most suitable system. These hydrogels were also assessed for their ability to be formulated as an injectable system.

The precipitated polyelectrolyte complexes are not injectable but the free polymers are easily injectable. Therefore to produce an injectable system complexation must be prevented. Polyelectrolyte complex formation is known to be disrupted by high salt concentrations (Lee et al., 2003). Therefore using a high concentration salt solution would produce an injectable liquid and after injection the salt can diffuse away to allow complex formation. This approach

was assessed for its potential to produce injectable polyelectrolyte complexes. This transition is represented in Figure 3-3, illustrating how complex formation after injection in the lower physiological salt concentration.

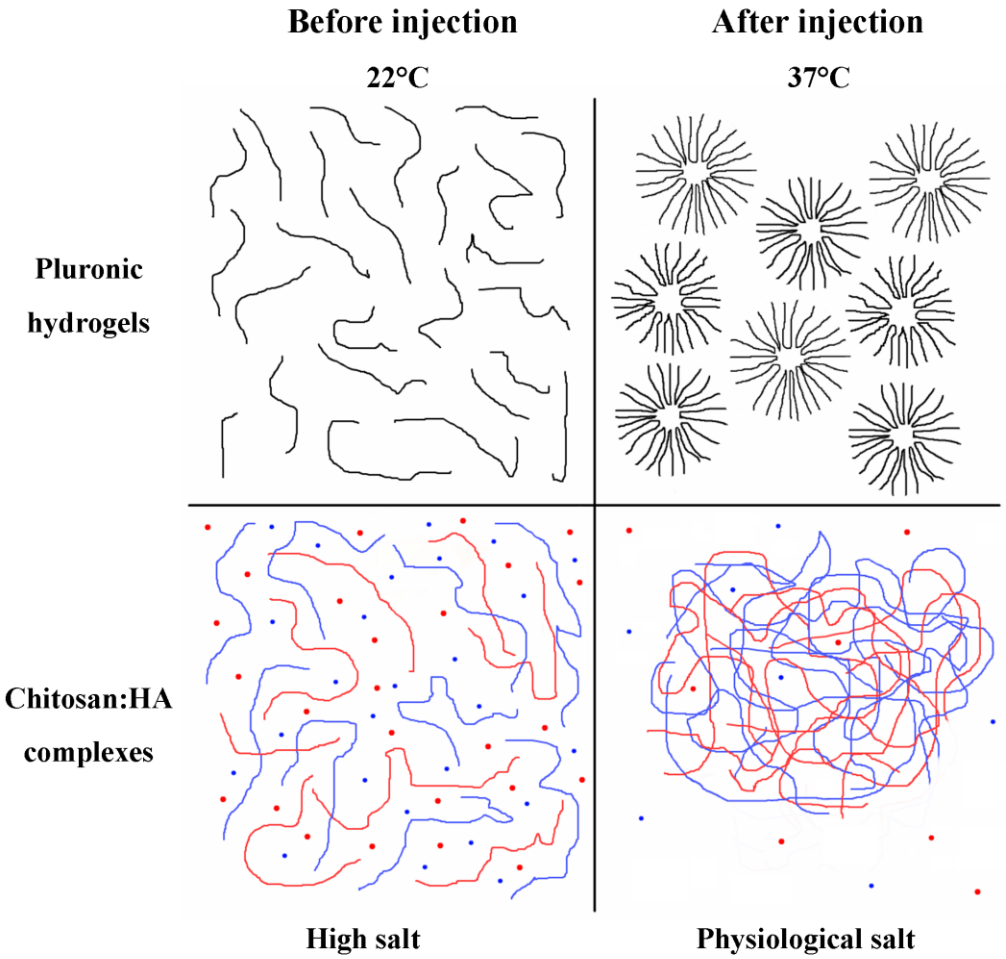

Figure 3-3 Schematic to show the factors driving hydrogel formation in the proposed injectable formulations.
Polymers are represented by lines and electrolytes by dots, colours represent charge and the key factor that causes hydrogel formation in both systems is identified, which is the salt concentration or temperature.

Chitosan is a material that is generally recognised as safe, but it has been shown to have some toxic effects (Liggins et al., 2004) and the effects of chitosan in the joint are less well known (Lu et al., 1999). Therefore a reduced chitosan concentration in these complexes may be an advantage to improve their biocompatibility and this was also investigated.

3.2 Materials and Methods

3.2.1 Materials

The materials used are detailed in section 2.1.

3.2.2 Pluronics

3.2.2.1 Pluronic solution preparation

Pluronic solutions were prepared using the method detailed in section 2.3.1.1.

3.2.2.2 Pluronic hydrogel preparation

Pluronic hydrogels were produced using the method described in section 2.3.1.2.

3.2.2.3 Pluronic hydrogel rheology

Rheology amplitude sweeps were carried out on Pluronic hydrogels as detailed in section 2.3.1.3.

3.2.2.4 Pluronic hydrogel degradation

Pluronic hydrogel degradation was assessed using the method described in section 2.3.1.4.

3.2.3 Hyaluronic Acid and Chitosan Polyelectrolyte Complexes

3.2.3.1 Hyaluronic acid and chitosan solution preparation

Solutions of hyaluronic acid and chitosan were prepared as described in section 2.3.2.1.

3.2.3.2 Hyaluronic acid and chitosan polyelectrolyte complex formation

Polyelectrolyte complexes were prepared as detailed in section 2.3.2.2 and the formation was assessed using the methods in section 2.3.2.2.

3.2.3.3 Rheology amplitude sweeps on polyelectrolyte complexes

Rheology amplitude sweeps on polyelectrolyte complexes were carried out using the method described in section 2.3.2.3.

3.2.3.4 Polyelectrolyte complex degradation

The degradation of polyelectrolyte complexes was assessed using the method described in section 2.3.2.4.

3.2.3.5 Effect on salt on complex formation

The effect of salt on polyelectrolyte complexes formation was analysed using the method described in section 2.3.2.5.

3.2.3.6 Complex formation by dialysis

Polyelectrolyte complexes were prepared by the dialysis method described in section 2.3.2.4. The formation of these complexes was analysed using the methods detailed in section 2.3.2.6.

3.3 Results

3.3.1 Pluronics

3.3.1.1 Pluronic hydrogel formation

Pluronic F127 is a thermogelling polymer with a lower critical transition temperature between liquid and gel forms. Hydrogel formation from this polymer is dependent on both polymer concentration and temperature. To assess the transition from liquid to gel a qualitative study was undertaken. This study investigated Pluronic F127 solutions at room temperature (22°C) (the temperature of the injected solution) and body temperature (37°C) to allow the identification of a concentration that would gel between these temperatures. This concentration would be a suitable concentration for an injectable hydrogel. After administration the Pluronic mixture will be exposed to a number of components that are naturally present within the joint and therefore the effect that salt and hyaluronic acid had on gelation was investigated.

Initial studies showed that the required concentration of Pluronic F127 was between 15% and 20% (w/v). The results of studies on Pluronic F127 solutions in this range are presented in Figure 3-4. Photographs were taken after vials had been left inverted for 1 minute, to show any flow that occurred in the samples. All concentrations in this range were found to be liquid at 22°C. At 37°C polymer concentrations of 17% and above produced a rigid gel. Concentrations of 15% and 16% produced less rigid gels, which showed some creep. The inclusion of a physiological salt concentration alone had no visual effect on the gel formation. Hydrogel formation was disrupted by the inclusion of hyaluronic acid at a physiologically relevant concentration (3.5mg/ml). No

hydrogel formed in the 15% solution and a greater creep was seen in 16%, 17% and 18% samples. When salt and HA were included together this seemed to reverse some of the disruptive effects seen. Solutions of 18% and below all exhibited reduced creep compared to when hyaluronic acid was included alone, Figure 3-4.

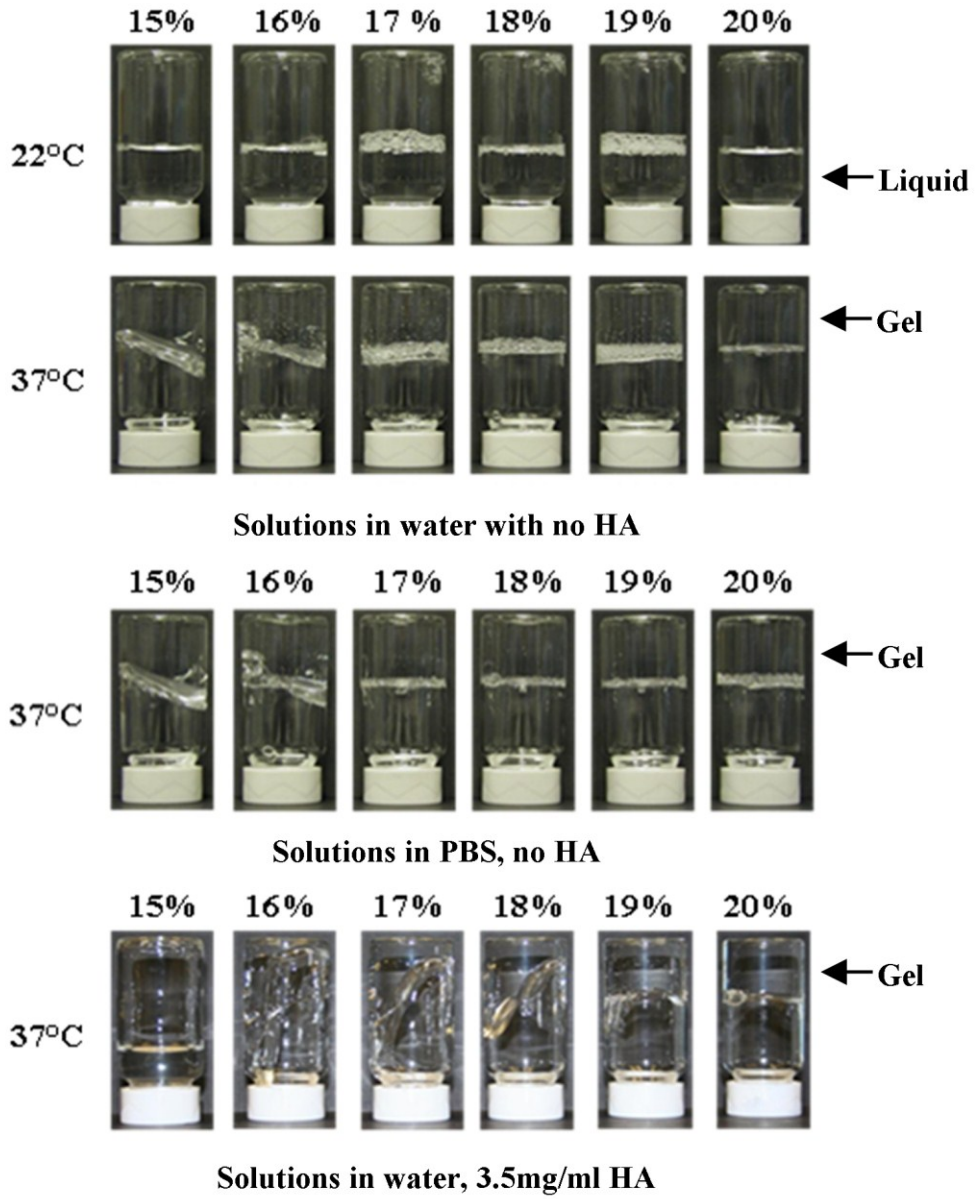

Figure 3-4 Photographs showing the thermal gelation of Pluronic F127 solutions in synovial relevant conditions.
Pluronic F127 solutions at concentrations between 15% and 20% (w/v) were prepared in water or PBS. Hyaluronic acid at 3.5mg/ml was included where indicated. The vials were photographed at the indicated temperature after being left inverted for 1 minute. The position of the Pluronic liquid or gel is indicated with an arrow.

From these results 16% solutions can be seen to be lowest concentration that gave a good hydrogel formation in all conditions. Further studies on the Pluronic system were conducted using this concentration. It is desirable to reduce the Pluronic concentration used as at high concentrations there are some concerns over toxicity and osmotic effects. A study on Pluronic F127 for ophthalmic applications concluded that a concentration of 16% was the maximum that is desirable (Talasaz et al., 2008). Although a different route of administration will be used here, it is likely that similar concentrations would be tolerated in the joint.

3.3.1.2 Analysis of hydrogel formation by rheology

Rheology can be used to investigate the internal strength and viscoelastic properties of materials. Rheology time sweeps can be used to monitor the change in the rheological parameters G′ and G″ with time. G′ is the storage modulus that represents the elastic (or solid) properties of a material and G″ is the loss modulus that represents the viscous (or liquid) properties. The changes in these parameters with time can therefore be used to monitor hydrogel formation quantitatively. The important features in rheology time sweeps that show hydrogel formation are the cross-over point where G′ first exceeds G″ (this is known as the gelation point) and the time over which the G′ and G″ continue to evolve.

For these samples rheology time sweeps were carried out at 37°C to mimic formation in the body. Room temperature solutions were added to the plate of the rheometer and measurements started as soon as possible afterwards. This

was done to mimic the temperature transition after injection. The results of this study are presented in Figure 3-5. Pluronic F127 solutions in water and those including HA included showed an instantaneous gelation and little change in G′ value during the study. The inclusion of physiological salt caused a slight retardation in gel formation. Gelation still occurred before measurements started but the G′ increased throughout the entire 30 minutes of the study. Inclusion of both salt and hyaluronic acid acted to reduce the negative effects seen with physiological salt alone. In this case the G′ rapidly evolved over the first 5 minutes before reaching a plateau.

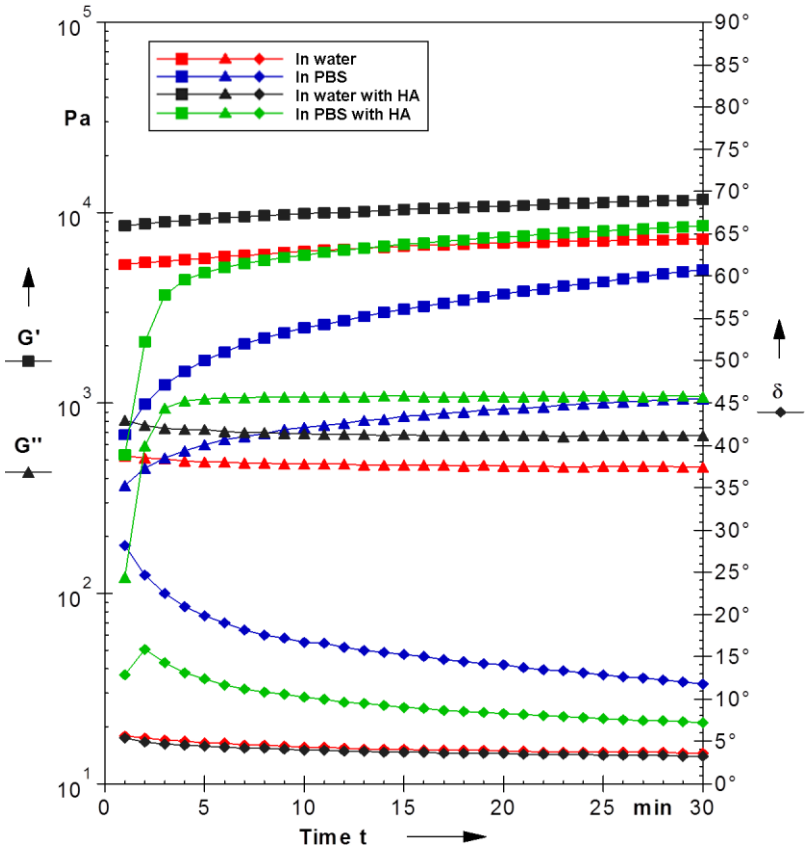

Figure 3-5 Rheology time sweeps showing Pluronic F127 hydrogel formation in synovial relevant conditions.
Rheology time sweeps were conducted at 37°C on Pluronic F127 solutions (16% (w/v)) with added synovial fluid components; PBS (pH 7.4) and/or HA (3.5mg/ml). G′ (squares) and G″ (triangles) are plotted on the primary y-axis; phase angle (δ- diamonds) is plotted on the secondary axis.

3.3.1.3 Gel integrity

The integrity and strength of formed hydrogels was assessed through the use of rheology amplitude sweeps, which investigate the responses of samples to increasing shear stresses. When interpreting stress amplitude sweeps there are two important features that represent gel integrity. Firstly is the value of G′ in the linear viscoelastic region (LVR); the LVR is where the value of G′ does not change with increasing shear stress. The other important feature is the yield stress; this is the value of the shear stress at the end of the LVR where G′ begins to fall. For both of these parameters, the higher the value the more resistant the gel is to shear stresses.

The results of rheology amplitude sweeps on 16% Pluronic hydrogels with added physiological components are presented in Figure 3-6. This figure shows both the raw results as well as the extracted G′ and yield stress values. This showed that strong and resistant hydrogels were formed. The inclusion of physiological salt and hyaluronic acid produced no significant changes in the G′ or yield stress.

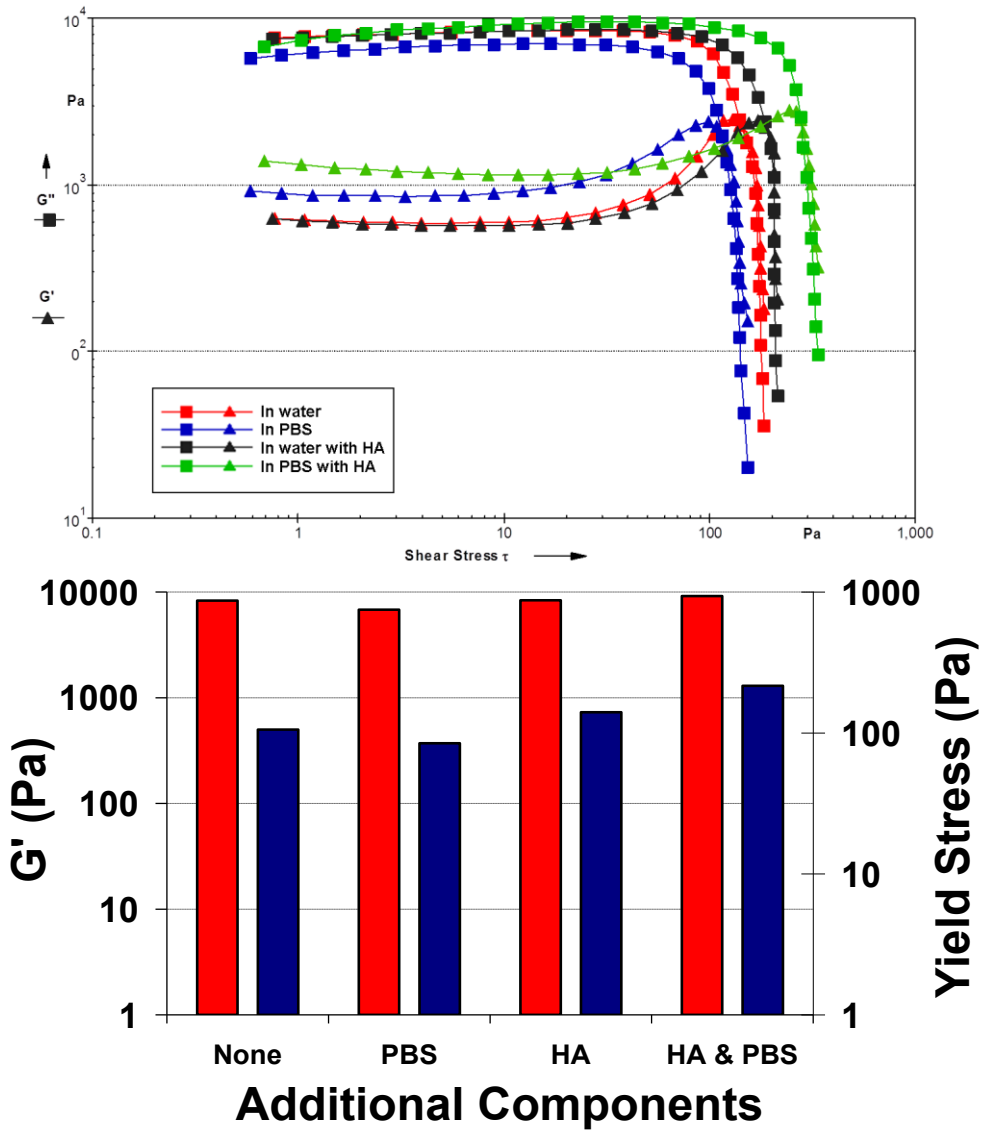

Figure 3-6 Rheology amplitude sweeps of Pluronic F127 hydrogels in synovial relevant conditions.
Rheology amplitude sweeps were carried out on Pluronic F127 hydrogels (16% (w/v)) at 37°C. Where indicated, PBS (pH 7.4) and/or HA (3.5mg/ml) were included. Top: Raw rheology amplitude sweep results. G′ (squares) and G″ (triangles) are plotted against shear stress. Bottom: Graph showing G′ and yield stress values extracted from raw results. G′ values- red; yield stress- blue.

3.3.1.4 Degradation

The degradation of Pluronic F127 hydrogels was investigated as stability over extended time periods is essential for the intended application. A degradation study was carried out with the gel retained within a dialysis membrane. The released Pluronic was quantified using a colourimetric assay. The results of this study are shown in Figure 3-7. This showed that the hydrogel lost over

half of its Pluronic content in 24 hours. The rate of diffusion of Pluronic across the dialysis membrane may have slowed the measured rate of degradation. This is supported by the fact that the Pluronic recovered from within the membrane after 24 hours was a liquid. This liquefaction shows another problem with the degradation of Pluronics. Hydrogel formation requires a critical concentration of Pluronic. When the concentration falls below this level the hydrogel will become liquefied, even though a relatively high concentration of Pluronic remains.

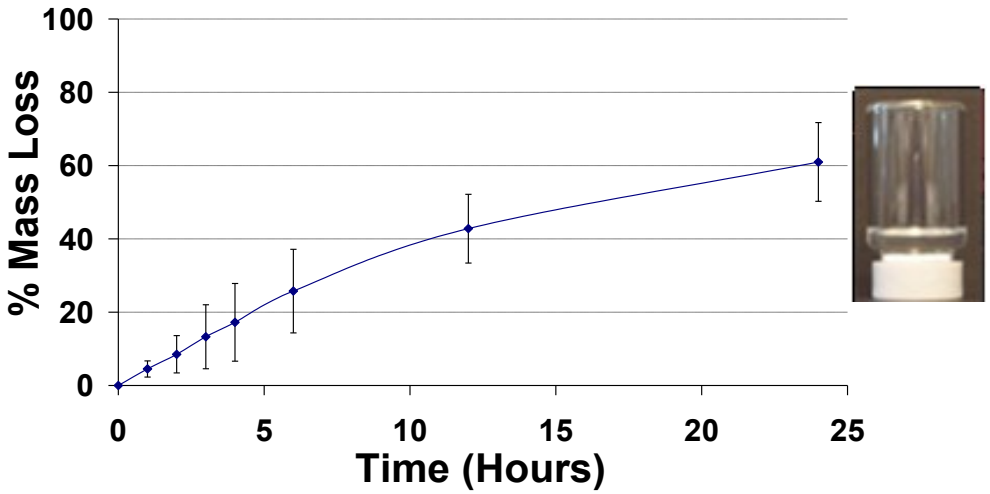

Figure 3-7 Graph showing Pluronic F127 loss during hydrogel degradation and a photograph of the recovered solution after 24 hours.
Pluronic F127 hydrogels (16% (w/v)) were held within a dialysis membrane (250 kDa molecular weight cut-off) at 37°C. PBS buffer was used as dialysate and was replaced at each time point. Mass of Pluronic in release buffer was assessed by a colourimetric assay. Photograph of recovered Pluronic solution after 24 hours of degradation at 37°C is shown, with vial inverted for 1 minute before the picture was taken.

3.3.2 Polyelectrolyte Complexes

3.3.2.1 Complex formation

Polyelectrolyte complexes form spontaneously from mixtures of negatively charged hyaluronic acid and positively charged chitosan. A reduced concentration of chitosan in the production of the polyelectrolyte complexes is desirable to keep possible toxic effects to a minimum. Therefore an initial

photographic study was conducted to investigate the effects of reducing chitosan concentration on complex formation, and the results are shown in Figure 3-8. The ratios of polymers in these complexes are expressed as the ratio of the charged group concentrations. This is the ratio of the amine groups of chitosan (Ch) to the carboxylate groups of hyaluronic acid (HA).

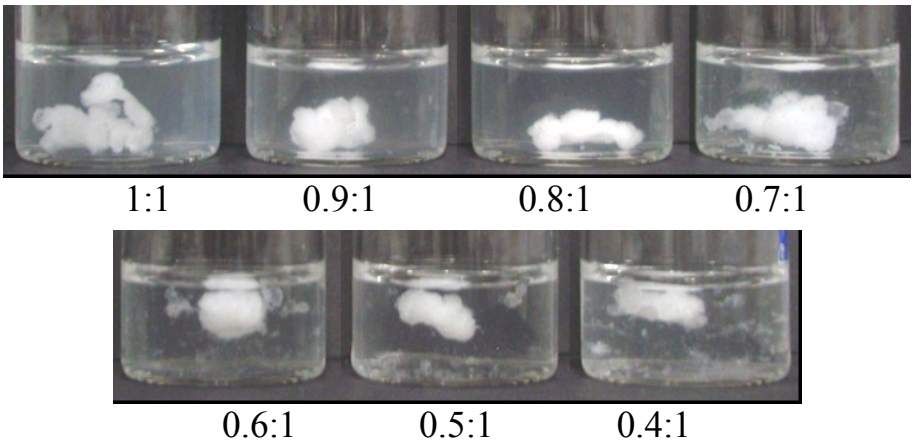

Figure 3-8 Photographs showing Ch:HA complexes of various polymer ratios prepared in water or ASF buffer.

Ch:HA complexes were prepared at the indicated polymer ratio in water or ASF. Complexes were incubated at 37°C for 60 minutes before photos were taken.

Salt is known to disrupt polyelectrolyte formation and this initial study therefore also investigated the effect that physiological salt concentrations had on complex formation. This was done by preparing complexes in artificial synovial fluid (ASF) buffer, which is a buffer mimetic of the salts present in synovial fluid. The results of this study are presented in Figure 3-8 and show that in water the 1:1 ratio produced compact and well defined complexes. As chitosan concentration decreased the complexes became smaller and less well defined with small exclusions from the main complex. In physiological salt the complexes formed but appeared less compact with a more fibrous structure. At lower chitosan concentrations there was a greater disruption when salt was present, which is shown in the 0.4:1 Ch:HA ratio complex which was almost totally disrupted in ASF buffer. A greater turbidity in the bulk solution was seen in ASF. This can be attributed to the polymer forming small complex particles, rather than becoming incorporated into the bulk complex.

The rate of complex formation was of interest as a rapid formation is required for this system. The kinetics of complex formation were investigated through photography of the forming complexes and rheology time sweeps. The results of the photographic study are shown in Figure 3-9 and show that precipitation occurred immediately and was followed by a slower contraction and condensation. This reorganisation occurred within 30 minutes after which time there was very little visual change. The polymer ratio does not visually affect the rate of complex formation and a similar precipitation and reorganisation was seen at all Ch to HA ratios studied between 0.5:1 and 1:1.

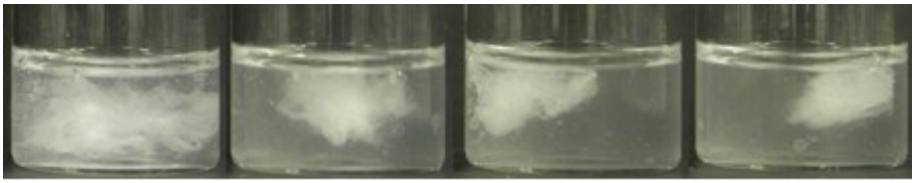

0 minutes 10 minutes 20 minutes 30 minutes

40 minutes 50 minutes 60 minutes

Ch:HA 1:1 complexes

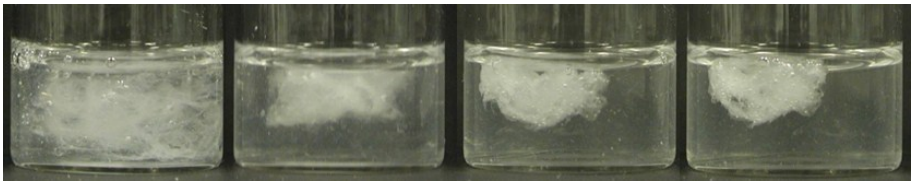

0 minutes 10 minutes 20 minutes 30 minutes

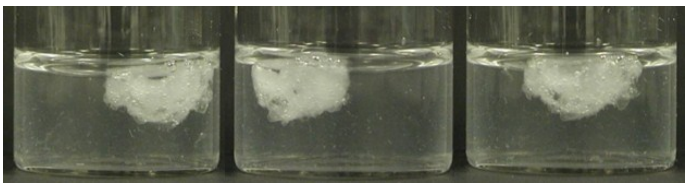

40 minutes 50 minutes 60 minutes

Ch:HA 0.7:1 complexes

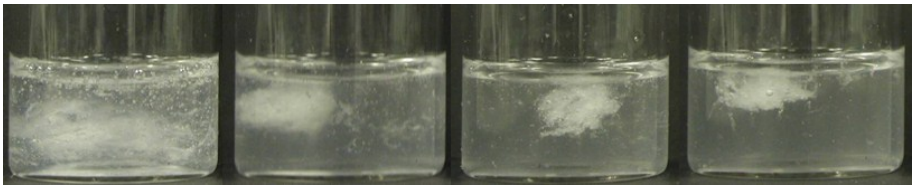

0 minutes 10 minutes 20 minutes 30 minutes

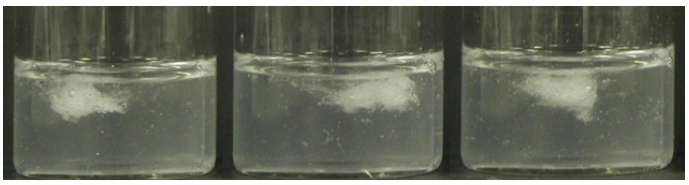

40 minutes 50 minutes 60 minutes

Ch:HA 0.5:1 complexes

Figure 3-9 Photographs showing the formation of Ch:HA complexes in water at different polymer ratios.

Chitosan and HA were mixed at varying ratios and incubated at 37°C. Photographs were taken at the indicated times.

The results of the rheology time sweeps, Figure 3-10, showed that gelation for the 1:1 ratio complexes occurred after around 30 minutes. The G′ value increased rapidly until after around 150 minutes. The phase angle (δ) can provide further information on complex formation. The phase angle shows the

relative levels of G′ to G″, with a smaller phase angle when there is higher relative G′. Changes in the phase angle can therefore show the overall formation of the complexes. The phase angle values confirmed what was seen in the G′ values. The phase angle rapidly decreased before levelling off after about 150 minutes showing that formation was complete. The 0.5:1 ratio complexes showed a similar overall time of formation (until the G′ and phase angle values were stable) but gelation (when G′ exceeded G″) took longer at around 60 minutes. The time of formation differed from the visual observations because the rheological measurements were carried out in a thin film and not a bulk solution, which slowed formation.

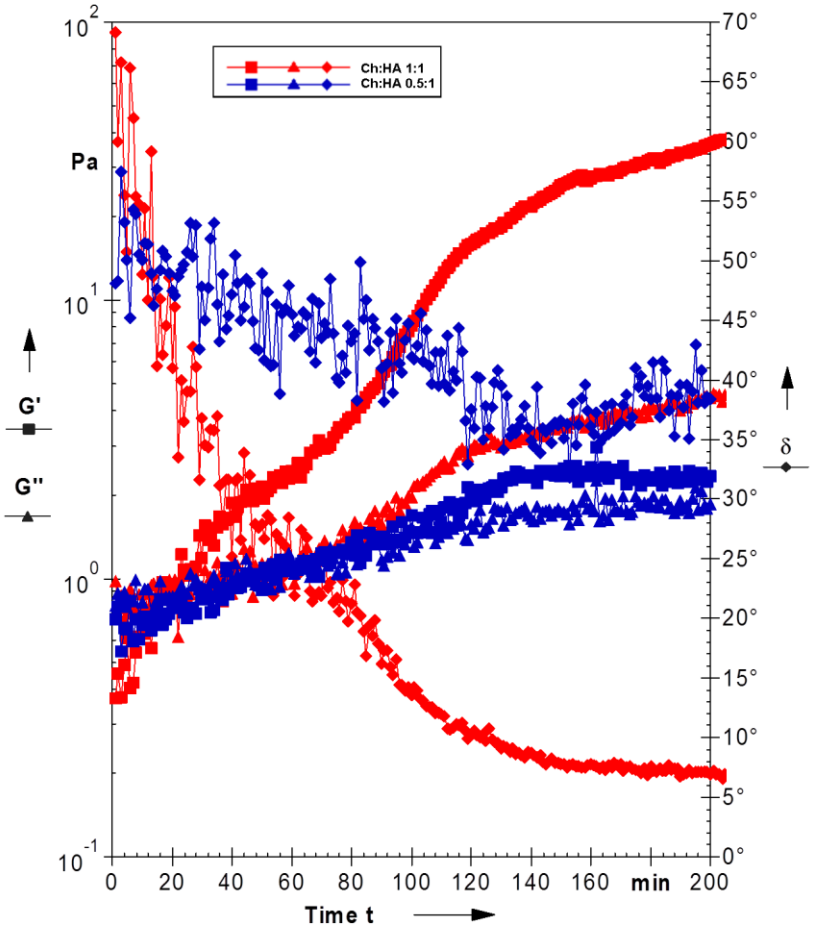

Figure 3-10 Rheology time sweeps showing the formation kinetics of Ch:HA complexes. Rheology time sweeps were conducted at 37°C. Chitosan and HA were mixed on the plate of the rheometer and measurements were started as soon as possible afterwards. G′ (squares) and G″ (triangles) are plotted on the primary y-axis; phase angle (δ- diamonds) is plotted on the secondary axis.

The formation of complexes *in vivo* will occur in the presence of other synovial fluid components. Therefore to investigate the effect that these compounds had on formation further rheology time sweeps were carried out and the results of this study are presented in Figure 3-11. Physiological salt was found to slightly delay complex gelation but did not affect the overall formation time. It also caused a slight reduction in the final G′ level which would suggest that salt also affects the overall complex strength. Inclusion of plasma proteins as well as salt (as ASFP) caused a more rapid complex gelation and formation. In this case gelation occurred almost instantaneously and formation was complete after about 60 minutes. The addition of protein also acted to slightly restore the G′ of the formed complexes but not to the level seen in complexes formed in water alone.

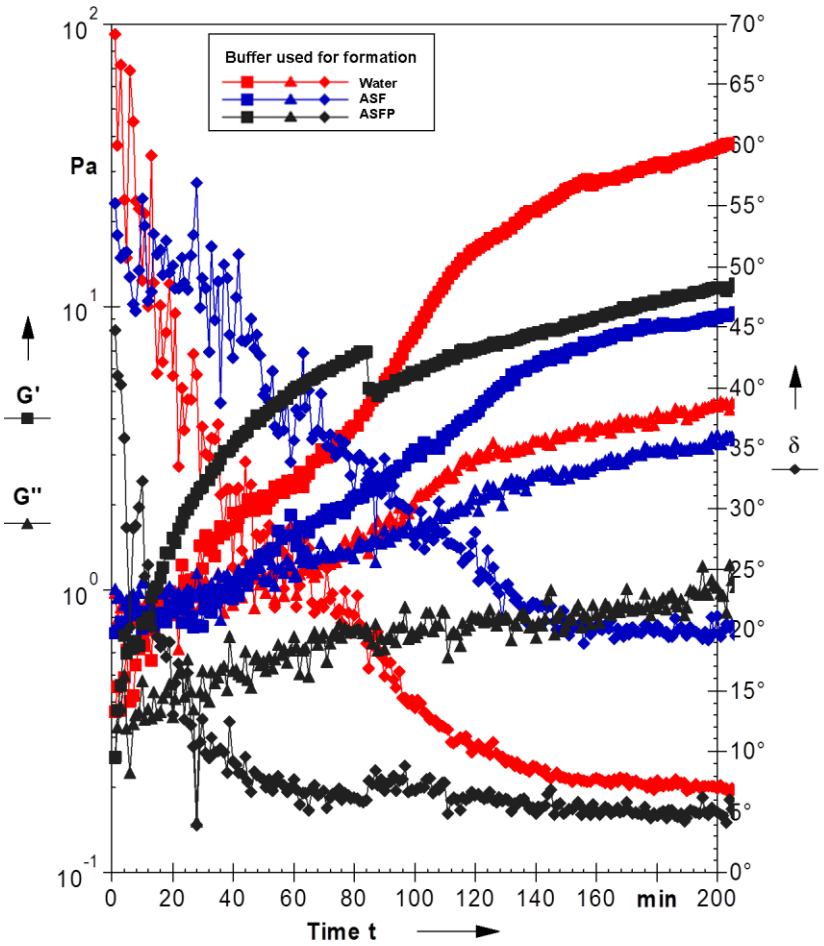

Figure 3-11 Rheology time sweeps showing the formation kinetics of Ch:HA complexes in synovial relevant conditions.
Rheology time sweeps were conducted at 37°C on mixtures of chitosan and HA at a 1:1 ratio. Chitosan and HA were mixed on the plate of the rheometer with any additional components and measurements were started as soon as possible afterwards. G′ (squares) and G″ (triangles) are plotted on the primary y-axis; phase angle (δ- diamonds) is plotted on the secondary axis.

3.3.2.2 Complex integrity

To assess the integrity and strength of the polyelectrolyte complexes rheology amplitude sweeps were used. Complexes were produced using different HA concentrations to investigate the ability to produce complexes with different rheological properties. Complexes are required that are resilient to the challenging forces experienced within the joint, however complexes which are too rigid may cause damage to the joint. The response of the joint to these complexes is unknown at the present time. The ability to produce complexes

with a variety of properties therefore allows complexes with optimal properties to be used once these have been determined.

The results of rheology amplitude sweeps on polyelectrolyte complexes are presented in Figure 3-12. These show that 1:1 ratio complexes were the most resistant to shear stress, exhibiting the highest G′ and yield stress values. At a HA concentration of 6mg/ml the G′ values for 1:1, 0.9:1 and 0.8:1 ratio complexes were all similar. At a ratio of 0.7:1 and below the G′ became significantly lowered ($P<0.001$). For complexes prepared using 3mg/ml HA, which was the concentration used previously, a more gradual decline in G′ was seen. Comparing consecutive ratios found significant differences between 1:1 and 0.9:1 ($P<0.01$); 0.8:1 and 0.7:1 ($P<0.01$); 0.6:1 and 0.5:1 ($P<0.05$) Ch:HA ratio complexes.

Complexes produced using 1.5mg/ml HA showed smaller differences in G′ values. A significant difference was found between 1:1 complexes and complexes of 0.6:1 and below ($P<0.05$). At all HA concentrations the yield stresses showed a more gradual decline as chitosan concentration was reduced and there were few significant differences. A comparison was then carried out on complexes with the same polymer ratios but produced using different HA concentrations. This found significant differences between 6mg/ml HA and both other concentrations in samples of 0.5:1 ratio and above ($P<0.001$).

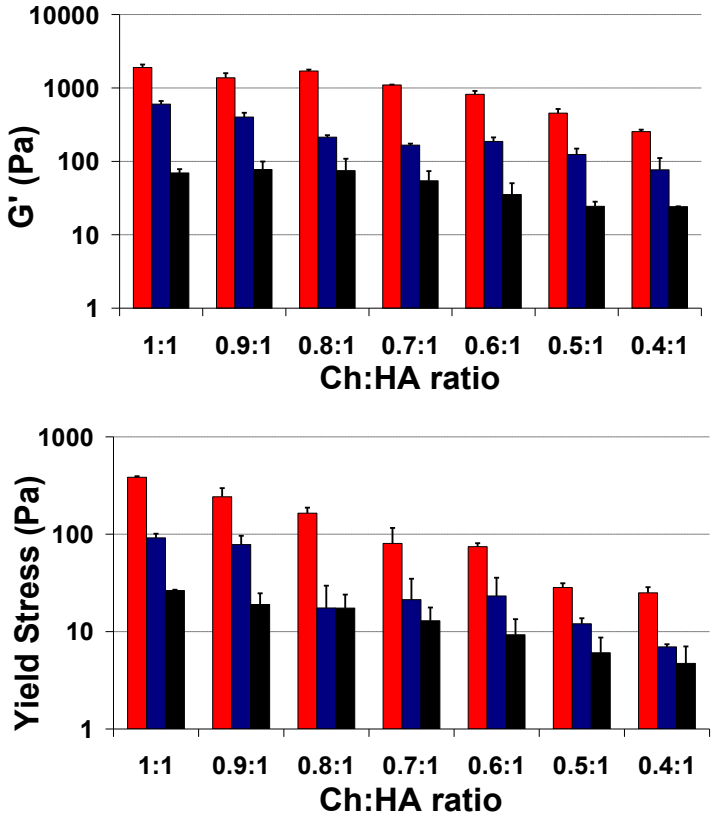

Figure 3-12 Graphs showing G′ and yield stress values for Ch:HA complexes.
G′ and yield stress values were extracted from rheology amplitude sweeps carried out on Ch:HA complexes formed at 37°C with the indicated polymer ratio. Top: G′ values in LVR; bottom: yield stress values. For both graphs the HA concentration used to prepare complexes was as follows: 6mg/ml- red; 3mg/ml- blue; 1.5mg/ml- black.

3.3.2.3 Complex degradation

The long term stability of these complexes is important for their use as a slow release delivery system. The degradation of these complexes was therefore assessed using a mass loss method. The results of this study are presented in Figure 3-13. Complexes incubated in water showed only a negligible mass loss for the 56 days of the study. Complexes incubated in a physiological salt concentration showed significantly greater level of degradation in both Ch:HA 1:1 and 0.5:1 ratio complexes ($P<0.001$). During the degradation an initial mass loss occurred over 2 weeks after which only a minimal mass loss occurred. A greater stability was found in the 1:1 ratio complexes as 69% of

the initial complex mass remained after 56 days whereas only 46% of the 0.5:1 ratio complexes remained ($P<0.001$).

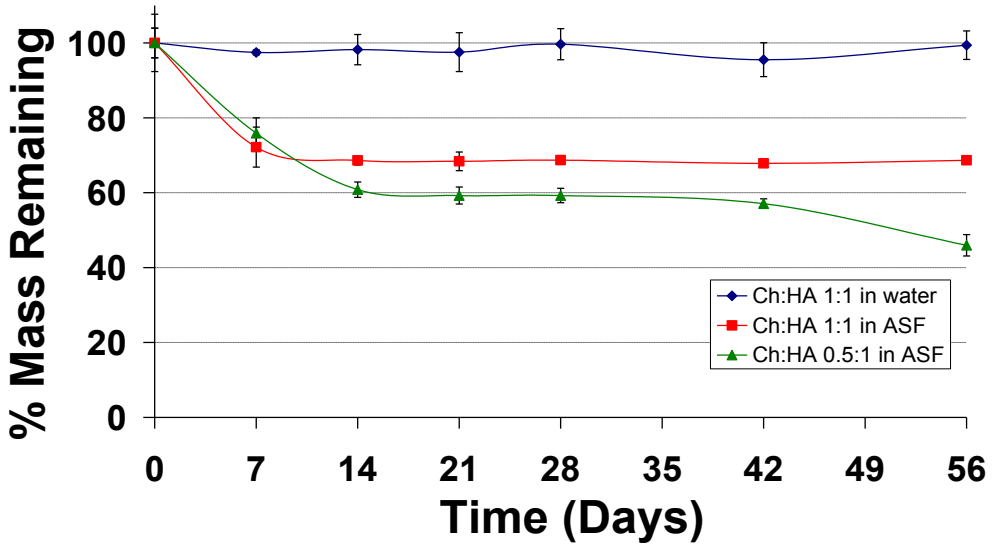

Figure 3-13 Mass degradation profiles of Ch:HA complexes in water or ASF.
Ch:HA complexes were prepared and then incubated in water or ASF at 37°C. Buffer was changed regularly and at each time point complexes were extracted, dried and weighed.

3.3.2.4 Evaluation of injectable formulation

To make an injectable formulation with these hydrogels it is proposed that complexation will be prevented by using salt. To investigate the feasibility of this method it was first necessary to investigate the effect that salt has on complex formation. This would allow the necessary concentration of salt required to prevent complexation to be determined.

The results of this photographic study are presented in Figure 3-14. This showed that the 1:1 ratio complexes were able to form in 0.3M salt or below. As salt concentration increased there was a gradual decrease in the definition of the complexes which took on a woolly appearance. At 0.4M salt concentration a very diffuse complex was visible. Then at 0.5M salt no complex formation was visible at all and the solution was easily passed

through a 25G needle. A 25G needle is the largest needle that can be used for intra-articular injection in rats. A 22G needle can be used for administration to humans but for ease of *in vivo* animal studies and patient comfort the use of a 25G needle is desirable. The 0.5:1 ratio complexes were visibly less stable in salt. A salt concentration of 0.4M entirely prevented complex formation and at a concentration of 0.3M only a very small diffuse complex was formed. In 0.2M salt and below the 0.5:1 ratio complexes were able to form into a compact and well defined form.

0M **0.1M** **0.2M** **0.3M** **0.4M** **0.5M**

Ch:HA 1:1

0M **0.1M** **0.2M** **0.3M** **0.4M** **0.5M**

Ch:HA 0.5:1

Figure 3-14 Photographs showing the effect of salt on Ch:HA complex formation.
Ch:HA complexes were prepared in the presence of increasing concentrations of NaCl. Mixtures were incubated at 37°C for 60 minutes to allow complex formation to occur before photographs were taken.

It was decided from these results to use a 0.5M concentration of sodium chloride to prevent complexation as this was the lowest concentration that completely prevented complex formation at all Ch:HA ratios. To investigate the formation of complexes from these high salt solutions a dialysis method was used. This method mimics the *in vivo* diffusion of salt that would allow complex formation to occur. Initially this dialysis formation method was investigated through photography of the forming complexes.

The results of this, presented in Figure 3-15, showed that for Ch:HA 1:1 complexes there was a rapid complex formation by this method. Small dispersed precipitates formed within 15 minutes of dialysis in both water and ASF buffer which was followed by a slower aggregation of these complexes for up until 60 minutes. After this time no further changes occurred. At the 1:1 ratio there were few differences between dialysis against water and ASF.

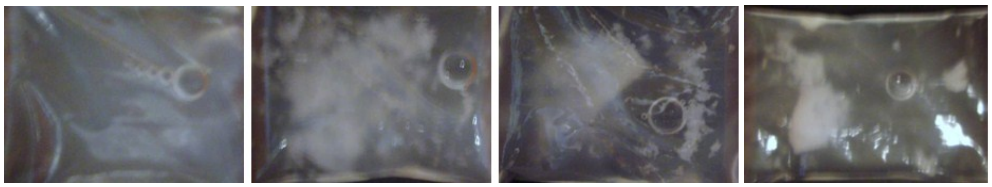

0 mins **15 mins** **30 mins** **60 mins**

Ch:HA 1:1 in water

0 mins **15 mins** **30 mins** **60 mins**

Ch:HA 1:1 in ASF

Figure 3-15 Photographs showing Ch:HA 1:1 complex formation by dialysis.
Solutions containing complex components were prepared in 0.5M NaCl. These mixtures were dialysed against water or ASF at 37°C with the buffer replaced every 15 minutes. Photographs were taken at each buffer change.

To further assess the formation using this method rheology amplitude sweeps were carried out on the forming complexes. This method used the whole solution from within the dialysis membrane and was done in order to assess the entire system and to provide a fair comparison between samples. This is different to the previous rheology amplitude sweeps which used extracted formed complexes. The important features in these results are therefore different. The first important feature is the appearance of a well defined linear viscoelastic region (LVR). The LVR is where the G′ value is constant with increasing shear stresses. The second important feature is the increase in G′ and yield stress values; this shows increases in the complex strength.

The results of this study are shown in Figure 3-16. These show that in 1:1 ratio complexes a detectable complex formation occurred in 15 minutes using both water and ASF buffer as the dialysate. A gradual increase in the G′ and yield stress was seen over 60 minutes and shows that a gradual and continued formation of complex occurred. These results confirm the observations made in the photographic study of these complexes.

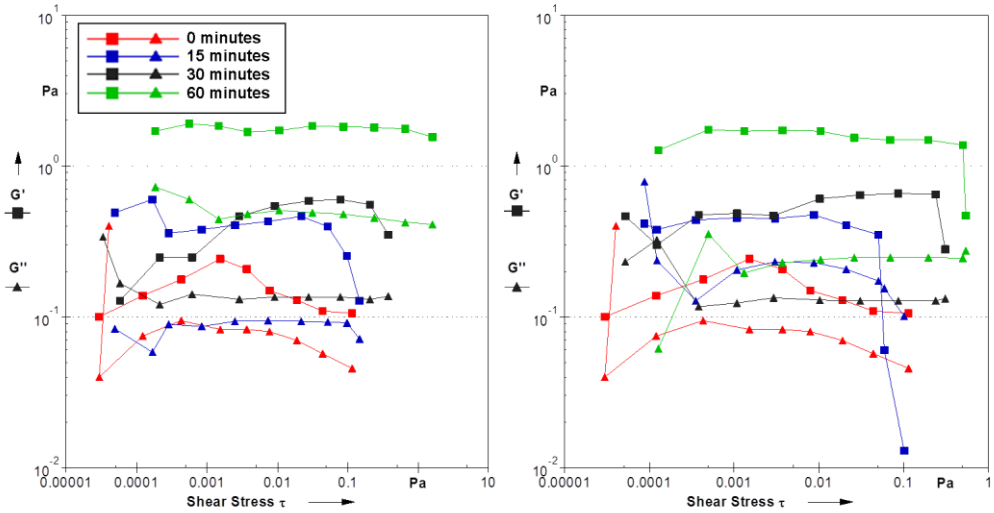

Figure 3-16 Rheology amplitude sweeps showing Ch:HA 1:1 complex formation by dialysis.
Solutions containing complex components were prepared in 0.5M NaCl. These mixtures were dialysed against water or ASF at 37°C with the buffer replaced every 15 minutes. Rheology amplitude sweeps were carried out on the recovered mixtures at 37°C. G′ (squares) and G″ (triangles) are plotted with against shear stress. Left: dialysis against water; Right: dialysis against ASF. Time of dialysis is shown in the legend and is the same for both graphs.

The dialysis formation method was also investigated with 0.5:1 ratio complexes. The photographs in this case seem to show a minimal formation of polyelectrolyte complex, Figure 3-17. However the photographs did not show the entire situation as they were taken through the dialysis membrane. The camera was not as able to cope with the dialysis membrane as the human eye and so observations in the laboratory showed further details. It was observed that a decent level of formation occurred in water, although only small, discrete complexes were formed. This formation was slower than occurred at the 1:1 ratio. Complex was visible after 30 minutes and changes were observed

throughout the 120 minutes of this study. Dialysis against ASF resulted in very little visible formation. Rheology amplitude sweeps on 0.5:1 Ch:HA ratio samples failed to show any measurable complex formation.

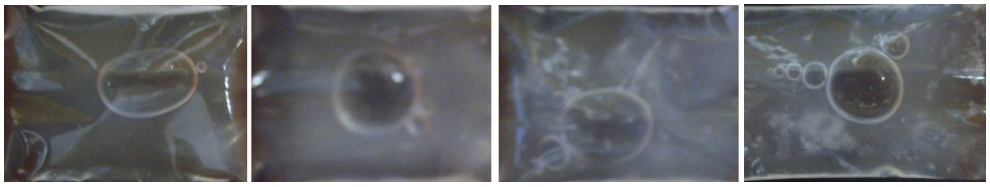

0 mins **15 mins** **30 mins** **120 mins**

Ch:HA 0.5:1 in water

0 mins **15 mins** **30 mins** **120 mins**

Ch:HA 0.5:1 in ASF

Figure 3-17 Photographs showing Ch:HA 0.5:1 complex formation by dialysis.
Solutions containing complex components were prepared in 0.5M NaCl. These mixtures were dialysed against water or ASF at 37°C with the buffer replaced every 15 minutes for 1 hour and then every 30 minutes. Photographs were taken at each buffer change.

3.4 Discussion

3.4.1 Pluronics

Pluronic F127 was found to be liquid in solutions below 20% (w/v) at 22°C. Hydrogels were produced at 37°C in solutions of 15% and above. These results are in line with what has been previously observed for Pluronic F127. Solutions below 16% were found to be unable to form a gel at 37°C and a 20% solution had a gelation temperature of just above 20°C (Chung et al., 2008, Malmsten and Lindman, 1992).

The effect that synovial fluid components had on complex formation was investigated. This produced contradictory results. For example the inclusion of a physiological salt concentration had no visual effect on gel formation. But the rheology study found that salt slowed gel formation and reduced resistance

to shear stress. However these methods looked at different factors. The visual studies looked at formed gels and creep under relaxed conditions. The rheology studies looked at the formation kinetics under dynamic shear stress.

Previous studies have also shown that a number of small molecules can affect the gelation temperature of Pluronic F127. Sodium chloride has been found to reduce gelation temperature (Guzman et al., 1992, Malmsten and Lindman, 1992, Vadnere et al., 1984), with urea and ethanol increasing gelation temperature (Vadnere et al., 1984). Therefore the addition of physiological salt in this study (as PBS) might have been expected to cause a reduction in gelation temperature. This was not seen, but as the 15% Pluronic solution in water was found to gel at 37°C this effect would have been hard to observe. No reduction in creep was seen with salt included which would have given an indication of a better hydrogel formation.

The disruption of hydrogels when hyaluronic acid was included may be due to HA being a large polymer. High molecular weight PEG has been observed to raise the gelation temperature of Pluronic F127 (Gilbert et al., 1987) and a similar effect with HA would account for the disruption that was observed. This may have been caused by the HA polymer chains reducing the mobility of the Pluronic polymer chains and therefore disrupting their organisation into micelles and hydrogels. The rheology amplitude sweeps showed a slight increase in yield stress when HA was included. This change could be explained by the HA polymer chains stretching throughout the gel and providing a greater physical strength. The inclusion of both salt and hyaluronic

acid reversed some of the disruptive effects seen with one additive alone. Salt would become associated with the HA as a counterion and this would act to shield the charges on HA as well as reducing the free salt. This would account for the reversal of the effects seen.

It was found that Pluronic F127 hydrogels were degraded within 24 hours. This rapid degradation is consistent with these hydrogels being physical gels. The degradation of these gels can occur simply through dissolution of the exterior of the gel. These results are similar to previous reports, where Pluronic F127 hydrogels were found to be rapidly degraded by surface dissolution within 24 hours (Jeong et al., 2002, Nanjawade et al., 2007, Chung et al., 2008).

The stability problems with Pluronics have been overcome by other investigators by the development of chemically modified Pluronic or Pluronic based systems. This has included cross-linked Pluronic hydrogels (Cohn et al., 2005), Pluronic chains linked end to end (Cohn et al., 2006), or Pluronics modified with other polymers (He et al., 2008, Ruel-Gariepy and Leroux, 2004, Kim and Park, 2002, Chung et al., 2008). However this approach has still not been able to produce hydrogels with the long term stability required for this delivery system.

3.4.2 Chitosan and Hyaluronic Acid Polyelectrolyte Complexes

A number of studies have been carried out on precipitated complexes between chitosan and HA. Generally the complexes have been produced and then dried

before use (Denuziere et al., 1998, Kim et al., 2004). The stoichiometry is often the only property investigated whilst the complexes are still in solution. Further studies were then carried out on the freeze dried complexes. It has also been most common for stoichiometric complexes to be investigated as this ensured that no excess polymer was present which would generally improve the biocompatibility. This leaves little relevant literature for comparison to the complexes produced in this study, which were in solution and used varying chitosan concentrations.

Initial investigations found that precipitated complexes were able to form using reduced chitosan concentrations. Complexes were also found to be stable in physiological salt concentrations. These results show that these complexes would be able to form under physiological conditions.

A rapid complex formation is required to prevent clearance from the joint before formation can occur. The polyelectrolyte complexes showed an immediate precipitation followed by a slower rearrangement. Complex formation was visually complete after 30 minutes, but rheology time sweeps showed changes continued for around 150 minutes. The differences between the visual observations and rheological results are due to the differences between these methods. Rheology was carried out on a thin film and this will limit the mobility of the polymers, and therefore a slower formation was observed. The rheology showed that 0.5:1 ratio complexes experience a slightly slower gelation, but overall formation time remained the same. This would be important *in vivo* as once the system is gelled it will not be subject to

clearance. Gelation refers to the whole system rather than the complexes alone as the rheology was carried out on the entire solution.

Some sudden drops were seen in G′ values during rheology time sweeps, Figure 3-11. These may be due to slippage occurring as the plate used in the rheology was smooth (Walls et al., 2003). Slippage may cause slight deviation for individual results but will not affect the overall rheology results as smooth plates were used for all studies and all rheology was repeated to ensure consistent results.

The effect that a number of synovial fluid components had on formation of these complexes was investigated. This study found that salt acted to slow formation. Salt will effectively shield the charges on the polymer, which reduces the interactions between polymers and causes slower formation.

However these complexes are not suitable for use as an injectable formulation. No investigations have been carried out into an injectable system using these polymers alone. A protocol of sequential injection or co-injection could be devised to allow injection, but this would be unlikely to give a good and repeatable complex formation. It would also increase the complexity of administration for this system. A formulation using salt to prevent complexation was therefore investigated.

It was first necessary to investigate the stability of the complexes in salt. Complexes between HA and chitosan were stable in salt concentrations of up

to 0.4M for 1:1 ratio complexes and up to 0.3M for 0.5:1 ratio complexes. The results for 1:1 ratio complexes agree with what has previously been reported. One previous study found that complexes between chitosan and HA did not form above 0.5M salt concentration (Lee et al., 2003).

The lower stability of 0.5:1 ratio complexes in salt can be explained by the formation of polyelectrolyte particles rather than a gel. Polyelectrolytes are known to form into particles when there is a high overall charge in the solution. This high overall charge can be due to salt or due to an imbalance in polymer concentrations. At the 0.5:1 ratio there is an imbalance in the polymers and therefore less salt is required to reach the overall charge where small polyelectrolyte particles form.

This stability in salt is better than some other polyelectrolyte complexes, for example chitosan with polyethyleneimine (Boughellam, 2007). The stability of these Ch:HA complexes is due to the compatibility of the polymers. Chitosan and HA both have low charge densities. There is one charge per residue for chitosan and one charge every other residue for HA (Denuziere et al., 1996, Luppi et al., 2009). These similar charge densities allow the polymers to bond tightly together and it has been suggested that this gives Ch:HA complexes their stability (Denuziere et al., 1996, Kim et al., 2004).

The use of salt can therefore produce an injectable liquid. Complex formation from this liquid could then be achieved by dialysis. The Ch:HA 1:1 ratio showed complex formation after 15 minute and little difference was seen

between dialysis against water and ASF. This shows that these complexes have potential as an injectable system.

The 0.5:1 Ch:HA ratio complexes showed a slower and less complete formation which can be explained by the lower stability of this ratio in salt. A greater reduction in salt is therefore needed before formation can occur which also prevents a more complete formation from occurring. The only question that arises with this formation method is the biocompatibility of the high salt concentrations. Studies have shown that this brief hypertonic challenge does not cause significant damage to chondrocytes *in vitro* (Boughellam, 2007).

Rheology amplitude sweeps showed that complexes with a wide range of rheological properties can be produced. The 1:1 ratio complexes produced the most resilient complexes. The 1:1 ratio is the stoichiometric ratio and theoretically gives the best interaction and incorporation of polymers. These studies were conducted on complexes which entirely covered the plate of the rheometer (which is its measuring surface). The measurements are therefore comparable and do not reflect changing amounts of complex.

The ideal rheological properties for these complexes within the joint are not known. The complexes need to be sufficiently resilient to shear stresses so that they are not immediately destroyed by the forces within the joint (Seireg and Arvikar, 1975, Sharma et al., 2007). They also need to be sufficiently flexible so that they don't cause damage to the joint (Gerwin et al., 2006, Sharma et al., 2007, Seireg and Arvikar, 1975). It has been shown that complexes with a

wide variety of rheological properties can be synthesised. Therefore if the complexes are found to not have the required properties during *in vivo* studies an alternative formulation could be used.

It was also interesting to note where the G′ and yield stress values were similar in complexes produced using different HA concentrations. The comparison was carried out between 1:1 complexes and complexes produced using double the HA concentration. In this comparison it would be expected that similar G′ and yield stress values would be found with the 0.5:1 ratio at the higher HA concentration. This would be the case if complex properties were only affected by polymer concentration. It was found that for the G′ similar values were found for 0.5:1 or 0.4:1 Ch:HA ratio complexes to the 1:1 ratio complexes using half the HA concentration. For yield stresses this same point occurred for the Ch:HA 0.6:1 ratio complexes. These results suggest that the properties of these complexes are affected by both the polymer ratio and concentration.

It was intended to assess the degradation of these complexes through the quantification of released polymer. This method allows the monitoring of individual complexes throughout their degradation and means that the degraded complex would be available for further analyses. Various methods have been published for the quantification of chitosan and HA; examples include the use of ninhydrin for the quantification of chitosan (Leane et al., 2004, Sahu et al., 2009, Shirosaki et al., 2009) and dye binding methods for both polymers (Wischke and Borchert, 2006, Park et al., 2005, Tang et al., 2007, Johnston, 2000). However none of these methods were able to assess the

release with the required sensitivity or were not able to be successfully reproduced in trial studies.

An alternative method was therefore required to monitor degradation. A mass loss method was chosen as this has been widely used to monitor the degradation of various hydrogels (Alexander and Shakesheff, 2006, Ferruti et al., 2005, Wu et al., 2007, Chung et al., 2008, Kim and Park, 2002, Tan et al., 2009).

The stability of these complexes in water shows the intrinsic stability of these complexes. The stability of these complexes in physiological salt is also impressive, with a significant proportion of complex remaining after 56 days. The degradation occurred in an initial burst which was followed by a period of minimal degradation which suggests that there is an initial loss of less well bound polymers from the surface leaving a strongly bonded core that is highly resilient to salt.

The level of degradation is similar to another study carried out on cross-linked hydrogels of chitosan and hyaluronic acid (Tan et al., 2009). Tan et al. found a gradual degradation over 28 days in PBS with around 60% of the complex remaining after this time. Similar degradation profiles were seen with different polymer ratios except when there was a large excess of one polymer (9:1 ratio). It is promising that the complexes in this study were produced without cross links but still have a similar degradation profile.

3.5 Conclusions

The results obtained from these hydrogel systems show that the polyelectrolyte system has the most promising and favourable properties for the intended application. The Pluronic F127 hydrogels showed a lack of stability as they lost over half their Pluronic content within 24 hours.

To improve the stability of Pluronic F127 hydrogels chemical crosslinking is a possible option. One of the attractions of the Pluronic polymers was the fact that they are a Food and Drug Administration approved material. Chemical modification would negate this advantage. Also the degradation of Pluronic hydrogels was so rapid that even with modifications it would be a challenge to produce hydrogels with the required stability. The maximum length of degradation that has been found with a chemically modified Pluronic F127 hydrogel was 14 days in a physiological buffer (Chung et al., 2008, Kim and Park, 2002).

However the results obtained for the polyelectrolyte system are promising. They show that complexes form rapidly, can be produced in an injectable form and have a high stability in physiological salt concentrations. Preliminary investigations also showed that these complexes are able to efficiently incorporate nanoparticles. The stability in salt is particularly encouraging as salt is known to be disruptive to polyelectrolytes.

These promising properties have therefore led to the selection of this system for further study and the elimination of the Pluronic F127 hydrogels. The

stability seen with the polyelectrolyte complexes has come under less demanding conditions than those found within the joint. It would be desirable to have covalent cross-links within the system to provide a greater stability that may be required *in vivo*. These cross-links would also help to stabilise the reduced chitosan complexes and improve their properties. The next chapter therefore investigates the synthesis of a modified hyaluronic acid and its inclusion into polyelectrolyte complexes.

CHAPTER 4 - SYNTHESIS OF A MODIFIED HYALURONIC ACID AND ITS INCORPORATION INTO POLYELECTROLYTE COMPLEXES

4.1 Introduction to Chemically Modified Hyaluronic Acids

A variety of chemical approaches have been investigated for modifying hyaluronic acid in order to improve its properties. Modified hyaluronic acids have been used for applications such as eye surgery, anti-adhesion films and cosmetics (Prestwich and Kuo, 2008). A number of products utilising modified HA have been approved and are currently marketed.

4.1.1 Types of Modification

4.1.1.1 Carboxylate group modifications

The structure of hyaluronic acid has two targets for chemical modification. These are the carboxylate group and the pendant hydroxyl group, which are illustrated in Figure 4-1. The carboxylate group in hyaluronic acid is the most common target for modifications.

At this site carbodiimide chemistry is the most common scheme used. Carbodiimides react with carboxylates and in the presence of nucleophiles, such as amines or hydrazides, facilitate the formation of amides or esters respectively. Hyaluronic acid is water soluble and poorly soluble in other solvents. This means that the water soluble carbodiimide 1-ethyl-3-(3-dimethylaminopropyl)carbodiimide (EDAC) has been widely used for HA modification. Examples of carbodiimide modifications include HA modified

with PEG (Moriyama et al., 1999); HA conjugated to a dye (Collis et al., 1998); and HA with pendant thiol groups by using a hydrazide (Pouyani et al., 1994, Shu et al., 2002) or cystamine as a nucleophile (Lee et al., 2007).

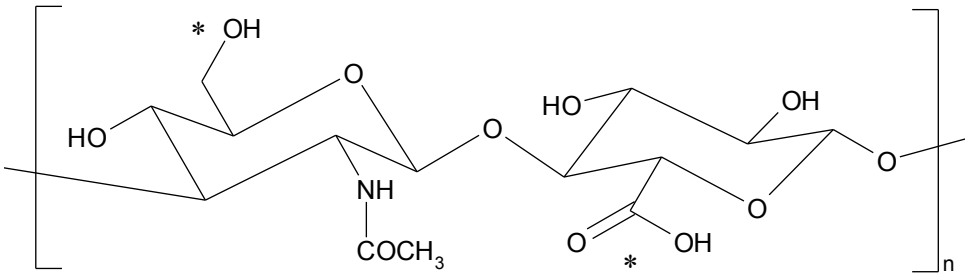

Figure 4-1 Structure of hyaluronic acid with the two most commonly modified groups marked with a star.

Other reactions using carbodiimides are also possible. The reaction of EDAC alone with HA produces an N-acylurea adduct. These adducts can produce hydrogels as the acylurea interacts with other carboxylates within HA leading to gelation (Kuo et al., 1991). There have also been attempts to cross-link HA through carbodiimide chemistry, examples include a conjugation using multivalent hydrazides (Prestwich and Kuo, 2008), or a biscarbodiimide (Kuo et al., 1991, Prestwich, 2001).

4.1.1.2 Hydroxyl group modifications

Modification of the pendant hydroxyl groups on hyaluronic acid is also possible. Hyaluronic acid also contains hydroxyl groups on its sugar rings, but these are sterically hindered and much more challenging to modify.

Hylans are a group of hyaluronic acids modified on their pendant hydroxyl groups and there are two main hylans with different modifications. Hylan A is a liquid HA and contains cross links between HA and proteins through the use

of formaldehyde (Band, 1998). Hylan B is a gel that is cross-linked through the use of divinylsulfone (DVS) (Band, 1998). DVS has also been used to cross-link HA with other polymers such as carboxymethyl cellulose and hydroxyethylcellulose (Sannino et al., 2004).

4.1.1.3 Other

Modifications that target both the carboxylate and hydroxyl groups on HA have been investigated. Epoxides can react with amino, carboxyl and hydroxyl groups. The reaction of bisepoxides with HA produces a cross-linked product (Lindqvist et al., 2002). An alternative reaction scheme used 2-chloro-1-methylpyridinium iodide to cause the formation of internal ester bonds between the HA hydroxyl and carboxylates (Barbucci et al., 2003, Barbucci et al., 2002).

4.1.2 Uses of Modified Hyaluronic Acid

4.1.2.1 Prevention of post-surgical adhesions

Modified hyaluronic acid hydrogels are widely used for the prevention of post-surgical adhesions. Post-surgical adhesions are internal scar tissue that causes aberrant internal adhesions. They can be caused by infection, trauma or surgical damage. The rate of adhesions after surgery can be very high and can cause complications including pain and infertility (Yeo and Kohane, 2008).

A number of modified hyaluronic acid hydrogels are commercially available for the prevention of adhesions. These include Seprafilm® (Genzyme, USA),

Incert®-S (Anika Therapeutics, USA), Hyalobarrier® (Nordic Pharma Group, France) and Hyaloglide® (Anika Therapeutics) (Prestwich and Kuo, 2008).

4.1.2.2 Viscosupplementation

Hyaluronic acid is used to restore the protective properties of synovial fluid that are lost in osteoarthritis. A number of the currently available HA preparations for viscosupplementation contain chemically modified HAs, see Table 1-1. For example Hylan GF-20 (Genzyme, USA) is a combination of hylan A (90%) and hylan B (10%) (Prestwich and Kuo, 2008).

4.1.2.3 Other uses

Hyaluronic acid has been widely used for cosmetic applications and modified HA has been used as a dermal filler. Products marketed as dermal fillers include Restylane® (Q-med, Sweden), Hylaform® and Puragen® (Mentor, USA) (Prestwich and Kuo, 2008). Modified HAs have also been used as wound dressings and as scaffolds for chondrocytes or dermal fibroblasts (Prestwich and Kuo, 2008).

4.1.3 Modified Hyaluronic Acid in Hydrogels

Many chemically modified hyaluronic acid derivatives have been incorporated into hydrogels and injectable hydrogels. An injectable HA hydrogel has been produced with HA conjugated to tyramine. Hydrogels were formed *in situ* through the action of HRP (horseradish peroxidise) (Lee et al., 2008). Another injectable hydrogel utilised separate cross-linking of HA and carboxymethyl cellulose to form an interpenetrating network (IPN) (Barbucci et al., 2010). An

IPN occurs where two crosslinked polymer networks become entangled with no bonding between the different polymers. These two hydrogels have been characterised but have not been investigated for any potential applications.

Pluronic F127 and HA have been cross-linked together through photopolymerisation. This produced hydrogels that degraded gradually over 28 days and gave a sustained protein release over 14 days *in vitro* (Kim and Park, 2002). An injectable system composed of HA conjugated to a thermosensitive polymer has also been produced. This system consisted of PNIPAM conjugated to chitosan which was then conjugated to HA (Chen and Cheng, 2009, Fang et al., 2008) and produced polymers with gelation temperatures around 30°C (Chen and Cheng, 2009, Fang et al., 2008). Hydrogels produced gave drug delivery over 2 days with hydrophilic drugs giving a burst release whereas hydrophobic drugs gave a more sustained delivery (Fang et al., 2008).

Hyaluronic acid derivatives have not however been incorporated into precipitated polyelectrolyte complexes. The closest example has been the production of polyelectrolyte particles using a modified chitosan (Wu et al., 2007). In this system PEG modified chitosan was used to improve the solubility of the system and avoid precipitated complexes.

4.1.4 Chapter Aims

The aim in this chapter was to produce and characterise a modified hyaluronic acid (HAM). This modification was the inclusion of cysteamine on the carboxylate groups through a reaction catalysed by EDAC and the structure of the HAM is shown in Figure 4-2.

The reaction was conducted in aqueous conditions and this is well known to produce low reaction yields (usually of around 30%). To overcome this three times the required molar amount of cysteamine was used. For this study the percentage modification of HA refers to the percentage of repeating units that have been modified. A 10% modification was aimed for. It was hoped that this would give increased stability but not interfere with the formation or biocompatibility of the complexes.

HAM was then used in polyelectrolyte complexes. The properties of these complexes were assessed and compared to those prepared with unmodified HA. It was hoped that HAM would produce more resilient complexes that were more resistant to degradation. This would allow complexes to survive within the joint for three months, which is the aim for this delivery system.

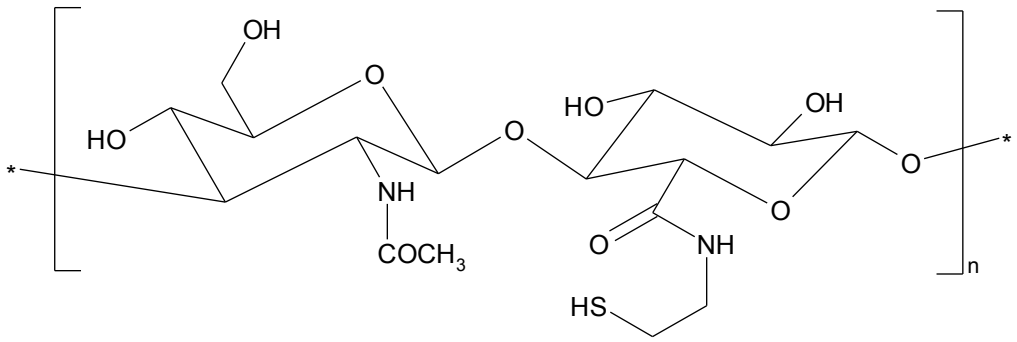

Figure 4-2 Structure of the cysteamine modified hyaluronic acid (HAM) used in this study.

4.2 Materials and Methods

4.2.1 Materials

The materials used are detailed in section 2.1.

4.2.2 Modified Hyaluronic Acid Preparation and Characterisation

4.2.2.1 Synthesis of modified hyaluronic acid

Modified hyaluronic acid was synthesised using the method in section 2.4.1.

4.2.2.2 Characterisation of modified hyaluronic acid

Modified hyaluronic acid was characterised using the method in section 2.4.2.

4.2.3 Polyelectrolyte Complex Preparation and Characterisation

4.2.3.1 Complex formation with modified hyaluronic acid

Modified hyaluronic acid was used in exactly the same way as unmodified hyaluronic acid. Complexes were prepared as detailed in section 2.3.2.2 and the formation was assessed using the methods in section 2.3.2.2.

4.2.3.2 Rheology amplitude sweeps

Rheology amplitude sweeps on complexes containing modified hyaluronic acid were carried out as described in section 2.3.2.3.

4.2.3.3 Complex degradation

The degradation of complexes containing modified hyaluronic acid was analysed using the method described in section 2.3.2.4.

4.2.3.4 Effect on salt on complex formation

The effect of salt on the formation of complexes containing modified hyaluronic acid was analysed using the method described in section 2.3.2.5.

4.2.3.5 Complex formation by dialysis

Complexes containing modified hyaluronic acid were prepared by the dialysis method described in section 2.3.2.4. The formation of these complexes was analysed using the methods detailed in section 2.3.2.6.

4.3 Results

4.3.1 Modified Hyaluronic Acid Synthesis and Characterisation

Hyaluronic acid was reacted with cysteamine and EDAC in a 1:3:4 molar ratio (HA monomer:cysteamine:EDAC). The reaction was carried out in aqueous solution at room temperature. The reaction resulted in the production of a modified hyaluronic acid, which will be referred to as HAM. Characterisation of the polymer using NMR was unsuccessful due to the viscosity of hyaluronic acid solutions limiting the sample concentration and therefore preventing characterisation of the modification.

Ellman's Test was therefore used to determine the concentration of incorporated sulfhydryl groups. This found the modification level to be 0.91%, Table 4-1, which is much lower than originally intended. Initial investigations found that even these low modification levels caused changes in the complex properties. The modified HA was stable in solution and did not spontaneously

form hydrogels. This was the desired situation and is an advantage of the low modification level.

Theoretical modification level	Actual modification	Standard Deviation
10%	0.91%	0.03

Table 4-1 Hyaluronic modification level in HAM as determined by Ellman's Test.

4.3.2 Characterisation of Complexes with Modified Hyaluronic Acid

4.3.2.1 Complex formation

A photographic study was undertaken to assess the formation of complexes with HAM. This study also investigated the ability of complexes to form in the presence of physiological salt. The results of this study are presented in Figure 4-3. This found that complexes were similar in appearance to those produced with unmodified HA. The complexes retained the compact and well defined form seen with Ch:HA complexes. As the chitosan concentration was reduced the Ch:HAM complexes became smaller and had a more fibrous appearance.

The only obvious difference between Ch:HAM and Ch:HA complexes was in the bulk solution. For Ch:HAM complexes this solution was cloudy at the 0.8:1 ratio and below, whereas at 0.9:1 and 1:1 ratios it was clear. The Ch:HA samples showed a slight turbidity that was consistent at all ratios. The turbidity in the Ch:HAM complexes varied between batches, for example the 1:1 complex produced in the formation study showed a turbid bulk solution, Figure 4-4. Physiological salt caused a slight disruption of the Ch:HAM complexes and increased their fibrous appearance. In all cases visible formation occurred and there was a degree of turbidity in the bulk solution.

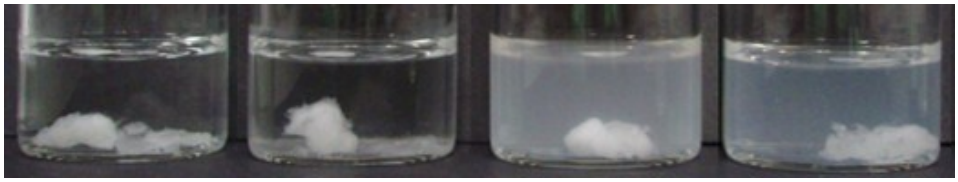

1:1 0.9:1 0.8:1 0.7:1

0.6:1 0.5:1 0.4:1

Complexes prepared in water

1:1 0.9:1 0.8:1 0.7:1

0.6:1 0.5:1 0.4:1

Complexes prepared in ASF

Figure 4-3 Photographs showing Ch:HAM complexes of various polymer ratios prepared in water or ASF buffer.

Ch:HAM complexes were prepared at the indicated polymer ratio in water or ASF. Complexes were incubated at 37°C for 60 minutes before photographs were taken.

The formation kinetics of Ch:HAM complexes were studied using the same methods as the Ch:HA complexes, which were a photographic study and rheology time sweeps. These results showed a dramatic change in formation with Ch:HAM complexes forming immediately into compact complexes, Figure 4-4, with little change observed after this. There was no visual difference in the kinetics of formation between Ch:HAM complexes at different polymer ratios.

0 minutes 10 minutes 20 minutes 30 minutes

40 minutes 50 minutes 60 minutes

Ch:HAM 1:1 complexes

0 minutes 10 minutes 20 minutes 30 minutes

40 minutes 50 minutes 60 minutes

Ch:HAM 0.7:1 complexes

0 minutes 10 minutes 20 minutes 30 minutes

40 minutes 50 minutes 60 minutes

Ch:HAM 0.5:1 complexes

Figure 4-4 Photographs showing the formation of Ch:HAM complexes at different polymer ratios in water.

Chitosan and HAM at varying ratios were mixed and incubated at 37°C. Photographs were taken at the indicated time.

The results of the rheology time sweeps are presented in Figure 4-5 and confirm the visual observations. Ch:HAM complexes appeared to exhibit an instantaneous gelation, but in reality this occurred before measurements could start. The formation of Ch:HAM complexes was complete after 60 minutes when the G′ value stabilised.

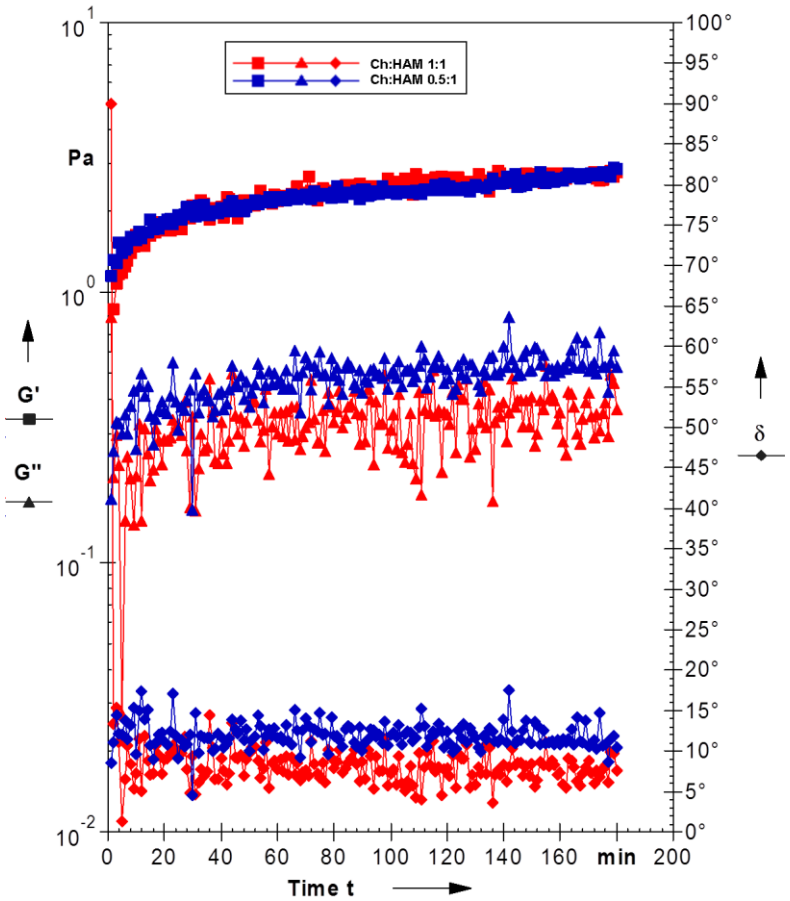

Figure 4-5 Rheology time sweeps showing the formation kinetics of Ch:HAM complexes. Rheology time sweeps were conducted at 37°C. Chitosan and HAM, at different ratios, were mixed on the plate of the rheometer and measurements were started as soon as possible afterwards. G′ (squares) and G″ (triangles) are plotted on the primary y-axis; phase angle (δ-diamonds) is plotted on the secondary axis.

The formation of complexes will occur within the joint. The effect that synovial fluid components had on formation was investigated through rheology time sweeps. These results, presented in Figure 4-6, showed that physiological salt caused a slowing in the formation of Ch:HAM complexes. There was a slight reduction in the final G′ value which suggests that salt also slightly reduces the overall complex strength. When protein was also included (as ASFP) the formation kinetics were similar to those in water but the final G′ value was still reduced. The presence of HA interfered with Ch:HAM complex formation, as the G′ evolved gradually over 150 minutes, rather than 60 minutes as previously observed.

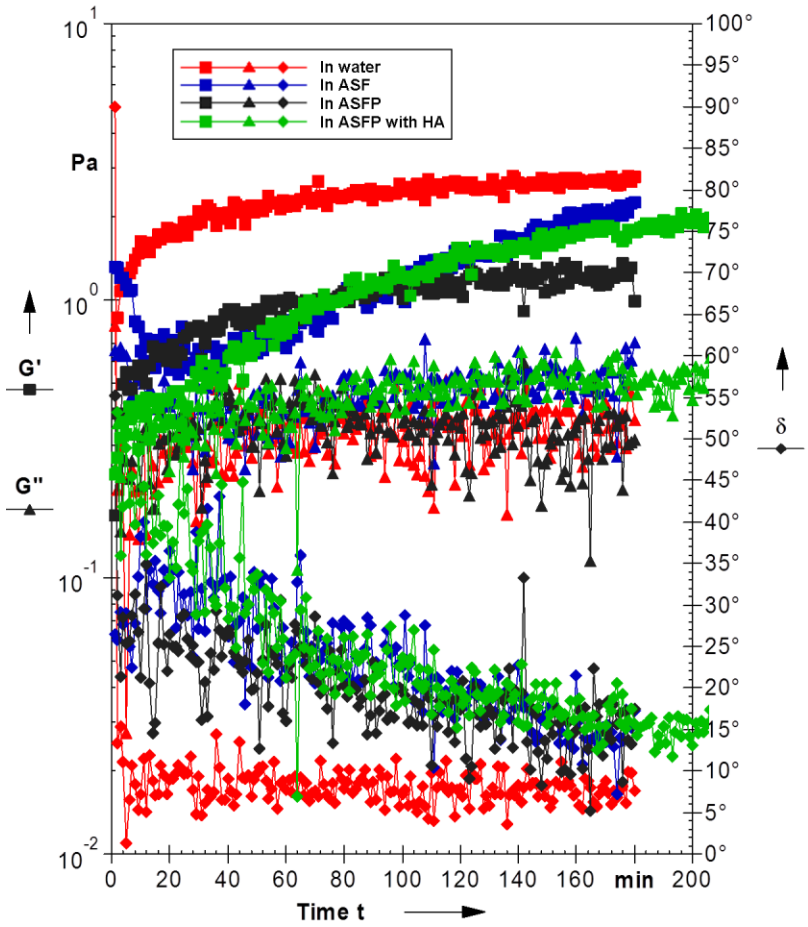

Figure 4-6 Rheology time sweeps showing the formation kinetics of Ch:HAM complexes under synovial relevant conditions.
Rheology time sweeps were conducted at 37°C on Ch:HAM 1:1 ratio complexes. Chitosan and HAM were mixed on the plate of the rheometer with any additional components and measurements were started as soon as possible afterwards. G′ (squares) and G″ (triangles) are plotted on the primary y-axis; phase angle (δ- diamonds) is plotted on the secondary axis. Buffer used for formation is shown in the legend.

4.3.2.2 Complex integrity

Rheology amplitude sweeps were conducted to assess the effect of HAM on complex strength. The key parameters of G′ and yield stress values from these amplitude sweeps are presented in Figure 4-7. These results showed that HAM caused an increase in gel strength of these complexes. At all polymer ratios studied Ch:HAM complexes had larger G′ and yield stress values than equivalent Ch:HA complexes. These differences between Ch:HA and Ch:HAM complexes were statistically significant ($P<0.05$) at ratios between 1:1 and 0.5:1 for both G′ and yield stress values. The increases in yield stresses were

relatively larger than those of the G′. The 0.9:1 ratio Ch:HAM complexes had the greatest G′ and yield stress values. This would suggest that the modification has slightly altered the charge ratios of these complexes. This is expected as the ratios and chitosan concentrations were not recalculated to take account of the lost carboxylate groups in HAM.

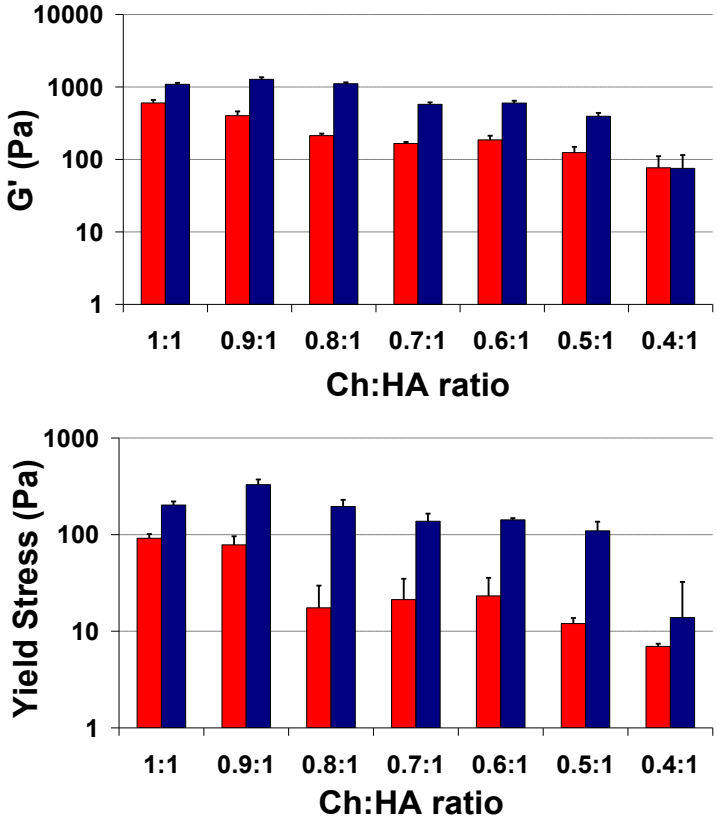

Figure 4-7 Graphs showing G′ and yield stress values for Ch:HA and Ch:HAM complexes.
G′ and yield stress values were extracted from rheology amplitude sweeps carried out on complexes at 37°C of the indicated polymer ratios. Top: G′ value in LVR; bottom: yield stress value. For both graphs: Ch:HA complexes- red; Ch:HAM complexes- blue.

4.3.2.3 Complex degradation

The long term stability of these complexes is a key property to allow for their use as a slow release delivery system. The effect of HAM on complex degradation was assessed using the mass degradation method used with the Ch:HA complexes. This showed that Ch:HAM complexes had a similar degradation profile to Ch:HA complexes, Figure 4-8. Ch:HAM complexes

were stable in ASF for the 56 days of the study and over 60% of the complex remained at the end of the study. The complexes showed an initial rapid mass loss over 2 weeks which was followed by minimal degradation. The Ch:HAM 1:1 complexes showed a more gradual initial degradation, with a significant difference found between Ch:HAM 1:1 and Ch:HA 1:1 complexes at 7 days ($P<0.001$), but no significant differences were found at other time points. Analysis of the 0.5:1 ratio complexes showed that HAM caused a significant difference ($P<0.01$) compared to Ch:HA complexes at 56 days only. This shows that at this lower chitosan concentration HAM stabilised the complexes.

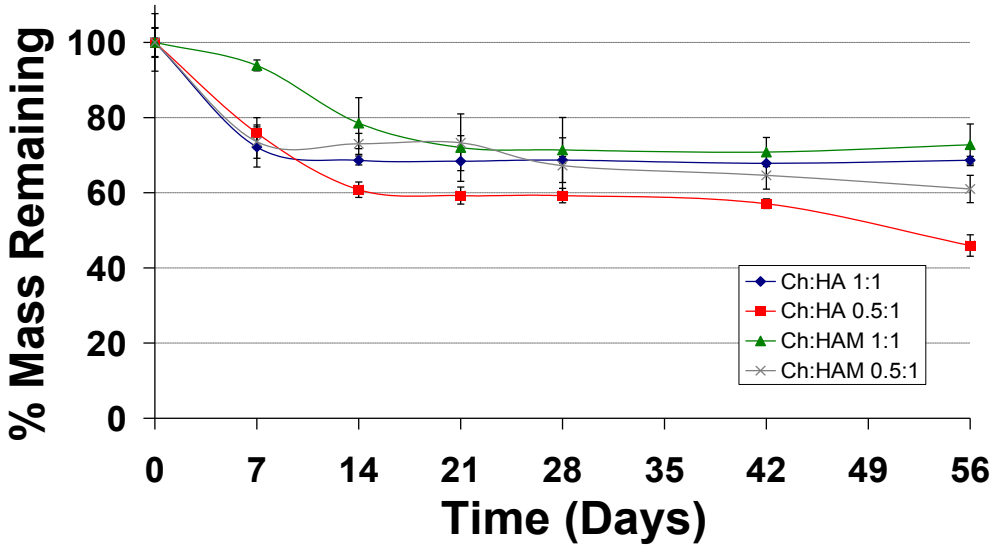

Figure 4-8 Mass degradation profiles of Ch:HA and Ch:HAM complexes in ASF.
Ch:HA and Ch:HAM complexes were prepared and were then incubated in ASF buffer at 37°C. Buffer was regularly changed and at each time point complexes were extracted, dried and weighed.

Due to the forces that can occur within joints it is important to not only consider the complex mass loss but also the effects that this has on the integrity and strength of the complexes. In order to assess these properties degraded samples were analysed using rheology amplitude sweeps. The results of this study are presented in Figure 4-9. This shows that despite the significant mass loss the complexes retained their integrity and much of their strength. The G′

values showed very little difference over the study period. The complexes appear to exhibit a slight increase in G′ after 4 weeks before dropping back after 8 weeks of degradation. The yield stress results showed a more gradual decline. This shows that there is a gradual loss of resistance to shear stresses whilst the overall structure and strength of the complexes is unaffected.

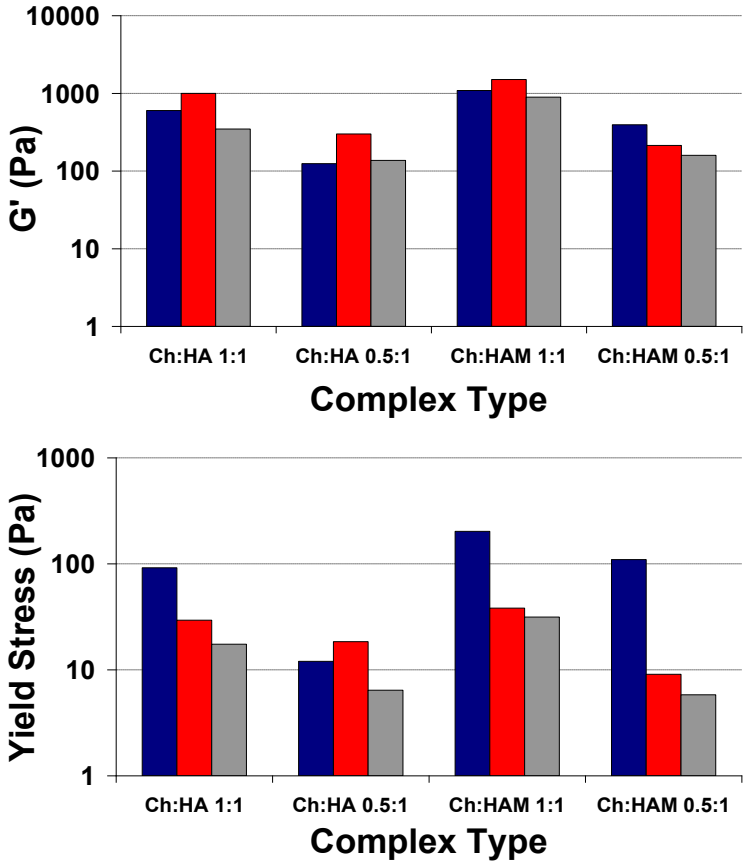

Figure 4-9 G′ and yield stress values for Ch:HA and Ch:HAM complexes during degradation in ASF.
G′ and yield stress values were extracted from rheology amplitude sweeps carried out on degraded complexes at 37°C. Top: G′ value in LVR; bottom: yield stress value. For both graphs, the time of degradation in ASF: 0 days- blue; 28 days- red; 56 days- grey.

This degradation study was extended to investigate the effect that protein had on complex degradation. The results of this study are presented in Figure 4-10. With protein present complex mass was found to increase during the study which could be explained by protein adsorption to the complexes. As proteins have a polyelectrolyte nature this would not be surprising as they can interact with the charges present on the polyelectrolyte complexes.

Complexes showed little change over the first 7 days, suggesting that during this period protein adsorption replaces the mass loss that was previously observed. This plateau was followed by a slow increase in complex mass until 28 days. After this point the complexes diverged with Ch:HAM complexes stabilising and Ch:HA complexes continuing to gain mass. The only statistically significant differences were found between all samples after 56 days ($P<0.001$); except between Ch:HAM 0.5:1 and Ch:HA 1:1 samples where the difference was not statistically significant.

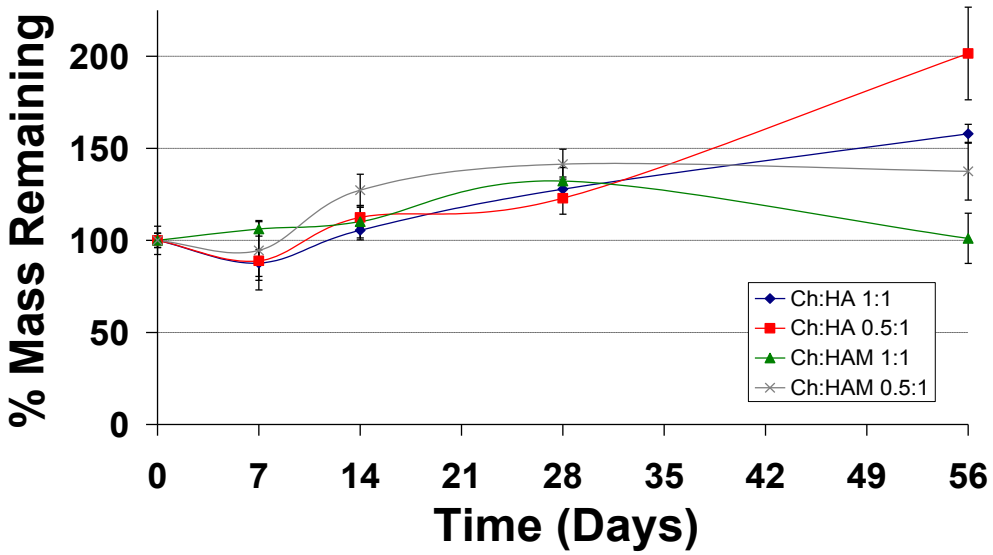

Figure 4-10 Mass degradation profiles of Ch:HA and Ch:HAM complexes in ASFP. Ch:HA and Ch:HAM complexes were prepared were then incubated in ASFP buffer at 37°C. Buffer was regularly changed and at each time point complexes were extracted, dried and weighed.

4.3.3 Evaluation of injectable formulation

4.3.3.1 Stability in salt

The aim was to produce an injectable formulation of these complexes. To achieve this salt was used to prevent complexation. Therefore the stability of Ch:HAM complexes in salt was important and this was assessed in a qualitative study. The results of this study are presented in Figure 4-11. At the Ch:HAM 1:1 ratio discrete compact complexes were formed in 0.1M NaCl and

below. At 0.2M and 0.3M salt a precipitated complex was produced which was more diffuse and is not well represented in the photographs. 0.4M and 0.5M NaCl gave a full disruption of Ch:HAM complexes. At the 0.5:1 Ch:HAM polymer ratio similar results were observed although a complete complex disruption occurred in 0.3M salt concentration and above. These results suggest that Ch:HAM complexes are slightly less stable in salt than Ch:HA complexes.

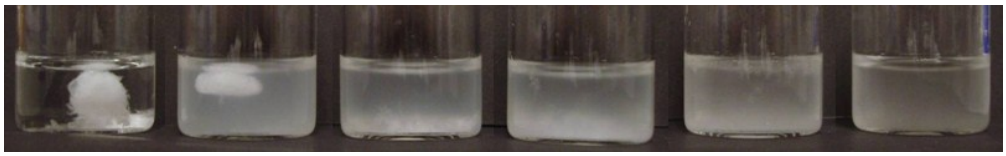

Figure 4-11 Photographs showing the effect of salt on Ch:HAM complex formation. Ch:HAM complexes were prepared in the presence of the indicated concentration of NaCl. Mixtures were incubated at 37°C for 60 minutes to allow complex formation to occur before photographs were taken. Top: Ch:HAM 1:1; Bottom: Ch:HAM 0.5:1.

4.3.3.2 Complex formation by dialysis

As the complexes showed a broadly similar stability in salt 0.5M NaCl would continue to be used to prevent complexation. The formation of Ch:HAM complexes using the dialysis formation method was then assessed. Photography of forming complexes and rheology amplitude sweeps were utilised for this. Ch:HAM 1:1 complexes exhibited a rapid precipitation followed by a contraction into discrete complexes over an hour, Figure 4-12.

0 mins **15 mins** **30 mins** **60 mins**

Ch:HAM 1:1 in water

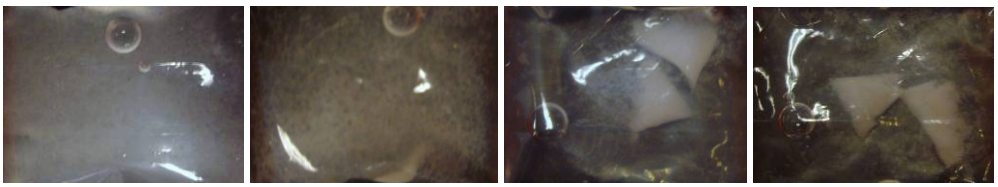

0 mins **15 mins** **30 mins** **60 mins**

Ch:HAM 1:1 in ASF

Figure 4-12 Photographs showing the formation of Ch:HAM 1:1 complexes by dialysis. Solutions containing complex components were prepared in 0.5M NaCl. These mixtures were dialysed against water or ASF at 37°C with the buffer replaced every 15 minutes. Photographs were taken at each buffer change.

These results were confirmed by the rheology amplitude sweeps, Figure 4-13. A detectable formation occurred within 15 minutes and little change occurred after this time. This suggests that the contraction seen does not affect the overall complex structure and strength. When ASF was used as the dialysate there was a greater formation of small complexes that were not incorporated into the main complex. The rheology results showed no difference in the initial formation. After this point there was a gradual increase in the G′, showing that ASF slightly slowed complex formation. Overall the formation of Ch:HAM 1:1 complexes was similar to that found with Ch:HA complexes.

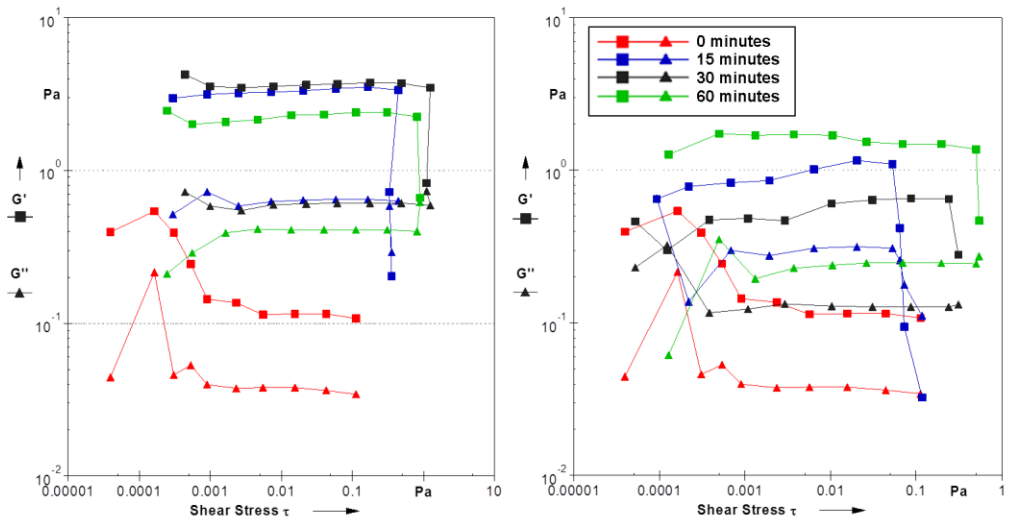

Figure 4-13 Rheology amplitude sweeps showing Ch:HAM 1:1 complex formation by dialysis.
Solutions containing complex components were prepared in 0.5M NaCl. These mixtures were dialysed against water or ASF at 37°C with the buffer replaced every 15 minutes. Rheology amplitude sweeps were carried out on the recovered mixtures at 37°C. G′ (squares) and G″ (triangles) are plotted against shear stress. Left: dialysis against water; Right: dialysis against ASF. Time of dialysis is shown in the legend and is the same for both graphs.

The 0.5:1 ratio was also investigated with the dialysis formation method. With water as the dialysate precipitation was seen within 15 minutes, Figure 4-14, and was followed by a contraction into discrete complexes over an hour. This was confirmed by rheology, where formation was detected after 45 minutes, Figure 4-15. The G′ and yield stress values slowly increased for the remainder of the study period. Dialysis against ASF caused a reduced complex formation with only a very diffuse formation visible after 15 minutes. Formation proceeded slowly and after 60 minutes a small discrete complex was formed. Rheology amplitude sweeps on these samples failed to detect any complex formation. These results show that HAM has a positive effect on formation at the 0.5:1 ratio and caused a greater formation than was seen with HA. However the formation is still affected by physiological salt in the reduced chitosan samples.

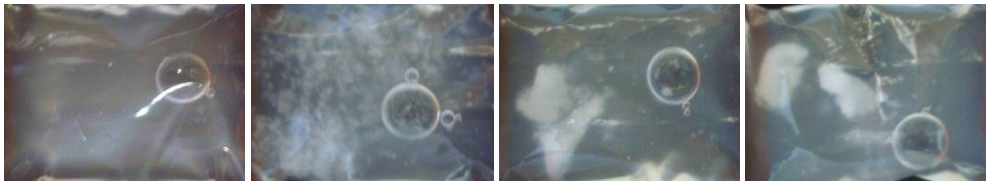

Figure 4-14 Photographs showing the formation of Ch:HAM 0.5:1 complexes by dialysis. Solutions containing complex components were prepared in 0.5M NaCl. These mixtures were dialysed against water or ASF at 37°C with the buffer replaced every 15 minutes. Photographs were taken at each buffer change.

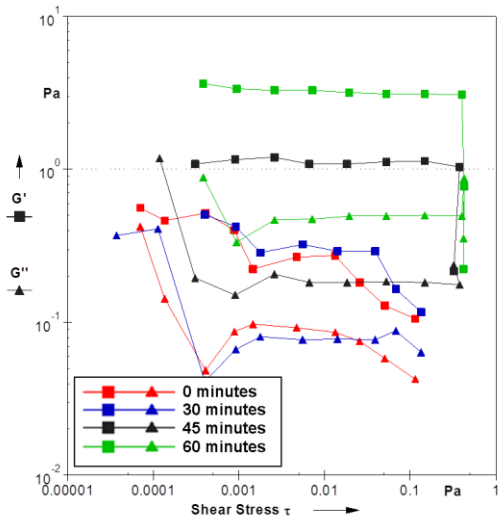

Figure 4-15 Rheology amplitude sweeps showing Ch:HAM 0.5:1 complex formation by dialysis.
Solutions containing complex components were prepared in 0.5M NaCl. These mixtures were dialysed against water at 37°C with the buffer replaced every 15 minutes. Rheology amplitude sweeps were carried on the recovered mixtures at 37°C. G′ (squares) and G″ (triangles) are plotted against shear stress. Time of dialysis is shown in the legend.

4.4 Discussion

4.4.1 Modified Hyaluronic Acid

A modified HA was successfully synthesised and characterised but the modification levels were below what was expected. HAM was found to have a modification level of 0.9% despite using a three fold excess of reactants to account for an expected low yield. The high molecular weight HA used in this

study limited the concentration that could be used due to the viscosity of the solution. This low concentration in aqueous conditions may account for the low reaction efficiency. The modification level was determined by Ellman's Test which measures the concentration of sulfhydryl groups present. Other methods for characterisation were investigated such as ^{1}H-NMR, which was not effective due to the viscosity of HA solutions limiting sample concentration.

High levels of HA modification have been achieved but generally these have involved more complex reaction schemes. The use of EDAC in combination with 1-hydroxybenzotriazole has produced substitution levels of 25 to 80% (Lee et al., 2007, Luo and Prestwich, 2001). Hydrazides with EDAC have been able to give substitution levels of 25 to 40% (Shu et al., 2002). These are exceptional and in general modification levels using EDAC have been below 10% (Moriyama et al., 1999, Ponedel'kina et al., 2008).

Other reaction schemes also have produced many substitutions of around 10%. For example a methacrylated HA needed a 6 to 10 fold excess of reactants to produce a 5 to 10% modification level (Leach et al., 2003). A method using 2-chloro-1-methylpyridinium iodide produced a 5 to 10% modification (Gamini et al., 2002). It has been reported that carbodiimide mediated conjugation to primary amines with HA results in negligible coupling (Luo and Prestwich, 2001). This paper was acting to promote an alternative reaction scheme and the results here show that although the reaction produced a much lower modification than intended a measurable modification was achieved.

4.4.2 Complexes with Modified Hyaluronic Acid

Complexes produced with HAM were visually similar to those produced with unmodified HA. This was the case at all polymer ratios and physiological salt caused only a slight disruption to the complexes. The only visual difference to Ch:HA complexes was in the bulk solution, which was more turbid with Ch:HAM complexes. The only exception was at 0.9:1 and 1:1 ratios, although these ratios showed turbidity on occasion. This turbidity can be explained by the formation of small polyelectrolyte particles, which usually occurs in high charge solutions. However the formed Ch:HA and Ch:HAM complexes have a similar mass. This shows that the increase in small complexes isn't at the expense of the precipitated complex. This suggests that these small complexes form out of any polymer that was not incorporated into the main complex. This may be driven by the ability of the modified HA to form cross-links.

The most significant and unexpected change when HAM was incorporated into complexes was a much more rapid complex formation. This was seen in the visual study where formation occurred during mixing, with few changes after this. It was also apparent through rheology time sweeps which showed that gelation occurred before measurements could start and the formation was complete after 60 minutes. This compared to Ch:HA complexes which showed visual changes over 30 minutes and rheological changes over around 150 minutes. This rapid formation is of great advantage for this project because after administration the complexes need to form before clearance from the joint occurs.

It is proposed that this increase in the speed of formation is due to the structure of complexes becoming locked due to the formation of cross-links. These cross-links also act to pull the complexes together more rapidly. The ratio of polymers had no effect on the speed of formation of the Ch:HAM complexes. This shows further advantages over the Ch:HA complexes where a slower formation was found with lower chitosan concentrations.

Investigations were carried out on the effect of physiological conditions on Ch:HAM complex formation. These found that physiological salt and the presence of unmodified hyaluronic acid caused a slowed complex formation. This would suggest that salt causes a slight disruption of complexes as they form. It would also suggest that HAM is not exclusively incorporated into the complexes when both HA and HAM are present. The incorporation of unmodified HA slows Ch:HAM complex formation as it is unable to cross-link. The kinetics are similar to those of Ch:HAM complexes alone which suggests that HAM is preferentially incorporated. This would be expected as cross-links can only form between HAM molecules. These results show that the formation of complexes with HAM was only slightly affected by the presence of synovial fluid constituents. Formation is faster than with unmodified HA under these conditions.

Rheology amplitude sweeps showed that HAM caused a significant increase in complex resistance to shear stress at ratios between 1:1 and 0.5:1. This was expected as the inclusion of covalent cross-links into the complexes should increase their stability and gel strength. Covalent bonds are strong bonds and

when formed across the entire complex would produce a resilient complex. It was also found that there was a greater relative increase in the yield stress compared to the G′. This is positive as it suggests that the resistance to shear stress has been increased without increasing the solidity of the complexes as much. Therefore these Ch:HAM complexes should be better able to withstand the physical challenges of the joint without being too rigid and causing damage (Seireg and Arvikar, 1975, Sharma et al., 2007, Gerwin et al., 2006).

It was also found that Ch:HAM complexes exhibited the greatest G′ and yield stress at the 0.9:1 ratio, which suggests that the modification has changed the charge ratios of these complexes. The modification of HA on the carboxylate group will have removed charges from the polymer. The modification was at a low level and so would not be expected to cause a discernible change in the complexes. However if there were inaccuracies in the original polymer characterisations then the calculated ratios may have been slightly inaccurate. Therefore despite the low level of modification the stoichiometry of the complexes may have been altered.

Ch:HAM complexes showed a similar degradation profile to Ch:HA complexes in ASF buffer. Ch:HAM 1:1 complexes showed a slower initial rate of degradation, which was statistically significant to Ch:HA 1:1 complexes at 7 days. After this time the degradation profile trended back towards that of Ch:HA 1:1 complexes and at the end of the study the overall degradation levels were very similar. This would suggest that the covalent bonds are able to increase the stability of these complexes.

The degradation of Ch:HA complexes showed that there was a stable core to the complexes. The mass loss observed has been attributed to the loss of loosely incorporated polymer chains on the surface. The increase in initial stability with Ch:HAM would therefore be due to these loosely incorporated polymer chains being more tightly held by covalent bonds which slows their release.

HAM did not affect the formation of the complex core and so similar degradation levels were seen compared to unmodified HA. Further studies under more challenging conditions would be required to see whether HAM was able to slow the degradation of this core. Ch:HAM 0.5:1 complexes show some evidence of this. They retained a significantly larger mass at 56 days compared to Ch:HA complexes. This suggests that HAM may also be able to stabilise the core of these complexes.

The stability of these complexes compares well to the degradation of other hydrogels produced using modified hyaluronic acids. One system used hyaluronic acid linked to Pluronic F127 (Kim and Park, 2002). These hydrogels showed an 80% mass loss over 20 days. A system that is more comparable to that produced here used hydrogels of covalently linked hyaluronic acid and chitosan (Tan et al., 2009). These hydrogels exhibited a slow and gradual degradation in PBS over 28 days of study. During this time around 20% to 40% of the hydrogel mass was lost depending on the exact hydrogel composition. These are very similar levels and rates of degradation to those seen with the Ch:HAM complexes produced here. However the

termination of the study after 28 days means that it is not possible to assess whether a plateau in degradation would occur as was seen in this study.

The rheology amplitude sweeps that were conducted on degraded samples gave further information on the degradation of the complexes. These showed that during the degradation there was little change in G′ values and a gradual decrease in yield stresses. This suggests that the mass lost from these complexes did not cause large structural and mechanical changes in complexes. The polymer lost is therefore most likely to be loosely associated on the surface.

To investigate the degradation of these complexes in more biologically relevant conditions a study was conducted where protein was also included. This found little change over the first week and then a gradual increase in mass. This would be due to protein being adsorbed onto the surface of these complexes. It is not surprising that this occurs as proteins are polyelectrolytes meaning that they can form electrostatic bonds with the complexes. The adsorption occurs gradually and initially replaced the mass loss that was seen in other studies. After 28 days there was a divergence in the remaining mass of complex with statistically significant differences between samples at 56 days. Ch:HAM complexes stabilised over this period which would suggest that a maximum protein binding has been reached. The Ch:HA 0.5:1 complexes continued to gain mass through this time. These complexes were the least stable in previous studies. This would suggest that the degradation in these complexes exposed a greater surface area over which protein could adsorb.

The production of injectable complexes was an aim of this study. In order to achieve this complexation would be prevented by salt. The effect that HAM had on complex formation in salt was therefore important. A study found that Ch:HAM complexes seemed to be slightly less stable in salt than Ch:HA complexes. This may be explained as the modification causes a reduction in the charges present on HA. This would reduce the electrostatic bonding between complexes meaning they were more easily disrupted.

The reduction in stability was only small and complexes were successfully prepared in physiological salt concentrations. It may provide an advantage though as a lower salt concentration could be used in the injectable formulation. These results suggest that the electrostatic charges drive the initial interaction between these two polymers and the covalent bonds form after these initial interactions. If covalent bonds played a role in the initial interactions Ch:HAM complexes would be expected to show a greater stability in salt as these bonds would be less affected by the salt.

The decreased stability of Ch:HAM complexes in salt gave concerns for the formation of complexes by the dialysis method. Experiments found that Ch:HAM complexes were able to form better than Ch:HA complexes by this method. This is particularly clear at the 0.5:1 ratio. Formation was clearly seen with Ch:HAM 0.5:1 complexes dialysed against water, and some formation was seen in dialysis against ASF. Whereas only a minimal formation was seen with Ch:HA 0.5:1 complexes. The formation of Ch:HAM 0.5:1 complexes

dialysed against water was confirmed by rheology. Rheology showed that formation was slower than for 1:1 ratio complexes.

Complexes with HAM seemed to show a lower stability in salt but gave a better formation by the dialysis method, which suggests that the cross-linking ability of HAM is still able to promote complex formation. The Ch:HAM 1:1 complexes showed a rapid precipitation during dialysis against both water and ASF. This was followed by contraction into discrete complexes over an hour which caused only a small and gradual rheological change. This suggests that the contraction does not affect the overall structure and bonding of the complexes. Overall these results show that Ch:HAM complexes are able to form rapidly by this method. The presence of physiological salt in the dialysis media only slightly disrupts and slows formation.

4.5 Conclusions

The results obtained show that the incorporation of HAM into polyelectrolyte complexes provides a number of advantages. These changes occurred despite the low level of modification achieved. The most striking result was the rapid formation of Ch:HAM complexes, which was much faster than observed for Ch:HA complexes. The speed of formation was not as obviously increased with the dialysis formation method. However there was a clear improvement in the overall formation of these complexes by dialysis, which was particularly evident in the 0.5:1 ratio complexes.

The degradation and resistance to stress also improved through the incorporation of HAM. The initial degradation in the 1:1 ratio complexes was slowed and the 0.5:1 ratio complexes were stabilised for longer. The rheology showed that Ch:HAM complexes exhibited higher G′ and yield stress values, with relatively larger increases in the yield stresses. These results suggest that the Ch:HAM complexes would be more resilient and long lived in the challenging environment of the joint. The positive effects of HAM mean that it will continue to be used through the rest of this project.

A number of other considerations arise from the results in this chapter and the previous chapter. The dialysis method showed a greater formation of small complexes not incorporated into the main complex. The effects of the dialysis formation method on the complex properties could therefore be important. The properties of complexes formed through this method will be assessed. Also the formation in the joint will occur in the presence of physiological salt and so dialysis in future studies will be carried out against ASF only. The results with reduced chitosan concentrations showed that there was a much worse formation below 0.5:1 ratio, therefore for the rest of this project only the 1:1 and 0.5:1 Ch:HA ratios will be investigated. Finally the results suggest interactions between these complexes and plasma proteins. This suggests that biological relevance of studies need to be further considered.

CHAPTER 5 - SYNTHESIS AND CHARACTERISATION OF DRUG LOADED PGA NANOPARTICLES

5.1 Introduction

Dexamethasone phosphate was selected as the drug for incorporation into this delivery system as it is currently used for the treatment of osteoarthritis by intra-articular injection. However its delivery could be improved and there is a particular lack of slow release delivery systems.

A composite delivery system of nanoparticles retained within a hydrogel has been proposed. A suitable hydrogel has been selected and so the nanoparticle component is required. The nanoparticles will be produced using poly(glycerol adipate) as this polymer has shown promising results with dexamethasone phosphate. These two components are introduced in more detail below.

5.1.1 Dexamethasone Phosphate

Dexamethasone phosphate (DXMP) is a synthetic glucocorticoid steroid and its structure is shown in Figure 5-1. Glucocorticoid steroids are used therapeutically to treat asthma and many other conditions as they have potent anti-inflammatory properties. Glucocorticoids also have immunosuppressive properties and are used to treat some autoimmune diseases such as rheumatoid arthritis. Due to these potent effects glucocorticoids have a wide range of side effects. Delivery systems that provide a sustained release of glucocorticoids are desirable as they would reduce the incidence and severity of side effects.

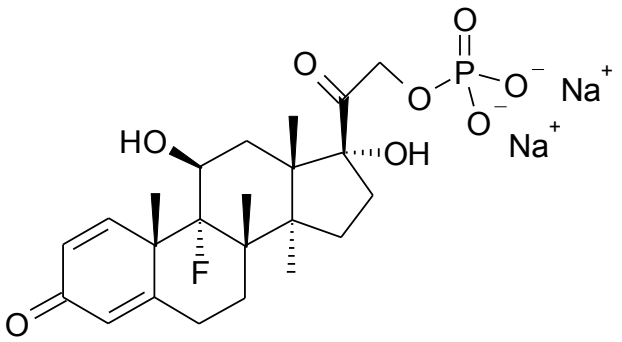

Figure 5-1 Chemical structure of dexamethasone phosphate.

Delivery systems for dexamethasone phosphate have included liposomes (Anderson et al., 2010) and polymeric particles (Karmouty-Quintana et al., 2010, Thote et al., 2005). PLGA microparticles of around 100μm were prepared by the emulsification solvent evaporation method (Thote et al., 2005). These particles had a drug loading of 8% and drug release was complete within 24 hours but was slowed by surface cross-linking to around 7 days (Thote et al., 2005). Calcium pyrophosphate microparticles (5-15 μm) gave a release of DXMP over 7 days (Karmouty-Quintana et al., 2010). This study did not look into the particle drug loading and so their true potential is hard to judge.

Many more delivery systems have been investigated using dexamethasone. Table 5-1 shows the size and drug loading data for a number of dexamethasone delivery systems. This form of the drug is only sparingly water soluble and so these systems have mainly aimed to improve its immediate delivery. The release from these particles was often complete in a day or two (Kim and Martin, 2006, Ramesh et al., 1999). Some systems have shown a more gradual release over longer periods (Song et al., 1997, Gomez-Gaete et al., 2007) with the maximum being 20 days (Wang et al., 2010). The size of particles had no relationship to loading levels or drug release.

Polymer	Preparation Method	Particle Size	Drug Loading (%)	Encapsulation Efficiency (%)	Reference
PLGA	E/S	125nm (±39)	16.0	79.6	(Song et al., 1997)
PLGA	E/S	240-270nm	11.0	55.0	(Panyam et al., 2004)
PLGA	E/S	400-600nm	13	79	(Kim and Martin, 2006)
PLGA	E/S	200nm	0.3	3	(Gomez-Gaete et al., 2007)
PLGA	E/S	200nm	10	50	(Wang et al., 2010)
PLGA	E/S	20µm	0.18	0.9	(Dawes et al., 2009)
PLGA	E/S	1µm	2.24	11.2	(Dawes et al., 2009)
PDLLA	E/S	40-60µm	5.2	52	(Ramesh et al., 1999)

Table 5-1 Physical and drug loading properties of particulate dexamethasone delivery systems.
Summary of key parameters of published polymer based dexamethasone delivery systems. E/S in preparation method refers to emulsification solvent evaporation particle formation method.

5.1.2 Poly(glycerol) Adipate

Poly(glycerol) adipate (PGA) is a polyester polymer produced from glycerol and adipic acid in a lipase catalysed reaction (Kallinteri et al., 2005). This produces a polymer that contains pendant hydroxyl groups and the polymer structure is shown in Figure 5-2. The pendant hydroxyl groups allow covalent modifications that can alter the polymer properties.

Nanoparticles loaded with dexamethasone phosphate have been prepared using PGA modified with acyl groups (Kallinteri et al., 2005, Puri et al., 2008). Steroids are known to interact with the acyl chains of fatty acids in cellular

membranes. The incorporation of acyl groups into PGA increases drug loading (Kallinteri et al., 2005) and improves the drug release profile (Puri et al., 2008).

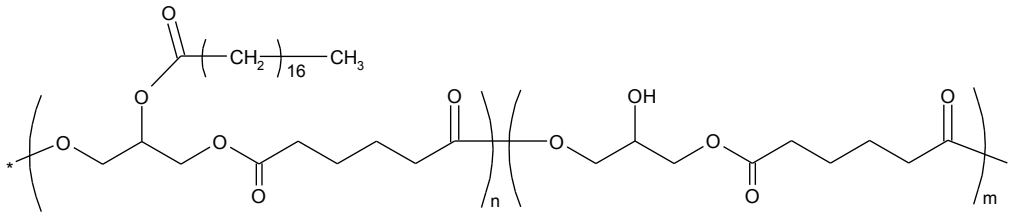

Figure 5-2 Chemical structure of poly(glycerol adipate) (PGA) polymer modified with 18 carbon acyl chains.
Structure of PGA polymer showing both the unmodified backbone residue (right) and stearoyl modified residue (left). PGA used for this study has 40% of repeating units modified, produced as a random co-polymer.

A study investigated various levels of acyl modification and different molecular weight PGA polymers (Kallinteri et al., 2005). This found the highest drug loading with 12kDa PGA which was 40% modified with stearoyl groups. This polymer produced particles of around 200nm with a drug loading level of 10% (Kallinteri et al., 2005). A study on PGA modified with octanoyl groups found that the interfacial deposition method gave higher drug loading levels than the emulsification solvent evaporation method (Puri et al., 2008). The higher loading levels gave a better release profile, with a gradual release over 14 days achieved (Puri et al., 2008).

5.1.3 Chapter Aims

PGA was chosen as the polymer used for the nanoparticles within this system as this polymer has shown high drug loading levels and promising sustained release with dexamethasone phosphate. Specifically, 12kDa PGA with 40% of its hydroxyl groups modified with C18 acyl (stearoyl) chains was chosen. This polymer has shown the highest dexamethasone phosphate loading levels in previous studies (Kallinteri et al., 2005).

This chapter characterised nanoparticles produced with 40% C18 modified 12kDa PGA loaded with DXMP. The physiochemical properties, drug loading and drug release were assessed. Nanoparticles loaded with rhodamine B isothiocyanate (RBITC) as a tracking dye were also synthesised and characterised. RBITC loaded PGA nanoparticles have been previously synthesised (Meng et al., 2007, Meng et al., 2006) and will be used to monitor the nanoparticles within the hydrogels in future studies.

5.2 Materials and Methods

5.2.1 Materials

The materials used are detailed in section 2.1.

5.2.2 PGA Polymer Modification

PGA polymer was modified with C18 acyl groups and characterised using the method described in section 2.5.1.

5.2.3 Nanoparticle Preparation and Characterisation

5.2.3.1 Nanoparticle preparation

Nanoparticles were prepared using the method in section 2.5.2. Unloaded, DXMP and RBITC loaded particles were prepared.

5.2.3.2 Separation of unencapsulated drug

Unencapsulated drug was removed from the prepared nanoparticles using the methods described in section 2.5.3.

5.2.3.3 Nanoparticle characterisation

The size and zeta potential of the particles were determined using the method described in section 2.5.4.

5.2.3.4 Determination of RBITC loading levels

RBITC loading levels were determined using the method in section 2.5.5.1.

5.2.3.5 Method development for DXMP loading levels

The direct method for DXMP loading determination was developed. The summary of the methods used is included in section 2.5.5.2.

5.2.3.6 Determination of DXMP loading levels

DXMP loading levels were determined using the indirect and optimised direct methods that are detailed in section 2.5.5.3.

5.2.3.7 Analysis of RBITC release

RBITC release from nanoparticles was determined using the method described in section 2.5.6.1.

5.2.3.8 Analysis of DXMP release

DXMP release was determined using the method in section 2.5.6.2.

5.3 Results

5.3.1 Polymer Characterisation

40% C18 modified PGA was synthesised as previously described (Kallinteri et al., 2005). This polymer was characterised by H^1-NMR to assess the percentage modification, as shown in Figure 5-3. The results of this confirmed that the PGA polymer had been successfully modified with 37.6% (standard deviation=0.76, n=3) stearoyl groups. This polymer was used for all subsequent nanoparticle studies.

5.3.2 Particle Size and Zeta Potential

Nanoparticles were successfully produced using the modified PGA polymer. The size and zeta potential of these particles were determined. Particles were loaded with dexamethasone phosphate, or the fluorescent label rhodamine B isothiocyanate, or were left unloaded as a control. The results of this show that all particles produced were less than 200nm in diameter, Table 5-2. The particles showed a very low polydispersity, which means that particles of a tightly defined size were produced. The particles also showed a small variability between batches. Empty nanoparticles were the largest, and a slight but significant reduction in diameter was seen when DXMP or RBITC were loaded into the particles ($P<0.01$).

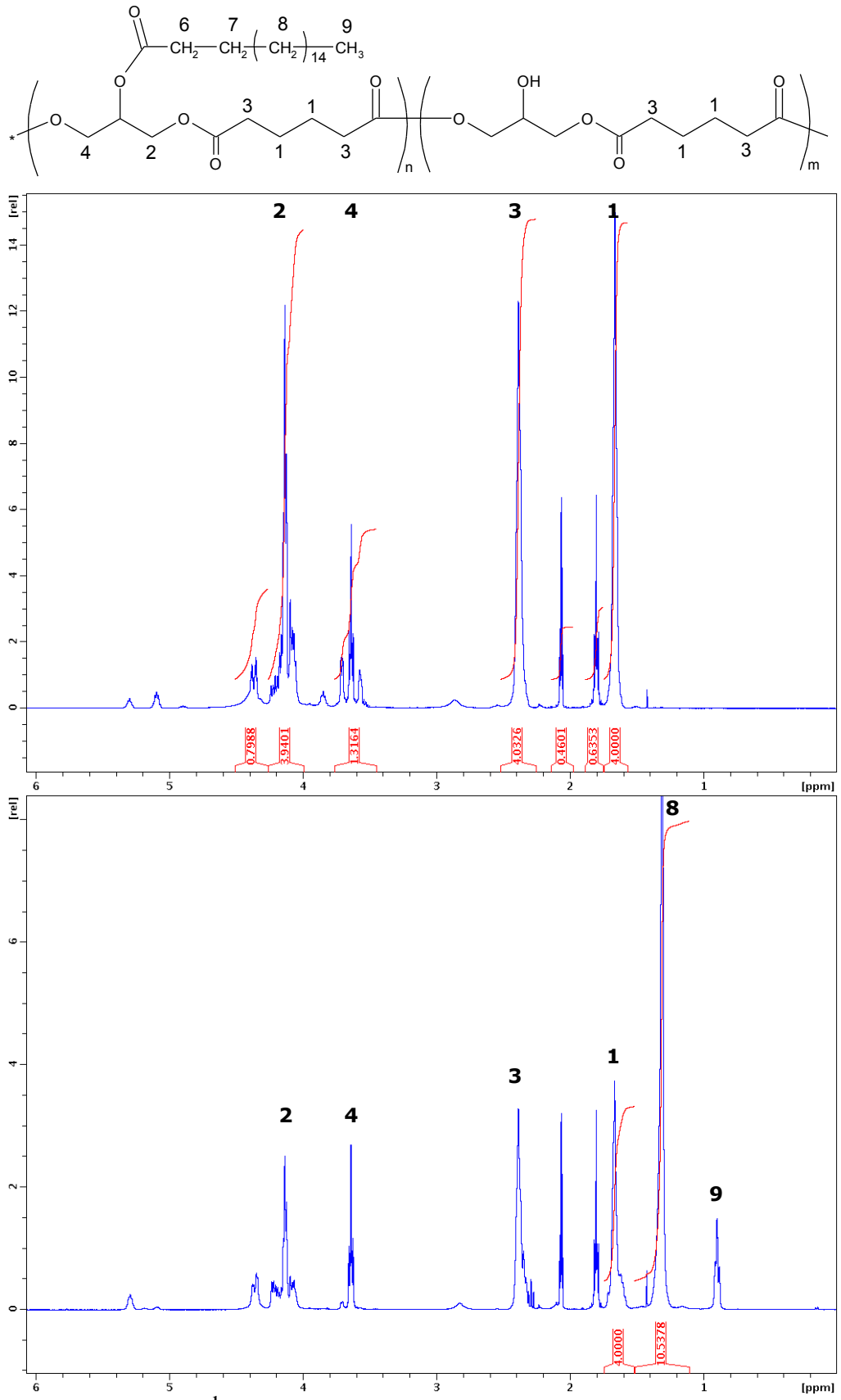

Figure 5-3 Assigned H[1]-NMR spectra of PGA polymer and modified derivative.
Top: Structure of C18 acyl modified PGA polymer with numbered groups corresponding to numbered NMR peaks. Middle: Assigned spectra of PGA backbone polymer. Bottom: Assigned spectra of C18 acyl modified PGA polymer.

The zeta potential of these particles was around -50mV in all cases, which would suggest that these particles are relatively stable in solution. Significant differences in zeta potential were found between all different nanoparticle samples ($P<0.001$). The empty nanoparticles had the least negative zeta potential and the DXMP loaded particles exhibited the most negative zeta potential.

Particle Type	Particle Diameter (nm)	Zeta Potential (mV)
Empty	176.9 (2.85) [0.068]	-39.8 (2.27)
DXMP loaded	167.3 (4.64) [0.097]	-58.6 (6.63)
RBITC loaded	164.9 (3.56) [0.136]	-49.8 (4.05)

Table 5-2 Particle size and zeta potential of 40% C18 substituted 12kDa PGA nanoparticles.
For particle diameter standard deviation values are given in round brackets and polydispersity values are given in square brackets (N=8). For zeta potential standard deviation values are given in round brackets (N=8).

5.3.3 Drug Loading

5.3.3.1 RBITC

The drug loading of PGA nanoparticles with RBITC was determined by fluorescence. The particles were disrupted using a mixture of acetone and methanol and the concentration of RBITC released into solution was then determined using a fluorescence spectrometer. The results of this found that almost 90% of the initially present RBITC was encapsulated into the particles, Table 5-3. As the amount of RBITC used was small this translated to low drug loading levels. However this is a sufficient loading to fluorescently label these nanoparticles and allows them to be used in monitoring the fate of nanoparticles within the polyelectrolyte complexes.

Encapsulation Efficiency (%)	Drug Loading (%)
89.0 (1.91)	0.45 (0.01)

Table 5-3 RBITC loading levels for 40% C18 substituted 12kDa PGA nanoparticles. Drug loading levels were determined by a direct method to assay the drug recovered from nanoparticles. RBITC concentrations were determined using fluorimetry. Standard deviations values are given in brackets (N=6).

5.3.3.2 DXMP method development

The drug loading of PGA nanoparticles with DXMP has previously been estimated using an indirect method (Kallinteri et al., 2005). It is desirable to use a direct method for this analysis to give a greater accuracy of results. A direct method involves the disruption of purified nanoparticles and measuring the recovered drug. The most common methods for direct drug loading determination use a solvent that solubilises both the polymer and the drug. Acetonitrile is a very common solvent for these methods (Thote et al., 2005, Gomez-Gaete et al., 2007). In the case of PGA this has not proven possible due to the limited solubility of this polymer. PGA is soluble in acetone, chloroform and few other solvents, and DXMP is not soluble in these solvents.

An alternative approach was therefore necessary, and a number of approaches were investigated with the results presented in Table 5-4. As PGA is a polyester it is susceptible to degradation by sodium hydroxide. DXMP is water soluble and therefore would be released into solution as the polymer is degraded. Treatment with sodium hydroxide visually appeared to disrupt the nanoparticles, and a pH corrected sample was analysed by HPLC to determine the DXMP concentration.

For this analysis nanoparticle samples containing a known amount of drug were required. These were produced by synthesising blank nanoparticles which were freeze dried and then spiked with a known amount of DXMP. The analysis of this reference sample found that this method was only able to recover 21.3% of the loaded drug. However 100% of a control sample of DXMP alone was recovered after this treatment. It is believed that the explanation for this maybe that the released fatty acids bind the steroid drug. To remove these fatty acids a hexane washing step was included. The same samples as before were used. This found that 33.9% of the drug in the spiked nanoparticle sample was recovered.

The failure of this approach led to the investigation of a biphasic system. This would be composed of one phase that was able to dissolve PGA and a second phase able to solubilise DXMP. The solvent for DXMP was chosen to be water and the solvent to dissolve PGA was to be either chloroform or dichloromethane. DXMP is unstable and will readily degrade in solution to dexamethasone. Dexamethasone is only sparing soluble in water and so the ability of this method to recover dexamethasone as well is essential for a fully accurate determination of drug loading. Results of this biphasic method found a good recovery of DXMP, which was 89% and above in all cases. The recovery of dexamethasone was less encouraging as it was under 5%. The recovery was similar with and without PGA present suggesting that dexamethasone is becoming partitioned into the organic phase of this system.

Extraction Method	Drug	Sample	Drug Recovery (%)
NaOH	DXMP	Drug alone	100.1
	DXMP	Blank NPs spiked with drug	21.3
NaOH/Hexane	DXMP	Blank NPs spiked with drug	33.9
DCM/water	DXMP	Drug alone	92.5
	Dex	Drug alone	1.56
	DXMP	Blank NPs spiked with drug	98.3
	Dex	Blank NPs spiked with drug	1.65
Chloroform/water	DXMP	Drug alone	89.0
	Dex	Drug alone	4.77
	DXMP	Blank NPs spiked with drug	108.0
	Dex	Blank NPs spiked with drug	3.00
DCM/water with analysis of DCM	DXMP	Blank NPs spiked with drug	95.4 (1.40)
	Dex	Blank NPs spiked with drug	99.0 (1.48)

Table 5-4 Method development for the extraction of DXMP from PGA nanoparticles. Drug recovery percentages using the methods trialled for extraction of DXMP and dexamethasone (Dex) from nanoparticles. Drug concentration was determined using HPLC. NaOH method used NaOH to degrade PGA, which was also combined with a hexane defatting. Direct extraction using DCM or chloroform and water was used, with the final method including analysis of DCM. For optimised method standard deviations are given in round brackets (N=3).

In order to overcome this problem the organic solvent phase could be analysed. These solvents are not considered to be water miscible and water miscibility is essential to allow the analysis by HPLC. Small quantities of dichloromethane diluted with methanol were found to be sufficiently water miscible to allow HPLC analysis. Therefore this solvent was utilised for further studies where the organic solvent was also analysed. The results of this found that 95.4% DXMP and 99.0% dexamethasone were recovered from drug spiked nanoparticle

samples. The high and repeatable recoveries make this method suitable for the determination of drug loading of nanoparticles and it will be therefore continue to be used for this purpose.

5.3.3.3 DXMP

The direct method, as developed above, was used along with a previously reported indirect method (Kallinteri et al., 2005) to determine drug loading levels. The indirect method collected and analysed the unencapsulated drug that was separated from loaded nanoparticles. Inaccuracies with this method are likely to occur if the free drug is not fully recovered from the column. In order to correct for this known drug concentrations were run through the column and the percentage recovery was determined. It was found that 80.1% (standard deviation=2.54, n=3) of free DXMP was recovered after passing through the column. This retention was corrected for and the drug loading was calculated using this method.

The results using the indirect method, Table 5-5, show an estimated drug loading of 8.98%. This value is much higher than was found when the direct method was used. The direct method showed a drug loading of 1.69% was achieved, which corresponds to an encapsulation efficiency of 4.29%. These lower values represent a more accurate estimation of the drug loading due to the fact that they used a validated direct method. The improved accuracy of the direct method can be seen by the smaller standard deviations.

Method	Encapsulation Efficiency (%)	Drug Loading (%)
Indirect	18.5 (3.99)	8.98 (1.94)
Direct	4.29 (0.52)	1.69 (0.24)

Table 5-5 DXMP drug loading levels for 40% C18 substituted 12kDa PGA nanoparticles. Drug loading levels were determined by an indirect method using drug recovered during particle purification or by a direct method on the drug recovered from formed particles. Drug concentrations were determined using HPLC. Standard deviation values are given in round brackets (for indirect method N=3; for direct method N=6).

5.3.4 Drug Release

5.3.4.1 RBITC

The RBITC loaded nanoparticles were needed for monitoring the fate of particles within complexes. To enable this, a low release of the fluorescent label was desirable to allow monitoring of the particles over extended time periods. A drug release study was therefore carried out on the RBITC loaded particles and the results of this study are shown in Figure 5-4. These results show that around 20% of the loaded RBITC is released over 14 days, and after this time a minimal RBITC release occurred. The level and speed of release was the same with and without serum proteins present. In contrast the release of free RBITC from the dialysis membrane occurred very rapidly and over 90% of RBITC escaped from the dialysis membrane within 2 days. The remaining RBITC was recovered from within the dialysis membrane.

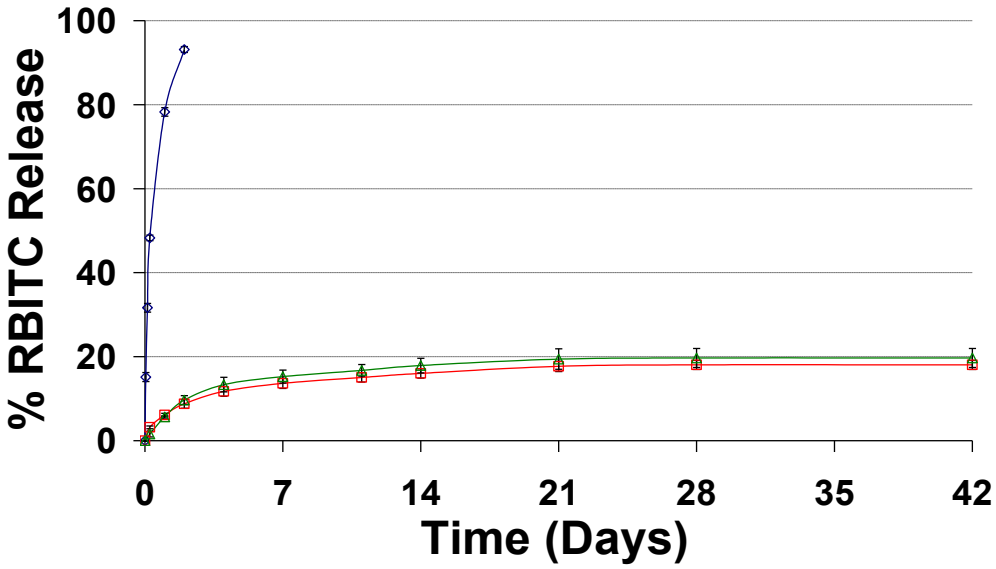

Figure 5-4 RBITC release from 40% C18 substituted 12kDa PGA nanoparticles.
RBITC release from nanoparticles was determined using a dialysis membrane to retain the nanoparticles. RBITC concentration was determined by fluorimetry. Blue- Release of free RBITC from dialysis membrane (N=3); Red- Release of RBITC loaded nanoparticles in ASF (N=3); Green- Release of RBITC loaded nanoparticles with serum in ASF (N=3).

5.3.4.2 DXMP

A sustained dexamethasone phosphate release from particles was an essential part of the proposed delivery system. The release of drug from 40% C18 modified 12kDa PGA nanoparticles was therefore determined. The results of the release experiment are shown in Figure 5-5. This found that these particles were able to give a gradual and sustained release over 28 days, and after this time 83.9% of the loaded drug had been released. This compared to the release of free DXMP from a dialysis membrane which was complete in less than 5 days, with most of this occurring within 1 day. These results show that PGA nanoparticles are able to retain DXMP and provide a sustained drug release.

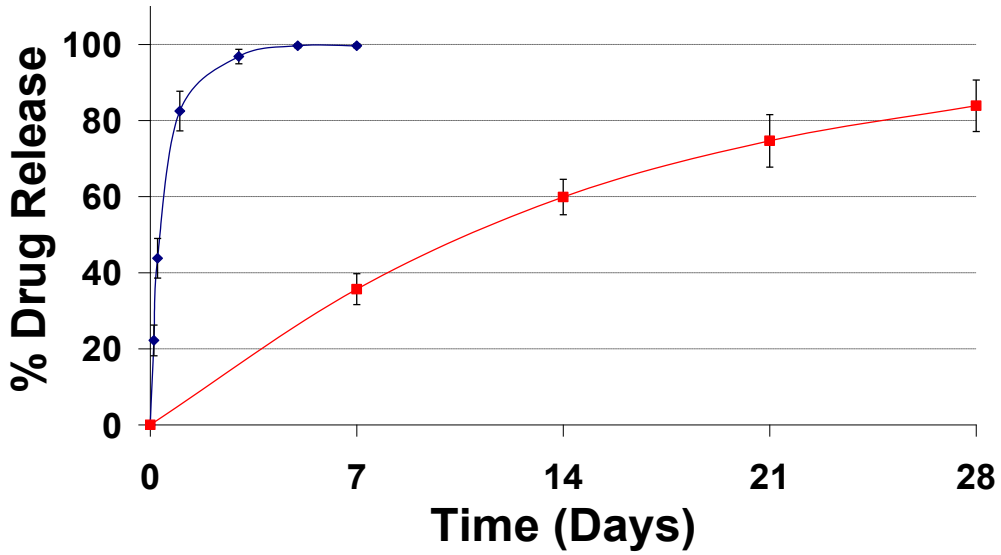

Figure 5-5 DXMP release from 40% C18 substituted 12kDa PGA nanoparticles.
DXMP release from nanoparticles was determined using a dialysis membrane to retain the nanoparticles. Drug concentrations were determined using HPLC. Blue- Release of free DXMP from dialysis membrane (N=3); Red- Release of DXMP loaded nanoparticles (N=4).

5.4 Discussion

5.4.1 Physical Properties of Nanoparticles

5.4.1.1 Size

Nanoparticles were prepared using 12kDa PGA which was 40% modified with stearoyl groups. In all cases these particles were found to be smaller than 200nm in diameter with a low polydispersity. Low polydispersity shows the particles have a tightly defined size range. There was also a low variability between nanoparticle batches, which shows a good reproducibility in the production of these particles. This is desirable as the physical properties can affect the other properties such as the drug release. Therefore a reproducible production of particles will give more accurate results in further studies.

The size of nanoparticles varied when different compounds were loaded into them. Empty nanoparticles were the largest (176nm) and a slight, but significant, reduction in diameter was seen when DXMP or RBITC were

loaded into the particles (167nm and 164nm respectively). This size change is likely to be due to interactions occurring between the drugs and the polymer, which cause a tighter binding within the particles and thus reduce their size (Puri et al., 2008). It is also possible that the drugs may be having an effect on the water and solvent interface causing a reduction in particle size (Puri et al., 2008).

The particle size is similar to previous reports of nanoparticles produced with 40% C18 modified 12kDa PGA. However the particles produced here are consistently slightly smaller than previous results. One previous study produced unloaded particles using 40% C18 modified 12kDa PGA and found them to have a size of 212nm (Kallinteri et al., 2005), this compares to 177nm for similar nanoparticles in this study. The same published study found that particles loaded with DXMP showed no size difference to unloaded particles (Kallinteri et al., 2005). However another study on PGA polymers with octanoyl substitutions found that DXMP loaded particles were consistently smaller than unloaded particles (Puri et al., 2008), as was found here.

RBITC loaded particles produced using 40% C18 modified 12kDa PGA have been reported with a size of 176nm (Meng et al., 2006), which again is slightly larger than produced here. The size differences to the particles produced in this project are small. They could be explained by small differences in polymer batches or by the different machine used to size the particles in this project.

5.4.1.2 Zeta potential

The PGA nanoparticles exhibited zeta potentials of around -50mV. A zeta potential in this range is considered to show that particles are relatively stable in solution. This is because a high surface charge prevents flocculation as it acts to repel particles from one another and thus reduces aggregation. The zeta potential became significantly more negative from empty nanoparticles, to RBITC loaded particles to DXMP loaded particles.

The charge on unloaded nanoparticles is likely to be due to the terminal carboxylate groups on the PGA polymer (Puri, 2007). Within particles the hydrophobic stearoyl groups will be shielded from the external aqueous environment. This will lead to the hydrophilic pendant hydroxyl groups and terminal carboxylate groups being orientated to the surface of the particles and thus produce a negative zeta potential.

The more negative zeta potential with DXMP incorporated into nanoparticles is likely to be due to the negative charge of this compound. The random incorporation of a negatively charged compound into nanoparticles would increase the negative charges present on the particle surface. However due to the hydrophobicity of the particle core it is unlikely that this incorporation would be random, and most likely occurs in the surface layers. RBITC is not negatively charged and so the more negative zeta potential when this compound is loaded must have an alternative explanation. The most likely cause is that the incorporation of RBITC causes a rearrangement of the polymer chains leading to an increase in the terminal carboxylate groups

exposed at the surface. The increase in carboxylate groups at the surface causes the increased negativity of the zeta potential.

The zeta potential values agree well with previous reports. The published study conducted using 40% C18 modified 12kDa PGA found that unloaded particles had a zeta potential of -25.9mV and DXMP loaded particles had a zeta potential -34.5mV (Kallinteri et al., 2005). Similar values were also found for unloaded and DXMP loaded particles using PGA with different substitutions (Puri et al., 2008). The values produced here were more negative with a zeta potential of -39.8mV for unloaded particles and -58.6mV for DXMP loaded particles. A study investigating 40% C18 modified 12kDa PGA nanoparticles loaded with RBITC found particles to have a zeta potential of -52.2mV (Meng et al., 2006). This is very similar to the value of -49.8mV which was obtained in this study.

The difference between loaded and unloaded particles is similar for the samples produced here and previous reports (Kallinteri et al., 2005). The differences would therefore seem to due slight differences in the polymer used for this study. Alternatively the production conditions for these particles have caused a greater proportion of the polymer carboxylate groups to become localised to the surface.

5.4.2 Drug Loading

The drug loading of nanoparticles is much more accurately determined using a direct method, which extracts the drug from the particles and then quantifies

this extracted drug. This contrasts to an indirect method where the unencapsulated drug is measured and the difference to the initial amount of drug added is assumed to be the drug loading. A direct method requires the disruption of particles to allow recovery of the drug. No method to do this was available for DXMP loaded PGA particles, so a method had to be developed. This extraction was not straightforward as there is no common solvent which would dissolve both the polymer and the drug. A more complex extraction than used for most nanoparticle systems was therefore required.

Two main approaches were investigated, which were a sodium hydroxide degradation of PGA and a biphasic extraction. The sodium hydroxide degradation was successful at disrupting PGA nanoparticles but did not give a good drug recovery. It was thought that this low recovery may be due to the stearoyl groups present in the polymer as these are known to bind steroid drugs such as DXMP (Puri, 2007). A hexane wash to remove the stearoyl groups only produced a small increase in drug recovery. This result suggests that DXMP remains associated with the stearoyl groups even when they are removed into the hexane layer.

The biphasic extraction used a solvent which dissolved PGA to disrupt the particles and water to solubilise the drug. To give a full analysis of the loading both DXMP and dexamethasone need to be quantified. Dexamethasone is more hydrophobic and the low recovery of this drug suggests that it is preferentially sequestered within the solvent phase of the system. The use of alternative solvents is not possible due to the limited solubility of PGA. Analysis of the

organic solvent was therefore needed and it was found that the small volumes of dichloromethane required were miscible in the HPLC mobile phase when diluted in methanol.

The biphasic extraction with analysis of dichloromethane and water provided an excellent recovery of both drugs. This method also gave consistent results with different samples. This validated method was therefore used for the determination of DXMP drug loading of PGA nanoparticles through the rest of this study.

The drug loading of DXMP was determined by both the developed direct method and a previously used indirect method (Kallinteri et al., 2005). With the indirect method the results obtained here (9% drug loading) were broadly similar to previous reports (10% drug loading) (Kallinteri et al., 2005). These results did not agree with the results obtained using the direct method, which found the loading to be around 1.7%. The direct method is a much more accurate method for determining the drug loading as the loaded drug is recovered from the particles. The direct method is only less accurate if the drug is not fully liberated from the particles as this would mean that it is unavailable for analysis. The direct method that was used here was validated using freeze dried nanoparticles spiked with known concentrations of drug and is therefore known to be accurate.

There is also the possibility that the direct method is providing an underestimate of the true drug loading. This could occur if there is an

incomplete release of the drug from the degraded nanoparticles. The incomplete release could be caused by the DXMP remaining associated with the solubilised PGA or it could become sequestered at the organic/aqueous phase boundary due to its amphipathic nature. Any drug that is not completely released would not be detected by the HPLC and so would lead to an underestimation of the drug loading. The validation studies run using dried nanoparticles spiked with known concentrations of drug were included to attempt to show that the losses by these causes were negligible.

The indirect method is likely to have errors due to the drug not being recovered from the column. This study attempted to correct for this by measuring the recovery of a known amount of DXMP from the complexes, but despite this the results did not agree with the direct method. The cause for this may be due to the drug binding to aggregated polymer present when the particles were synthesised, or drug binding strongly to the column so that it is not eluted. Aggregated particles were removed by filtration but visually appeared to be of small quantities. Also the concentration of free drug in the nanoparticle samples is not known. Therefore the correction applied from the recovery of the known DXMP concentration may also be causing an over or underestimation of the actual concentration. This would occur if the column retention was not varying linearly with the concentration applied. Overall it is not entirely clear why there were quite such inaccuracies with the indirect method.

The DXMP drug loading found was lower than expected. Other nanoparticle systems have managed higher dexamethasone phosphate loading levels. One study produced PLGA microparticles of around 250nm by the emulsification solvent evaporation method that had a drug loading level of 11% (Panyam et al., 2004, Thote et al., 2005). The interfacial deposition method is known to give poor loading levels of hydrophilic drugs due to the accessible aqueous phase present during formation. However PGA showed better DXMP loading using the interfacial deposition compared to the emulsification solvent evaporation method (Puri, 2007). Although the DXMP loadings achieved here are lower than previous reports with PGA and PLGA, they are still a good loading compared to many steroid loaded particles.

The encapsulation efficiency of RBITC into nanoparticles was very high with around 90% of the available drug loaded into particles. This high efficiency is due to the hydrophobicity of this drug and to the small amount of drug used in the encapsulation process. As RBITC is hydrophobic it is favourable for it to become encapsulated within the hydrophobic polymer matrix. Only a low drug loading of RBITC in the particles was required as the drug was intended as a fluorescent label for tracking the nanoparticles.

5.4.3 Drug Release

Drug release from nanoparticles can be assessed by a number of methods. The main challenge for assessing drug release from particles is the separation of particles from the release medium. The most commonly used methods are to retain particles within a dialysis bag or to separate release medium from the

particles. Ultrafiltration methods utilising pressurised ultrafiltration cells and centrifugal ultrafiltration cells have also been used. Each of these methods has its own advantages and disadvantages.

The use of a dialysis membrane adds a barrier into the system which means that the measured release is also dependent on the diffusion of drug across the membrane. Such a method also maintains a high concentration of particles within the membrane which may affect the partitioning of drug between polymer and solution (Washington, 1990, Redhead, 1997). This can alter the concentration gradient which drives the movement of drug across the dialysis membrane.

Separation methods use filtration or centrifugation to separate release medium from the particles. This method becomes more difficult with smaller particles as separation becomes more difficult and can take longer. Ultrafiltration involves additional forces to facilitate the separation. These methods again struggle with small particles as fine filters require greater pressure to achieve filtration. They also risk clogging of the filter and loosing particles onto the membrane which will have major effects on the quality of any data produced by this method.

For this project the dialysis membrane method was chosen. With the nanoparticles used in this project it was the easiest method to use. The problems associated with diffusion across the dialysis membrane can be minimised by using a control sample of free drug for comparison. This can

reveal whether effects seen are due to release from the particles or due to a delayed diffusion across the membrane. Also the remaining solutions at the end of the studies can be analysed to ensure that 100% of the drug present is recovered, identifying any problems of drug binding to the dialysis membrane.

The RBITC loaded particles were to be used as fluorescently labelled particles for monitoring the fate of particles incorporated into hydrogels. It was therefore desired that the particles exhibited a low release so that the label remained within the particles. The release was found to be low with only 20% of the loaded RBITC released during the study period. The majority of this release occurred rapidly within the first 7 days. 96.1% of the original loaded RBITC was recovered at the end of the study; this includes both the released drug and that recovered from the particles. This release is similar to that previously seen for PGA particles loaded with RBITC (Meng et al., 2006).

An alternative strategy would have been to covalently attach RBITC to PGA. With the pendant hydroxyl groups present in PGA this would have been possible and would have almost eliminated the release of the label from particles. However no method had been developed for this modification. As the release of RBITC from particles was low it was decided that these particles would be used to allow more work to be carried out on the combined delivery system. Also a fluorescently modified PGA polymer would have altered the particles physiochemical properties and thus the behaviour of the particles produced.

Previous investigations with different modified PGA polymers have shown that the 40% stearoyl modified 12kDa polymer should have the best sustained release profile with DXMP (Kallinteri et al., 2005, Puri et al., 2008). The previous results suggested that this polymer should give a release over around 30 days (Puri et al., 2008). It was found in the present study that these particles gave a gradual release of 80% of loaded drug over 28 days. This is a very good slow release for dexamethasone phosphate from nanoparticles.

This length of release is far in excess of all previous systems, with a release over 7 days being the longest achieved (Karmouty-Quintana et al., 2010, Thote et al., 2005). Other steroid drugs have rarely shown release over such an extended period. The maximum period of release that has been achieved with dexamethasone is 20 days (Wang et al., 2010). This slow release from PGA has been attributed to the acyl groups within the modified polymer having a high affinity for steroid drugs (Puri, 2007). The strong retention of DXMP allows the extended and gradual drug release observed.

5.5 Conclusions

Nanoparticles have been produced using 40% C18 modified 12kDa PGA that have promising properties for the intended application. The particles have a well defined and reproducible size just under 200nm. Particles with a well defined size were desired as they will give a better characterisation of the combined hydrogel and nanoparticle system. The actual size was not an essential property for the particles in this system. Particles were desired that

would be taken up by phagocytosis if they were released from the hydrogels, which gives a maximum size for particles of around 15μm.

The loading of DXMP was lower than has previously been observed. However the development and use of a direct method for the loading determination gives confidence in the accuracy of the results. The release of DXMP was as expected from previous reports and occurred over 28 days as a slow, sustained release with no initial burst. This period of release exceeds all other published nanoparticle delivery systems for dexamethasone and dexamethasone phosphate. With the aims of this project, although a high drug loading is desirable, a good sustained release profile is extremely important. Therefore these PGA particles show good promise for this delivery system.

In general it is expected that larger particles will give a longer release. Using larger particles or improving the drug loading of the particles may well provide benefits to this delivery system. At this stage it was desired to produce a system which proves the concept of a delivery system with a hydrogel retaining nanoparticles. It was not desired to do a large amount of work to optimise the particles and the nanoparticles produced already give a better release than any other system. The use of nanoparticles also ensures that any released particles will be taken up by synovial macrophages and deliver drug to where it is needed. But this does leave this portion of the delivery system as an area for potential future improvements.

CHAPTER 6 - EVALUATION OF NANOPARTICLE LOADED POLYELECTROLYTE COMPLEXES AS COMPOSITE DELIVERY SYSTEM

6.1 Introduction to Composite Delivery Systems

Generally drug delivery systems are designed to be as simple as possible. This is because a simple system has many advantages. A simple system will be easier to produce, characterise and manufacture. Also when there are many interacting elements there is a possibility of unexpected properties being exhibited *in vivo* that were not identified during *in vitro* testing. However even in a simple system this risk remains. Perhaps the biggest reason for producing a simple delivery system is that it is easier and more likely for regulatory approval to be obtained.

Due to these advantages for simple drug delivery systems there have been very few systems that have combined a hydrogel and nanoparticles. A simpler system is the directly loading of a hydrogel with drug, and a number of such systems have been produced (Van Tomme et al., 2008). These approaches are briefly reviewed below.

6.1.1 Hydrogel Delivery Systems

Hydrogels contain large volumes of water entrapped within their structure and in general also have large internal pores (Hamidi et al., 2008). This means that small molecules are unlikely to be well retained within a hydrogel by physical

entrapment alone. However larger molecules such as proteins are more likely to be retained.

The success of loading a protein into a hydrogel can be seen where human growth hormone was incorporated into hydrogels produced from hyaluronic acid and Pluronic F127 (Kim and Park, 2002). The release of this protein showed an initial burst over the first 24 hours, and was followed by a sustained release over the next 10 days. During this period over 60% of the hydrogel mass was lost suggesting that drug release was driven by hydrogel degradation.

Hydrogel systems containing small molecule drugs have also been produced, including a system loaded with dexamethasone (Kim et al., 2011). Kim et al. used a hydrogel produced by the action of horseradish peroxidise on a HA modified with tyramine. This system gave a sustained *in vitro* drug release over 30 days, and a similar release *in vivo*. Another delivery system used PEG based hydrogels to give a sustained release of paclitaxel over 50 days with very small initial burst (Zentner et al., 2001). However when this system was loaded with protein a much faster release over 10 days was observed. This observation suggests molecular weight was not the most important factor and that paclitaxel was interacting with the hydrogel to give the slower release seen.

The differences between drugs show that ability to directly load a drug into a hydrogel depends on the specific properties of both components. The release rate of the drug from the hydrogel will also be affected by these properties. Therefore a system using drug directly loaded into a hydrogel has less

flexibility for use with new drugs as the properties cannot be accurately predicted and need to be checked with any new drug that is loaded.

6.1.2 Hydrogel Composite Delivery Systems

Hydrogels can be synthesised to hold and retain many different things other than drugs and proteins. For tissue engineering applications hydrogels are often utilised to produce cell scaffolds and so are loaded with cells (Tan et al., 2009, Chen and Cheng, 2009). Colloidal drug delivery systems can also be loaded into hydrogels, and this includes nanoparticles as well as other systems such as liposomes. One system used liposomes incorporated into hydrogels composed of chitosan-β-glycerophosphate (Ruel-Gariepy et al., 2002). This temperature sensitive polymer had been previously found to produce hydrogels unsuitable for the direct loading of drug (Ruel-Gariepy et al., 2000). The combined liposome and hydrogel system gave a slow drug release of between 50% and 70% of loaded drug over 14 days (Ruel-Gariepy et al., 2002).

Relatively few drug delivery systems have investigated the incorporation of nanoparticles into a hydrogel. There are such systems that have been loaded with dexamethasone (Cascone et al., 2002, Kim and Martin, 2006). The first of these systems used poly(vinyl alcohol) hydrogels to retain PLGA nanoparticles (Cascone et al., 2002). PLGA nanoparticles loaded into poly(vinyl alcohol) hydrogels showed a slower drug release than free nanoparticles. There was an almost complete drug release in 21 days but a significant initial burst release occurred. Another composite system for dexamethasone retained PLGA nanoparticles within an alginate hydrogel (Kim and Martin, 2006). This system

was able to provide a sustained release over 15 days, but the release from free nanoparticles was found to be only slightly more rapid.

Another study used a very different approach that resulted in a similar system. This used aggregating nanoparticles which formed a system with similar characteristics to one where nanoparticles were retained within a hydrogel (Wang et al., 2010). Two different surface modified PLGA nanoparticles were used to achieve this. This system gave a sustained release of dexamethasone over 60 days (Wang et al., 2010). This is an impressive length of release and exceeds that achieved with nanoparticles retained in a hydrogel. The free particles were also found to give a significantly faster release.

6.1.3 Chapter Aims

This chapter investigated the incorporation of nanoparticles into polyelectrolyte complexes composed of hyaluronic acid and chitosan. The incorporation and release of particles was investigated. The properties of the complexes that have previously been measured were also assessed. This allowed the identification of any effects that the incorporation of nanoparticles had on the complex properties. It was hoped that no negative effects would be found and that nanoparticles may further stabilise the system.

It was also important to assess the properties of complexes produced by the dialysis method. This chapter also investigated the properties of dialysis formed composites to ensure that this formation method produced complexes with the required properties.

Finally this chapter investigated the drug release from these composites. It was hoped that a delivery of three months could be achieved with this system. However a release greater than 1 month would give an improvement over currently available therapies. The release from complexes loaded with dexamethasone crystals was also investigated to assess the necessity of the nanoparticle portion of this delivery system.

6.2 Materials and Methods

6.2.1 Materials

The materials used are detailed in section 2.1.

6.2.2 Composite Preparation and Characterisation

6.2.2.1 Composite preparation

Composites were prepared and the formation characterised using the methods described in section 2.6.1.

6.2.2.2 Determination of nanoparticle incorporation into composites

The level of incorporation of nanoparticles into complexes was determined using the method detailed in section 2.6.3.

6.2.2.3 Rheology amplitude sweeps on composites

Rheology amplitude sweeps on composites were carried out as described in section 2.6.2.

6.2.2.4 Composite degradation

Composite degradation was determined using the method described in section 2.6.2.

6.2.2.5 Nanoparticle release from composites

Nanoparticle release from composites was determined using the method detailed in section 2.6.5.

6.2.2.6 Enzyme degradation of composites

Nanoparticle release from composites incubated with hyaluronidase was determined using the method described in section 2.6.6.

6.2.2.7 Effect on salt on composite formation

The effect of salt on the formation of composites was analysed using the method described in section 2.6.7.

6.2.2.8 Composite formation by dialysis

Composites were prepared by the dialysis method described in section 2.6.8.1 and their formation of these complexes was analysed using the methods detailed in section 2.6.8.1.

6.2.2.9 Characterisation of composites formed by dialysis

Formed composites prepared by the dialysis formation method were characterised using the same methods as used for bulk formed composites, as described in section 2.6.8.2.

6.2.3 Analysis of Drug Release from Composites

6.2.3.1 DXMP release from drug loaded composites

Dexamethasone phosphate release from composites was determined using the method in section 2.7.1.

6.2.3.2 Dexamethasone crystal preparation and characterisation

Dexamethasone crystal suspensions were prepared and characterised using the methods detailed in section 2.7.2.1.

6.2.3.3 Drug release from dexamethasone loaded complexes

Dexamethasone release from complexes was determined using the method described in section 2.7.2.2.

6.3 Results

6.3.1 Characterisation of Composites

6.3.1.1 Composite formation

To initially investigate the formation of nanoparticle loaded complexes a photographic study was undertaken and the results of this study are presented in Figure 6-1. Complex formation appeared to be similar to that observed when nanoparticles were not present. Ch:HA complexes showed a rapid initial precipitation followed by a rearrangement into a tight complex over around 30 minutes, which is identical to the observations on Ch:HA complexes without nanoparticles. The formation of Ch:HAM complexes was also unaffected by the presence of nanoparticles and showed an instantaneous precipitation and complex formation with little change over the study period.

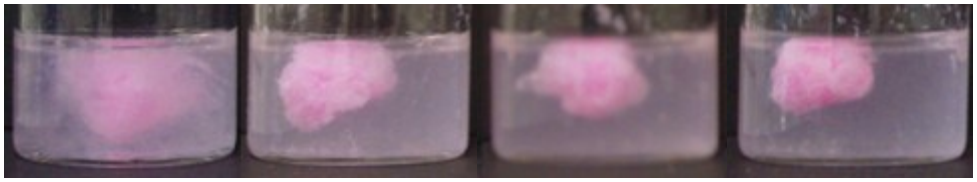

0 minutes 10 minutes 30 minutes 60 minutes

Ch:HA 1:1 complexes

0 minutes 10 minutes 30 minutes 60 minutes

Ch:HA 0.5:1 complexes

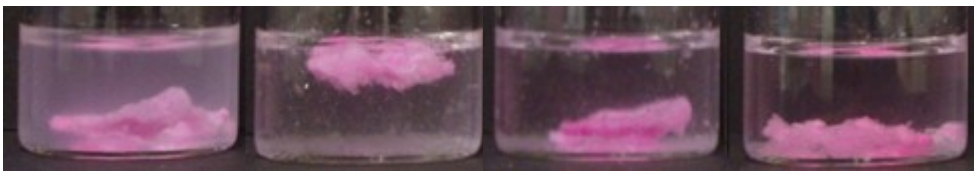

0 minutes 10 minutes 30 minutes 60 minutes

Ch:HAM 1:1 complexes

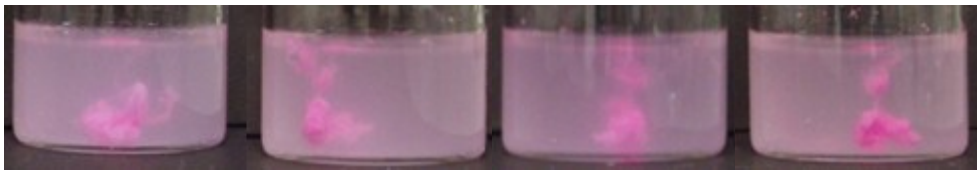

0 minutes 10 minutes 30 minutes 60 minutes

Ch:HAM 0.5:1 complexes

Figure 6-1 Photographs showing the formation of different polymer ratio Ch:HA and Ch:HAM complexes loaded with RBITC nanoparticles in water.
Chitosan, HA/HAM and nanoparticles were mixed at the indicated ratio and incubated at 37°C. Photographs were taken at the indicated times.

This initial photographic study was conducted using RBITC loaded particles. It was hoped that the pink colour of these particles would provide an indication to the distribution of particles within the complexes. This showed that the particles appeared to be quite evenly distributed within the complexes as they had a relatively even colouring. It appeared that Ch:HA complexes in particular exhibited a lower concentrations of particles near the surface as less coloured areas were visible. However this macroscopic inspection only provided an indication of the distribution and further studies would be necessary to determine the true particle distribution.

These complexes will form after injection into the joint and therefore in the presence of a physiological salt concentration. Therefore it was important to check that the composites were able to form under these conditions. The results of a qualitative study to assess this are presented in Figure 6-2. These results show that salt seemed to cause a slight disruption to the nanoparticle loaded complexes. The complexes produced have a more fibrous and less compact appearance, however complexes were still able to form in all cases.

Ch:HA 1:1 Ch:HA 0.5:1 Ch:HAM 1:1 Ch:HAM 0.5:1

Figure 6-2 Photographs showing Ch:HA and Ch:HAM complexes at different polymer ratios loaded with RBITC nanoparticles prepared in ASF.
Chitosan, HA/HAM and nanoparticles were mixed at the indicated ratio and incubated at 37°C. Photographs were taken after 60 minutes.

To further analyse the kinetics of composite formation rheology time sweeps were carried out on Ch:HA and Ch:HAM complexes at the 1:1 ratio. The results of these investigations are presented in Figures 6-3 and 6-4. The Ch:HA 1:1 ratio complexes showed that the presence of nanoparticles slightly slowed initial complex formation, Figure 6-3. The cross-over point of G′ and G″ is delayed from around 20 minutes without nanoparticles to around 60 minutes when nanoparticles were present. When the phase angle (δ) values are examined further differences become evident. The phase angle of the Ch:HA sample without nanoparticles became steady after 150 minutes which suggests that the complexes were undergoing very little change after this point. In the sample containing nanoparticles the phase angle did not stabilise after 150 minutes which suggests that formation continued for longer in this sample.

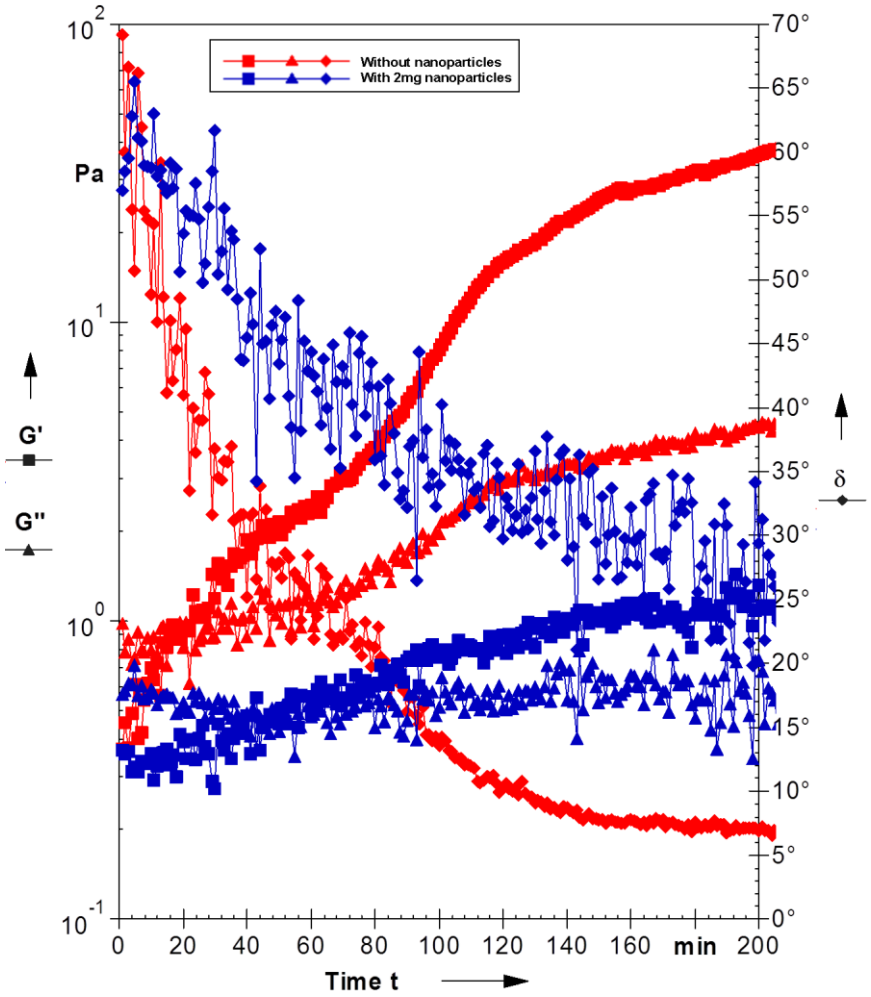

Figure 6-3 Rheology time sweeps showing the formation kinetics of Ch:HA complexes loaded with nanoparticles.
Rheology time sweeps were conducted at 37°C on Ch:HA 1:1 complexes. Chitosan, HA and PGA nanoparticles were mixed on the plate of the rheometer and measurements were started as soon as possible afterwards. G′ (squares) and G″ (triangles) are plotted on the primary y-axis; phase angle (δ- diamonds) is plotted on the secondary axis.

The results obtained with Ch:HAM 1:1 ratio complexes showed that for these samples the addition of nanoparticles had very little effect on the speed of formation, Figure 6-4. The formation remained extremely rapid with an instantaneous gelation and no change after 20 minutes. The formation was also unaffected by different amounts of nanoparticles. Increasing nanoparticle levels can be seen to increase the G′ value of the complexes suggesting that this addition is strengthening the complexes. Further examination reveals that the final phase angle of these samples remains constant. This implies that the presence of nanoparticles may be increasing the strength of the complexes but

without affecting the overall solidity of the complexes; both the G′ and G″ are being increased proportionally.

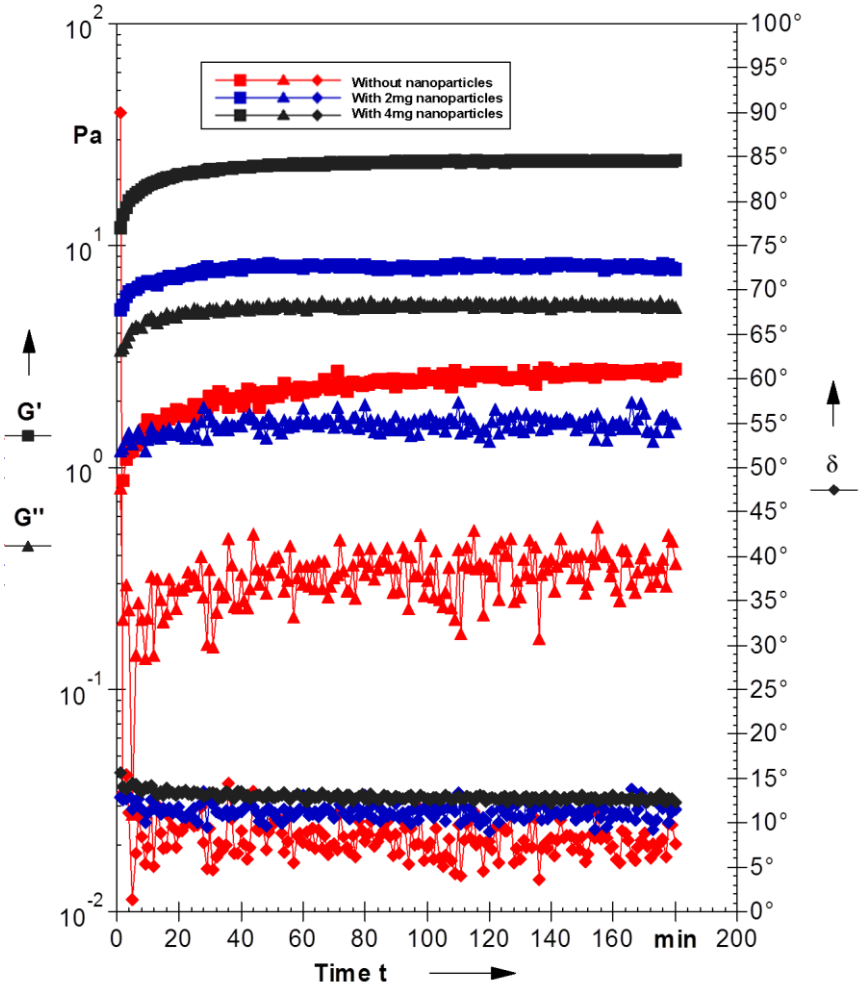

Figure 6-4 Rheology time sweeps showing the formation kinetics of Ch:HAM complexes loaded with nanoparticles.
Rheology time sweeps were conducted at 37°C on Ch:HAM 1:1 complexes. Chitosan, HAM and PGA nanoparticles were mixed on the plate of the rheometer and measurements were started as soon as possible afterwards. G′ (squares) and G″ (triangles) are plotted on the primary y-axis; phase angle (δ- diamonds) is plotted on the secondary axis.

6.3.1.2 Nanoparticle incorporation levels

The incorporation of nanoparticles into the polyelectrolyte complexes was an important part of this delivery system. In order for a sustained drug release to occur a high proportion of the nanoparticles added need to be incorporated into the complexes. No specific mechanism was used with these nanoparticles to ensure their uptake. However as the particles have been shown to have high

zeta potentials it was hoped that the surface charge would be sufficient to cause incorporation of particles into the complexes. It was therefore very important to analyse the particle incorporation to and the fluorescent labelled nanoparticles were used to allow this measurement to be carried out more easily.

RBITC loaded particles were included in the preparation of complexes. After formation had occurred the composites were separated using nylon mesh filters of 30µm pore size. This size was chosen as it is closest to the size limit for phagocytosis (Greis et al., 1994) which means that any particles or complex material which passed through these filters would be likely taken up by the phagocytes present within the joint. The solution that passed through the filter was analysed using a fluorimeter, to allow the quantification of the particles present and the calculation of the incorporated particles. The results of this study are shown in Figure 6-5.

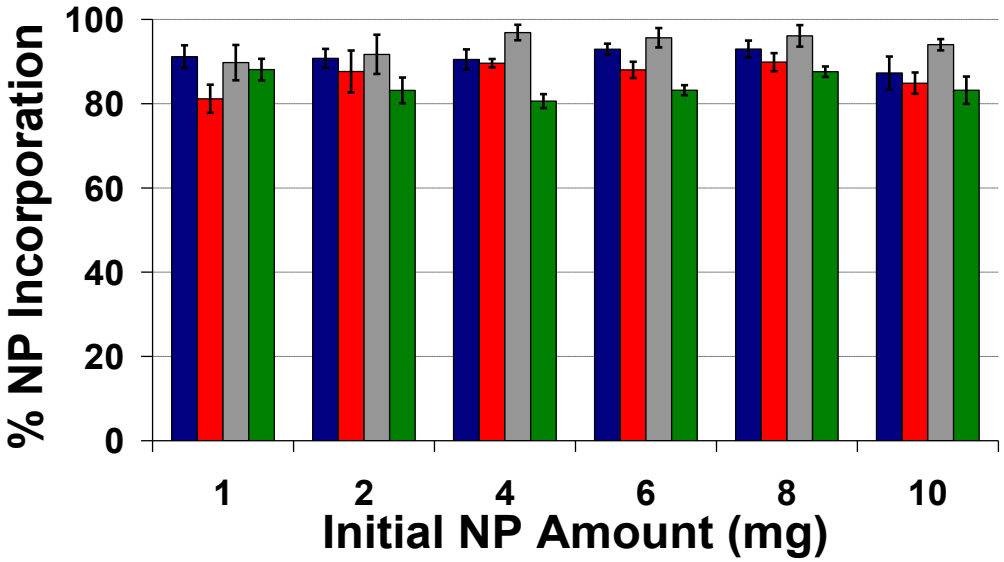

Figure 6-5 Graphs showing nanoparticle incorporation levels into Ch:HA and Ch:HAM complexes.
Chitosan, HA/HAM and RBITC loaded nanoparticles (NP) were mixed together and incubated at 37°C in a water bath for 60 minutes. Complexes were removed and the remaining solution was analysed using a fluorimeter to estimate the nanoparticle incorporation into complexes. Ch:HA 1:1- blue; Ch:HA 0.5:1- red; Ch:HAM 1:1- grey; Ch:HAM 0.5:1- green.

These results show that in all cases very high nanoparticle incorporations were achieved. All complex types and all nanoparticle loading levels studied gave an incorporation of over 80%, and even at high nanoparticle levels no decrease in incorporation was seen. Statistical analysis of the results revealed no significant differences between complexes of the same type with different nanoparticle loading levels. Comparing different complex types at the same loading levels revealed a number of significant differences. The most relevant were between Ch:HAM 0.5:1 ratio samples and all other samples when an initial amount of nanoparticles between 4mg and 6mg was used ($P<0.01$). Also Ch:HA 0.5:1 ratio samples showed significant differences to both 1:1 ratio samples with 6mg or 8mg initial nanoparticles ($P<0.05$). With the 1mg initial loading significant differences were found between the Ch:HA 0.5:1 ratio samples and all other samples ($P<0.05$).

To better understand the incorporation of nanoparticles into the complexes it was desired to use an imaging technique to provide a visualisation of the particles within the complexes. Cryo-SEM (scanning electron microscopy) was utilised as it is a technique that allows the internal structure of samples to be imaged. However it proved very difficult to produce reproducible and accurate images of these complexes. The images produced (data not shown) seem to show that the nanoparticles were not as evenly distributed as it appeared from visual inspection. This was supported by fluorescent microscopy studies carried out on complexes loaded with fluorescently labelled nanoparticles. These showed an uneven distribution of particles within the complexes (data not shown), however no clear images were produced with this technique.

6.3.1.3 Complex integrity

Rheology amplitude sweeps were conducted to assess the complex strength. From the raw data the G′ and yield stress values were extracted and these are presented in Figure 6-6. Samples of 0.7:1 ratio were run in addition to help show any trends with changing chitosan concentration. The results show that in almost all cases nanoparticles act to increase the complex strength. It is also interesting to note that the complex strength increases in the order: unloaded complexes; RBITC loaded composites; DXMP loaded composites. In the majority of cases, as shown in Table 6-1, the differences between these different complex types were statistically significant ($P<0.05$).

Complex Type	No NP v RBITC	No NP v DXMP	RBITC v DXMP
Ch:HA 1:1	√/√	√/√	√/√
Ch:HA 0.7:1	√/√	√/√	√/X
Ch:HA 0.5:1	X/√	√/√	√/√
Ch:HAM 1:1	√/√	√/√	√/X
Ch:HAM 0.7:1	√/X	√/√	√/√
Ch:HAM 0.5:1	√/X	√/X	X/X

Table 6-1 Table showing significant differences in rheology results between nanoparticle loaded complexes.
Significant differences ($P<0.05$) between rheology results different nanoparticle loaded complexes. First value refers to G′ value and second value to yield stress value. √ indicates a significant difference and X indicates that difference was not significant.

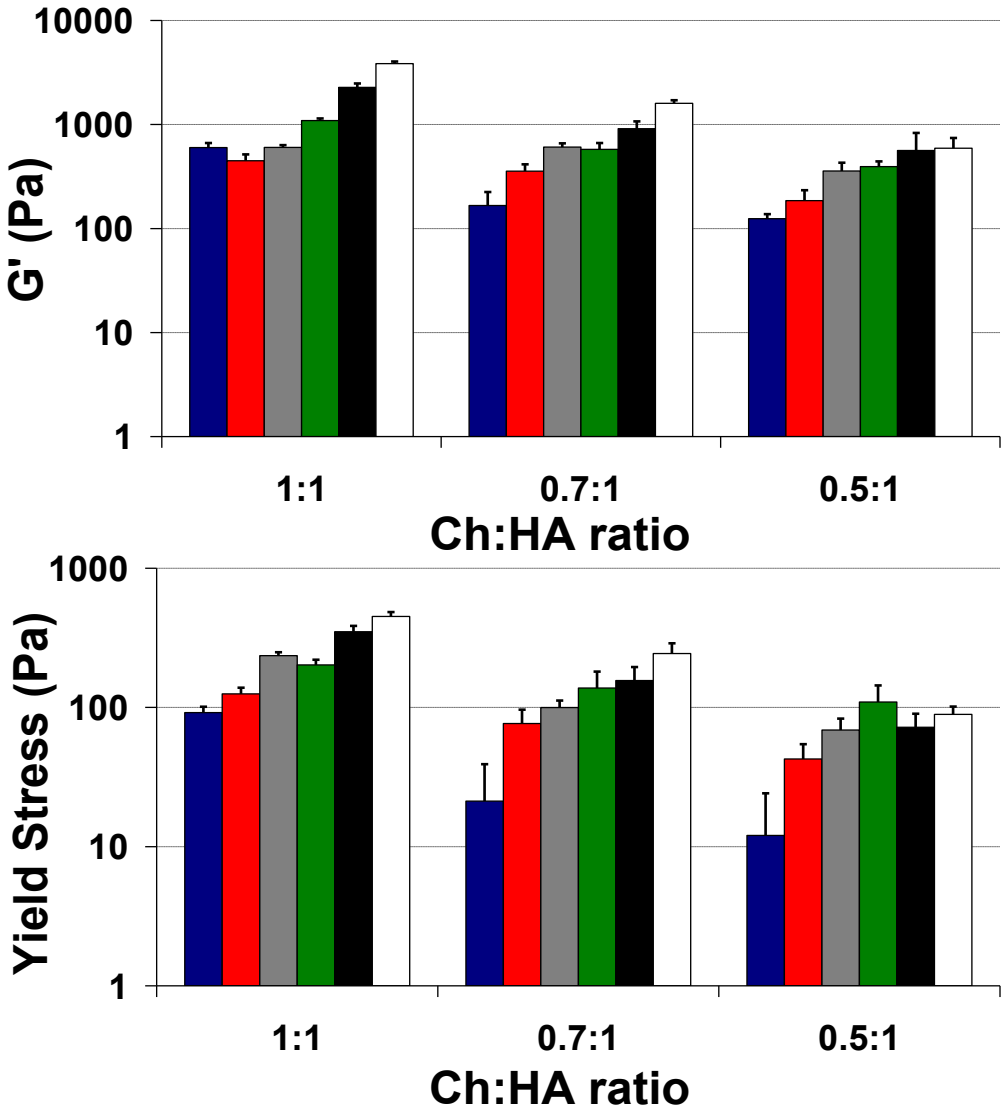

Figure 6-6 Graphs showing G′ and yield stress values for Ch:HA and Ch:HAM complexes loaded with nanoparticles.
G′ and yield stress values were extracted from rheology amplitude sweeps carried out at 37°C on complexes loaded with nanoparticles where indicated. Top: G′ value in LVR; bottom: yield stress value. For both graphs: Ch:HA- blue; Ch:HA with RBITC loaded NP- red; Ch:HA with DXMP loaded NP- grey; Ch:HAM- green; Ch:HAM with RBITC loaded NP- black; Ch:HAM with DXMP loaded NP- white.

The presence of nanoparticles seemed to have a greater effect on the strength of Ch:HA complexes compared to Ch:HAM complexes. The Ch:HAM 0.5:1 ratio samples were the least affected by the addition of nanoparticles with no significant differences between the yield stresses. The G′ and yield stress values for the Ch:HAM 0.5:1 samples still exceeded the highest values for Ch:HA 0.5:1 samples. This shows that the use of HAM rather than HA in the complexes gives a higher strength than the addition of nanoparticles.

6.3.1.4 Composite degradation

In order for this delivery system to be useful for a sustained drug release, long term stability of the composites was required. The degradation of nanoparticle loaded complexes was therefore assessed using a mass degradation method. The results of studies in both ASF and ASFP are presented in Figure 6-7.

The degradation in ASF was found to be slower and more gradual with nanoparticles present. The degradation of complexes without nanoparticles, Figure 4-8, showed a rapid initial mass loss over 14 days followed by a plateau. The nanoparticle loaded complexes showed no rapid initial degradation, only a gradual mass loss throughout the study period. A higher mass of complex remained at the end of the study than with unloaded complexes, around 75% compared to between 45% and 60% for complexes alone. The difference was statistically significant ($P<0.05$) for all complex types except Ch:HAM 1:1 complexes.

In ASFP the degradation of 0.5:1 ratio samples showed a gradual degradation to a level similar to that seen with ASF, Figure 6-7. However without nanoparticles these samples showed a steady increase in mass, Figure 4-10. The 1:1 ratio samples both showed a similar degradation profile in ASFP to that seen without nanoparticles. Smaller increases in mass were observed, with a significant difference ($P<0.01$) in the Ch:HA 1:1 samples at 56 days. Overall it seems that the addition of nanoparticles increased the degradation in ASFP as lower final masses remained. Extensive adsorption of protein was seen in the complexes without nanoparticles. Therefore the decreases in mass seen may be

due to a reduction in protein adsorption. These results highlight the effects that protein can have on these complexes. The use of ASFP increases the deviation in the results showing that a more diverse response occurs when protein is present.

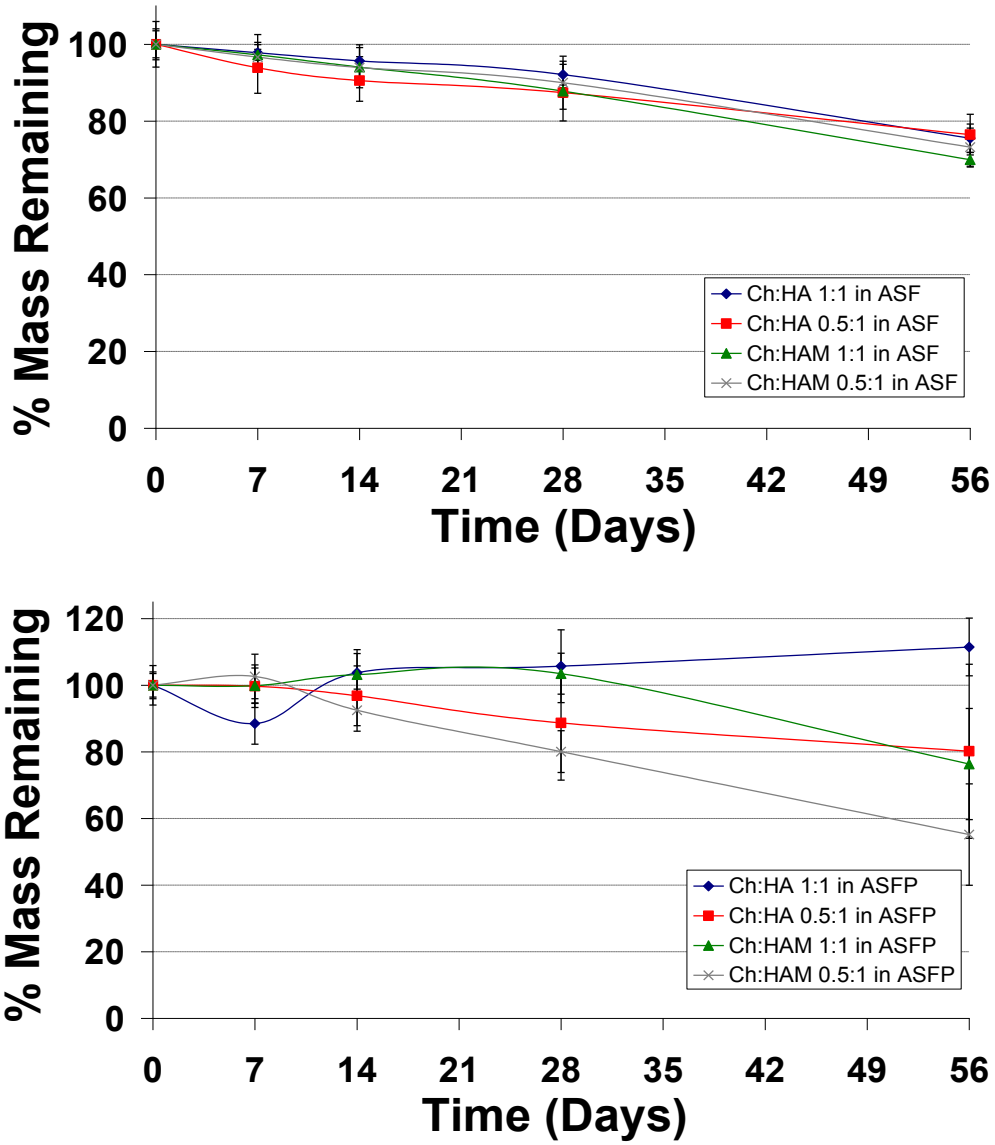

Figure 6-7 Mass degradation profiles of Ch:HA and Ch:HAM complexes loaded with nanoparticles.
Ch:HA and Ch:HAM complexes loaded with PGA nanoparticles were prepared and then incubated in buffer at 37°C. Buffer was regularly changed and at each time point complexes were extracted, dried and weighed. Buffer and complex type used are detailed in the legend.

The mass loss from the complexes is not the only important factor during their degradation. The integrity and strength of the complexes must be retained to allow the complexes to withstand the forces that occur within joints. Rheology

amplitude sweeps were carried out on samples degraded in ASF to assess the integrity and strength of the complexes during degradation and the results are presented in Figure 6-8.

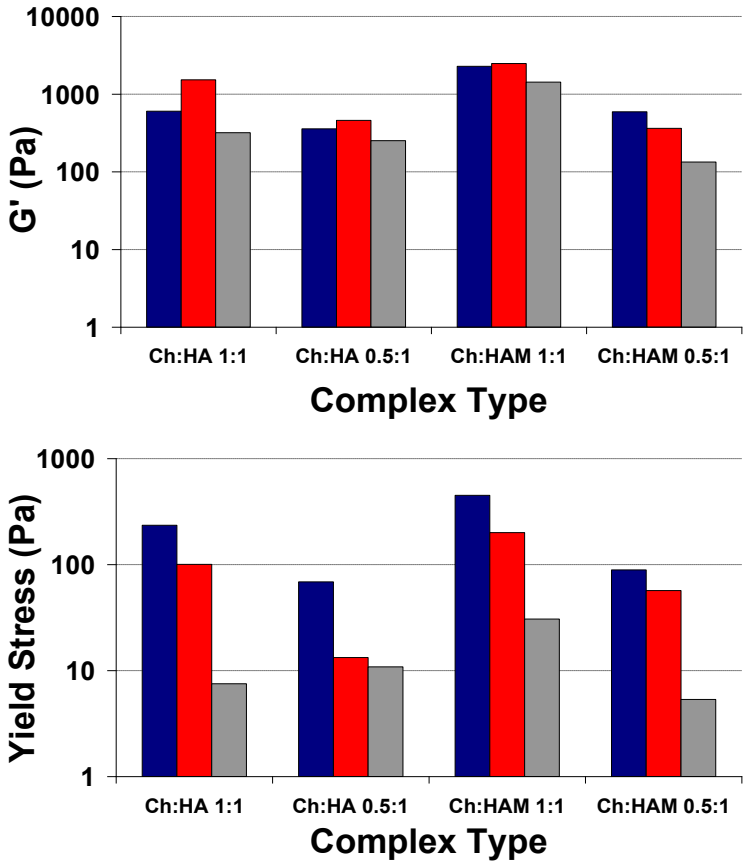

Figure 6-8 G′ and yield stress values for Ch:HA and Ch:HAM complexes loaded with nanoparticles during degradation in ASF.
G′ and yield stress values were extracted from rheology amplitude sweeps carried out on ASF degraded complexes loaded with nanoparticles at 37°C. Top: G′ value in LVR; bottom: yield stress value. For both graphs, time of degradation: 0 days- blue; 28 days- red; 56 days- grey.

The results were very similar to those obtained from complexes without nanoparticles, Figure 4-9. A small increase is observed in G′ values in the first 28 days, which is followed by a slight decrease after 56 days. The yield stress values show a gradual but larger decrease over the study period. This shows that there is a gradual loss of resistance to shear stress whilst the overall structure and strength of the complexes is minimally affected.

6.3.1.5 Nanoparticle release

This composite delivery system is designed to retain nanoparticles within the joint and therefore the nanoparticles need to be retained within the complexes. To ensure that this was the case the release of nanoparticles from the complexes was investigated. This was carried out using the fluorescently labelled nanoparticles as this allowed easy quantification of released particles. The results of this study are presented in Figure 6-9.

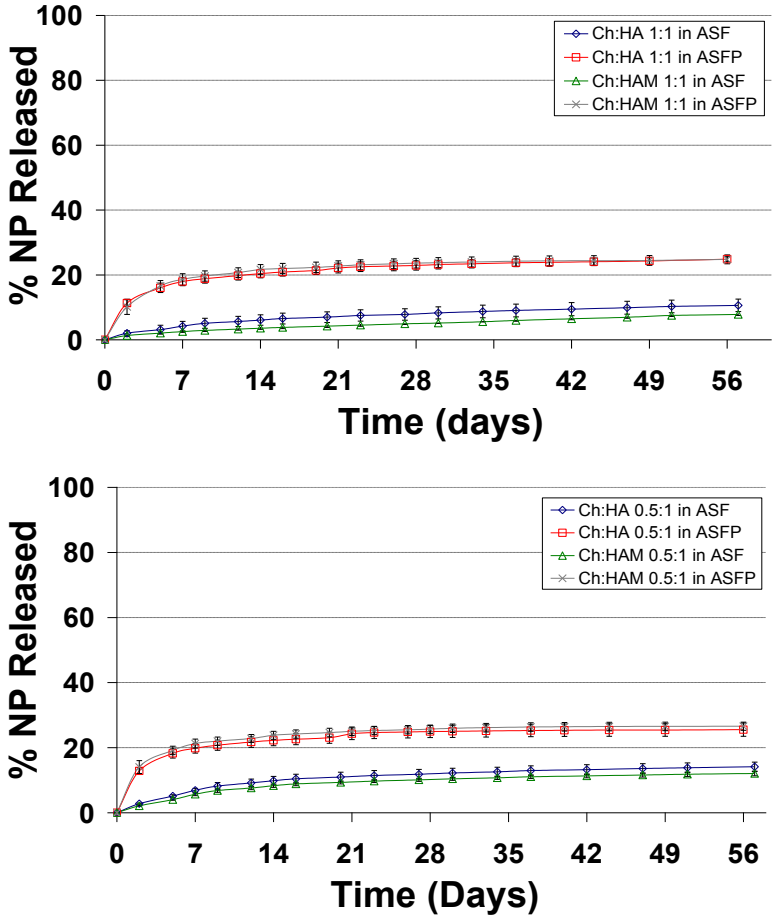

Figure 6-9 Release profiles of nanoparticles from composites incubated in buffer. Ch:HA and Ch:HAM complexes loaded with nanoparticles (NP) containing RBITC were prepared and then incubated in buffer at 37°C. Buffer was regularly changed and release of nanoparticles was determined by fluorimetery. Buffer and complex type used are detailed in the legend.

It was found that only a low release of particles occurred from the complexes. This release occurred rapidly and after 7 days minimal further release occurred. In all samples a maximum of 25% of the loaded nanoparticles were released

during the 56 days of the study. Significant differences were found between release in ASF and ASFP ($P<0.01$), with a higher release occurring in the presence of protein. A significantly higher release was also found in 0.5:1 ratio samples compared to 1:1 ratio samples ($P<0.01$).

6.3.1.6 Enzymatic degradation of complexes

In the osteoarthritic joint a number of catabolic enzymes are present. Many of these enzymes are proteinases and would not be expected to have any effect on the carbohydrate based polymers used in these complexes. Hyaluronic acid is a component of synovial fluid and so is naturally degraded by the enzyme hyaluronidase (HAase). There is no consensus as to whether this enzyme is present within the joint. However HAase can be used to give more challenging degradation conditions to allow the potential of these complexes to be assessed. The complexes were incubated in the presence of HAase and the particle release was monitored to show the enzyme degradation. The results of this investigation are shown in Figure 6-10.

A formate buffer of pH 4.5 was used for this investigation as this is the optimal pH for HAase activity. The particle release with formate buffer is very similar to that seen with ASF. A significantly greater degradation and particle release occurred in the presence of enzyme ($P<0.01$). The composites incubated with enzyme showed an initial phase of between 7 and 21 days where the particle release was no different to samples incubated in buffer. After this initial lag the 1:1 ratio complexes showed a gradual and sustained degradation. The complexes prepared with HAM showed a longer lag period and lower

degradation than HA samples, however the differences were not statistically significant. After 56 days at the end of the study the complexes were disrupted using a high concentration of hyaluronidase leading to the recovery of around 20% to 30% of the loaded nanoparticles from the 1:1 ratio complexes. These results show that even under challenging conditions these complexes show a high level of stability.

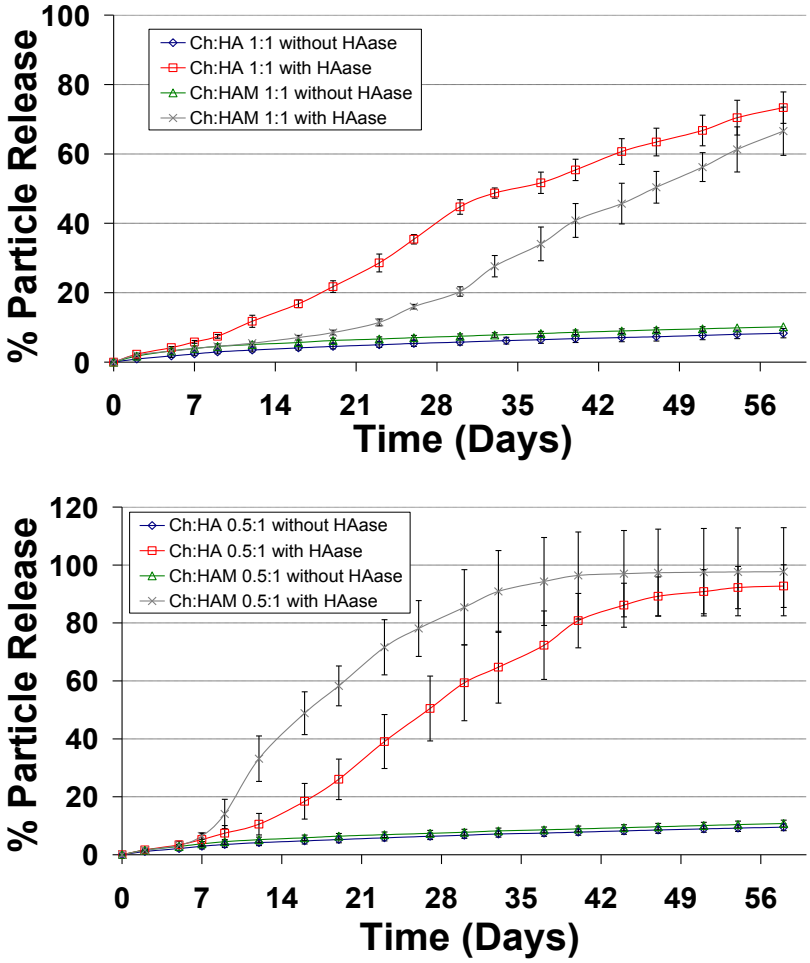

Figure 6-10 Release profile of nanoparticles from composites during hyaluronidase degradation.
Ch:HA and Ch:HAM complexes loaded with nanoparticles (NP) containing RBITC were prepared and then incubated in formate buffer (pH 4.5) at 37°C. In indicated samples 3U of HAase (0.6 U/ml) was also included in the buffer. Buffer was regularly changed and release of nanoparticles was determined by fluorimetery. Complex type used is detailed in the legend.

The 0.5:1 ratio complexes showed a faster degradation in the presence of enzyme than the 1:1 ratio complexes, Figure 6-10. There was only a significant difference in the degradation level between 35 and 56 days ($P<0.01$). At this

polymer ratio the complexes containing HAM showed a faster degradation than occurred with complexes containing HA; however the differences were not significant. The 0.5:1 ratio complexes also showed a more complete degradation with only 5% to 10% of the loaded nanoparticles being recovered at the end of the study.

6.3.2 Evaluation of Injectable Formulation

6.3.2.1 Stability in salt

In order to produce an injectable formulation for this delivery system complexation will be prevented by salt. The effect that nanoparticles have on the complex stability in salt is therefore important and was investigated using photography of the composites formed in increasing salt concentrations. Fluorescently labelled nanoparticles were used to give a visual indication of the nanoparticle incorporation and distribution. The results of this study are presented in Figure 6-11. At the 1:1 ratio discrete compact complexes were formed in 0.2M NaCl and below. At 0.3M and 0.4M salt a diffuse precipitated complex was produced, and a full disruption occurred with 0.5M NaCl.

For the 0.5:1 ratio a complete complex disruption occurred in a salt concentration of 0.3M and above. Composites prepared using HA formed into discrete compact complexes in 0.2M NaCl and below, whereas HAM produced discrete compact complexes in NaCl concentrations of 0.1M and below.

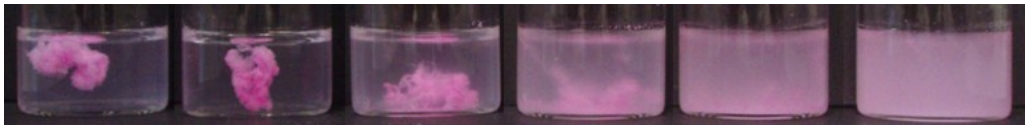

0M 0.1M 0.2M 0.3M 0.4M 0.5M

Ch:HA 1:1 complexes

0M 0.1M 0.2M 0.3M 0.4M 0.5M

Ch:HA 0.5:1 complexes

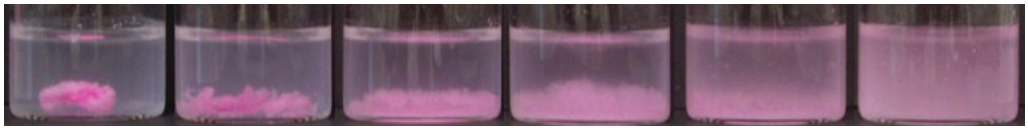

0M 0.1M 0.2M 0.3M 0.4M 0.5M

Ch:HAM 1:1 complexes

0M 0.1M 0.2M 0.3M 0.4M 0.5M

Ch:HAM 0.5:1 complexes

Figure 6-11 Photographs showing the effect of salt on composite formation.
Complexes including RBITC loaded nanoparticles were prepared in the presence of the indicated concentration of NaCl. Mixtures were incubated at 37°C for 60 minutes to allow complex formation to occur before photographs were taken.

6.3.2.2 Composite formation by dialysis

From the mixtures prepared in 0.5M NaCl a dialysis formation method was utilised to form complexes. This method mimicked the reduction in salt that would occur *in vivo* through diffusion. The formation of composites by this method were analysed by photography and rheology amplitude sweeps.

The results of the photographic study are presented in Figure 6-12, and show that this method was able to produce a visible complex formation in all cases. Ch:HA 1:1 samples showed the best visible formation with a rapid precipitation within 15 minutes, followed by a contraction and aggregation of the complex over 60 minutes. There appeared to be an even distribution of nanoparticles in these samples.

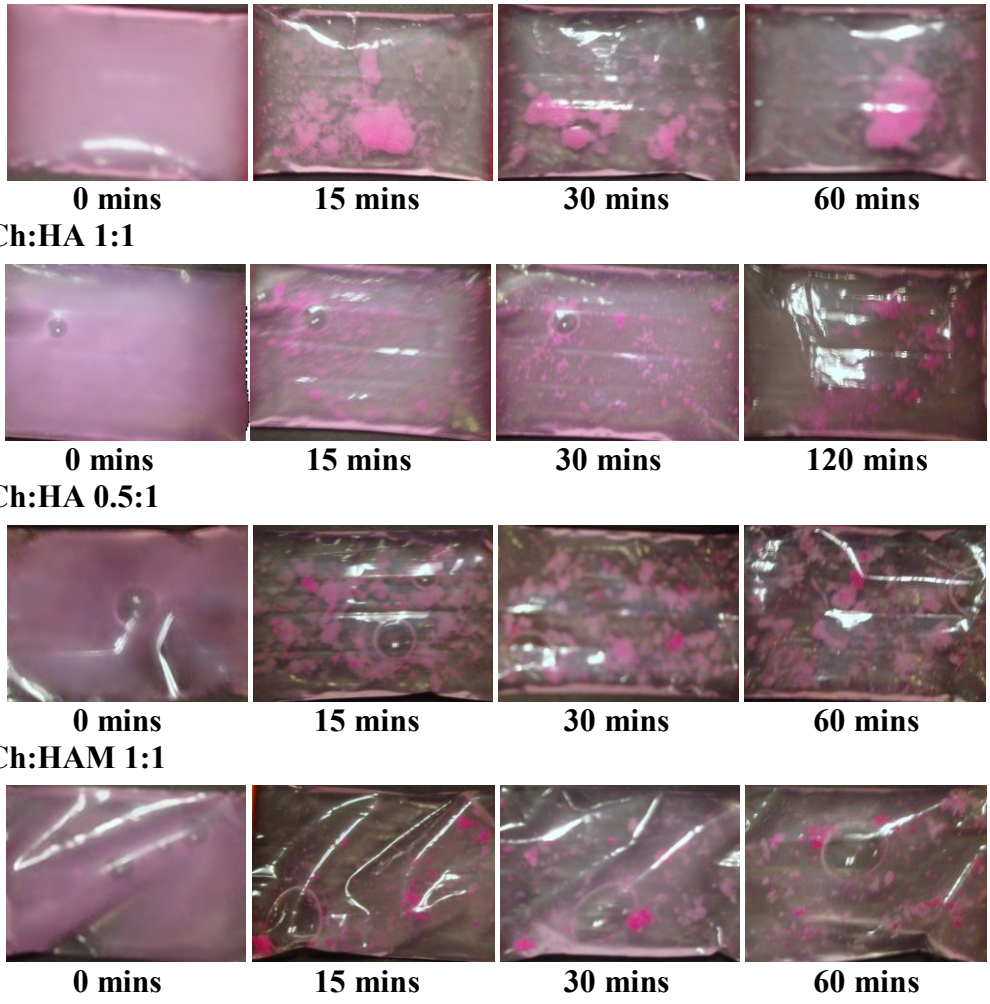

Figure 6-12 Photographs showing formation of composites by dialysis.
Solutions containing composite components (including RBITC loaded nanoparticles) were prepared in 0.5M NaCl. These mixtures were dialysed against ASF at 37°C with the buffer replaced every 15 minutes. Photographs were taken at each buffer change.

Ch:HAM 1:1 ratio samples also showed a good visual formation, which occurred into small discrete complexes, Figure 6-12. After an initial rapid precipitation very little rearrangement occurred. In these samples there appeared to be a less even distribution of particles with a small number of complexes appearing to be enriched with nanoparticles.

The samples at the 0.5:1 ratio showed an impaired formation by this method, but a rapid precipitation still occurred, Figure 6-12. For the Ch:HA 0.5:1 complexes this was followed by a much slower rearrangement over the course

of 120 minutes into small discrete complexes. The Ch:HAM 0.5:1 complexes showed no changes after 30 minutes, and formed a number of small discrete complexes.

The results of the rheology time sweeps are presented in Figure 6-13. These back up the visual observations. They found that in all samples except Ch:HA 0.5:1 a detectable formation occurred. Ch:HAM 1:1 ratio composites showed the most rapid formation, with complex detectable after 15 minutes. Despite the lack of visual changes after this point, the rheology revealed a gradual strengthening. Complexation was detected in Ch:HA 1:1 ratio composites after 30 minutes, with a gradual increase in complex strength after this time. The Ch:HAM 0.5:1 ratio composites showed a slower formation, with complex detected after 60 minutes.

To ensure that formation was not differently affected by drug loaded nanoparticles a further study was undertaken using these particles and the results of this photographic study are presented in Figure 6-14. These photographs show that the DXMP loaded nanoparticles do not cause any visible changes. The Ch:HA 1:1 ratio samples still produced the largest complexes. The other samples produced similar small discrete complexes.

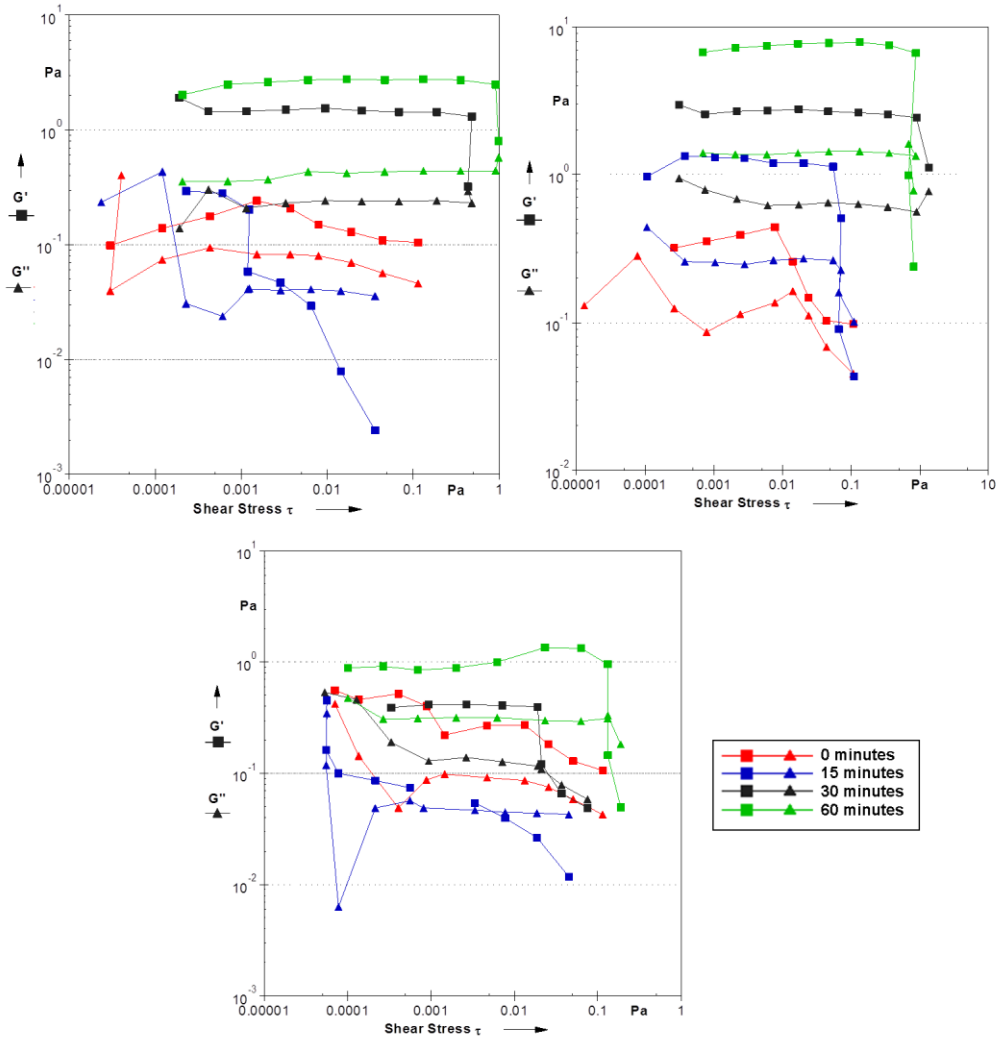

Figure 6-13 Rheology amplitude sweeps showing composite formation by dialysis. Solutions containing composite components were prepared in 0.5M NaCl. These were dialysed against ASF at 37°C with the buffer replaced every 15 minutes. Rheology amplitude sweeps were carried out on the recovered mixtures at 37°C. G′ (squares) and G″ (triangles) are plotted against shear stress. Top left: Ch:HA 1:1; Top right: Ch:HAM 1:1; Bottom: Ch:HAM 0.5:1. The time of dialysis is shown in the legend and is the same for all graphs.

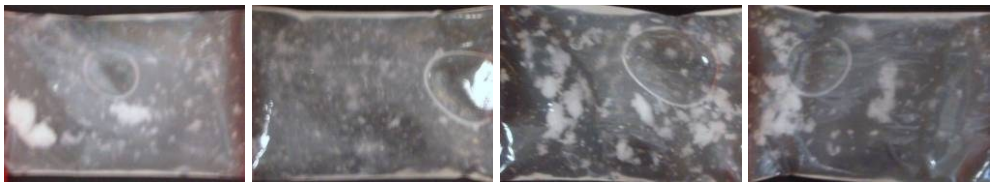

Ch:HA 1:1 **Ch:HA 0.5:1** **Ch:HAM 1:1** **Ch:HAM 0.5:1**

Figure 6-14 Photographs showing formation of drug loaded composites by dialysis. Solutions containing complex components (including DXMP loaded nanoparticles) were prepared in 0.5M NaCl. These mixtures were dialysed against ASF at 37°C with the buffer replaced every 15 minutes. After 60 minutes of dialysis photographs were taken.

6.3.2.3 Nanoparticle incorporation levels

The studies conducted into the dialysis formation method have shown that the complexes appear different to the bulk formed complexes. The effect that the dialysis formation method had on the other properties of the complexes was therefore investigated. The incorporation of nanoparticles is an essential property and so the incorporation study was repeated using dialysis formed samples. The results of this study are presented in Figure 6-15.

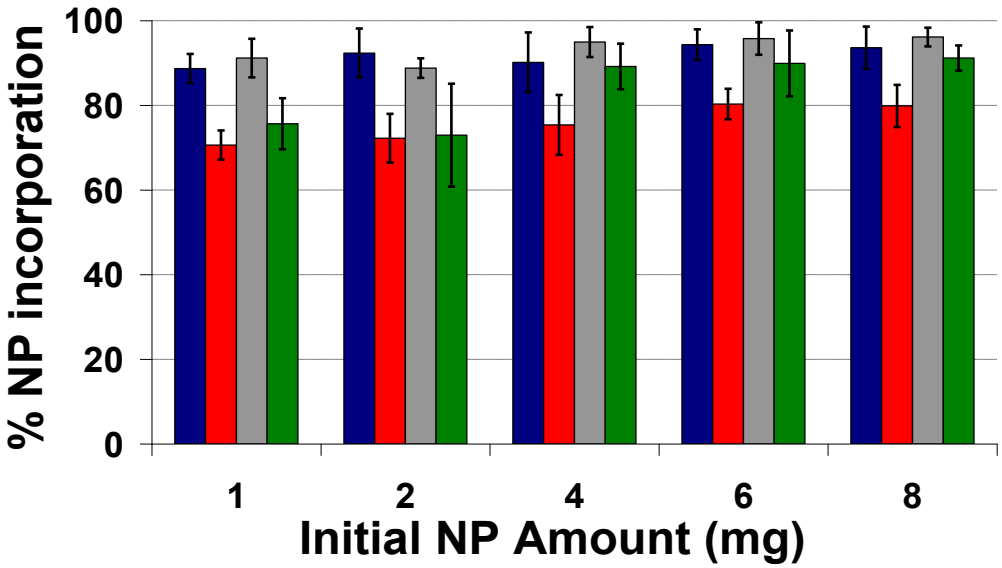

Figure 6-15 Graph showing nanoparticle incorporation levels into Ch:HA and Ch:HAM complexes formed by dialysis.
Solutions containing complex components (including RBITC loaded nanoparticles (NP)) were prepared in 0.5M NaCl. These mixtures were dialysed for 60 minutes against ASF at 37°C with the buffer replaced every 15 minutes. Complexes were removed and remaining solution was analysed using a fluorimeter to estimate the nanoparticle incorporation into complexes. Ch:HA 1:1- blue; Ch:HA 0.5:1- red; Ch:HAM 1:1- grey; Ch:HAM 0.5:1- green.

The results show that high levels of incorporation occurred with this formation method. The loading levels were over 70% for 0.5:1 ratio samples and over 85% for the 1:1 ratio complexes. For the majority of samples there was no significant difference between the bulk formed complexes and the dialysis formed complexes. The exception was the Ch:HA 0.5:1 samples which showed a significant difference in loading at loading levels of 1, 2 and 6mg ($P<0.05$). Incorporation levels were consistently lower with the dialysis formation

method. Comparing different complex types only found significant differences between the Ch:HA 0.5:1 ratio samples and both 1:1 ratio samples.

6.3.2.4 Complex integrity

The visual differences in the complexes produced by the dialysis method meant it was important to assess the strength of these complexes. This was done through rheology amplitude sweeps on dialysis formed complexes and the results of this study are presented in Figure 6-16. These results show that 1:1 ratio complexes exhibited a slightly increased G′ and yield strength compared to the bulk formed complexes. In contrast the 0.5:1 ratio complexes show a decreased G′ and yield strength values compared to bulk formed complexes. In the case of Ch:HAM 0.5:1 these values are reduced dramatically. These results suggest that the 1:1 ratio complexes are stronger when produced by the dialysis method, whereas the 0.5:1 ratio produced weaker complexes.

6.3.2.5 Degradation

The long term stability of these composites in ASF was assessed using a mass degradation method and the results of this study are presented in Figure 6-17. The dialysis formed complexes exhibited a gradual degradation over the 56 day study period, which is an identical response to that seen with bulk formed complexes. The mass remaining at the end of the study in complexes produced by dialysis (between 50% and 70%) was slightly lower than for bulk formed complexes (between 70% and 75%). The only statistically significant difference in the degradation between bulk formed and dialysis formed complexes was in Ch:HA 0.5:1 ratio samples beyond 14 days ($P<0.01$).

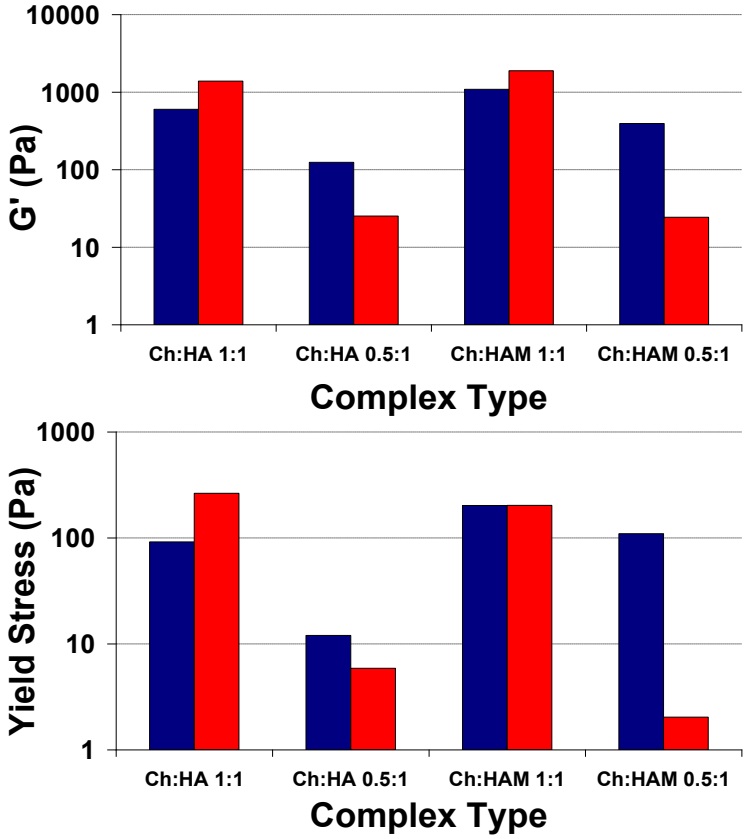

Figure 6-16 G′ and yield stress values for Ch:HA and Ch:HAM complexes loaded with nanoparticles prepared by dialysis.
G′ and yield stress values were extracted from rheology amplitude sweeps carried out on 1:1 ratio composites at 37°C. Top: G′ value in LVR; bottom: yield stress value. For both graphs: bulk formation method- blue; dialysis formation method- red.

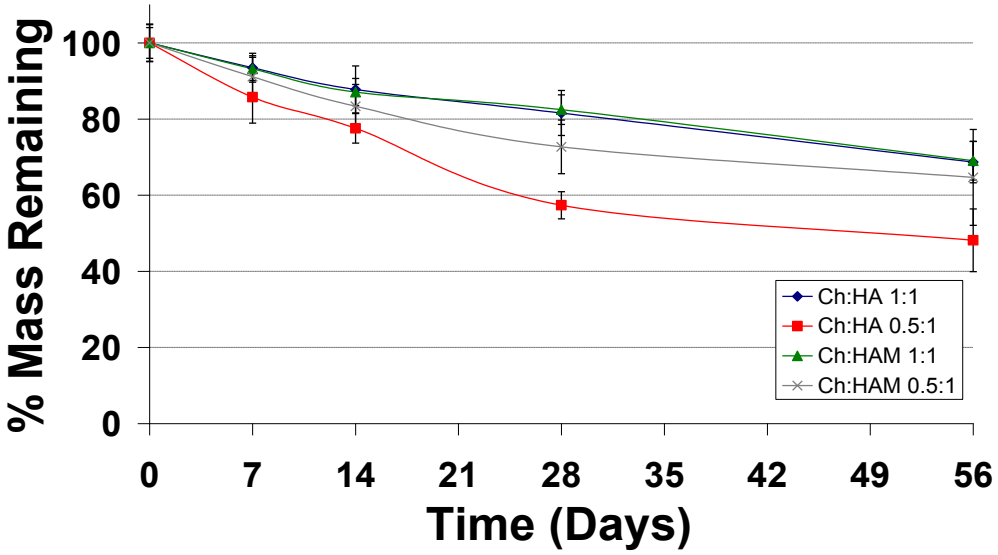

Figure 6-17 Mass degradation profiles in ASF of Ch:HA and Ch:HAM composites formed by the dialysis method.
Ch:HA and Ch:HAM complexes loaded with PGA nanoparticles were prepared by the dialysis method and then incubated in ASF buffer at 37°C. Buffer was regularly changed and at each time point complexes were extracted, dried and weighed.

6.3.2.6 Particle release

The particle release from the dialysis formed composites was analysed using fluorescently labelled nanoparticles. This study found that only a very small amount of nanoparticles were released from the complexes during the 56 day study, Figure 6-18. The release was lower than that seen for bulk formed complexes, and significant differences in the particle release were found for all complex types except Ch:HAM at the 1:1 ratio ($P<0.01$). Ch:HA 1:1 complexes showed a significant difference after 9 days until the end of the study ($P<0.01$), Ch:HA 0.5:1 complexes after 5 days ($P<0.001$), and Ch:HAM 0.5:1 complexes after 7 days ($P<0.001$).

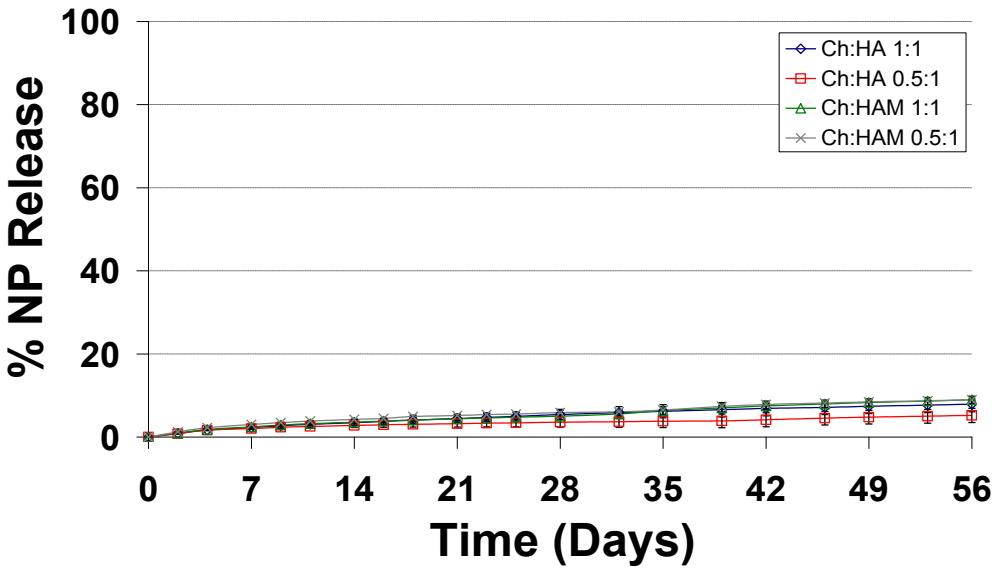

Figure 6-18 Release profiles of nanoparticles from composites prepared by dialysis. Ch:HA and Ch:HAM complexes loaded with PGA nanoparticles (NP) were prepared by dialysis and then incubated in ASF buffer at 37°C. Buffer was regularly changed and release of nanoparticles was determined by fluorimetery.

6.3.2.7 Enzymatic degradation of composites

As well as the degradation in biologically relevant buffer it was desired to test the composites under more challenging conditions as the conditions experienced within the joint are likely to be quite challenging. A high

concentration of hyaluronidase was chosen to provide a challenging test of the stability of these complexes. The enzymatic degradation was monitored by the release of fluorescently labelled nanoparticles from the complexes. The results of this study are shown in Figure 6-19.

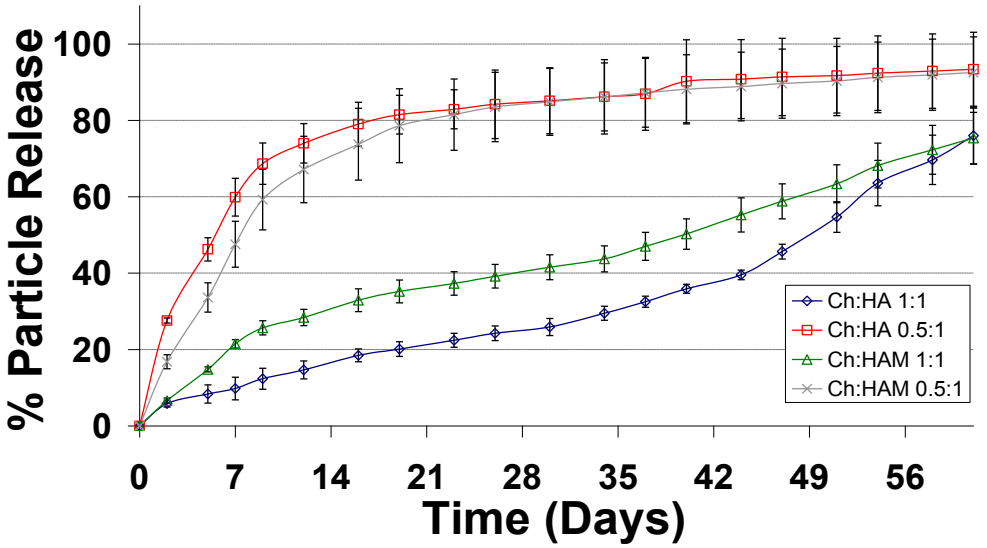

Figure 6-19 Release profile of nanoparticles from composites prepared by dialysis during hyaluronidase degradation.
Ch:HA and Ch:HAM complexes loaded with PGA nanoparticles (NP) were prepared by dialysis and then incubated in formate buffer (pH 4.5) containing HAase (3U) at 37°C. Buffer was regularly changed and release of nanoparticles was determined by fluorimetery.

In the bulk formed complexes there was an initial phase where the release was the same as composites incubated in buffer alone. For the dialysis formed samples this initial phase of low degradation was not seen, Figure 6-19. The 1:1 ratio composites exhibited a constant degradation throughout the study period. The Ch:HA 1:1 exhibited a slightly slower initial degradation rate compared to Ch:HAM 1:1 ratio complexes, but this difference was not significant. A slight increase in the degradation rate of Ch:HA 1:1 complexes occurred after 35 days. This caused the degradation of this sample to trend back towards the degradation profile of Ch:HAM 1:1 complexes. At the end of the study around 30% of the loaded nanoparticles were recovered from the 1:1

ratio composites. In the 1:1 ratio samples there was no significant differences between the dialysis formed composites and the bulk formed composites.

The 0.5:1 ratio composites showed a rapid initial degradation and around 60% of loaded particles were released in 7 days, Figure 6-19. After this the degradation slowed and a gradual release occurred for the rest of the study period. At the end of the study around 10% of the loaded nanoparticles were recovered from these complexes. The 0.5:1 ratio samples did show a significantly faster initial degradation rate compared to the bulk formed composites. The Ch:HA 0.5:1 samples showed a significant difference between 5 and 23 days ($P<0.001$) and for Ch:HAM 0.5:1 samples a significant difference occurred between 5 and 9 days ($P<0.001$).

6.3.3 Drug Release from Composite Delivery System

6.3.3.1 Dexamethasone phosphate

The proposed delivery system aims to give a sustained release of dexamethasone phosphate over a period of up to three months. This length of sustained delivery was required to allow drug release to occur for the minimum recommended period between intra articular administrations of steroids. Any drug release of over 1 month would provide an improvement on currently available treatments. The drug release from the nanoparticle and polyelectrolyte composite system was an essential property of the system and was therefore investigated.

This experiment investigated complexes incubated directly in buffer; there was no need for a dialysis membrane with the large complexes. The buffer removed at each time point was filtered through a 30μm filter to allow any large particles to be returned to the release medium. The type A synovial lining cells within the joint have a macrophage like activity. The size limit for uptake by these cells means that any particles under 30μm can be considered to have been released as they will be cleared from the joint. The dexamethasone phosphate concentration in the release medium was analysed using the protocol used for the determination of DXMP nanoparticle loading. This resulted in the recovery of all drug whether free or from intact released nanoparticles.

The results of this study are presented in Figure 6-20 and Table 6-2. Figure 6-20 shows the result of a number of control experiments that were carried out. These include the release of DXMP from a dialysis membrane and from PGA nanoparticles, which was determined in chapter 5. The release of free DXMP from the polyelectrolyte complexes was also determined. These results show that the release of free drug from the complexes was extremely rapid with over 90% released within 7 days in all cases. Rate of DXMP release from polyelectrolyte complexes was thus only slightly slower rate of release than was observed for free DXMP from a dialysis membrane.

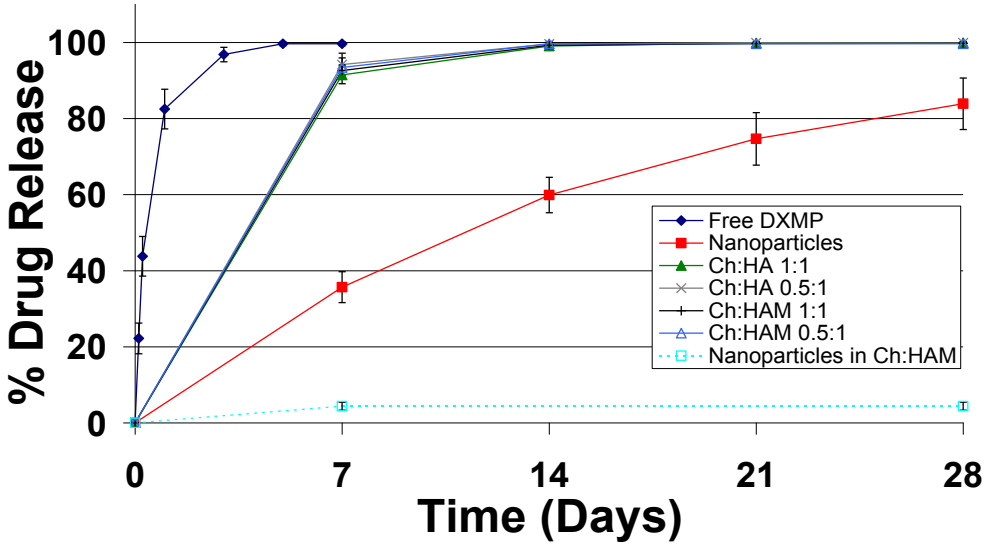

Figure 6-20 Drug release profiles for dexamethasone phosphate from PGA nanoparticles and polyelectrolyte complexes.
Release of dexamethasone phosphate from various formulations in ASF at 37°C. DXMP concentrations were determined by HPLC. The samples used were: free DXMP in dialysis membrane; PGA nanoparticles in dialysis membrane; free DXMP in Ch:HA and Ch:HAM complexes; PGA nanoparticles retained in Ch:HAM 1:1 complexes.

Complex Type	Unincorporated Recovery (%)	Release after 7 Days (%)	Recovery at 56 Days (%)	Total Recovery (%)
Ch:HA 1:1	18.4 (2.8)	3.26 (0.57)	58.3 (4.3)	80.0 (7.2)
Ch:HA 0.5:1	16.5 (3.5)	0.0 (0.0)	62.1 (6.5)	78.7 (3.7)
Ch:HAM 1:1	17.5 (3.8)	4.38 (1.05)	61.2 (5.8)	83.1 (10.5)
Ch:HAM 0.5:1	12.4 (0.62)	0.0 (0.0)	60.9 (6.0)	73.3 (6.0)
Ch:HA 1:1 Dialysis	17.6 (1.0)	0.0 (0.0)	60.8 (5.9)	78.4 (4.9)
Ch:HA 0.5:1 Dialysis	19.2 (1.5)	0.0 (0.0)	59.7 (3.8)	78.9 (4.6)
Ch:HAM 1:1 Dialysis	16.8 (1.9)	0.0 (0.0)	58.2 (3.3)	75.0 (5.0)
Ch:HAM 0.5:1 Dialysis	15.3 (3.5)	0.0 (0.0)	61.6 (6.8)	77.7 (3.3)

Table 6-2 Dexamethasone phosphate release and recovery from PGA nanoparticles loaded into polyelectrolyte complexes.
Release of dexamethasone phosphate from composites incubated in ASF at 37°C. DXMP concentrations were determined using HPLC. 'Dialysis' in complex type indicates that complex was produced using the dialysis formation method.

Figure 6-20 and Table 6-2 show the results for DXMP release from nanoparticle and polyelectrolyte composites. Firstly these results show that the incorporation levels of DXMP loaded nanoparticles were similar to those

observed with RBITC loaded nanoparticles. In all cases an incorporation of over 80% was seen. Drug release was only detected from two samples which were the two 1:1 ratio samples produced by the bulk formation method, shown in Figure 6-20. After the release study had been conducted for 56 days the remaining complexes were disrupted using hyaluronidase to allow the recovery of any unreleased drug. This found that around 55% to 60% of the initially loaded drug was recovered from the delivery system.

6.3.3.2 Dexamethasone crystals

To determine whether it was necessary to incorporate a nanoparticle component into the delivery system the direct incorporation of dexamethasone crystals into complexes was assessed. These crystals were composed of the sparingly soluble steroid dexamethasone rather than the water soluble DXMP used in the nanoparticles in this study. It was first necessary to size the crystals in a dexamethasone suspension as large crystals have been shown to cause irritation in the joint. Intra articularly delivered steroid crystal formulations therefore have a tightly defined size of under 20µm (Derby et al., 2008). As the crystals produced were expected to be in the micrometre range a Coulter counter was used to size the crystals.

Representative results of the dexamethasone crystal sizing are presented in Figure 6-21. The crystals produced had a mean size of 13.4µm and a median of 9.93µm. Only a few particles were larger than 20µm, and a larger proportion were 5µm or smaller.

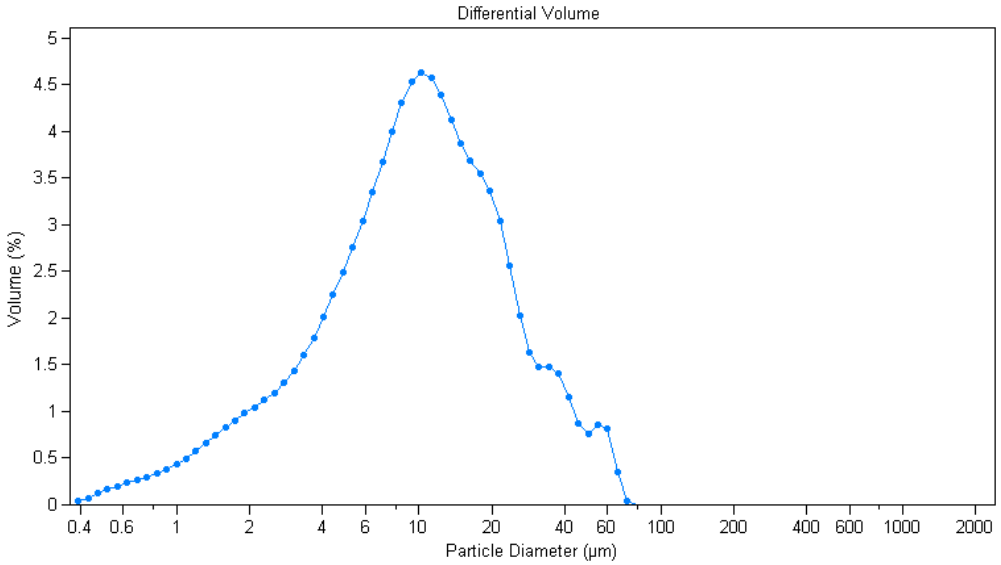

Figure 6-21 Size distribution of dexamethasone crystals determined by Coulter counter. Dexamethasone suspension was prepared in water and crystal size was determined using a Coulter counter.

These crystals were incorporated into polyelectrolyte complexes in the same manner and amount as nanoparticles and the release was determined. The results of this release study are shown in Figure 6-22 and show that the crystal loaded complexes provided a gradual and sustained drug release over around 90 days. No initial burst was observed and the release rate was consistent until it slowed as a complete release was reached.

It was necessary to ensure that this result was not simply an effect of the limited solubility of dexamethasone in water. In order to accomplish this, a control sample of dexamethasone crystals retained within dialysis membrane was utilised. The results of this showed that the dexamethasone release by dissolution alone occurred within 28 days and was significantly different ($P<0.001$) to the release from complexes. A further control sample was analysed to ensure that the effect seen was not due to dexamethasone binding to hyaluronic acid. This sample consisted of dexamethasone crystals and hyaluronic acid retained within a dialysis membrane. The release from this

sample was identical to that seen with dexamethasone crystals alone and was significantly different ($P<0.001$) to the release from complexes.

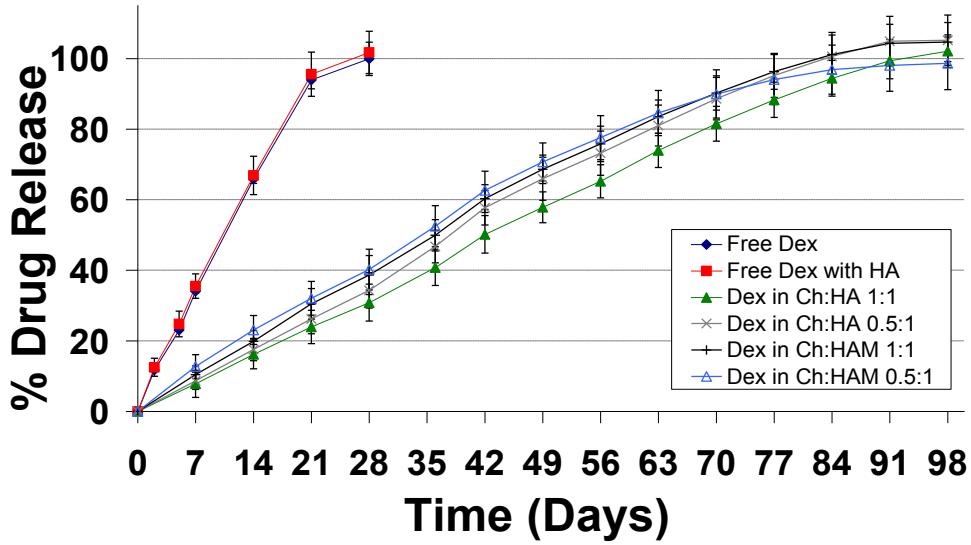

Figure 6-22 Drug release profiles of dexamethasone from polyelectrolyte complexes. Release of dexamethasone (Dex) crystals from various formulations in ASF at 37°C. Dexamethasone concentrations were determined by HPLC. Samples used were: free Dex in dialysis membrane; free Dex and HA in dialysis membrane; free Dex in Ch:HA and Ch:HAM complexes.

6.4 Discussion

6.4.1 Composite Properties

Complexes loaded with nanoparticles were synthesised and the properties of these composites were investigated. The incorporation of nanoparticles had few effects on the properties of the complexes. It was also found that the complexes were able to hold and retain high levels of nanoparticles showing the potential of chitosan and HA complexes as a drug delivery system.

The formation of complexes was not visually affected by the presence of nanoparticles. In the photographic study no differences were observed between complexes prepared in the presence or absence of nanoparticles. The formation of nanoparticle loaded complexes was largely unaffected by the presence of a

physiological salt concentration. A slight disruption was observed in salt as the composites took on a more fibrous and less compact appearance. However the complexes were still able to form into the discrete precipitated complexes that are desired.

The formation kinetics were slightly altered by the presence of nanoparticles and different effects were seen between complexes containing HA and HAM. For Ch:HA 1:1 ratio complexes the nanoparticles slowed formation. The gelation of the system (which is the point where G′ and G″ cross-over so that G′ becomes the larger value) was delayed from around 20 minutes to around 60 minutes. The phase angle also revealed that the samples prepared with nanoparticles continued to form for longer than the 150 minutes that samples without nanoparticles took.

The kinetics of formation with Ch:HAM complexes showed very little difference when nanoparticles were included. The formation remained extremely rapid and the only difference was an increase in the final G′ value of the complexes. This value also increased with higher nanoparticle loading levels suggesting that nanoparticles act to strengthen the composites, and this was found to be the case through rheology amplitude sweeps.

The reason for this difference in formation between the two types of hyaluronic acid is unclear. The most likely explanation would be that the nanoparticles do disrupt formation slightly. HAM has been shown to have positive effects on formation which were attributed to the formation of covalent bonds. Therefore

composites prepared with HA showed some disruption due to the disruptive effect of nanoparticles. However the positive effects of HAM outweighed the disruptive effects of the nanoparticles giving the better formation observed.

The successful incorporation of nanoparticles into the polyelectrolyte complexes was important for the use of these complexes as a delivery system. It was found that in all cases very high nanoparticle incorporations (over 80%) were achieved. Significant differences in incorporation were found between 0.5:1 and 1:1 ratio samples which shows that the polymer ratio can have effects on the complex properties and the 1:1 ratio provided the optimal properties for this system.

The high incorporation levels show that the surface charge of the nanoparticles was sufficient to ensure their incorporation into complexes. The nanoparticle surface charge interacts with the charges on the polyelectrolyte polymers and drives their incorporation into complexes. No other studies have looked at the incorporation level of nanoparticles into hydrogels as most systems gel entirely ensuring the incorporation of all included nanoparticles. The precipitation of the complexes used here therefore could have been a drawback, but the high particle incorporations prove that this is not the case.

An interesting observation from the nanoparticle incorporation study was that no decrease in incorporation was seen at high nanoparticle levels. At the highest loading levels studied the mass of nanoparticles approached 50% of the mass of the complex. At this level it may well be expected that nanoparticle

loading would affect the structure of the complexes and reduce the incorporation. The loading of nanoparticles is mainly a packing phenomenon and therefore the volume ratios are more important. To investigate this further it was decided to measure the volume of the complexes formed and calculate the percentage volume that nanoparticles take up.

The results of these volume calculations are shown in Table 6-3 and show that despite approaching a high percentage of the complex mass, the volume of the nanoparticles is much lower. The highest value occurs with the smaller 0.5:1 complexes with 8mg of nanoparticles where the nanoparticles take up 31% of the complex volume, rather than 55% of the complex mass. These lower values explain why the complexes are able to hold such high masses of nanoparticles efficiently and seems to confirm that the complex nanoparticle holding capacity is limited by space filling concerns. This theory could be investigated further by producing complexes loaded with higher nanoparticle levels to find the maximum loading that can be achieved.

Initial Loading Level (mg)	Particle volume as percentage of 1:1 complex volume	Particle volume as percentage of 0.5:1 complex volume
2	3.85	7.69
4	7.69	15.38
6	11.54	23.08
8	15.38	30.77

Table 6-3 Volume ratios of nanoparticles to polyelectrolyte complexes.
Theoretical percentage volume that various amounts of nanoparticles occupy compared to polyelectrolyte complex volume. Polyelectrolyte complex volume was measured using a 1ml syringe.

The method used to estimate nanoparticle incorporation used RBITC loaded particles. The solution that remained after complex formation was analysed using a fluorimeter to quantify the particles present and allow the calculation of

incorporated particles. This method does not directly measure the incorporated nanoparticles and so does have the potential for inaccuracy. The resilience of the polyelectrolyte complexes prevented the development of a direct method for nanoparticle incorporation determination. Measuring the fluorescence whilst the label is still incorporated into nanoparticles could also introduce errors into the results, because the binding of the label into the nanoparticles may cause some quenching of the fluorescence. To reduce this error a standard curve of fluorescence against nanoparticle concentration was produced and used for this study. The standard deviations of these results show that despite the limitations of the method used the results showed a good reproducibility.

The distribution of nanoparticles within complexes appeared, on visual inspection, to be even throughout when using RBITC loaded nanoparticles, which have a pink colour. It appeared that Ch:HA complexes exhibited lower concentrations of particles near the surface. However this macroscopic inspection could only provide an indication of the particle distribution. To investigate this further cryo-SEM and fluorescence microscopy were used in an attempt to reveal the true distribution of the nanoparticles. Unfortunately neither of these methods was able to produce clear and definitive images. They did give an indication that the nanoparticles were not evenly distributed through the complexes, but they remained separate and not aggregated even when densely packed. Aggregation is not desired as it would cause uncontrolled increases in particle size which could lead to large aggregates which may reduce the tolerability *in vivo*. The failure to produce clear images means that further work would be required to confirm this.

It was also found that the addition of nanoparticles caused an increase in complex strength through rheology amplitude sweeps on composites. Nanoparticles gave a greater increase in strength with Ch:HA complexes compared to Ch:HAM complexes. This result conflicts with those of the rheology time sweep studies which suggested that the Ch:HA complexes were slightly disrupted by the presence of nanoparticles. As the amplitude sweeps were carried out on formed complexes it may explain these differences. The greater increase in strength of Ch:HA complexes could be accounted for by the fact that HAM produces covalent bonds within the complex structure. The strength of these bonds therefore overshadows the increase in strength due to nanoparticles that was seen in the Ch:HA complexes.

It was found that the complex strength increases from unloaded complexes to RBITC loaded composites to DXMP loaded composites. This observation could be explained by the differences in zeta potential in the nanoparticles as the increase in negativity of zeta potentials followed the same pattern. There were no significant differences in the nanoparticle incorporation efficiencies with different nanoparticles. This suggests that this effect does not occur simply through the incorporation of a greater amount of nanoparticles. It is more likely that the higher charges influence the bonding of the particles within the complex. This may cause a tighter bonding that would account for the increases in strength observed.

The degradation of composites in ASF was slow and gradual, which contrasts the initial rapid degradation seen in complexes without nanoparticles. A greater

mass of complex remained at the end of the study period when nanoparticles were included. These observations suggest that the nanoparticles stabilise the complexes, which agrees with the increase in strength seen in the rheology amplitude sweeps.

The strength and integrity of the composites during their degradation was also studied and found that small changes occurred in G′ values and greater changes were seen in yield stress values. The yield stress values showed a gradual decrease over the study period, which shows that complexes remain physically resilient throughout their degradation. This would allow complexes to resist the physical stresses in the joint after a period of chemical degradation. The results presented are only single measurements of each sample due to the sample requirements making repeated measurements not possible within this project. Therefore these results were included to give an indication that the strength of the complexes was not destroyed during their degradation.

The conditions used in the mass degradation study are much less challenging than the potential conditions within the joint. Therefore to investigate a more challenging degradation it was decided to investigate the degradation of complexes with enzymes. Hyaluronidase was selected as the enzyme to be used as it is present within the joint and degrades hyaluronic acid, which is one of the components of this delivery system. To assess the degradation by this method it was decided to monitor particle release from degrading composites.

This enzyme degradation study wasn't directly biologically relevant to the osteoarthritic joint. The use of a high enzyme concentration was an easy way to assess complex stability in more challenging conditions. Hyaluronidase is present within the healthy and osteoarthritic joint (Nagaya et al., 1999), and for example HYAL-2 is present on the cell surface through a GPI-linkage (Volpi et al., 2009). Despite the presence of this enzyme within the joint it is not clear whether it is biologically active. The hyaluronidase enzymes have an optimal activity at acidic pHs (around pH 4.5) as they are lysosomal enzymes and are inactive at a neutral pH. The natural pH of synovial fluid is 7.4 and is not affected by osteoarthritis. For this study a formate buffer of pH 4.5 was used which will allow enzyme degradation to occur. The activity of HAase used was approximately 100 times the potential activity from synovial fluid (Nagaya et al., 1999).

It was necessary to ensure that the release seen was not just due to degradation in the buffer, so therefore the release of particles from complexes incubated in buffer was also examined. This found that only a low level of particle release occurred during incubation in buffer with an initial rapid release over the first 7 days and only a minimal release after that. 0.5:1 ratio samples exhibited a higher particle release than 1:1 ratio samples. Overall these complexes were able to retain the nanoparticles loaded into them.

These results would suggest that the nanoparticles became tightly bound into the complex structure. Any particles that were not tightly bound were quickly released and account for the initial rapid release. Overall this shows that these

complexes are likely to be suitable for a drug delivery system. The drug loaded nanoparticles will be retained and allow a slow release to occur. It also indicates that the 1:1 ratio complexes have the optimal properties.

The particle release when the composites were incubated with HAase was found initially to be unaffected by the enzyme. After this initial period a gradual and sustained degradation occurred in the 1:1 ratio complexes, whereas the 0.5:1 ratio complexes exhibited a significantly more rapid degradation. At the end of the study between 20% and 30% of the loaded nanoparticles were recovered from 1:1 ratio complexes, whereas less than 10% of the loaded nanoparticles were recovered from 0.5:1 ratio complexes. These results show that these complexes exhibit a high stability even under challenging conditions. The 0.5:1 ratio complexes showed a more rapid and complete degradation which suggests that the 1:1 ratio complexes exhibit the optimal properties. The degradation that occurred due to HAase gives confidence that these complexes would be fully degraded *in vivo* and therefore would not remain indefinitely within the joint, which could cause more problems and joint damage.

This stability during incubation with enzyme compares well to cross-linked hyaluronic acid hydrogels (Lee et al., 2008). Lee et al. found that hydrogels were degraded over 48h in 2.5 U/ml HAase, which is a much faster degradation than the polyelectrolyte complexes in the present study. This suggests that the incorporation of HA into these polyelectrolyte complexes protects it from degradation. However the present study used a lower HAase concentration of 0.6 U/ml, which will reduce the degradation seen. To fully

disrupt the complexes at the end of the study a concentration of 30U/ml was required which confirms that the polyelectrolyte complexes protected HA from degradation by HAase.

Differences were observed in the response of the complexes produced with HA or HAM to degradation by HAase. However these differences depended on the polymer ratios used and were not statistically significant. The low level of modification present in HAM does not therefore affect its susceptibility to degradation by HAase.

One aspect of the complexes that has not been investigated is their internal structure. Attempts have been made to determine this using cryo-SEM, however a clear image of the internal structure was not produced. There are a number of reasons for this but it mainly was due to the samples having unfavourable properties for cryo-SEM. The complexes were very tough which gave problems when fracturing. Often a scrape rather than a fracture occurred which is not suitable for imaging. When a fracture did occur it was often very rough and uneven which limits the resolution that the SEM image can achieve. The polyelectrolyte nature of the polymers also gave problems with the presence of charge, which again limits the imaging possible.

There is a question of the reliability of any images produced as water is integral to the complexes. It is likely that the presence of water affects the complex structure and so the freezing process may therefore alter the structure. This highlights a wider problem in the imaging of aqueous based hydrogels and

other aqueous systems. There is a lack of techniques available to study these systems within their natural aqueous environment. The processing of these systems by drying or crystallisation to render them suitable for current techniques will alter the structure. A novel technique to image the internal structure of aqueous systems within their natural environment is required to overcome these problems.

6.4.2 Dialysis Formation Method

The dialysis formation method was investigated with nanoparticle loaded complexes. With the increases in strength and stability seen with nanoparticles included into complexes it was important to assess any effects nanoparticles had on the dialysis formation method.

An initial study found no major differences in the concentration of salt required to prevent complex formation compared to when nanoparticles were not present. The reduction in stability in salt seen with HAM compared to HA was reversed when nanoparticles were added. A concentration of 0.5M NaCl produced a complete disruption of complex formation in all cases and for many samples a concentration of 0.4M was sufficient. If the higher salt concentration proves to be problematic for the tolerability of this system then a lower salt concentration may be able to alleviate this problem.

The formation of composites using the dialysis method was successful with both RBITC and DXMP loaded nanoparticles. Visually a good formation occurred for all samples, although the 1:1 ratios showed the greatest formation

and Ch:HA 0.5:1 ratio complexes showed the worst formation. The formation was found to be slower in the 0.5:1 ratio samples. These visual observations were confirmed by the rheology results. The rheology also revealed a gradual strengthening of the complexes after the initial precipitation that was not obvious from the photographic study. Overall these results confirm that the dialysis method is suitable for producing nanoparticle loaded complexes.

Visual inspection of complexes showed an even distribution of nanoparticles in the Ch:HA 1:1 ratio samples with a less even distribution of particles in other samples. In these cases there appeared to be a small number of complexes that were enriched with nanoparticles. The limitations of visual inspection were revealed with cryo-SEM images obtained on bulk formed complexes. Unfortunately cryo-SEM images of the dialysis formed complexes were not of sufficient quality to identify the nanoparticles present. The distribution of the particles within the dialysis formed complexes remains to be determined. However it seems unlikely with the data collected in this study that the distribution is entirely even.

The production of a number of smaller complexes occurred with the dialysis formation method which causes an increase in the surface area of the complexes. Therefore it might be expected to cause changes in the complex degradation, particle retention and drug release properties. The properties of dialysis formed complexes were investigated to ensure that the complexes were still suitable for the intended application.

It was found that the nanoparticle incorporation efficiencies were consistently lower with the dialysis formation method. These differences were significant in the Ch:HA 0.5:1 ratio samples and both 1:1 ratio samples. It might be expected that the dialysis method would have massively reduced the incorporation of nanoparticles as the slower formation allows a greater chance for the particles to escape incorporation into the complexes. The high incorporations show that these complexes would still be suitable using this formation method. The reductions in the 0.5:1 ratio complexes show that the 1:1 ratio complexes have better properties using this formation method.

Rheology amplitude sweeps revealed that this formation method had effects on the complex strength and different effects were seen with different ratio complexes. The 1:1 ratio complexes exhibit a slightly increased strength, whereas the 0.5:1 ratio complexes showed a decrease in strength and the Ch:HAM 0.5:1 showed a dramatic reduction in strength. The results suggest that the dialysis formation method is advantageous for the structure of the 1:1 ratio complexes, but is disruptive of 0.5:1 ratio samples. The reliability of these results is limited as no repeats were carried out in this project for these data. However the similar results seen with samples at the same polymer ratio help to show that these results are likely to be an accurate representation.

The improved strength of the 1:1 ratio complex may be due to the dialysis formation method giving better polymer incorporation into the complexes. It has been reported that for optimal formation of polyelectrolyte complexes that it is necessary to conduct the mixing at conditions where interaction does not

occur and then adjust the conditions so that interaction and formation can occur (Berger et al., 2004). The dialysis formation method provides this and so this may account for the improved strength seen for the 1:1 ratio complexes. For the 0.5:1 ratio samples it may be that the decreased stability in salt has a greater effect, with this slowing the formation and preventing the optimal complex formation seen with the 1:1 ratio complexes.

The degradation of dialysis formed complexes in ASF buffer followed a similar gradual pattern to complexes produced using the bulk formation method. In all cases a slightly lower mass remained at the end of the study, but the only significant difference was in the Ch:HA 0.5:1 ratio samples. These results show that the reductions seen in stability were small and the complexes retain a sufficient stability for the intended application.

The release of loaded nanoparticles also followed a similar pattern to that seen with bulk formed complexes. The release was more gradual than for bulk formed complexes and a lower overall release occurred. This shows that the retention of nanoparticles by the complexes was not hindered by the dialysis formation method and was, in fact, slightly improved. These results may be explained by the slightly lower incorporations seen with the dialysis method. The reduction is likely to be due to the removal of the least well bound particles and as these particles no longer bind to the complexes they will no longer be released, causing the slightly reduced levels of particle release that were seen. Also as these particles were the least well bound and could account for the initial burst seen with the bulk formed complexes. Therefore their

removal would also account for the reduction in this initial burst seen with dialysis formed complexes.

The particle release in the presence of hyaluronidase was affected by the dialysis formation method. The initial period of minimal degradation with the bulk formed complexes was not seen with dialysis formed samples. For the 1:1 ratio complexes there was no significant difference between the degradation in the complexes produced by the two formation methods. A similar amount of nanoparticles were also recovered at the end of the degradation study. These results show that the 1:1 ratio complexes are still stable under challenging conditions when formed by the dialysis method.

The 0.5:1 ratio complexes exhibited a significantly faster degradation when they were produced by the dialysis method, causing a release of around 60% of the loaded particles within 7 days. However the release then slowed and at the end of the study around 10% of the loaded nanoparticles were recovered, which is similar to the recovery from the bulk formed complexes. Overall it can be seen that the 0.5:1 complexes have a lower stability than the 1:1 ratio. As this study was not conducted using a directly biologically relevant enzyme concentration this does not necessarily mean that the reduced chitosan complexes would not be suitable as a delivery system.

These results show that some of the effects of the dialysis formation method appear to be contradictory. For example the increase in complex strength is not matched by an increase in stability. However many of these differences were

not significant. It may be that the increase in strength of the 1:1 ratio samples may represent a more complete formation rather than a formation of stronger complexes. This situation would account for the similar or slightly reduced stability seen. Other results show a better agreement with the slight reduction in nanoparticle incorporation being able to explain the reduction in particle release, as discussed above.

The 0.5:1 ratio complexes show a more consistent negative impact with the dialysis formation method, showing a decreased strength, nanoparticle incorporation and stability. The 0.5:1 ratio complexes are closer to the polymer ratio where complex formation was not possible. Therefore this more demanding formation method may be expected to show the less optimal properties at this polymer ratio. However the properties of the 0.5:1 ratio complexes are still promising in general and they are worthy of further consideration but it can be clearly seen that the 1:1 ratio complexes provide the optimal properties.

6.4.3 Drug Release

6.4.3.1 Dexamethasone phosphate

The drug release from the composites is a key property for the delivery system. Dexamethasone phosphate was the chosen drug and these DXMP loaded nanoparticles gave a sustained release over 28 days. The determination of DXMP release from the composites has however proven challenging. The low incorporation levels of DXMP into nanoparticles meant that only low levels of

drugs were available for analysis of the release, which made detection of the released drug challenging.

The full release profile was not successfully determined in this study. However around 60% of the initially loaded drug was recovered after 56 days of the release study. A small release over the first 7 days was detected and only 75% to 80% of the loaded drug was recovered. It is likely that the unaccounted drug was released and not detected. If release was occurring at just below the 2% detection limit throughout the study then the majority of this missing drug can be accounted for. Together these results suggest that a gradual drug release is occurring. It can also be seen that the complexes retained drug for longer than 56 days. These results show that these composites have the ability to act as a controlled release delivery system.

It would be advantageous to determine the full release profile as this would provide confirmation of the potential of complexes loaded with nanoparticles. The sensitivity of the assay allows detection of around 2% of the loaded drug, and buffer in the release experiment was analysed every 7 days. This sensitivity would have been sufficient for the experiment if the release had occurred over the 90 days that was desired. A method with a higher sensitivity could be used to produce a full release profile with this system.

These results suggest that these complexes may have a release that was slower than intended, which is a very unusual situation for a drug delivery system. The rate of release during *in vitro* studies is unlikely to be repeated under *in vivo*

conditions and the release is likely to be significantly faster. This gives hope that the desired release can be achieved in more biologically relevant or *in vivo* studies.

It is important that the delivery system is able to maintain a sufficient drug concentration. Many sustained release delivery systems use the same dose as in an immediate release formulation but deliver it over an extended time period. Current intra-articular formulations of DXMP use around 2-4mg of drug (Gerwin et al., 2006), with most of this dose lost rapidly to the blood. A sustained release system may be able to utilise much lower amounts of drug and yet still provide a therapeutic effect. Calculations have shown that the current system, in a 2ml formulation for human knee, is capable of maintaining a concentration of around 20nM in the joint. This was calculated assuming that the entire drug amount was cleared and replaced every hour. The half-life of DXMP in the joint is known to be around 1.5 hours (Larsen et al., 2008), and so these calculations provide a conservative estimate. A concentration of 20nM exceeds the EC_{50} of this drug and would hopefully be sufficient to cause clinical effects.

The drug release from nanoparticles retained within hydrogels has varied considerably with the system used. In systems incorporating dexamethasone the period of release has varied from around 10 days to around 60 days (Cascone et al., 2002, Kim and Martin, 2006, Wang et al., 2010). A system composed of an alginate gel retaining PLGA nanoparticles was the most similar to the system in this study (Kim and Martin, 2006). It was found that

free dexamethasone was very rapidly released from the hydrogel. This release was slowed by encapsulation into nanoparticles and slowed further by incorporation of nanoparticles into hydrogels. A similar pattern of release was seen in the present study but over longer time scales than the 10 days seen in the alginate system.

The system reported in the literature that has provided a release over the longest period was composed of aggregating nanoparticles (Wang et al., 2010). This system was able to provide a complete release of dexamethasone over a period of 60 days. The release was significantly slowed compared to free nanoparticles, which exhibited release over 20 days (Wang et al., 2010). The comparison to the system here is limited by the lack of a full release profile and the different drug used. Dexamethasone phosphate was used for the present study and this drug is more water soluble than dexamethasone. Therefore the release of DXMP would be expected to be quicker than that of dexamethasone and so the length of retention observed with these complexes is impressive.

The recovery of dexamethasone phosphate from the complexes after 56 days is even more impressive when the release of free drug from the hydrogels is considered. The release of free DXMP from polyelectrolyte complexes was found to be quite rapid and occurred within 7 days. It can therefore be assumed that any drug released from nanoparticles within the complexes will be rapidly released to the surrounding media. The release of DXMP from particles in solution was almost complete after 28 days which might suggest that the release from the composite system would occur over a similar time scale. The

much slowed release could be due to the compact structure of the complexes excluding water. This would therefore slow the degradation of the nanoparticles and hence the rate of drug release.

It can also be noted from these results that the incorporation rates of DXMP loaded nanoparticles were similar to those observed with RBITC loaded nanoparticles. This is an encouraging result as it shows that these drug loaded particles are equally well retained and gives confidence that the results obtained with the fluorescently labelled particles are likely to give a good indication of the properties of the complexes loaded with DXMP nanoparticles.

This high retention of drug throughout the release study suggests that the particles are well retained throughout the study, as occurred with RBITC loaded nanoparticles. The initial nanoparticle release seen with RBITC loaded nanoparticles would be able to cause the small burst release of DXMP seen in bulk formed samples. The results of the incorporation and release of nanoparticles also provide encouragement that this system could be adapted for use with nanoparticles loaded with other drugs in the future in the confidence that they are likely to exhibit similar properties.

6.4.3.2 Dexamethasone crystals

To simplify the system the incorporation of dexamethasone crystals into the complexes was considered as a possible alternative delivery system. These crystals have a limited solubility and so have been used as a slow release system for intra articular administration (Derendorf et al., 1986). However

large crystals can cause irritation and damage within the joint so commercially available steroid crystal formulations have a tightly defined size of under 20μm (Derby et al., 2008). The crystals used for this study were prepared from laboratory chemicals and so did not have a tightly defined size. The crystals were mostly smaller than 20μm and so provide a good enough sample for this investigative study. A more tightly defined crystal sample could be prepared for future studies with these complexes.

The release study found that these crystal loaded complexes produced a sustained drug release for a period of around 90 days, which was not simply due to solubility effects or binding to HA. Hyaluronic acid has a hydrophobic patch within its structure that could potentially bind to the hydrophobic steroid. If binding occurred this could have provided an explanation for the slow release seen. It would therefore seem likely that the slow drug release from dexamethasone crystals is also an effect of the compact structure of the complexes excluding water. This reduction in available water and the limited solubility of dexamethasone could account for the slow release.

This slow release exceeds any seen from a drug directly incorporated into a hydrogel. A system using a dexamethasone suspension retained within a cross-linked hyaluronic acid hydrogel showed a complete drug release over 28 days (Kim et al., 2011). These complexes therefore show a vastly improved drug release profile and have potential as a directly loaded system with dexamethasone.

Further study of these crystal loaded complexes is required to determine their full potential. The issues with the biocompatibility of crystals may prove problematic during *in vivo* studies and with the long term tolerability of the treatment. If this is the case it may mean that the nanoparticle loaded system still retains advantages. However the ability of the directly loaded system to provide the desired 3 month delivery makes it worthy of further study.

Comparing the release of free dexamethasone phosphate and dexamethasone when directly loaded into the complexes is very interesting. The phosphate group which is present in DXMP makes this molecule more hydrophilic than dexamethasone, but this is the only difference between the two molecules. Therefore it would seem that the difference in release is due to the hydrophobicity of the compound.

The fact that dexamethasone is in a crystalline state rather than in solution will undoubtedly slow the drug release as it must first be dissolved before it can be released. The results from the dissolution of free crystals show that this factor alone does not explain the differences in release. The exclusion of water from the complexes is likely to slow the dissolution of dexamethasone and would therefore slow the release. It is also likely that dexamethasone is better retained within the complexes due to its hydrophobicity and together these factors account for the slow release that was found.

6.5 Conclusions

The results within this chapter show that complexes were able to hold and retain nanoparticles. The complexes are able to hold high levels of nanoparticles whilst maintaining a high incorporation efficiency. The presence of nanoparticles had few effects on the complex properties and did in fact slightly improve the properties of the complexes. The nanoparticles were also retained very well, which would be sufficient to allow a drug release over 3 months as is desired.

The results found a significant difference in nanoparticle release with and without protein present. Protein was also found to affect the degradation of composites. It would be advantageous to conduct further investigations to determine the effects of protein on complex properties. However it is questionable whether further *in vitro* studies are required with more biological relevance or whether it is more useful to conduct *in vivo* studies as an *in vitro* study can never fully mimic *in vivo* conditions. The current data on this system shows its potential and *in vivo* studies would give more useful results.

The dialysis formation method was also able to produce nanoparticle loaded complexes. This formation method had very little effect on the 1:1 ratio complexes, with a slight decrease in particle incorporation, a slight increase in strength and a slight decrease in particle release seen. The 0.5:1 ratio complexes were more greatly affected by the formation method, with a significant reduction in nanoparticle incorporation, strength and stability found. These results highlight the limitations of the reduced chitosan ratio and shows

that the 1:1 ratio complexes have the optimal properties. The 0.5:1 ratio complexes still have properties that make them suitable for continued consideration. This is especially true as the projected improved compatibility of this ratio has not been assessed.

The release of dexamethasone phosphate from these composites was not successfully determined and further study is required in order to determine this release. The low drug concentrations proved a challenge in the HPLC analysis and the use of a method with a higher sensitivity would help. The drug determination would also be less challenging if the drug loading levels of the PGA nanoparticles could be improved, and would also increase the capacity for drug delivery with this system. Overall however the system shows promise as there was a high retention of drug within the system for 56 days.

The loading of dexamethasone crystals directly into the complexes produced an unexpected alternative delivery system. With this system a drug delivery for the desired three month period was achieved, but much further study is required to fully understand this system. It is also very important to investigate the compatibility with the crystal component in this system. The negative effects of crystals within the joint may be prevented through these complexes; however it is not known to what extent this would occur. To fully assess the viability of this delivery system the compatibility needs to be investigated. The other properties of the crystal loaded complexes have not been investigated; however the sustained drug release results make these properties less important

as they show these complexes are stable and have similar to those previously investigated.

Large differences seen between hydrophobic and hydrophilic drugs loaded directly into the complexes. This system has the potential to be extended to including other drugs. The hydrophilic or hydrophobic properties of the drug could determine the more suitable system to provide a sustained release. Hydrophobic drugs can potentially be directly incorporated into the complexes and this is an easier system to produce and also avoids the necessity to investigate the nanoparticles and their drug loading. The observed release here may be due to the drug crystals used in this study, but until studies are conducted with further hydrophobic drugs it is not possible to be sure. Hydrophilic drugs were rapidly released when directly incorporated into complexes and therefore nanoparticles are essential to allow a sustained release. These options provide this system with the potential to deliver a wide variety of drugs.

CHAPTER 7 - GENERAL CONCLUSIONS

7.1 Summary and Conclusions

This project started with the aim of investigating potential drug delivery systems for osteoarthritis. Through a review of the literature this was developed to focus on producing an intra-articular system capable of providing a slow release of the corticosteroid dexamethasone phosphate. The aim was to produce a delivery system capable of providing a sustained drug delivery over at least three months. This period of delivery exceeds what is possible for most delivery systems and therefore a system of an injectable hydrogel incorporating a nanoparticle drug delivery was proposed.

Polyelectrolyte complexes between hyaluronic acid and chitosan were investigated as the hydrogel portion of this system. These complexes showed a great potential as a base for a slow release drug delivery system as they had a high stability and resilience. The complexes also showed promise that a drug release over the desired time scales could be achieved. Unfortunately the full release profile of dexamethasone phosphate from nanoparticle loaded complexes was not successfully determined, and this limits the conclusions that can be drawn. However, around 60% of the initially loaded drug at the end of the 56 day release study was recovered which shows that the system is capable of retaining drug for long periods. Further study is therefore required to determine the full drug release profile to overcome the current uncertainty. However the initial release seen and the recovery of unreleased drug at the end of the study showed the promise of this system.

Dexamethasone crystals loaded directly into complexes were investigated as an alternative system that avoided the incorporation of nanoparticles. The removal of the nanoparticles is desirable as this simplifies the system. This gives a greater likelihood that no unexpected results will be found during *in vivo* studies and also that regulatory approval will be gained. The directly loaded system was able to provide a sustained drug delivery over 90 days and therefore has a great potential, but the crystals do raise questions over compatibility. The extremely promising drug release from this system make it worthy of further study, as this exceeds the delivery from any previously reported delivery system of this type.

The results gathered show the potential of this system to have a wide variety of drugs incorporated. For hydrophilic drugs the nanoparticle portion of this delivery system is essential whereas poorly soluble compounds can be directly loaded into complexes. Overall this system therefore has the potential to provide a sustained release for many drugs.

The drug loading of the PGA nanoparticles was lower than expected. This loading was determined using a direct method that was developed and validated during this project. The particles did however provide a release in line with what was expected, with a sustained release of DXMP over 28 days, which exceeds what has been found with most nanoparticle systems. Improving the drug loading levels of the nanoparticles, either through further work with PGA or through the use of an alternative polymer, would provide many advantages for this system. It would allow a higher drug concentration to

be maintained within the joint and would also allow for easier analysis of the drug released. The project aimed to provide evidence that this delivery system was capable of providing a drug release over a minimum of three months. Therefore although further work could have been carried out to improve the drug loading it was decided that within the time limitations of this project it was more important to study the combined nanoparticle and complex system. This leaves the nanoparticles as an area of this system which can be improved.

This project also investigated a modified hyaluronic acid (HAM). This polymer was produced with a low modification level to ensure that the polyelectrolyte characteristics were not lost. The incorporation of HAM into complexes was able to improve their properties with a greater resilience and slower degradation observed; also a much more rapid formation was found. The cause of the increase in the formation speed was not definitively identified as the structure of HAM was not fully determined. Ellman's Test confirmed that cysteamine had been successfully incorporated but the full structure of HAM was not confirmed. This leaves open the possibilities that unexpected reactions had occurred, such as the formation of an N-acylurea adduct with EDAC. Therefore further investigations to fully characterise HAM are required.

A high salt concentration was used to prevent complex formation and produce an injectable formulation of this system. Formation of complexes in the lab from these high salt solutions was achieved through dialysis, to mimic the diffusion of salt that would occur *in vivo*. This method was able to successfully produce complexes and had few negative effects on the complex properties.

The salt concentrations required may prove to cause problems with the compatibility of the system, however previous studies have shown that chondrocytes can survive this hypertonic shock. It may prove that HAM has further advantages here as it appeared to reduce the salt concentration required to disrupt complexation. This would allow a lower salt concentration to be used which would reduce the potential compatibility problems.

It was desired to utilise the lowest possible concentration of chitosan as it potentially causes inflammation within the joint; although its effects in the joint are not entirely clear. The use of a reduced chitosan concentration had some negative impact on the complex properties; however they still showed promising properties for the intended application. As the compatibility of the complexes has not yet been investigated the reduced chitosan concentration samples may well prove to have advantages that are more important than the small reductions in strength and stability.

It has also not been possible to conduct any *in vivo* studies in the current project. There is always the risk that any system will produce unexpected results *in vivo* due to the much more challenging conditions. It is therefore important that this system is investigated *in vivo* to confirm that the promise shown by this system *in vitro* follows through.

7.2 Future Work

There are a number of studies that are required to overcome some of the shortcomings that haven't been fully addressed in the current work. The work

that is most needed to prove the value of this system is further release studies, and in particular the determination of the full DXMP release profile from PGA nanoparticles loaded into polyelectrolyte complexes. The failure to achieve this is likely to have been due to the slow rate of drug release and the sensitivity of the HPLC assay used. Improving the drug loading or using a more accurate analysis method would be able to determine the drug release profile.

Another factor that has not been investigated is the biocompatibility and toxicity of HAM, so a study to investigate this is therefore very important. The complexes have shown promising properties without using HAM, so if it proves to have an unacceptable toxicity then the system can continue to be investigated using unmodified hyaluronic acid. There is also a need for further studies to fully determine the structure of HAM, to help explain the effects that HAM had on the complexes. It is also possible that a version of HAM with a higher percentage modification may provide further advantages, and this could also be investigated.

This system has shown great *in vitro* potential as a drug delivery system and now requires studying *in vivo* to ensure that this potential is fulfilled. The first factor that these studies would need to focus on is the compatibility of this system, as this has not been investigated in this study. The exact physical properties of the complexes required to ensure that they do not cause damage to the joint are not known and it is hoped that the 1:1 ratio complexes will not damage the joint. If it is found that they do damage the joint then the physical properties of the complexes can be adjusted by varying the polymer ratio and

concentrations and this will hopefully allow complexes with appropriate properties to be produced.

Studies of the *in vivo* drug release and the effectiveness of this system against an osteoarthritis disease model would provide very good evidence as to its efficacy. Osteoarthritis is a disease of the entire synovial joint, which has often been overlooked in animal models (Bonnet and Walsh, 2005). Corticosteroids in osteoarthritis act to reduce the synovial inflammation and do not affect the cartilage. Therefore any animal model used to study this system needs to include the changes seen in the synovial membrane. One possible model that could be used is collagen induced arthritis, although this is a rheumatoid arthritis model it shows many of the required characteristics of osteoarthritis. The methods for these animal studies also need to be considered as normally drug release is monitored in the blood. As this system is aiming for a local delivery to the joint and is applying low drug concentrations it is likely that monitoring via the blood may prove problematic. Synovial fluid sampling has many challenges but would provide better information for this system. Monitoring the animals for clinical improvement may also give good information on the clinical efficacy of the system.

Further studies are required into the system with dexamethasone crystals directly loaded into complexes as it has so far only been investigated in terms of drug release. The compatibility of this system must be carefully evaluated as crystals are known to be damaging within the joint. Steroids crystals with a tightly defined size have been administered to the joint to minimise the risk of

joint damage. Further work is also required to investigate this system with the dialysis formation method required to produce the injectable formulation.

Looking wider and the results show that this delivery system has a potential to be developed with other drugs. The system can be formulated with or without nanoparticles depending on the drug properties. The PGA backbone polymer used for the production of the nanoparticles can be modified to alter its properties and allow different drugs to be incorporated (Kallinteri et al., 2005, Puri, 2007). Other nanoparticle systems could also potentially be used with this system. These possibilities give many options for further investigations and show a great potential for this system.

This system also has the potential to be adapted for other applications beyond osteoarthritis. Hyaluronic acid hydrogels have been used for anti-adhesion and wound healing applications. There is the potential that these complexes could be adapted for these applications, with or without drug loading. It is likely that drug loaded hydrogels would also provide advantages in these areas. Hydrogel patches have also been used as a topically applied drug delivery system. The aqueous nature of the hydrogels acts to increase the skin permeability allowing the delivery of the drug. The tough and resilient complexes produced in this study have the potential to be used as part of a hydrogel based patch system. Another potential use for a long term depot forming system is as a base for an environmental activated drug delivery system. This system would release small bursts of drug when triggered over a long time period and would provide further advantages as drug would only be released when needed.

REFERENCES

AFONSO, V., CHAMPY, R., MITROVIC, D., COLLIN, P. & LOMRI, A. (2007) Reactive oxygen species and superoxide dismutases: role in joint diseases. *Joint Bone Spine,* 74**,** 324-329.

AIGNER, T., BERTLING, W., STOSS, H., WESELOH, G. & VONDERMARK, K. (1993) Independent expression of fibril-forming collagen-I, collagen-II, and collagen-III in chondrocytes of human osteoarthritic cartilage. *Journal of Clinical Investigation,* 91**,** 829-837.

AIGNER, T., GLUCKERT, K. & VONDERMARK, K. (1997) Activation of fibrillar collagen synthesis and phenotypic modulation of chondrocytes in early human osteoarthritic cartilage lesions. *Osteoarthritis and Cartilage,* 5**,** 183-189.

AIGNER, T., HAAG, J., MARTIN, J. & BUCKWALTER, J. (2007) Osteoarthritis: aging of matrix and cells - going for a remedy. *Current Drug Targets,* 8**,** 325-331.

AIGNER, T., HEMMEL, A., NEUREITER, D., GEBHARD, P. M., ZEILER, G., KIRCHNER, T. & MCKENNA, L. (2001) Apoptotic cell death is not a widespread phenomenon in normal aging and osteoarthritic human articular knee cartilage -a study of proliferation, programmed cell death (apoptosis), and viability of chondrocytes in normal and osteoarthritic human knee cartilage. *Arthritis and Rheumatism,* 44**,** 1304-1312.

AIGNER, T., SACHSE, A., GEBHARD, P. M. & ROACH, H. I. (2006) Osteoarthritis: pathobiology-targets and ways for therapeutic intervention. *Advanced Drug Delivery Reviews,* 58**,** 128-149.

AL-HANBALI, O., ONWUZO, N. M., RUTT, K. J., DADSWELL, C. M., MOGHIMI, S. M. & HUNTER, A. C. (2007) Modification of the Stewart biphasic colorimetric assay for stable and accurate quantitatitive determination of Pluronic and Tetronic block copolymers for application in biological systems. *Analytical Biochemistry,* 361**,** 287-293.

ALAAEDDINE, N., DI BATTISTA, J. A., PELLETIER, J. P., KIANSA, K., CLOUTIER, J. M. & MARTEL-PELLETIER, J. (1999) Differential effects of IL-8, LIF (pro-inflammatory) and IL-11 (anti-inflammatory) on TNF-alpha-induced PGE(2) release and on signalling pathways in human OA synovial fibroblasts. *Cytokine,* 11**,** 1020-1030.

ALEXANDER, C. & SHAKESHEFF, K. M. (2006) Responsive polymers at the biology/materials science interface. *Advanced Materials,* 18**,** 3321-3328.

ALFORD, J. W. & COLE, B. J. (2005) Cartilage restoration, part 1 - basic science, historical perspective, patient evaluation, and treatment options. *American Journal of Sports Medicine,* 33**,** 295-306.

ANDERSON, J. M. & SHIVE, M. S. (1997) Biodegradation and biocompatibility of PLA and PLGA microspheres. *Advanced Drug Delivery Reviews,* 28**,** 5-24.

ANDERSON, R., FRANCH, A., CASTELL, M., PEREZ-CANO, F. J., BRAEUER, R., POHLERS, D., GAJDA, M., SISKOS, A. P., KATSILA, T., TAMVAKOPOULOS, C., RAUCHHAUS, U., PANZNER, S. & KINNE, R. W. (2010) Liposomal encapsulation enhances and prolongs the anti-inflammatory effects of water-soluble dexamethasone phosphate in experimental adjuvant arthritis. *Arthritis Research & Therapy,* 12**,** R147.

ARDEN, N. & COOPER, C. (Eds.) (2006) *Osteoarthritis handbook,* London, Taylor and Francis.

ARTHRITIS CARE (2004) OA nation. London: Arthritis Care.

ASPDEN, R. M. (2011) Obesity punches above its weight in osteoarthritis. *Nature Reviews Rheumatology,* 7**,** 65-68.

ATHANASOU, N. A. (1995) Synovial macrophages. *Annals of the Rheumatic Diseases,* 54**,** 392-394.

ATIK, O. S. (1990) Leukotriene-B4 and prostaglandin-E2-like activity in synovial-fluid in osteoarthritis. *Prostaglandins Leukotrienes and Essential Fatty Acids,* 39**,** 253-254.

BAJPAI, A. K., SHUKLA, S. K., BHANU, S. & KANKANE, S. (2008) Responsive polymers in controlled drug delivery. *Progress in Polymer Science,* 33**,** 1088-1118.

BAND, P. A. (1998) Hyaluronan derivatives: chemistry and clinical applications. *Chemistry, Biology and Medical Applications of Hyaluronan and Its Derivatives.*

BAO, J. P., CHEN, W. P. & WU, L. D. (2011) Lubricin: a novel potential biotherapeutic approaches for the treatment of osteoarthritis. *Molecular Biology Reports,* 38**,** 2879-2885.

BARBUCCI, R., CONSUMI, M., LAMPONI, S. & LEONE, G. (2003) Polysaccharides based hydrogels for biological applications. *Macromolecular Symposia,* 204**,** 37-58.

BARBUCCI, R., GIARDINO, R., DE CAGNA, M., GOLINI, L. & PASQUI, D. (2010) Inter-penetrating hydrogels (IPHs) as a new class of injectable polysaccharide hydrogels with thixotropic nature and interesting mechanical and biological properties. *Soft Matter,* 6**,** 3524-3532.

BARBUCCI, R., LAMPONI, S., BORZACCHIELLO, A., AMBROSIO, L., FINI, M., TORRICELLI, P. & GIARDINO, R. (2002) Hyaluronic acid hydrogel in the treatment of osteoarthritis. *Biomaterials,* 23**,** 4503-4513.

BARKSBY, H. E., HUI, W., WAPPLER, I., PETERS, H. H., MILNER, J. M., RICHARDS, C. D., CAWSTON, T. E. & ROWAN, A. D. (2006) Interleukin-1 in combination with oncostatin M up-regulates multiple genes in chondrocytes - implications for cartilage destruction and repair. *Arthritis and Rheumatism,* 54**,** 540-550.

BARRERA, P., BLOM, A., VAN LENT, P., VAN BLOOIS, L., BEIJNEN, J. H., VAN ROOIJEN, N., MALEFIJT, M. C. D., VAN DE PUTTE, L. B. A., STORM, G. & VAN DEN BERG, W. B. (2000) Synovial macrophage depletion with clodronate-containing liposomes in rheumatoid arthritis. *Arthritis and Rheumatism,* 43**,** 1951-1959.

BASTOW, E. R., BYERS, S., GOLUB, S. B., CLARKIN, C. E., PITSILLIDES, A. A. & FOSANG, A. J. (2008) Hyaluronan synthesis and degradation in cartilage and bone. *Cellular and Molecular Life Sciences,* 65**,** 395-413.

BECK, L. R., COWSAR, D. R., LEWIS, D. H., COSGROVE, R. J., RIDDLE, C. T., LOWRY, S. L. & EPPERLY, T. (1979) New long-acting injectable microcapsule system for the administration of progesterone. *Fertility and Sterility,* 31**,** 545-551.

BELLAMY, N., CAMPBELL, J., ROBINSON, V., GEE, T., BOURNE, R. & WELLS, G. (2005a) Intraarticular corticosteroid for treatment of osteoarthritis of the knee. *Cochrane Database of Systematic Reviews***,** CD005328.

BELLAMY, N., CAMPBELL, J., ROBINSON, V., GEE, T., BOURNE, R. & WELLS, G. (2005b) Viscosupplementation for the treatment of osteoarthritis of the knee. *Cochrane Database of Systematic Reviews***,** CD005321.

BENITO, M. J., VEALE, D. J., FITZGERALD, O., VAN DEN BERG, W. B. & BRESNIHAN, B. (2005) Synovial tissue inflammation in early and late osteoarthritis. *Annals of the Rheumatic Diseases,* 64**,** 1263-1267.

BERGER, J., REIST, M., MAYER, J. M., FELT, O. & GURNY, R. (2004) Structure and interactions in chitosan hydrogels formed by complexation or aggregation for biomedical applications. *European Journal of Pharmaceutics and Biopharmaceutics,* 57**,** 35-52.

BETRE, H., LIU, W., ZALUTSKY, M. R., CHILKOTI, A., KRAUS, V. B. & SETTON, L. A. (2006) A thermally responsive biopolymer for intra-articular drug delivery. *Journal of Controlled Release,* 115**,** 175-182.

BIAS, P., LABRENZ, R. & ROSE, P. (2001) Sustained-release dexamethasone palmitate - Pharmacokinetics and efficacy in patients with activated inflammatory osteoarthritis of the knee. *Clinical Drug Investigation,* 21**,** 429-436.

BLOM, A. B., LENT, P. L., LIBREGTS, S., HOLTHUYSEN, A. E., VAN DER KRAAN, P. M., VAN ROOIJEN, N. & VAN DEN BERG, W. B. (2007) Crucial role of macrophages in matrix metalloproteinase-mediated cartilage

destruction during experimental osteoarthritis - involvement of matrix metalloproteinase 3. *Arthritis and Rheumatism,* 56**,** 147-157.

BLOM, A. B., VAN LENT, P., HOLTHUYSEN, A. E. M., VAN DER KRAAN, P. M., ROTH, J., VAN ROOIJEN, N. & VAN DEN BERG, W. B. (2004) Synovial lining macrophages mediate osteophyte formation during experimental osteoarthritis. *Osteoarthritis and Cartilage,* 12**,** 627-635.

BONDESON, J., WAINWRIGHT, S. D., LAUDER, S., AMOS, N. & HUGHES, C. E. (2006) The role of synovial macrophages and macrophage-produced cytokines in driving aggrecanases, matrix metalloproteinases, and other destructive and inflammatory responses in osteoarthritis. *Arthritis Research & Therapy,* 8**,** R187.

BONNET, C. S. & WALSH, D. A. (2005) Osteoarthritis, angiogenesis and inflammation. *Rheumatology,* 44**,** 7-16.

BOUGHELLAM, I. (2007) Injectable composites for intra-articular delivery. *School of Pharmacy.* Nottingham, University of Nottingham.

BOZDAG, S., CALIS, S., KAS, H. S., ERCAN, M. T., PEKSOY, I. & HINCAL, A. A. (2001) In vitro evaluation and intra-articular administration of biodegradable microspheres containing naproxen sodium. *Journal of Microencapsulation,* 18**,** 443-456.

BRAGDON, B., BERTONE, A. L., HARDY, J., SIMMONS, E. J. & WEISBRODE, S. E. (2001) Use of an isolated joint model to detect early changes induced by intra-articular injection of paclitaxel-impregnated polymeric microspheres. *Journal of Investigative Surgery,* 14**,** 169-182.

BRANDT, K. D., DOHERTY, M. & LOHMANDER, L. S. (Eds.) (2003) *Osteoarthritis,* Oxford, Oxford University Press.

BRANDT, K. D., SMITH, G. N. & SIMON, L. S. (2000) Intraarticular injection of hyaluronan as treatment for knee osteoarthritis - What is the evidence? *Arthritis and Rheumatism,* 43**,** 1192-1203.

BREWER, E., COLEMAN, J. & LOWMAN, A. (2011) Emerging technologies of polymeric nanoparticles in cancer drug delivery. *Journal of Nanomaterials***,** 408675.

BROWN, K. E., LEONG, K., HUANG, C. H., DALAL, R., GREEN, G. D., HAIMES, H. B., JIMENEZ, P. A. & BATHON, J. (1998) Gelatin/chondroitin 6-sulfate microspheres for the delivery of therapeutic proteins to the joint. *Arthritis and Rheumatism,* 41**,** 2185-2195.

BUCKWALTER, J. A., MANKIN, H. J. & GRODZINSKY, A. J. (2005) Articular cartilage and osteoarthritis. IN PELLEGRINI, V. D. (Ed.) *Instructional Course Lectures: Volume 54.* American Academy of Orthopaedic Surgeons.

BURGESS, D. J. & DAVIS, S. S. (1988) Potenial use of albumin microspheres as a drug delivery system: 2. In vivo deposition and release of steroids. *International Journal of Pharmaceutics,* 46**,** 69-76.

BURSTEIN, D. (2006) MRI for development osteoarthritis drugs of disease-modifying. *NMR in Biomedicine,* 19**,** 669-680.

BURT, H. M., TSALLAS, A., GILCHRIST, S. & LIANG, L. S. (2009) Intra-articular drug delivery systems: overcoming the shortcomings of joint disease therapy. *Expert Opinion on Drug Delivery,* 6**,** 17-26.

BUTOESCU, N., SEEMAYER, C. A., FOTI, M., JORDAN, O. & DOELKER, E. (2009) Dexamethasone-containing PLGA superparamagnetic microparticles as carriers for the local treatment of arthritis. *Biomaterials,* 30**,** 1772-1780.

CAFAGGI, S., RUSSO, E., CAVIGLIOLI, G., PARODI, B., STEFANI, R., SILLO, G., LEARDI, R. & BIGNARDI, G. (2008) Poloxamer 407 as a solubilising agent for tolfenamic acid and as a base for a gel formulation. *European Journal of Pharmaceutical Sciences,* 35**,** 19-29.

CAI, X.-J. & XU, Y.-Y. (2011) Nanomaterials in controlled drug release. *Cytotechnology,* 63**,** 319-323.

CASCONE, M. G., POT, P. M., LAZZERI, L. & ZHU, Z. H. (2002) Release of dexamethasone from PLGA nanoparticles entrapped into dextran/poly(vinyl alcohol) hydrogels. *Journal of Materials Science-Materials in Medicine,* 13**,** 265-269.

CATTERALL, J. B. & CAWSTON, T. E. (2003) Drugs in development: bisphosphonates and metalloproteinase inhibitors. *Arthritis Research & Therapy,* 5**,** 12-24.

CAWSTON, T. E. & WILSON, A. J. (2006) Understanding the role of tissue degrading enzymes and their inhibitors in development and disease. *Best Practice & Research in Clinical Rheumatology,* 20**,** 983-1002.

CEPONIS, A., WARIS, E., MONKKONEN, J., LAASONEN, L., HYTTINEN, M., SOLOVIEVA, S. A., HANEMAAIJER, R., BITSCH, A. & KONTTINEN, Y. T. (2001) Effects of low-dose, noncytotoxic, intraarticular liposomal clodronate on development of erosions and proteoglycan loss in established antigen-induced arthritis in rabbits. *Arthritis and Rheumatism,* 44**,** 1908-1916.

CHEN, J. P. & CHENG, T. H. (2009) Preparation and evaluation of thermo-reversible copolymer hydrogels containing chitosan and hyaluronic acid as injectable cell carriers. *Polymer,* 50**,** 107-116.

CHEN, T. H., EMBREE, H. D., BROWN, E. M., TAYLOR, M. M. & PAYNE, G. F. (2003) Enzyme-catalyzed gel formation of gelatin and chitosan: potential for in situ applications. *Biomaterials,* 24**,** 2831-2841.

CHUA, P. H., NEOH, K. G., SHI, Z. & KANG, E. T. (2008) Structural stability and bioapplicability assessment of hyaluronic acid-chitosan polyelectrolyte multilayers on titanium substrates. *Journal of Biomedical Materials Research Part A,* 87A**,** 1061-1074.

CHUNG, H. J., LEE, Y. H. & PARK, T. G. (2008) Thermo-sensitive and biodegradable hydrogels based on stereocomplexed Pluronic multi-block copolymers for controlled protein delivery. *Journal of Controlled Release,* 127**,** 22-30.

COHN, D., LANDO, G., SOSNIK, A., GARTY, S. & LEVI, A. (2006) PEO-PPO-PEO-based poly(ether ester urethane)s as degradable reverse thermo-responsive multiblock copolymers. *Biomaterials,* 27**,** 1718-1727.

COHN, D., SOSNIK, A. & GARTY, S. (2005) Smart hydrogels for in situ generated implants. *Biomacromolecules,* 6**,** 1168-1175.

CURTISS, P. H. (1964) Changes produced in the synovial membrane and synovial fluid by disease. *Journal of Bone and Joint Surgery-American Volume,* 46**,** 873-888.

DAHL, L. B., DAHL, I. M. S., ENGSTROMLAURENT, A. & GRANATH, K. (1985) Concentration and molecular-weight of sodium hyaluronate in synovial-fluid from patients with rheumatoid-arthritis and other arthropathies. *Annals of the Rheumatic Diseases,* 44**,** 817-822.

DAVIDSON, R. K., WATERS, J. G., KEVORKIAN, L., DARRAH, C., COOPER, A., DONELL, S. T. & CLARK, I. M. (2006) Expression profiling of metalloproteinases and their inhibitors in synovium and cartilage. *Arthritis Research and Therapy,* 8**,** R124.

DAWES, G. J. S., FRATILA-APACHITEI, L. E., MULIA, K., APACHITEI, I., WITKAMP, G. J. & DUSZCZYK, J. (2009) Size effect of PLGA spheres on drug loading efficiency and release profiles. *Journal of Materials Science-Materials in Medicine,* 20**,** 1089-1094.

DE LA FUENTE, M., SEIJO, B. & ALONSO, M. J. (2008) Novel hyaluronan-based nanocarriers for transmucosal delivery of macromolecules. *Macromolecular Bioscience,* 8**,** 441-450.

DE RIENZO, F., SAXENA, P., FILOMIA, F., CASELLI, G., COLACE, F., STASI, L., GIORDANI, A. & MENZIANI, M. C. (2009) Progress towards the identification of new aggrecanase inhibitors. *Current Medicinal Chemistry,* 16**,** 2395-2415.

DEAN, G., HOYLAND, J. A., DENTON, J., DONN, R. P. & FREEMONT, A. J. (1993) Mast-cells in the synovium and synovial-fluid in osteoarthritis. *British Journal of Rheumatology,* 32**,** 671-675.

DENUZIERE, A., FERRIER, D., DAMOUR, O. & DOMARD, A. (1998) Chitosan-chondroitin sulfate and chitosan-hyaluronate polyelectrolyte complexes: biological properties. *Biomaterials,* 19**,** 1275-1285.

DENUZIERE, A., FERRIER, D. & DOMARD, A. (1996) Chitosan-chondroitin sulfate and chitosan-hyaluronate polyelectrolyte complexes. Physico-chemical aspects. *Carbohydrate Polymers,* 29**,** 317-323.

DERBY, R., LEE, S. H., DATE, E. S., LEE, J. H. & LEE, C. H. (2008) Size and aggregation of corticosteroids used for epidural injections. *Pain Medicine,* 9**,** 227-234.

DERENDORF, H., MOLLMANN, H., GRUNER, A., HAACK, D. & GYSELBY, G. (1986) Pharmacokinetics and pharmacodynamics of glucocorticoid suspensions after intraarticular administration. *Clinical Pharmacology & Therapeutics,* 39**,** 313-317.

DIJKGRAAF, L. C., DEBONT, L. G. M., BOER, G. & LIEM, R. S. B. (1995) The structure, biochemistry, and metabolism of osteoarthritic cartilage - a review of the literature. *Journal of Oral and Maxillofacial Surgery,* 53**,** 1182-1192.

DREIER, R., GRASSEL, S., FUCHS, S., SCHAUMBURGER, J. & BRUCKNER, P. (2004) Pro-MMP-9 is a specific macrophage product and is activated by osteoarthritic chondrocytes via MMP-3 or a MT1-MMP/MMP-13 cascade. *Experimental Cell Research,* 297**,** 303-312.

DUMITRIU, S. & CHORNET, E. (1998) Inclusion and release of proteins from polysaccharide-based polyion complexes. *Advanced Drug Delivery Reviews,* 31**,** 223-246.

DUNN, A. R. (2010) Eighty-seven percent of 66 adult patients with advanced osteoarthritis of the knee subjected to treatment with intra-articular injections of human growth hormone avoid a total knee arthroplasty. *Osteoarthritis and Cartilage,* 18**,** S38.

EL-HEFIAN, E. A. & YAHAYA, A. H. (2010) Rheological study of chitosan and its blends: an overview. *Maejo International Journal of Science and Technology,* 4**,** 210-220.

ELRON-GROSS, I., GLUCKSAM, Y. & MARGALIT, R. (2009) Liposomal dexamethasone-diclofenac combinations for local osteoarthritis treatment. *International Journal of Pharmaceutics,* 376**,** 84-91.

FANG, J. Y., CHEN, J. P., LEU, Y. L. & HU, H. W. (2008) Temperature-sensitive hydrogels composed of chitosan and hyaluronic acid as injectable carriers for drug delivery. *European Journal of Pharmaceutics and Biopharmaceutics,* 68**,** 626-636.

FARAHAT, M. N., YANNI, G., POSTON, R. & PANAYI, G. S. (1993) Cytokine expression in synovial membranes of patients with rheumatoid-arthritis and osteoarthritis. *Annals of the Rheumatic Diseases,* 52**,** 870-875.

FESSI, H., PUISIEUX, F., DEVISSAGUET, J. P., AMMOURY, N. & BENITA, S. (1989) Nanocapsule formation by interfacial polymer deposition

following solvent displacement. *International Journal of Pharmaceutics,* 55**,** R1-R4.

FICHTER, M., KORNER, U., SCHOMBURG, J., JENNINGS, L., COLE, A. A. & MOLLENHAUER, J. (2006) Collagen degradation products modulate matrix metalloproteinase expression in cultured articular chondrocytes. *Journal of orthopaedic research : official publication of the Orthopaedic Research Society,* 24**,** 63-70.

FREDHEIM, G. E. & CHRISTENSEN, B. E. (2003) Polyelectrolyte complexes: interactions between lignosulfonate and chitosan. *Biomacromolecules,* 4**,** 232-239.

FURUZAWA-CARBALLEDA, J. & ALCOCER-VARELA, J. (1999) Interleukin-8, interleukin-10, intercellular adhesion molecule-1 and vascular cell adhesion molecule-1 expression levels are higher in synovial tissue from patients with rheumatoid arthritis than in osteoarthritis. *Scandinavian Journal of Immunology,* 50**,** 215-222.

GAMINI, A., PAOLETTI, S., TOFFANIN, R., MICALI, F., MICHIELIN, L. & BEVILACQUA, C. (2002) Structural investigations of cross-linked hyaluronan. *Biomaterials,* 23**,** 1161-1167.

GARNETT, M. C. (1999) Gene-delivery systems using cationic polymers. *Critical Reviews in Therapeutic Drug Carrier Systems,* 16**,** 147-207.

GARNETT, M. C., FERRUTI, P., RANUCCI, E., SUARDI, M. A., HEYDE, M. & SLEAT, R. (2009) Sterically stabilized self-assembling reversibly cross-linked polyelectrolyte complexes with nucleic acids for environmental and medical applications. *Biochemical Society Transactions,* 37**,** 713-716.

GERWIN, N., HOPS, C. & LUCKE, A. (2006) Intraarticular drug delivery in osteoarthritis. *Advanced Drug Delivery Reviews,* 58**,** 226-242.

GIATROMANOLAKI, A., SIVRIDIS, E., MALTEZOS, E., ATHANASSOU, N., PAPAZOGLOU, D., GATTER, K. C., HARRIS, A. L. & KOUKOURAKIS, M. I. (2003) Upregulated hypoxia inducible factor-1 alpha and -2 alpha pathway in rheumatoid arthritis and osteoarthritis. *Arthritis Research & Therapy,* 5**,** R193-R201.

GILBERT, J. C., RICHARDSON, J. L., DAVIES, M. C., PALIN, K. J. & HADGRAFT, J. (1987) The effect of solutes and polymers on the gelation properties of Pluronic F-127 solutions for controlled drug delivery. *Journal of Controlled Release,* 5**,** 113-118.

GOLDRING, M. B. & GOLDRING, S. R. (2007) Osteoarthritis. *Journal of Cellular Physiology,* 213**,** 626-634.

GOMEZ-GAETE, C., TSAPIS, N., BESNARD, M., BOCHOT, A. & FATTAL, E. (2007) Encapsulation of dexamethasone into biodegradable polymeric nanoparticles. *International Journal of Pharmaceutics,* 331**,** 153-159.

GRABOWSKI, P. S., WRIGHT, P. K., VANTHOF, R. J., HELFRICH, M. H., OHSHIMA, H. & RALSTON, S. H. (1997) Immunolocalization of inducible nitric oxide synthase in synovium and cartilage in rheumatoid arthritis and osteoarthritis. *British Journal of Rheumatology,* 36**,** 651-655.

GREIS, P. E., GEORGESCU, H. I., FU, F. H. & EVANS, C. H. (1994) Particle-induced synthesis of collagenase by synovial fibroblasts - an immunocytochemical study. *Journal of Orthopaedic Research,* 12**,** 286-293.

GUZMAN, M., GARCIA, F. F., MOLPECERES, J. & ABERTURAS, M. R. (1992) Polyoxyethylene-polyoxypropylene block copolymer gels as sustained-release vehicles for subcutaneous drug administration. *International Journal of Pharmaceutics,* 80**,** 119-127.

HAMERMAN, D. & KLAGSBRUN, M. (1985) Osteo-arthritis - emerging evidence for cell-interactions in the breakdown and remodeling of cartilage. *American Journal of Medicine,* 78**,** 495-499.

HAMIDI, M., AZADI, A. & RAFIEI, P. (2008) Hydrogel nanoparticles in drug delivery. *Advanced Drug Delivery Reviews,* 60**,** 1638-1649.

HAMMAN, J. H. (2010) Chitosan based polyelectrolyte complexes as potential carrier materials in drug delivery systems. *Marine Drugs,* 8**,** 1305-1322.

HANS, M. L. & LOWMAN, A. M. (2002) Biodegradable nanoparticles for drug delivery and targeting. *Current Opinion in Solid State & Materials Science,* 6**,** 319-327.

HARAOUI, B., PELLETIER, J. P., CLOUTIER, J. M., FAURE, M. P. & MARTELPELLETIER, J. (1991) Synovial-membrane histology and immunopathology in rheumatoid-arthritis and osteoarthritis – in vivo effects of antirheumatic drugs. *Arthritis and Rheumatism,* 34**,** 153-163.

HARDING, S. E., HILL, S. E. & MITCHELL, J. R. (Eds.) (1995) *Biopolymer Mixtures,* Nottingham, Nottingham University Press.

HAYASHI, M., MUNETA, T., TAKAHASHI, T., JU, Y. J., TSUJI, K. & SEKIYA, I. (2010) Intra-articular injections of bone morphogenetic protein-7 retard progression of existing cartilage degeneration. *Journal of Orthopaedic Research,* 28**,** 1502-1506.

HAYWOOD, L., MCWILLIAMS, D. F., PEARSON, C. I., GILL, S. E., GANESAN, A., WILSON, D. & WALSH, D. A. (2003) Inflammation and angiogenesis in osteoarthritis. *Arthritis and Rheumatism,* 48**,** 2173-2177.

HE, C. L., KIM, S. W. & LEE, D. S. (2008) In situ gelling stimuli-sensitive block copolymer hydrogels for drug delivery. *Journal of Controlled Release,* 127**,** 189-207.

HENROTIN, Y., KURZ, B. & AIGNER, T. (2005) Oxygen and reactive oxygen species in cartilage degradation: friends or foes? *Osteoarthritis and Cartilage,* 13**,** 643-654.

HILL, C. L., HUNTER, D. J., NIU, J., CLANCY, M., GUERMAZI, A., GENANT, H., GALE, D., GRAINGER, A., CONAGHAN, P. & FELSON, D. T. (2007) Synovitis detected on magnetic resonance imaging and its relation to pain and cartilage loss in knee osteoarthritis. *Annals of the Rheumatic Diseases,* 66**,** 1599-1603.

HOFFMAN, A. S. (2002) Hydrogels for biomedical applications. *Advanced Drug Delivery Reviews,* 54**,** 3-12.

HOGENMILLER, M. S. & LOZADA, C. J. (2006) An update on osteoarthritis therapeutics. *Current Opinion in Rheumatology,* 18**,** 256-260.

HOLLAND, T. A. & MIKOS, A. G. (2003) Advances in drug delivery for articular cartilage. *Journal of Controlled Release,* 86**,** 1-14.

HORISAWA, E., HIROTA, T., KAWAZOE, S., YAMADA, J., YAMAMOTO, H., TAKEUCHI, H. & KAWASHIMA, Y. (2002a) Prolonged anti-inflammatory action of DL-lactide/glycolide copolymer nanospheres containing betamethasone sodium phosphate for an intra-articular delivery system in antigen-induced arthritic rabbit. *Pharmaceutical Research,* 19**,** 403-410.

HORISAWA, E., KUBOTA, K., TUBOI, I., SATO, K., YAMAMOTO, H., TAKEUCHI, H. & KAWASHIMA, Y. (2002b) Size-dependency of DL-lactide/glycolide copolymer particulates for intra-articular delivery system on phagocytosis in rat synovium. *Pharmaceutical Research,* 19**,** 132-139.

HORTON, W. E., YAGI, R., LAVERTY, D. & WEINER, S. (2005) Overview of studies comparing human normal cartilage with minimal and advanced osteoarthritic cartilage. *Clinical and Experimental Rheumatology,* 23**,** 103-112.

HOU, W. S., LI, W. J., KEYSZER, G., WEBER, E., LEVY, R., KLEIN, M. J., GRAVALLESE, E. M., GOLDRING, S. R. & BROMME, D. (2002) Comparison of cathepsins K and S expression within the rheumatoid and osteoarthritic synovium. *Arthritis and Rheumatism,* 46**,** 663-674.

INOUE, A., TAKAHASHI, K. A., ARAI, Y., TONOMURA, H., SAKAO, K., SAITO, M., FUJIOKA, M., FUJIWARA, H., TABATA, Y. & KUBO, T. (2006) The therapeutic effects of basic fibroblast growth factor contained in gelatin hydrogel microspheres on experimental osteoarthritis in the rabbit knee. *Arthritis and Rheumatism,* 54**,** 264-270.

ISHIHARA, T., KUBOTA, T., CHOI, T. & HIGAKI, M. (2009) Treatment of experimental arthritis with stealth-type polymeric nanoparticles encapsulating betamethasone phosphate. *Journal of Pharmacology and Experimental Therapeutics,* 329**,** 412-417.

JAGUR-GRODZINSKI, J. (2010) Polymeric gels and hydrogels for biomedical and pharmaceutical applications. *Polymers for Advanced Technologies,* 21**,** 27-47.

JEONG, B., KIM, S. W. & BAE, Y. H. (2002) Thermosensitive sol-gel reversible hydrogels. *Advanced Drug Delivery Reviews,* 54**,** 37-51.

JIANG, D. H., ZOU, J., HUANG, L. X., SHI, Q., ZHU, X. S., WANG, G. L. & YANG, H. L. (2010) Efficacy of intra-articular injection of celecoxib in a rabbit model of osteoarthritis. *International Journal of Molecular Sciences,* 11**,** 4106-4113.

JOHNSON, A. R., PAVLOVSKY, A. G., ORTWINE, D. F., PRIOR, F., MAN, C. F., BORNEMEIER, D. A., BANOTAI, C. A., MUELLER, W. T., MCCONNELL, P., YAN, C., BARAGI, V., LESCH, C., ROARK, W. H., WILSON, M., DATTA, K., GUZMAN, R., HAN, H. K. & DYER, R. D. (2007) Discovery and characterization of a novel inhibitor of matrix metalloprotease-13 that reduces cartilage damage in vivo without joint fibroplasia side effects. *Journal of Biological Chemistry,* 282**,** 27781-27791.

JOHNSTON, A. P. R., SUCH, G. K., NG, S. L. & CARUSO, F. (2011) Challenges facing colloidal delivery systems: from synthesis to the clinic. *Current Opinion in Colloid & Interface Science,* 16**,** 171-181.

JONES, A., REGAN, M., LEDINGHAM, J., PATTRICK, M., MANHIRE, A. & DOHERTY, M. (1993) Importance of placement of intraarticular steroid injections. *British Medical Journal,* 307**,** 1329-1330.

KABANOV, A. V. & KABANOV, V. A. (1998) Interpolyelectrolyte and block ionomer complexes for gene delivery: physicochemical aspects. *Advanced Drug Delivery Reviews,* 30**,** 49-60.

KALLINTERI, P., HIGGINS, S., HUTCHEON, G. A., ST POURCAIN, C. B. & GARNETT, M. C. (2005) Novel functionalized biodegradable polymers for nanoparticle drug delivery systems. *Biomacromolecules,* 6**,** 1885-1894.

KARMOUTY-QUINTANA, H., TAMIMI, F., MCGOVERN, T. K., GROVER, L. M., MARTIN, J. G. & BARRALET, J. E. (2010) Sustained steroid release in pulmonary inflammation model. *Biomaterials,* 31**,** 6050-6059.

KIM, D. H. & MARTIN, D. C. (2006) Sustained release of dexamethasone from hydrophilic matrices using PLGA nanoparticles for neural drug delivery. *Biomaterials,* 27**,** 3031-3037.

KIM, K. S., PARK, S. J., YANG, J. A., JEON, J. H., BHANG, S. H., KIM, B. S. & HAHN, S. K. (2011) Injectable hyaluronic acid-tyramine hydrogels for the treatment of rheumatoid arthritis. *Acta Biomaterialia,* 7**,** 666-674.

KIM, M. R. & PARK, T. G. (2002) Temperature-responsive and degradable hyaluronic acid/Pluronic composite hydrogels for controlled release of human growth hormone. *Journal of Controlled Release,* 80**,** 69-77.

KIM, S. J., SHIN, S. R., LEE, K. B., PARK, Y. D. & KIM, S. I. (2004) Synthesis and characteristics of polyelectrolyte complexes composed of chitosan and hyaluronic acid. *Journal of Applied Polymer Science,* 91**,** 2908-2913.

KIM, Y., LARKIN, A. L., DAVIS, R. M. & RAJAGOPALAN, P. (2010) The design of in vitro liver sinusoid mimics using chitosan-hyaluronic acid polyelectrolyte multilayers. *Tissue Engineering Part A,* 16**,** 2731-2741.

KLATT, A. R., PAUL-KLAUSCH, B., KLINGER, G., KUEHN, G., RENNO, J. H., BANERJEE, M., MALCHAU, G. & WIELCKENS, K. (2009) A critical role for collagen II in cartilage matrix degradation: collagen II induces pro-inflammatory cytokines and MMPs in primary human chondrocytes. *Journal of Orthopaedic Research,* 27**,** 65-70.

KONTTINEN, Y. T., MANDELIN, J., LI, T. F., SALO, J., LASSUS, J., LILJESTROM, M., HUKKANEN, M., TAKAGI, M., VIRTANEN, I. & SANTAVIRTA, S. (2002) Acidic cysteine endoproteinase cathepsin K in the degeneration of the superficial articular hyaline cartilage in osteoarthritis. *Arthritis and Rheumatism,* 46**,** 953-960.

KUO, J. W., SWANN, D. A. & PRESTWICH, G. D. (1991) Chemical modification of hyaluronic-acid by carbodiimides. *Bioconjugate Chemistry,* 2**,** 232-241.

LARSEN, C., OSTERGAARD, J., LARSEN, S. W., JENSEN, H., JACOBSEN, S., LINDEGAARD, C. & ANDERSEN, P. H. (2008) Intra-articular depot formulation principles: role in the management of postoperative pain and arthritic disorders. *Journal of Pharmaceutical Sciences,* 97**,** 4622-4654.

LE GRAVERAND-GASTINEAU, M. P. H. (2010) Disease modifying osteoarthritis drugs: facing development challenges and choosing molecular targets. *Current Drug Targets,* 11**,** 528-535.

LEACH, J. B., BIVENS, K. A., PATRICK, C. W. & SCHMIDT, C. E. (2003) Photocrosslinked hyaluronic acid hydrogels: natural, biodegradable tissue engineering scaffolds. *Biotechnology and Bioengineering,* 82**,** 578-589.

LEE, F., CHUNG, J. E. & KURISAWA, M. (2008) An injectable enzymatically crosslinked hyaluronic acid-tyramine hydrogel system with independent tuning of mechanical strength and gelation rate. *Soft Matter,* 4**,** 880-887.

LEE, H., MOK, H., LEE, S., OH, Y. K. & PARK, T. G. (2007) Target-specific intracellular delivery of siRNA using degradable hyaluronic acid nanogels. *Journal of Controlled Release,* 119**,** 245-252.

LEE, J. W., KIM, S. Y., KIM, S. S., LEE, Y. M., LEE, K. H. & KIM, S. J. (1999) Synthesis and characteristics of interpenetrating polymer network

hydrogel composed of chitosan and poly(acrylic acid). *Journal of Applied Polymer Science,* 73**,** 113-120.

LEE, K. Y., PARK, W. H. & HA, W. S. (1997) Polyelectrolyte complexes of sodium alginate with chitosan or its derivatives for microcapsules. *Journal of Applied Polymer Science,* 63**,** 425-432.

LEE, S. B., LEE, Y. M., SONG, K. W. & PARK, M. H. (2003) Preparation and properties of polyelectrolyte complex sponges composed of hyaluronic acid and chitosan and their biological behaviors. *Journal of Applied Polymer Science,* 90**,** 925-932.

LI, N. G., SHI, Z. H., TANG, Y. P., WANG, Z. J., SONG, S. L., QIAN, L. H., QIAN, D. W. & DUAN, J. A. (2011) New hope for the treatment of osteoarthritis through selective inhibition of MMP-13. *Current Medicinal Chemistry,* 18**,** 977-1001.

LIAO, Y. H., JONES, S. A., FORBES, B., MARTIN, G. P. & BROWN, M. B. (2005) Hyaluronan: Pharmaceutical characterization and drug delivery. *Drug Delivery,* 12**,** 327-342.

LIGGINS, R. T., CRUZ, T., MIN, W., LIANG, L., HUNTER, W. L. & BURT, H. M. (2004) Intra-articular treatment of arthritis with microsphere formulations of paclitaxel: biocompatibility and efficacy determinations in rabbits. *Inflammation Research,* 53**,** 363-372.

LINDQVIST, U., TOLMACHEV, V., KAIREMO, K., ASTROM, G., JONSSON, E. & LUNDQVIST, H. (2002) Elimination of stabilised hyaluronan from the knee joint in healthy men. *Clinical Pharmacokinetics,* 41**,** 603-613.

LITTLE, C. B., FLANNERY, C. R., HUGHES, C. E., MORT, J. S., ROUGHLEY, P. J., DENT, C. & CATERSON, B. (1999) Aggrecanase versus matrix metalloproteinases in the catabolism of the interglobular domain of aggrecan in vitro. *Biochemical Journal,* 344**,** 61-68.

LOPEZ-GARCIA, F., VAZQUEZ-AUTON, J. M., GIL, F., LATOORE, R., MORENO, F., VILLALAIN, J. & GOMEZ-FERNANDEZ, J. C. (1993) Intraarticular therapy of experimental arthritis with a derivative of triamcinolone acetonide incorporated in liposomes. *Journal of Pharmacy and Pharmacology,* 45**,** 576-578.

LU, J. X., PRUDHOMMEAUX, F., MEUNIER, A., SEDEL, L. & GUILLEMIN, G. (1999) Effects of chitosan on rat knee cartilages. *Biomaterials,* 20**,** 1937-1944.

LU, Y., ZHANG, G. Q., SUN, D. X. & ZHONG, Y. Q. (2007) Preparation and evaluation of biodegradable flubiprofen gelatin micro-spheres for intra-articular administration. *Journal of Microencapsulation,* 24**,** 515-524.

LUO, Y. & PRESTWICH, G. D. (2001) Hyaluronic acid-N-hydroxysuccinimide: a useful intermediate for bioconjugation. *Bioconjugate Chemistry,* 12**,** 1085-1088.

LUPPI, B., BIGUCCI, F., MERCOLINI, L., MUSENGA, A., SORRENTI, M., CATENACCI, L. & ZECCHI, V. (2009) Novel mucoadhesive nasal inserts based on chitosan/hyaluronzite polyelectrolyte complexes for peptide and protein delivery. *Journal of Pharmacy and Pharmacology,* 61**,** 151-157.

MACGREGOR, A. J., ANTONIADES, L., MATSON, M., ANDREW, T. & SPECTOR, T. D. (2000) The genetic contribution to radiographic hip osteoarthritis in women - results of a classic twin study. *Arthritis and Rheumatism,* 43**,** 2410-2416.

MALMSTEN, M. & LINDMAN, B. (1992) Self-assemblt in aqueous block copolymer solutions. *Macromolecules,* 25**,** 5440-5445.

MATHY-HARTERT, M., HOGGE, L., SANCHEZ, C., DEBY-DUPONT, G., CRIELAARD, J. M. & HENROTIN, Y. (2008) Interleukin-1 beta and interleukin-6 disturb the antioxidant enzyme system in bovine chondrocytes: a possible explanation for oxidative stress generation. *Osteoarthritis and Cartilage,* 16**,** 756-763.

MAVRAKI, A. & CANN, P. M. (2009) Friction and lubricant film thickness measurements on simulated synovial fluids. *Proceedings of the Institution of Mechanical Engineers Part J-Journal of Engineering Tribology,* 223**,** 325-335.

MAZZETTI, I., GRIGOLO, B., PULSATELLI, L., DOLZANI, P., SILVESTRI, T., ROSETI, L., MELICONI, R. & FACCHINI, A. (2001) Differential roles of nitric oxide and oxygen radicals in chondrocytes affected by osteoarthritis and rheumatoid arthritis. *Clinical Science,* 101**,** 593-599.

MCDEVITT, C. A., PAHL, J. A., AYAD, S., MILLER, R. R., URATSUJI, M. & ANDRISH, J. T. (1988) Experimental osteoarthritic articular-cartilage is enriched in guanidine-soluble type-VI collagen. *Biochemical and Biophysical Research Communications,* 157**,** 250-255.

MCINNES, I. B., LEUNG, B. P., FIELD, M., WEI, X. Q., HUANG, F.-P., STURROCK, R. D., KINNINMONTH, A., WEIDNER, J., MUMFORD, R. & LIEW, F. Y. (1996) Production of nitric oxide in the synovial membrane of rheumatoid and osteoarthritis patients. *Journal of Experimental Medicine,* 184**,** 1519-1524.

MENG, W., PARKER, T. L., KALLINTERI, P., WALKER, D. A., HIGGINS, S., HUTCHEON, G. A. & GARNETT, M. C. (2006) Uptake and metabolism of novel biodegradable poly(glycerol-adipate) nanoparticles in DAOY monolayer. *Journal of Controlled Release,* 116**,** 314-321.

MENSITIERI, M., AMBROSIO, L., IANNACE, S., NICOLAIS, L. & PERBELLINI, A. (1995) Viscoelastic evaluation of different knee

osteoarthritis therapies. *Journal of Materials Science-Materials in Medicine,* 6**,** 130-137.

MEZGER, T. G. (2006) *The rheology handbook,* Hannover, Germany, Vincentz Network.

MIERISCH, C. M., COHEN, S. B., JORDAN, L. C., ROBERTSON, P. G., BALIAN, G. & DIDUCH, D. R. (2002) Transforming growth factor-beta in calcium alginate beads for the treatment of articular cartilage defects in the rabbit. *Arthroscopy-the Journal of Arthroscopic and Related Surgery,* 18**,** 892-900.

MISHRA, B., PATEL, B. B. & TIWARI, S. (2010) Colloidal nanocarriers: a review on formulation technology, types and applications toward targeted drug delivery. *Nanomedicine- Nanotechnology Biology and Medicine,* 6**,** 9-24.

MOMBERGER, T. S., LEVICK, J. R. & MASON, R. M. (2005) Hyaluronan secretion by synoviocytes is mechanosensitive. *Matrix Biology,* 24**,** 510-519.

MONKKONEN, J., LIUKKONEN, J., TASKINEN, M., HEATH, T. D. & URTTI, A. (1995) Studies on liposome formulations for intra-articular delivery of clodronate. *Journal of Controlled Release,* 35**,** 145-154.

MORELAND, L. W. (2003) Intra-articular hyaluronan (hyaluronic acid) and hylans for the treatment of osteoarthritis: mechanisms of action. *Arthritis Research & Therapy,* 5**,** 54-67.

MORIYAMA, K., OOYA, T. & YUI, N. (1999) Hyaluronic acid grafted with poly(ethylene glycol) as a novel peptide formulation. *Journal of Controlled Release,* 59**,** 77-86.

MOUNTZIARIS, P. M., SING, D. C., CHEW, S. A., TZOUANAS, S. N., LEHMAN, E. D., KASPER, F. K. & MIKOS, A. G. (2011) Controlled release of anti-inflammatory siRNA from biodegradable polymeric microparticles intended for intra-articular delivery to the temporomandibular joint. *Pharmaceutical Research,* 28**,** 1370-1384.

MOUNTZIARIS, P. M., SING, D. C., MIKOS, A. G. & KRAMER, P. R. (2010) Intra-articular microparticles for drug delivery to the TMJ. *Journal of Dental Research,* 89**,** 1039-1044.

MUMPER, R. J., MILLS, B. J. A., RYO, U. Y. & JAY, M. (1992) Polymeric microspheres for radionuclide synovectomy containing neutron-activated Ho-166. *Journal of Nuclear Medicine,* 33**,** 398-402.

MURATA, M., YUDOH, K. & MASUKO, K. (2008) The potential role of vascular endothelial growth factor (VEGF) in cartilage - How the angiogenic factor could be involved in the pathogenesis of osteoarthritis? *Osteoarthritis and Cartilage,* 16**,** 279-286.

MYERS, S. L., BRANDT, K. D., EHLICH, J. W., BRAUNSTEIN, E. M., SHELBOURNE, K. D., HECK, D. A. & KALASINSKI, L. A. (1990)

Synovial inflammation in patients with early osteoarthritis of the knee *Journal of rheumatology,* 17**,** 1662-1669.

NAGASE, H. & KASHIWAGI, M. (2003) Aggrecanases and cartilage matrix degradation. *Arthritis Research & Therapy,* 5**,** 94-103.

NAGASE, H., VISSE, R. & MURPHY, G. (2006) Structure and function of matrix metalloproteinases and TIMPs. *Cardiovascular Research,* 69**,** 562-573.

NAGAYA, H., YMAGATA, T., YMAGATA, S., IYODA, K., ITO, H., HASEGAWA, Y. & IWATA, H. (1999) Examination of synovial fluid and serum hyaluronidase activity as a joint marker in rheumatoid arthritis and osteoarthritis patients (by zymography). *Annals of the Rheumatic Diseases,* 58**,** 186-188.

NAKAMURA, H., YOSHINO, S., KATO, T., TSURUHA, J. & NISHIOKA, K. (1999) T-cell mediated inflammatory pathway in osteoarthritis. *Osteoarthritis and Cartilage,* 7**,** 401-402.

NANJAWADE, B. K., MANVI, F. V. & MANJAPPA, A. S. (2007) In situ-forming hydrogels for sustained ophthalmic drug delivery. *Journal of Controlled Release,* 122**,** 119-134.

NATIONAL COLLABORATING CENTRE FOR CHRONIC CONDITIONS (2008) Osteoarthritis: national clinical guideline for care and management in adults., London: Royal College of Physicians.

NIGROVIC, P. A. & LEE, D. M. (2007) Synovial mast cells: role in acute and chronic arthritis. *Immunological Reviews,* 217**,** 19-37.

NISHIDE, M., KAMEI, S., TAKAKURA, Y., TAMAI, S., TABATA, Y. & IKADA, Y. (1999) Fate of biodegradable DL-lactic acid oligomer microspheres in the articulus. *Journal of Bioactive and Compatible Polymers,* 14**,** 385-398.

NUESCH, E., RUTJES, A. W. S., TRELLE, S., REICHENBACH, S. & JUNI, P. (2009) Doxycycline for osteoarthritis of the knee or hip. *Cochrane Database of Systematic Reviews***,** CD007323.

OEHLER, S., NEUREITER, D., MEYER-SCHOLTEN, C. & AIGNER, T. (2002) Subtyping of osteoarthritic synoviopathy. *Clinical and Experimental Rheumatology,* 20**,** 633-640.

OSTALOWSKA, A., BIRKNER, E., WIECHA, M., KASPERCZYK, S., KASPERCZYK, A., KAPOLKA, D. & ZON-GIEBEL, A. (2006) Lipid peroxidation and antioxidant enzymes in synovial fluid of patients with primary and secondary osteoarthritis of the knee joint. *Osteoarthritis and Cartilage,* 14**,** 139-145.

PAGE THOMAS, D. P., KING, B., STEPHENS, T. & DINGLE, J. T. (1991) In vivo studies of cartilage regeneration after damage induced by catabolin/interleukin-1. *Annals of the Rheumatic Diseases,* 50**,** 75-80.

PANYAM, J., WILLIAMS, D., DASH, A., LESLIE-PELECKY, D. & LABHASETWAR, V. (2004) Solid-state solubility influences encapsulation and release of hydrophobic drugs from PLGA/PLA nanoparticles. *Journal of Pharmaceutical Sciences,* 93**,** 1804-1814.

PARAJO, Y., D'ANGELO, I., WELLE, A., GARCIA-FUENTES, M. & ALONSO, M. J. (2010) Hyaluronic acid/chitosan nanoparticles as delivery vehicles for VEGF and PDGF-BB. *Drug Delivery,* 17**,** 596-604.

PEAT, G., THOMAS, E., DUNCAN, R., WOOD, L., HAY, E. & CROFT, P. (2006) Clinical classification criteria for knee osteoarthritis: performance in the general population and primary care. *Annals of the Rheumatic Diseases,* 65**,** 1363-1367.

PELLETIER, J. P. & MARTEL-PELLETIER, J. (2007) DMOAD developments present and future. *Bulletin of the NYU Hospital for Joint Diseases,* 65**,** 242-248.

PELLETIER, J. P., MARTEL-PELLETIER, J. & ABRAMSON, S. B. (2001) Osteoarthritis, an inflammatory disease - potential implication for the selection of new therapeutic targets. *Arthritis and Rheumatism,* 44**,** 1237-1247.

PELLETIER, J. P., RAYNAULD, J. P., ABRAM, F., HARAOUI, B., CHOQUETTE, D. & MARTEL-PELLETIER, J. (2008) A new non-invasive method to assess synovitis severity in relation to symptoms and cartilage volume loss in knee osteoarthritis patients using MRI. *Osteoarthritis and Cartilage,* 16**,** S8-S13.

POLLARD, T. C. B., GWILYM, S. E. & CARR, A. J. (2008) The assessment of early osteoarthritis. *Journal of Bone and Joint Surgery-British Volume,* 90B**,** 411-421.

POUYANI, T., HARBISON, G. S. & PRESTWICH, G. D. (1994) Novel hydrogels of hyaluronic-acid - synthesis, surface-morphology, and solid-state NMR. *Journal of the American Chemical Society,* 116**,** 7515-7522.

PREHM, P. & SCHUMACHER, U. (2004) Inhibition of hyaluronan export from human fibroblasts by inhibitors of multidrug resistance transporters. *Biochemical Pharmacology,* 68**,** 1401-1410.

PRESTWICH, G. D. (2001) Biomaterials from chemically-modified hyaluronan. *Glyocoforum: http://www.glycoforum.gr.jp/science/hyaluronan/HA18/HA18E.html*.

PRESTWICH, G. D. & KUO, J. (2008) Chemically-modified HA for therapy and regenerative medicine. *Current Pharmaceutical Biotechnology,* 9**,** 242-245.

PURI, S. (2007) Novel functionalized polymers for nanoparticle formulations with anti cancer drugs. *School of Pharmacy*. Nottingham, University of Nottingham.

PURI, S., KALLINTERI, P., HIGGINS, S., HUTCHEON, G. A. & GARNETT, M. C. (2008) Drug incorporation and release of water soluble drugs from novel functionalised poly(glycerol adipate) nanoparticles. *Journal of Controlled Release,* 125**,** 59-67.

QVIST, P., BAY-JENSEN, A. C., CHRISTIANSEN, C., DAM, E. B., PASTOUREAU, P. & KARSDAL, M. A. (2008) The disease modifying osteoarthritis drug (DMOAD): is it in the horizon? *Pharmacological Research,* 58**,** 1-7.

RAMESH, D. V., TABATA, Y. & IKADA, Y. (1999) Bioabsorbable microspheres for local drug release in the articulus. *Journal of Bioactive and Compatible Polymers,* 14**,** 137-149.

RANI, M., AGARWAL, A. & NEGI, Y. S. (2010) Review: chitosan based hydrogel polymeric beads - as drug delivery system. *Bioresources,* 5**,** 2765-2807.

RAO, J. P. & GECKELER, K. E. (2011) Polymer nanoparticles: preparation techniques and size-control parameters. *Progress in Polymer Science,* 36**,** 887-913.

RATCLIFFE, J. H., HUNNEYBALL, I. M., SMITH, A., WILSON, C. G. & DAVIS, S. S. (1984) Preparation and evaluation of biodegradable polymeric systems for the intra-articular delivery of drugs. *Journal of Pharmacy and Pharmacology,* 36**,** 431-436.

RATCLIFFE, J. H., HUNNEYBALL, I. M., WILSON, C. G., SMITH, A. & DAVIS, S. S. (1987) Albumin microspheres for intraarticular drug delivery - investigation of their retention in normal and arthritic knee joints of rabbits. *Journal of Pharmacy and Pharmacology,* 39**,** 290-295.

REDHEAD, H. M. (1997) Drug loading of biodegradable nanoparticles for site specific drug delivery. *School of Pharmacy.* Nottingham, University of Nottingham.

RENGEL, Y., OSPELT, C. & GAY, S. (2007) Proteinases in the joint: clinical relevance of proteinases in joint destruction. *Arthritis Research & Therapy,* 9.

ROPES, M. W., ROSSMEISL, E. C. & BAUER, W. (1940) The origin and nature of normal human synovial fluid. *Journal of Clinical Investigation,* 19**,** 795-799.

ROSSINI, M., VIAPIANA, O., RAMONDA, R., BIANCHI, G., OLIVIERI, I., LAPADULA, G. & ADAMI, S. (2009) Intra-articular clodronate for the treatment of knee osteoarthritis: dose ranging study vs hyaluronic acid. *Rheumatology,* 48**,** 773-778.

ROTHENFLUH, D. A., BERMUDEZ, H., O'NEIL, C. P. & HUBBELL, J. A. (2008) Biofunctional polymer nanoparticles for intra-articular targeting and retention in cartilage. *Nature Materials,* 7**,** 248-254.

ROTHWELL, A. G. & BENTLEY, G. (1973) Chondrocyte multiplication in osteoarthritic articular cartilage. *The Journal of bone and joint surgery. British volume,* 55**,** 588-94.

RUEL-GARIEPY, E., CHENITE, A., CHAPUT, C., GUIRGUIS, S. & LEROUX, J. C. (2000) Characterization of thermosensitive chitosan gels for the sustained delivery of drugs. *International Journal of Pharmaceutics,* 203**,** 89-98.

RUEL-GARIEPY, E., LECLAIR, G., HILDGEN, P., GUPTA, A. & LEROUX, J. C. (2002) Thermosensitive chitosan-based hydrogel containing liposomes for the delivery of hydrophilic molecules. *Journal of Controlled Release,* 82**,** 373-383.

RUEL-GARIEPY, E. & LEROUX, J. C. (2004) In situ-forming hydrogels - review of temperature-sensitive systems. *European Journal of Pharmaceutics and Biopharmaceutics,* 58**,** 409-426.

RUETTGER, A., SCHUELER, S., MOLLENHAUER, J. A. & WIEDERANDERS, B. (2008) Cathepsins B, K, and L are regulated by a defined collagen type II peptide via activation of classical protein kinase C and p38 MAP kinase in articular chondrocytes. *Journal of Biological Chemistry,* 283**,** 1043-1051.

RYDELL, N. & BALAZS, E. A. (1971) Effect of intra-articular injection of hyaluronic acid on clinical symptoms of osteoarthritis and on granulation tissue formation. *Clinical Orthopaedics and Related Research***,** 25-32.

SADOUK, M. B., PELLETIER, J.-P., TARDIF, G., KIANSA, K., CLOUTIER, J.-M. & MARTEL-PELLETIER, J. (1995) Human synovial fibroblasts coexpress IL-1 receptor type I and type II mRNA: the increased level of the IL-1 receptor in osteoarthritic cells is related to an increased level of the type I receptor. *Laboratory Investigation,* 73**,** 347-355.

SAKKAS, L. I. & PLATSOUCAS, C. D. (2007) The role of T cells in the pathogenesis of osteoarthritis. *Arthritis and Rheumatism,* 56**,** 409-424.

SALTER, D. M. (1993) Tenascin is increased in cartilage and synovium from arthritic knees. *British Journal of Rheumatology,* 32**,** 780-786.

SANDELL, L. J. & AIGNER, T. (2001) Articular cartilage and changes in arthritis - an introduction: cell biology of osteoarthritis. *Arthritis Research,* 3**,** 107-113.

SANNINO, A., MADAGHIELE, M., CONVERSANO, F., MELE, G., MAFFEZZOLI, A., NETTI, P. A., AMBROSIO, L. & NICOLAIS, L. (2004) Cellulose derivative-hyaluronic acid-based microporous hydrogels cross-linked through divinyl sulfone (DVS) to modulate equilibrium sorption capacity and network stability. *Biomacromolecules,* 5**,** 92-96.

SARAVANAN, M., BHASKAR, K., MAHARAJAN, G. & PILLAI, K. S. (2011) Development of gelatin microspheres loaded with diclofenac sodium for intra-articular administration. *Journal of Drug Targeting,* 19**,** 96-103.

SCHMOLKA, I. R. (1972) Artificial skin: part 1. Preparation and properties of Pluronic F-127 gels for treatment of burns. *Journal of Biomedical Materials Research,* 6**,** 571-582.

SCHUMACHER, H. R. (2003) Aspiration and injection therapies for joints. *Arthritis & Rheumatism-Arthritis Care & Research,* 49**,** 413-420.

SCOTT, J. E. (1998) Secondary and tertiary structures of hyaluronan in aqueous solution: some biological consequences. *Glycoforum: http://www.glycoforum.gr.jp/science/hyaluronan/HA02/HA02E.html*.

SCOTT, J. E. & HEATLEY, F. (1999) Hyaluronan forms specific stable tertiary structures in aqueous solution: a (13)C NMR study. *Proceedings of the National Academy of Sciences of the United States of America,* 96**,** 4850-4855.

SCOTT, J. E. & HEATLEY, F. (2002) Biological properties of hyaluronan in aqueous solution are controlled and sequestered by reversible tertiary structures, defined by NMR spectroscopy. *Biomacromolecules,* 3**,** 547-553.

SECHRIEST, V. F., MIAO, Y. J., NIYIBIZI, C., WESTERHAUSEN-LARSON, A., MATTHEW, H. W., EVANS, C. H., FU, F. H. & SUH, J. K. (1999) GAG-augmented polysaccharide hydrogel: a novel biocompatible and biodegradable material to support chondrogenesis. *Journal of Biomedical Materials Research,* 49**,** 534-541.

SEIFARTH, C., CSAKI, C. & SHAKIBAEI, M. (2009) Anabolic actions of IGF-I and TGF-beta 1 on Interleukin-1 beta-treated human articular chondrocytes: evaluation in two and three dimensional cultures. *Histology and Histopathology,* 24**,** 1245-1262.

SEIREG, A. & ARVIKAR, R. J. (1975) The prediction of muscular load sharing and joint forces in the lower extremities during walking. *Journal of Biomechanics,* 8**,** 89-102.

SELLAM, J. & BERENBAUM, F. (2010) The role of synovitis in pathophysiology and clinical symptoms of osteoarthritis. *Nature Reviews Rheumatology,* 6**,** 625-635.

SHARMA, A., KOMISTEK, R. D., RANAWAT, C. S., DENNIS, D. A. & MAHFOUZ, M. R. (2007) In vivo contact pressures in total knee arthroplasties. *Journal of Arthroplasty,* 22**,** 404-416.

SHIOZAKI, M., MAEDA, K., MIURA, T., KOTOKU, M., YAMASAKI, T., MATSUDA, I., AOKI, K., YASUE, K., IMAI, H., UBUKATA, M., SUMA, A., YOKOTA, M., HOTTA, T., TANAKA, M., HASE, Y., HAAS, J., FRYER, A. M., LAIRD, E. R., LITTMANN, N. M., ANDREWS, S. W., JOSEY, J. A., MIMURA, T., SHINOZAKI, Y., YOSHIUCHI, H. & INABA, T. (2011) Discovery of (1S,2R,3R)-2,3-dimethyl-2-phenyl-1-

sulfamidocyclopropanecarboxylates: novel and highly selective aggrecanase inhibitors. *Journal of Medicinal Chemistry,* 54**,** 2839-2863.

SHU, X. Z., LIU, Y. C., LUO, Y., ROBERTS, M. C. & PRESTWICH, G. D. (2002) Disulfide cross-linked hyaluronan hydrogels. *Biomacromolecules,* 3**,** 1304-1311.

SILVA, M. D., THOMAS, D. P. P., HAZLEMAN, B. L. & WRAIGHT, P. (1979) Liposomes in arthritis - new approach. *Lancet,* 313**,** 1320-1322.

SMITH, M. D., TRIANTAFILLOU, S., PARKER, A., YOUSSEF, P. P. & COLEMAN, M. (1997) Synovial membrane inflammation and cytokine production in patients with early osteoarthritis. *Journal of Rheumatology,* 24**,** 365-371.

SOFAT, N. (2009) Analysing the role of endogenous matrix molecules in the development of osteoarthritis. *International Journal of Experimental Pathology,* 90**,** 463-479.

SONG, C. X., LABHASETWAR, V., MURPHY, H., QU, X., HUMPHREY, W. R., SHEBUSKI, R. J. & LEVY, R. J. (1997) Formulation and characterization of biodegradable nanoparticles for intravascular local drug delivery. *Journal of Controlled Release,* 43**,** 197-212.

SPERLING, L. H. & MISHRA, V. (1996) The current status of interpenetrating polymer networks. *Polymers for Advanced Technologies,* 7**,** 197-208.

STERN, R., KOGAN, G., JEDRZEJAS, M. J. & SOLTES, L. (2007) The many ways to cleave hyaluronan. *Biotechnology Advances,* 25**,** 537-557.

STRATTON, L. P., DONG, A. C., MANNING, M. C. & CARPENTER, J. F. (1997) Drug delivery matrix containing native protein precipitates suspended in a poloxamer gel. *Journal of Pharmaceutical Sciences,* 86**,** 1006-1010.

SUH, J. K. F. & MATTHEW, H. W. T. (2000) Application of chitosan-based polysaccharide biomaterials in cartilage tissue engineering: a review. *Biomaterials,* 21**,** 2589-2598.

SUTTON, S., CLUTTERBUCK, A., HARRIS, P., GENT, T., FREEMAN, S., FOSTER, N., BARRETT-JOLLEY, R. & MOBASHERI, A. (2009) The contribution of the synovium, synovial derived inflammatory cytokines and neuropeptides to the pathogenesis of osteoarthritis. *Veterinary Journal,* 179**,** 10-24.

TALASAZ, A. H. H., GHAHREMANKHANI, A. A., MOGHADAM, S. H., MALEKSHAHI, M. R., ATYABI, F. & DINARVAND, R. (2008) In situ gel forming systems of poloxamer 407 and hydroxypropyl cellulose or hydroxypropyl methyl cellulose mixtures for controlled delivery of vancomycin. *Journal of Applied Polymer Science,* 109**,** 2369-2374.

TAN, H. P., CHU, C. R., PAYNE, K. A. & MARRA, K. G. (2009) Injectable in situ forming biodegradable chitosan-hyaluronic acid based hydrogels for cartilage tissue engineering. *Biomaterials,* 30**,** 2499-2506.

THAKKAR, H., SHARMA, R. K., MISHRA, A. K., CHUTTANI, K. & MURTHY, R. S. R. (2004a) Celecoxib incorporated chitosan microspheres: in vitro and in vivo evaluation. *Journal of Drug Targeting,* 12**,** 549-557.

THAKKAR, H., SHARMA, R. K., MISHRA, A. K., CHUTTANI, K. & MURTHY, R. S. R. (2004b) Efficacy of chitosen microspheres for controlled intra-articular of celecoxib in inflamed joins. *Journal of Pharmacy and Pharmacology,* 56**,** 1091-1099.

THOTE, A. J., CHAPPELL, J. T., GUPTA, R. B. & KUMAR, R. (2005) Reduction in the initial-burst release by surface crosslinking of PLGA microparticles containing hydrophilic or hydrophobic drugs. *Drug Development and Industrial Pharmacy,* 31**,** 43-57.

TUNCAY, M., CALIS, S., KAS, H. S., ERCAN, M. T., PEKSOY, I. & HINCAL, A. A. (2000a) Diclofenac sodium incorporated PLGA (50 : 50) microspheres: formulation considerations and in vitro/in vivo evaluation. *International Journal of Pharmaceutics,* 195**,** 179-188.

TUNCAY, M., CALIS, S., KAS, H. S., ERCAN, M. T., PEKSOY, I. & HINCAL, A. A. (2000b) In vitro and in vivo evaluation of diclofenac sodium loaded albumin microspheres. *Journal of Microencapsulation,* 17**,** 145-155.

TURKER, S., ERDOGAN, S., OZER, Z. Y., ERGUN, E. L., TUNCEL, M., BILGILI, H. & DEVECI, S. (2005) Scintigraphic imaging of radiolabelled drug delivery systems in rabbits with arthritis. *International Journal of Pharmaceutics,* 296**,** 34-43.

VADNERE, M., AMIDON, G., LINDENBAUM, S. & HASLAM, J. L. (1984) Thermodynamic studies on the gel sol transition of some Pluronic polyols. *International Journal of Pharmaceutics,* 22**,** 207-218.

VAN DEN BERG, W. B. (2002) Lessons from animal models of arthritis. *Current rheumatology reports,* 4**,** 232-9.

VAN LENT, P., BLOM, A. B., VAN DER KRAAN, P., HOLTHUYSEN, A. E. M., VITTERS, E., VAN ROOIJEN, N., SMEETS, R. L., NABBE, K. & VAN DEN BERG, W. B. (2004) Crucial role of synovial lining macrophages in the promotion of transforming growth factor beta-mediated osteophyte formation. *Arthritis and Rheumatism,* 50**,** 103-111.

VAN TOMME, S. R., STORM, G. & HENNINK, W. E. (2008) In situ gelling hydrogels for pharmaceutical and biomedical applications. *International Journal of Pharmaceutics,* 355**,** 1-18.

VASCONCELLOS, F. C., SWISTON, A. J., BEPPU, M. M., COHEN, R. E. & RUBNER, M. F. (2010) Bioactive polyelectrolyte multilayers: hyaluronic acid mediated B lymphocyte adhesion. *Biomacromolecules,* 11**,** 2407-2414.

VOLPI, N., SCHILLER, J., STERN, R. & SOLTES, L. (2009) Role, metabolism, chemical modifications and applications of hyaluronan. *Current Medicinal Chemistry,* 16**,** 1718-1745.

VONDERMARK, K., GAUSS, V., VONDERMARK, H. & MULLER, P. (1977) Relationship between cell-shape and type of collagen synthesized as chondrocytes lose their cartilage phenotype in culture. *Nature,* 267**,** 531-532.

WALLS, H. J., CAINES, S. B., SANCHEZ, A. M. & KHAN, S. A. (2003) Yield stress and wall slip phenomena in colloidal silica gels. *Journal of Rheology,* 47**,** 847-868.

WALSH, D. A., BONNET, C. S., TURNER, E. L., WILSON, D., SITU, M. & MCWILLIAMS, D. F. (2007) Angiogenesis in the synovium and at the osteochondral junction in osteoarthritis. *Osteoarthritis and Cartilage,* 15**,** 743-751.

WANG, J. J., ZENG, Z. W., XIAO, R. Z., XIE, T. A., ZHOU, G. L., ZHAN, X. R. & WANG, S. L. (2011) Recent advances of chitosan nanoparticles as drug carriers. *International Journal of Nanomedicine,* 6**,** 765-774.

WANG, Q., WANG, J., LU, Q., DETAMORE, M. S. & BERKLAND, C. (2010) Injectable PLGA based colloidal gels for zero-order dexamethasone release in cranial defects. *Biomaterials,* 31**,** 4980-4986.

WARD, S. T., WILLIAMS, P. L. & PURKAYASTHA, S. (2008) Intra-articular corticosteroid injections in the foot and ankle: a prospective 1-year follow-up investigation. *Journal of Foot & Ankle Surgery,* 47**,** 138-144.

WASHINGTON, C. (1990) Drug release from microdisperse systems - a critical-review. *International Journal of Pharmaceutics,* 58**,** 1-12.

WILLIAMS, A. S., CAMILLERI, J. P., GOODFELLOW, R. M. & WILLIAMS, B. D. (1996) A single intra-articular injection of liposomally conjugated methotrexate suppresses joint inflammation in rat antigen-induced arthritis. *British Journal of Rheumatology,* 35**,** 719-724.

WITTENBERG, R. H., WILLBURGER, R. E., KLEEMEYER, K. S. & PESKAR, B. A. (1993) In-vitro release of prostaglandins and leukotrienes from synovial tissue, cartilage, and bone in degenerative joint diseases. *Arthritis and Rheumatism,* 36**,** 1444-1450.

WOOLF, A. D. & PFLEGER, B. (2003) Burden of major musculoskeletal conditions. *Bulletin of the World Health Organization,* 81**,** 646-656.

WU, J., WANG, X. F., KEUM, J. K., ZHOU, H. W., GELFER, M., AVILA-ORTA, C. A., PAN, H., CHEN, W. L., CHIAO, S. M., HSIAO, B. S. & CHU, B. (2007) Water soluble complexes of chitosan-g-MPEG and hyaluronic acid. *Journal of Biomedical Materials Research Part A,* 80A**,** 800-812.

XU, H., EDWARDS, J., BANERJI, S., PREVO, R., JACKSON, D. G. & ATHANASOU, N. A. (2003) Distribution of lymphatic vessels in normal and

arthritic human synovial tissues. *Annals of the Rheumatic Diseases,* 62**,** 1227-1229.

XU, L., PENG, H., GLASSON, S., LEE, P. L., HU, K., IJIRI, K., OLSEN, B. R., GOLDRING, M. B. & LI, Y. (2007) Increased expression of the collagen receptor discoidin domain receptor 2 in articular cartilage as a key event in the pathogenesis of osteoarthritis. *Arthritis and Rheumatism,* 56**,** 2663-2673.

YANG, L., CARLSON, S. G., MCBURNEY, D. & HORTON, W. E. (2005) Multiple signals induce endoplasmic reticulum stress in both primary and immortalized chondrocytes resulting in loss of differentiation, impaired cell growth, and apoptosis. *Journal of Biological Chemistry,* 280**,** 31156-31165.

YEO, Y. & KOHANE, D. S. (2008) Polymers in the prevention of peritoneal adhesions. *European Journal of Pharmaceutics and Biopharmaceutics,* 68**,** 57-66.

YOSHIDA, M., SAI, S., MARUMO, K., TANAKA, T., ITANO, N., KIMATA, K. & FUJII, K. (2004) Expression analysis of three isoforms of hyaluronan synthase and hyaluronidase in the synovium of knees in osteoarthritis and rheumatoid arthritis by quantitative real-time reverse transcriptase polymerase chain reaction. *Arthritis Research & Therapy,* 6**,** R514-R520.

YU, G.-E., DENG, Y., DALTON, S., WANG, Q.-G., ATTWOOD, D., PRICE, C. & BOOTH, C. (1992) Micellisation and gelation of triblock copoly(oxyethylene/oxypropylene/oxyet hylene), F127. *Journal of the Chemical Society, Faraday Transactions,* 88**,** 2537-2544.

YU, L. & DING, J. D. (2008) Injectable hydrogels as unique biomedical materials. *Chemical Society Reviews,* 37**,** 1473-1481.

ZENTNER, G. M., RATHI, R., SHIH, C., MCREA, J. C., SEO, M. H., OH, H., RHEE, B. G., MESTECKY, J., MOLDOVEANU, Z., MORGAN, M. & WEITMAN, S. (2001) Biodegradable block copolymers for delivery of proteins and water-insoluble drugs. *Journal of Controlled Release,* 72**,** 203-215.

APPENDIX I

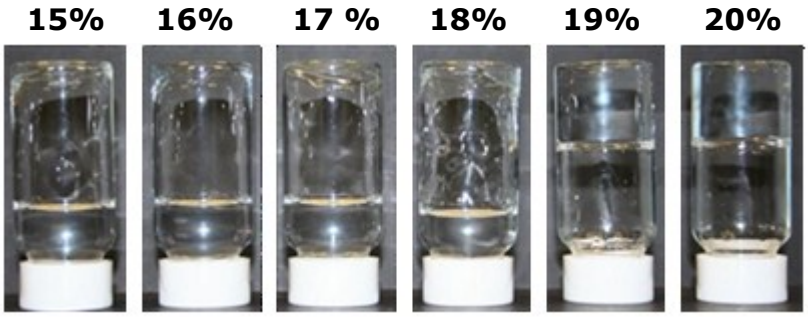

Solutions in PBS, 0.0035g/ml HA, 22°C

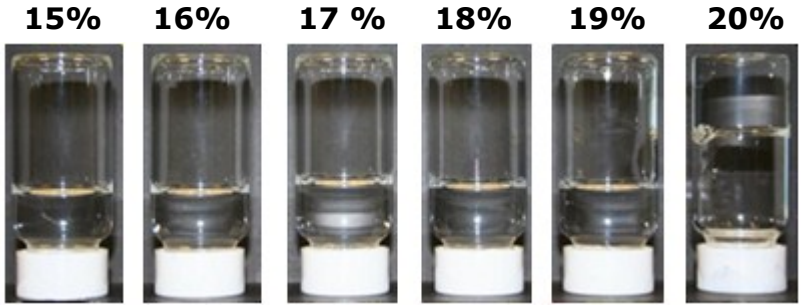

Solutions in water, 0.0035g/ml HA, 22°C

Photographs showing the gelation of Pluronic F127 solutions in synovial relevant conditions.

Pluronic F127 solutions at concentrations between 15% and 20%(w/v) were prepared in water or PBS. Hyaluronic acid at 3.5mg/ml was included where indicated. The vials were photographed at the indicated temperature after being inverted for 1 minute

APPENDIX II

Raw size and zeta potential distributions

Size distributions and zeta potentials were determined using a Malvern Zetasizer Nano ZS (Malvern Instruments Ltd, UK) at 25°C. Size was determined by dynamic light scattering and zeta potential by laser doppler micro-electrophoresis.

Blank Nanoparticles

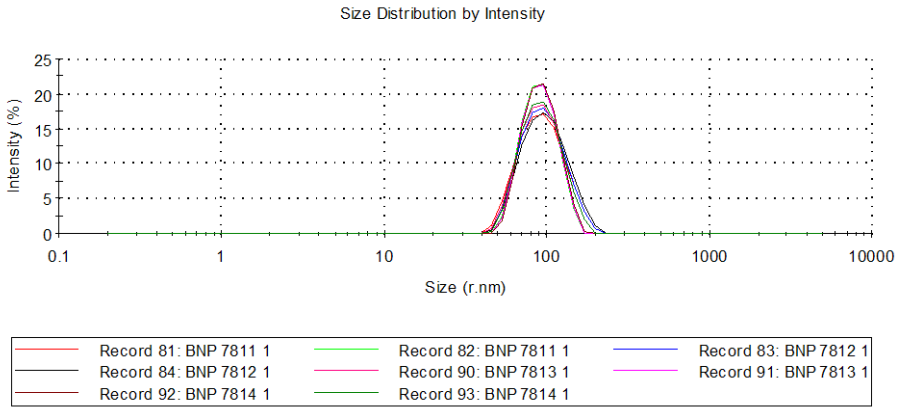

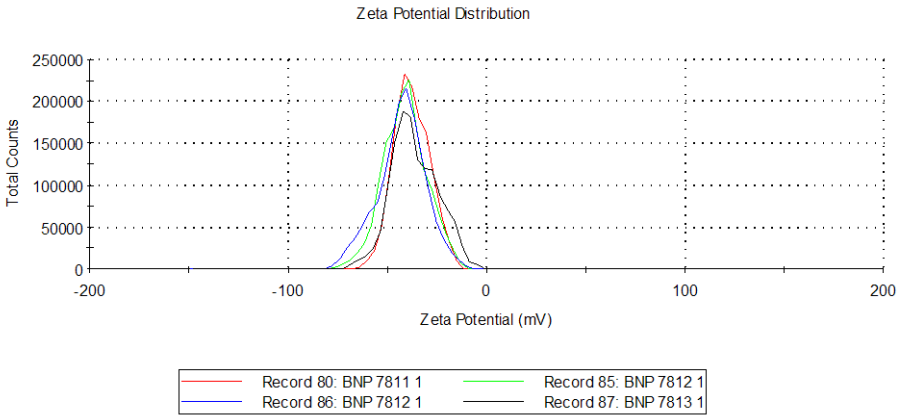

DXMP loaded nanoparticles

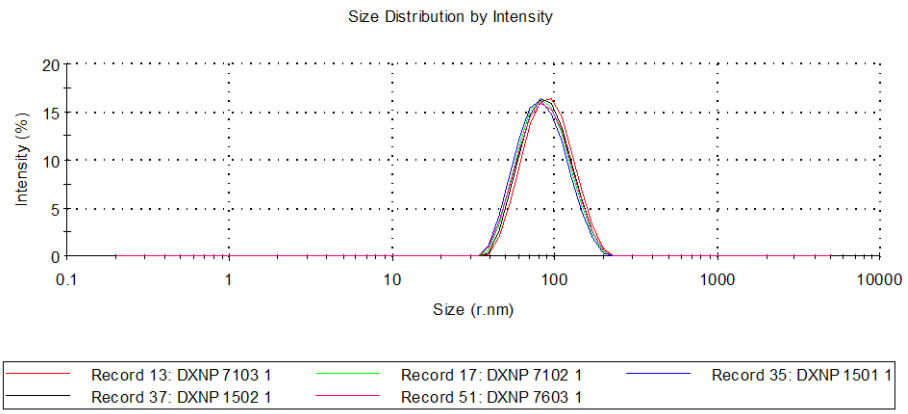

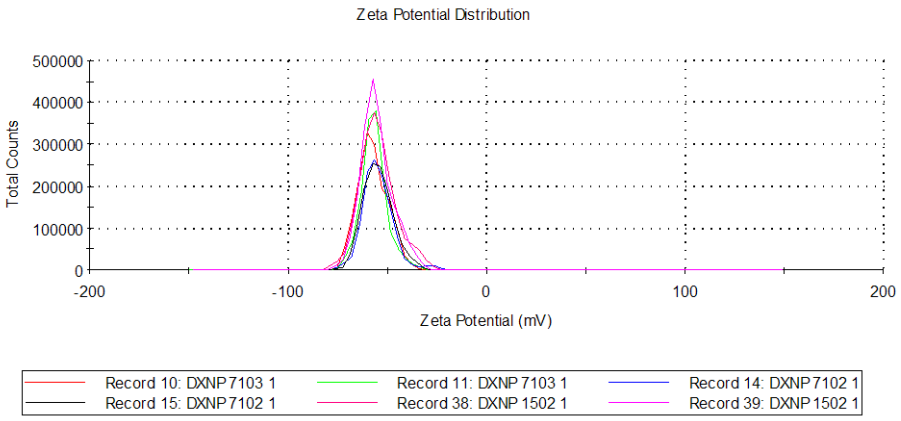

RBITC loaded nanoparticles